

Lincoln University Digital Thesis

Copyright Statement

The digital copy of this thesis is protected by the Copyright Act 1994 (New Zealand).

This thesis may be consulted by you, provided you comply with the provisions of the Act and the following conditions of use:

- you will use the copy only for the purposes of research or private study
- you will recognise the author's right to be identified as the author of the thesis and due acknowledgement will be made to the author where appropriate
- you will obtain the author's permission before publishing any material from the thesis.



COMPUTER SIMULATION OF ROCKFALLS -
APPLICATION TO ROCKFALLS AT FOX GLACIER,
WEST COAST, NEW ZEALAND

A thesis
submitted in partial fulfilment
of the requirements for the Degree of
Master of Engineering
(in Rock Engineering)
at
Department of Natural Resources Engineering,
Lincoln University

by

D.N.P.Rayudu

Lincoln University

1997

Abstract of a thesis submitted in partial fulfilment of the requirements for the degree of
Master of Engineering (M.E.) in Rock Engineering

COMPUTER SIMULATION OF ROCKFALLS -
APPLICATION TO ROCKFALLS AT FOX GLACIER,
WEST COAST, NEW ZEALAND.

by

Rayudu, D.N.Prasad.

This thesis reviews computer simulation of rockfalls in general and an attempt has been made to analyse and predict rockfalls at Fox Glacier, West Coast, New Zealand, using rockfall simulation programs. A comprehensive comparison of five rockfall simulation programs was carried out to help decide upon which program is the best to use for a detailed analysis of rockfalls. It was found from the comparison that the program *Rockfal2* is the best to use for this purpose.

Certain differences were noted with *Rockfal2* and so it was modified using Visual Basic, based in MSEXCEL™. Additional randomness has been incorporated to variate the starting position and velocity of the boulder, and to generate boulder trajectories and display them in graphical form.

The modified program *WinRock* was used to simulate rockfalls at Fox Glacier. Back analyses were carried out (using the boulder distribution from past rockfalls, as surveyed and recorded in the field), to find the representative coefficients of restitution that are essential to accurately simulate rockfalls. These coefficients were subsequently used to simulate and predict rockfalls in future. Conclusions were drawn that rockfalls at Undercite Creek are relatively stable (with an exception that boulders in excess of 5.5m diameter have more potential to reach the access road) and the Cone Rock rockfalls may increase in due course.

An overall assessment of rockfall hazards for all the degrading slopes at Fox Glacier was carried out using the Rockfall Hazard Rating System (1993) and CAN/CSA (1991) guidelines. This assessment identified and “quantified” the hazard that is involved with various slopes. From the hazard analysis it was found that the probability of fatalities are under the proposed and published acceptable limits for major civil engineering projects world-wide.

An attempt was made to find out an easy means of obtaining the coefficient of restitution by easy laboratory methods. Investigation of a correlation between Schmidt number and the coefficient of restitution (of a steel ball bouncing on a rock slab clamped to the ground) revealed good results (correlation coefficient = 0.89). This indicates that a good correlation may also exist between Schmidt number and the restitution coefficient when a rock impacts rock.

Acknowledgments

I am grateful to many for completing this research project and I would like to thank the following for helping and guiding me for a successful completion:

- Ministry of Foreign Affairs and Trade (MFAT), New Zealand - for sponsoring me by offering a scholarship for my studies in New Zealand.
- Dr. Laurie Richards - for providing guidance, support and sharing wisdom and beer throughout my studies in New Zealand.
- Dr. Tim Davies - for providing guidance, support and feedback for my project.
- Gordon Elliott (Golder Associates Inc., U.S.A.) - for providing the code for program *Rockfal2* and allowing me to change the original program.
- Brian Paterson - for providing photographs, diagrams and reports about the rockfalls at Fox Glacier.
- Tony Preston (DOC) - for providing assistance during my visits to the site and providing information regarding rockfall recordings at the site.
- Dr. David Bell, Robert Spiers, and Cathy Knight (Geology Dept., Uni. of Canterbury) - for providing technical support, instruments, and rock samples for my laboratory tests.
- Sylvia Butters (Elliott & Sinclair Ltd.) - for providing topography maps of the site.
- Rick Diehl - for technical help.
- Pascal Balley and Mariana Poh - for helping me with the boulder survey at the site.
- Ramesh and Rajani Rayudu (my brother and S.I.L.) - for being there.
- My family - for the support.
- Helen Rouse and Paul Scholes - for proof reading and feedback for my thesis.
- Staff at D.N.R.E - for good discussions in the staff room.
- Fellow postgrads at D.N.R.E - for providing a friendly environment and for playing table tennis with me.
- Indian community in Christchurch - for providing moral support.

Table of Contents

Abstract.....	iii
Acknowledgments.....	iv
Table of Contents.....	v
List of Figures.....	xi
List of Photos.....	xiv
List of Tables.....	xv
List of Abbreviations and Symbols.....	xvi
1.0 Introduction.....	1
1.1 Introduction.....	1
1.1.1 Definition of Rockfalls	1
1.2 Study Site.....	3
1.3 Aim and Objectives	6
1.4 Thesis Structure	7
2.0 Literature Review.....	8
2.1 Introduction.....	8
2.2 Rockfall Phenomenon.....	8
2.2.1 Rockfall Parameters.....	9
2.2.2 Definition of Terms Used in Rockfall Mitigation Design	10
2.3 Research on Rockfalls	11
2.3.1 Empirical Methods.....	12
2.3.1.1 <i>In Situ</i> Tests	12
2.3.1.2 Physical Modelling	15
2.3.2 Computer Modelling of Rockfalls	16
2.3.2.1 Simulation Methods.....	17
2.4 Protection Measures.....	18
2.4.1 Active Methods.....	20
2.4.2 Passive Methods	20
2.5 Rockfall Hazard Analysis Systems.....	20

2.6 Conclusions.....	21
2.7 Summary.....	22
3.0 Comparison Of Simulation Programs.....	23
3.1 Introduction.....	23
3.1.1 Assumptions	23
3.1.2 Computer Simulation of Rockfalls	23
3.1.2.1 The General Algorithm.....	24
3.2 Comparison of Simulation Programs.....	25
3.2.1 Assumptions for Comparison	25
3.2.2 Criteria for Comparison.....	25
3.2.3 Input Parameters	26
3.2.3.1 Boulder Information	26
3.2.3.2 Initial Conditions of The Boulder.....	26
3.2.3.3 Properties of Slope.....	27
3.2.3.4 Coordinates of Slope Cells	27
3.2.4 Simulation Logistics	28
3.2.4.1 Initial Movement of The Boulder	29
3.2.4.2 Free Falling.....	29
3.2.4.3 Impact and Bouncing	30
3.2.4.3.1 Calculation of Impact Coordinates	31
3.2.4.3.2 Calculation of Reflected Velocities	31
3.2.4.4 Transition from Bounce Mode to Roll Mode	38
3.2.4.5 Rolling and Sliding.....	39
3.2.4.6 Stopping.....	43
3.2.4.7 Summary of Logistics Comparison	44
3.2.5 Probabilistic Analysis	44
3.2.6 Overall Performance	46
3.2.6.1 Simulation Details	46
3.2.6.2 Simulation Results	47
3.2.6.3 Summary of Results.....	56
3.3 Conclusions and Recommendations	57
3.3.1 Conclusions for Each Program	58
3.3.2 Recommendations.....	60

3.4 Summary.....	61
4.0 Modification of The Program <i>Rockfal2</i>.....	62
4.1 Introduction.....	62
4.2 Modifications Made to The Program.....	62
4.2.1 Randomising Starting Position and Velocity of The Boulder	63
4.2.2 Generating 20 Representative Boulder Trajectories	63
4.2.3 Improving The Aesthetics of The Program	64
4.3 “ <i>WinRock</i> ”-The Modified Program of The Original <i>Rockfal2</i>	64
4.3.1 Input for The Program <i>WinRock</i>	66
4.3.1.1 Run Identification	66
4.3.1.2 Boulder Information	66
4.3.1.3 Initial Conditions	66
4.3.1.4 Simulation Details	67
4.3.1.5 Slope Information	68
4.3.2 Rockfall Simulation Using The Program <i>WinRock</i>	68
4.3.3 Output from The Program.....	68
4.4 Comparison of Program Output from <i>Rockfal2</i> and <i>WinRock</i>	74
4.5 Advantages of <i>WinRock</i> Over <i>Rockfal2</i>	75
4.6 Comparison of Trajectories From <i>WinRock</i> With Those from <i>CADMA</i> and <i>RF</i>	75
4.7 Bugs and Rules of The Program <i>WinRock</i>	77
4.8 Summary	78
5.0 Rockfall Analyses at Undercite Creek, Fox Glacier.....	79
5.1 Introduction.....	79
5.2 Rockfall History at Undercite Creek.....	79
5.3 Site Description.....	81
5.3.1 Location	81
5.3.2 Geology and Geomorphology.....	81
5.3.3 Environment.....	84
5.4 Back-Analysis of Past Rockfalls.....	84
5.4.1 Field Investigation	85
5.4.2 Computer Simulation.....	89
5.4.2.1 Input Parameters	89
5.4.2.1.1 Boulder Information	90

5.4.2.1.2 Initial Conditions	90
5.4.2.1.3 Simulation Details	90
5.4.2.1.4 Slope Information	91
5.4.2.2 Iterations to Find The Values of The Coefficients.....	91
5.5 Prediction of Rockfalls at Undercite Creek	94
5.5.1 Sections Used for The Analysis.....	95
5.5.2 Simulation Results	95
5.6 Conclusions.....	97
5.7 Summary	99
6.0 Assessment Of Rockfall Hazard To The Access Road At Fox Glacier.....	100
6.1 Introduction.....	100
6.2 Rockfall Hazard Rating System (RHRS).....	100
6.2.1 Slope Inventory	101
6.2.2 Preliminary Rating.....	102
6.2.3 Detailed Rating	103
6.3 Detailed Rating for the Slopes at Fox Glacier	103
6.4 Risk Assessment of Rockfalls at Fox Glacier.....	106
6.4.1 Criteria for Detailed Risk Analysis.....	106
6.4.2 Scope Definition	107
6.4.3 Hazard Identification	107
6.4.4 Risk Estimation and Calculation	107
6.4.4.1 Event Tree Analysis.....	108
6.4.4.2 Risk Calculation.....	109
6.4.4.2.1 Moving Vehicle / Falling Rock	110
6.4.4.2.2 Moving Vehicle / Fallen Rock.....	112
6.5 Comparison Between Assessed Risk and Acceptable Risk.....	115
6.6 Conclusions and Discussion	117
6.7 Summary	120
7.0 Laboratory Tests To Find The Coefficient of Restitution.....	121
7.1 Introduction.....	121
7.1.1 Importance of The Restitution Coefficients.....	121
7.2 Background on Restitution Coefficients.....	123
7.3 Obtaining a Relation Between The Schmidt Number and Restitution Coefficient .	124

7.3.1 Experimental Procedure To Find The Restitution Coefficient	124
7.3.1.1 Experimental Setup To Find The Restitution Coefficient	125
7.3.2 Method of Finding The Schmidt Number of Rock.....	127
7.3.3 Correlation Between Schmidt Number and Restitution Coefficient	128
7.4 Obtaining The Coefficient of Restitution of Rock-Rock Impacts From Steel-Rock Impacts	130
7.5 Conclusions and Discussion	132
7.6 Summary.....	132
8.0 Conclusions and Discussion.....	133
8.1 Introduction.....	133
8.2 Achieving Three Main Objectives.....	133
8.3 Overall Conclusions.....	134
8.3.1 Computer Simulation of Rockfalls	134
8.3.2 Review of Rockfall Problems at Fox Glacier	135
8.3.3 Coefficient of Restitution.....	136
8.4 How helpful was this research?	136
8.5 Future Work.....	137
Appendix A.....	139
A.1 Logistics Involved In The Program Rockfal2.....	139
A.1.1 "Bounce" Mode Algorithms	139
A.1.2 "Roll" Mode Algorithms.....	143
A.2 Calculation Sequence.....	145
Appendix B.....	150
Appendix C.....	154
Appendix D.....	159
D.1 Detailed RHRS Rating for Undercite Creek at Fox Glacier	159
D.1.1 Slope Height.....	159
D.1.2 Ditch Effectiveness	159
D.1.3 Average Vehicle Risk (AVR)	160
D.1.4 Percent of Decision Sight Distance (DSD).....	160
D.1.5 Roadway Width	162

D.1.6 Geologic Character 162

 D.1.6.1 Structural Condition..... 162

 D.1.6.2 Rock Friction 163

D.1.7 Block Size or Volume of Rockfall Per Event 164

D.1.8 Climate and Presence of Water on Slope..... 164

D.1.9 Rockfall History..... 164

References.....167

Modified Program *WinRock*.....floppy disk

List of Figures

Figure 1-1: Diagram showing a typical rockfall.....	2
Figure 1-2: Location map showing the access roads and the Fox Glacier (Scale 1:5000). ...	4
Figure 3-1: Flow chart showing the general algorithm for computer simulation of rockfalls.	24
Figure 3-2: Configuration of the block before and after the impact (Azzoni <i>et al.</i> 1995)...	36
Figure 3-3: Different possibilities for the block at the impact (Azzoni <i>et al.</i> 1995).....	37
Figure 3-4: Definition of rolling problem in the assumed $OX'Y'$ reference frame.....	42
Figure 3-5: Profile of the slope used for overall comparison of simulation programs.	46
Figure 3-6: Boulder trajectory (Rockfall).	48
Figure 3-7: Velocity graph for the whole slope (CRSP).	49
Figure 3-8: Velocity distribution at analysis point (CRSP).....	49
Figure 3-9: Bounce height graph for the whole slope (CRSP).	49
Figure 3-10: Boulder trajectories simulated by the program <i>CRSP</i>	49
Figure 3-11: Maximum boulder travel in horizontal direction (Rockfal2).....	50
Figure 3-12: Percentage of boulders reaching specified X-coordinates (Rockfal2).....	50
Figure 3-13: Boulder velocity at analysis point (Rockfal2).	50
Figure 3-14: Percentage of boulders exceeding given velocities at analysis point (Rockfal2).	51
Figure 3-15: Boulder height above ground at analysis point (Rockfal2).....	51
Figure 3-16: Percentage of boulders exceeding given heights at analysis point (Rockfal2).	51
Figure 3-17: Trajectories of the boulders (RF).	52
Figure 3-18: Plot showing the histogram of run out distances (CADMA).....	53
Figure 3-19: Boulder trajectories (CADMA).	54
Figure 3-20: Average bounce heights at particular distances (CADMA).....	54
Figure 3-21: Average velocities at respective distances (CADMA).....	55
Figure 3-22: Plots showing the statistics at analysis point (CADMA).....	55
Figure 4-1: Layout of the main sheet of the program <i>WinRock</i>	65
Figure 4-2: EXCEL sheet showing the input for slope.....	67
Figure 4-3: Output data from the program <i>WinRock</i>	70
Figure 4-4: Statistical output data from the program <i>WinRock</i>	70

Figure 4-5: Maximum boulder travel in horizontal direction (<i>WinRock</i>).....	71
Figure 4-6: Percentage of boulders reaching specified X-coordinates (<i>WinRock</i>).	71
Figure 4-7: Boulder velocity distribution at analysis point (<i>WinRock</i>).	72
Figure 4-8: Percentage of boulders exceeding given velocities at analysis point (<i>WinRock</i>).	72
Figure 4-9: Boulder height above ground surface at analysis point (<i>WinRock</i>).	73
Figure 4-10: Percentage of boulders exceeding given heights at analysis point (<i>WinRock</i>).	73
Figure 4-11: Boulder trajectories for the slope analysed (<i>WinRock</i>).	74
Figure 4-12: Boulder trajectories (<i>CADMA</i>).....	76
Figure 4-13: Boulder trajectories (<i>RF</i>).	76
Figure 5-1: Map of Undercite Creek - Yellow Creek area showing geomorphic features and geologic structure (courtesy: Brian Paterson).....	83
Figure 5-2: Boulder mapping at the Undercite Creek (original size A3).	87
Figure 5-3: Topographic map of Undercite Creek - Yellow Creek area showing location of topographic cross-sections (courtesy: Brian Paterson).	88
Figure 5-4: Slope profile used for the back-analysis (cross-section C-C').....	92
Figure 5-5: Hand-drawn map of the zoning used by the Department Of Conservation for recording rockfalls (courtesy: DOC).	94
Figure 6-1: Event tree analysis for Undercite Creek.	108
Figure 6-2: Comparison between risks of fatalities due to rockfalls with published and proposed acceptable risk criteria.	116
Figure 8-1: Schematic diagram showing the three main research objectives and the main conclusions from each chapter.....	134
Figure C-1: Details of section C-C' along with some boulder trajectories (<i>WinRock</i>).	154
Figure C-2: Details of section B-B' along with some boulder trajectories (<i>WinRock</i>).	155
Figure C-3: Details of section Y-Y' along with some boulder trajectories (<i>WinRock</i>).	155
Figure C-4: Details of section Y'-C' along with some boulder trajectories (<i>WinRock</i>).	156
Figure C-5: Details of section X-X' along with some boulder trajectories (<i>WinRock</i>).	156
Figure C-6: Details of section X'-C' along with some boulder trajectories (<i>WinRock</i>).	157

Figure C-7: Details of section Z-Z' along with some boulder trajectories (*WinRock*)...... 157

Figure C-8: Details of section Z'-C' along with some boulder trajectories (*WinRock*). ... 158

List of Photos

Photo 1-1: Aerial view of Undercite Creek fan after the January 1994 rockfall.	5
Photo 5-1: Aerial photograph of the site taken during January 1997 (courtesy: Brian Paterson).	80
Photo 5-2: Photograph taken from the ground showing the whole slope of Undercite Creek.	82
Photo 5-3: Photograph showing the reference point used for the survey.	86
Photo 6-1: Photo showing a boulder that rolled down on to the walking track at Yellow Creek.	102
Photo 7-1: Experimental setup to find the coefficient of restitution.	126
Photo 7-2: Method of clamping the rock slab tight to the ground.	126
Photo 7-3: Schmidt hammer used for the experiments (Type L).	127

List of Tables

Table 2-1: Classification of remedial measures for rock slopes (Martin 1988).....	19
Table 3-1: Summary of boulder details to be specified for each program.....	26
Table 3-2: Summary of initial conditions of boulder to be specified for each program.....	26
Table 3-3: Summary of specifying slope properties in each program.....	28
Table 3-4: Summary of boulder starting conditions for each program.....	30
Table 3-5: Summary of criteria used to simulate transition from bounce mode to roll mode.....	39
Table 3-6: Criteria used to terminate calculations.	44
Table 3-7: Comparison of <i>all</i> of the simulation logistics used by respective programs.....	45
Table 3-8: Randomness incorporated in respective programs.	45
Table 3-9: Parameter values used for the rockfall simulation.	47
Table 3-10: Summary of results at the point of analysis	56
Table 5-1: Summary of iterations carried out to find the parameter values.	93
Table 6-1: Preliminary rating system.....	102
Table 6-2: Summary sheet of the rockfall hazard rating system	104
Table 6-3: Rockfall hazard rating for slopes at Fox Glacier.....	105
Table 6-4: Frequency severity matrix and action guide.....	106
Table 6-5: Summary of calculated probabilities of fatalities and accidents at Undercite Creek.	115
Table 7-1: Types of rock specimens used for the tests.	128
Table 7-2: Schmidt number and restitution coefficients of different types of rocks.	128
Table 7-3: r^2 and correlation coefficient values for different types of rocks.	130
Table A-1: Conditions for the initial travel mode for the program <i>Rockfal2</i>	146
Table D-1: Required decision sight distance according to AASHTO standards (1991). ..	161
Table D-2: Rockfall hazard field data sheet.	166

List of Abbreviations and Symbols

AADT	annual average daily traffic volume
AASHTO	American Association for State Highway and Transport Officials
ASD	actual sight distance of a portion of highway
DOC	Department Of Conservation, New Zealand.
DSD	decision sight distance (AASHTO 1990)
CSA	Canadian Standards Association
CRSP	Colorado Rockfall Simulation Program
EDM	Electronic Distance Measurement Theodolite
F_1	friction function used by Elliott (1992)
F_2	scaling function used by Elliott (1992)
F_v	average fraction of the highway occupied by vehicles
FPS	Foot, Pound, Second system of units
I	moment of inertia
ISRM	International Society for Rock Mechanics
K_i	initial kinetic energy
K_r	final kinetic energy
L_c	length of a highway rock cut
L_{dsd}	length of the decision sight distance for a specific vehicle speed (AASHTO 1990)
L_{rf}	length of the road effected by a rockfall
N_a	number of vehicle/rock accidents resulting from a specific number of rocks reaching the road in a given time period
N_r	number of rocks that reach the road annually
N_v	number of vehicles at risk which is equal to the number of vehicles that pass through the cut per day or are stationary within the cut for a given period
P(A)	probability of a rock hitting a vehicle or a vehicle hitting a rock
PDSD	percentage decision sight distance
P(L:T)	probability of loss of life of an individual given a rock hits the individual's vehicle (Morgan 1992)
P(H)	probability of a hazardous event occurring (Morgan 1992)
P(S)	probability that a rock hits a vehicle and is therefore the combination of
P(H)	and P(S:H) from Morgan (1992)

P(S:H)	probability of spatial impact given the event or the probability that a vehicle occupies the portion of the road effected by a rockfall (Morgan 1992)
P(T:S)	probability of temporal impact given spatial impact (Morgan 1992) or the probability that a vehicle occupies the rockfall path when the rock impacts the road
PAV	probability of a rockfall/vehicle accident of an individual vehicle
R	coefficient of restitution
RHRS	Rockfall Hazard Rating System
RMR	Raock Mass Rating
R_n	normal coefficient of restitution
R_t	tangential coefficient of restitution
SF	scaling factor used by Pfeiffer and Bowen (1989)
SI	International System of units
SMR	Slope Masss Rating
USDOT	United States Department of Transportation
V_i	initial velocity
V_{in}	initial normal velocity
V_{it}	initial tangential velocity
V_{ix}	initial velocity in x direction of the global cartesian system
V_{iy}	initial velocity in y direction of the global cartesian system
V_r	final velocity
V_m	final normal velocity
V_{rt}	final tangential velocity
V_{rx}	final velocity in x direction of the global cartesian system
V_{ry}	final velocity in y direction of the global cartesian system
V_v	average vehicle speed which is assumed to be equal to the posted speed limit
V_x	velocity in x direction of the global cartesian system
V_y	velocity in y direction of the global cartesian system
f(F)	friction function used by Pfeiffer and Bowen (1989)
g	acceleration due to gravity
h	initial height of the steel ball
h'	rebound height of the steel ball after the impact
m	mass of the rock

r	radius of the boulder
Δ	angular displacement
α	angle of trajectory with respect to the global cartesian system
β_i	angle of impact relative to the ground surface
β_r	angle of rebound relative to the ground surface
ε	coefficient of restitution of energy
λ	rolling friction coefficient used by Elliott (1992)
θ	angle of plane
ω_i	initial rotational velocity
ω_r	final rotational velocity

Chapter 1

INTRODUCTION

1.1 Introduction

“Beware of rockfalls” (see cover page); this is a very common sign seen on New Zealand highways. Rockfalls pose a serious problem in areas where steep terrain is in close proximity to developed areas or transportation corridors. Rockfalls can cause traffic delays, damage, injury, and death to users of the highways. New Zealand, with a large area of steep terrain, is prone to such hazards.

In 1982, a rock fell on a vehicle killing a woman and disabling her father while delayed in traffic on British Columbia Highway 99 (Bunce 1994). People in the town of Nainital, in the state of Uttar Pradesh, India have been living under constant threat of rockfalls and rock avalanches since the early nineteenth century (Joshi and Pant 1990). Martin (1988) stated that rockfalls, small rockslides and raveling are the most chronic problems on transportation routes in mountainous areas of North America; millions of dollars are spent annually on maintenance and remedial measures to provide protection against such hazards. These are just a few examples of the rockfall hazard which indicate the seriousness of the problem. Hence, there is a need to understand and predict rockfall behaviour so that effective rockfall analysis and design can be carried out in the areas where there is a potential for rockfall hazard.

1.1.1 Definition of Rockfalls

Rockfalls should be distinguished from rock avalanches and debris flows. Rockfalls involve extremely rapid movement (under gravity), of individual rock boulders of a limited size which behave individually (Figure 1-1), whereas rock avalanches involve huge

volumes of mass movement. In a rock avalanche, a part or the whole slope (which may consist of facial and bed rock) collapses suddenly. Debris flows include movement of earth along with water.

Varnes (1978) defines a rockfall as a free fall of rocks through the air, with leaping, bouncing or rolling of fragments. Spang (1987) and Spang and Rautenstrauch (1988) have reviewed the definition of the term 'rockfall' and note that there is no general agreement as to the volume which characterises a rockfall event. However, the phenomenon is generally accepted as having the following characteristics (Richards 1988):

- The event involves a single block or group of blocks which become detached from the rock face.
- Each falling block behaves more or less independently of other blocks.
- There is temporary loss of ground contact and high acceleration during the descent.
- The blocks attain significant kinetic energy during their descent.

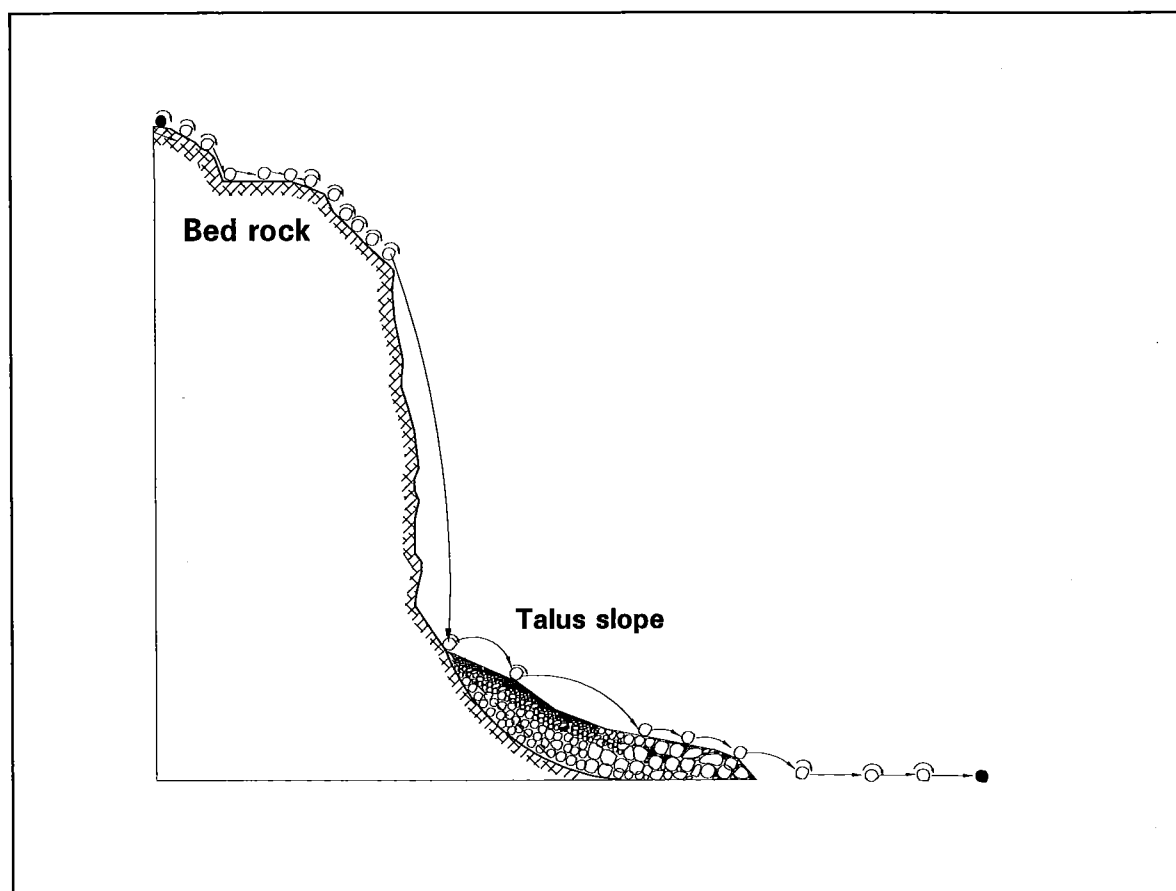


Figure 1-1: Diagram showing a typical rockfall

1.2 Study Site

The Fox and Franz Josef Glaciers (see map in Figure 1-2) are national tourist icons for New Zealand, where annual visitor numbers to the Glaciers are about 400,000, generating about \$40 million worth of business (Tourism Resource Consultants 1995). The glaciers are said to be a main natural tourist attraction with visitor numbers on a par with Mount Cook and Milford Sound. The tourist industry at the glacier villages depends mainly upon the accessibility of the glaciers, as the normal visitor to the glaciers only visits the most accessible glacier. The access roads are prone to natural hazards such as rockfalls, debris flows, and flooding. Due to the size of this glacier visitor industry and its significance to both the local economy and the national tourist industry, the maintenance of the visitor access to the glaciers is of prime importance to the West Coast economy.

Since August 1992, the Undercite Creek catchment of the Fox Glacier (see map in Figure 1-2) has undergone an increased rate of erosion. Several large slips, occurring during times of prolonged intense rainfall, have stripped vegetation cover, top soil, and underlying fractured bedrock from a substantial part of the drainage basin. Debris from the catchment has blocked the access road on several occasions. Finally, in January 1994, collapse of the eastern side and part of the western side of the basin, produced between 1 and 1.35 million cubic meters of material, most of which was deposited on the debris cone directly underneath the catchment (Photo 1-1).

Due to the blockage of the Northern Bank access road (See map in Figure 1-2), a temporary access road has been established along the flood plain of the Fox river, as the extension of the Southern Bank access road to the Fox Glacier is not feasible on engineering grounds. This temporary access to the glacier is under constant threat from rockfalls from the Undercite Creek, flooding due to Fox river, and also the lateral movement of the river. Erosion at the Undercite Creek catchment slope is highly active at present as the bed rock now exposed, consists of very weak inter-layered schist with open fissures. Toppling failure is also a possibility as the schist fabric dips into the slope. Hence there is a high possibility of rockfalls in the near future.

With visitor safety in mind, it is essential to review rockfall problems at the Fox Glacier. Landslides and other forms of mass movement can be predicted by monitoring the movement of the slope sometimes, but the localised nature and sudden occurrence of

rockfalls makes this prediction much more difficult. Because the rockfalls occur with little if any warning, prediction methods are needed to assess their behaviour so that appropriate engineering measures can be taken; these may involve re-location of the road or construction of protection measures such as a catch ditch between the road and debris cone.

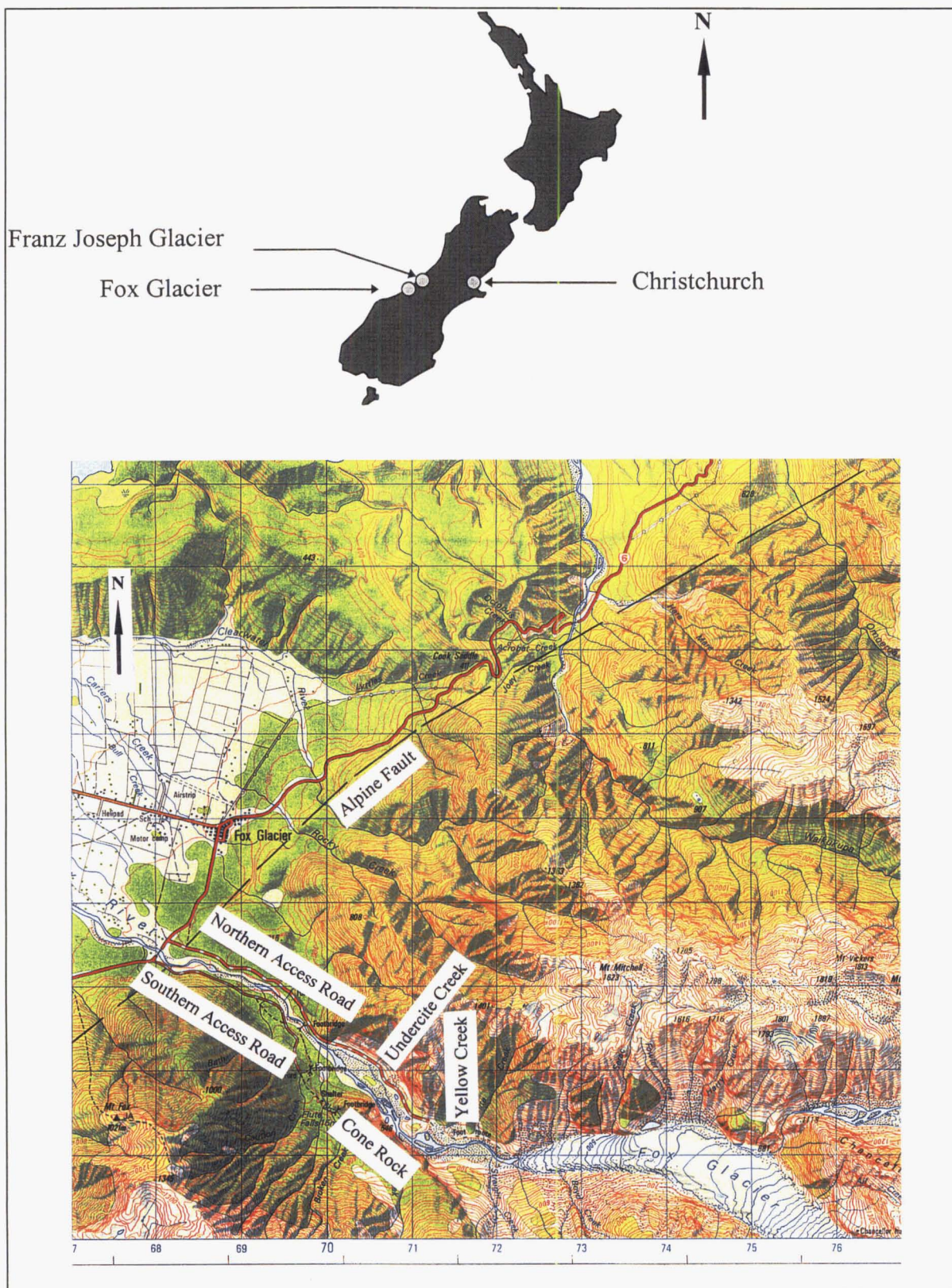


Figure 1-2: Location map showing the access roads and the Fox Glacier (Scale 1:11050).

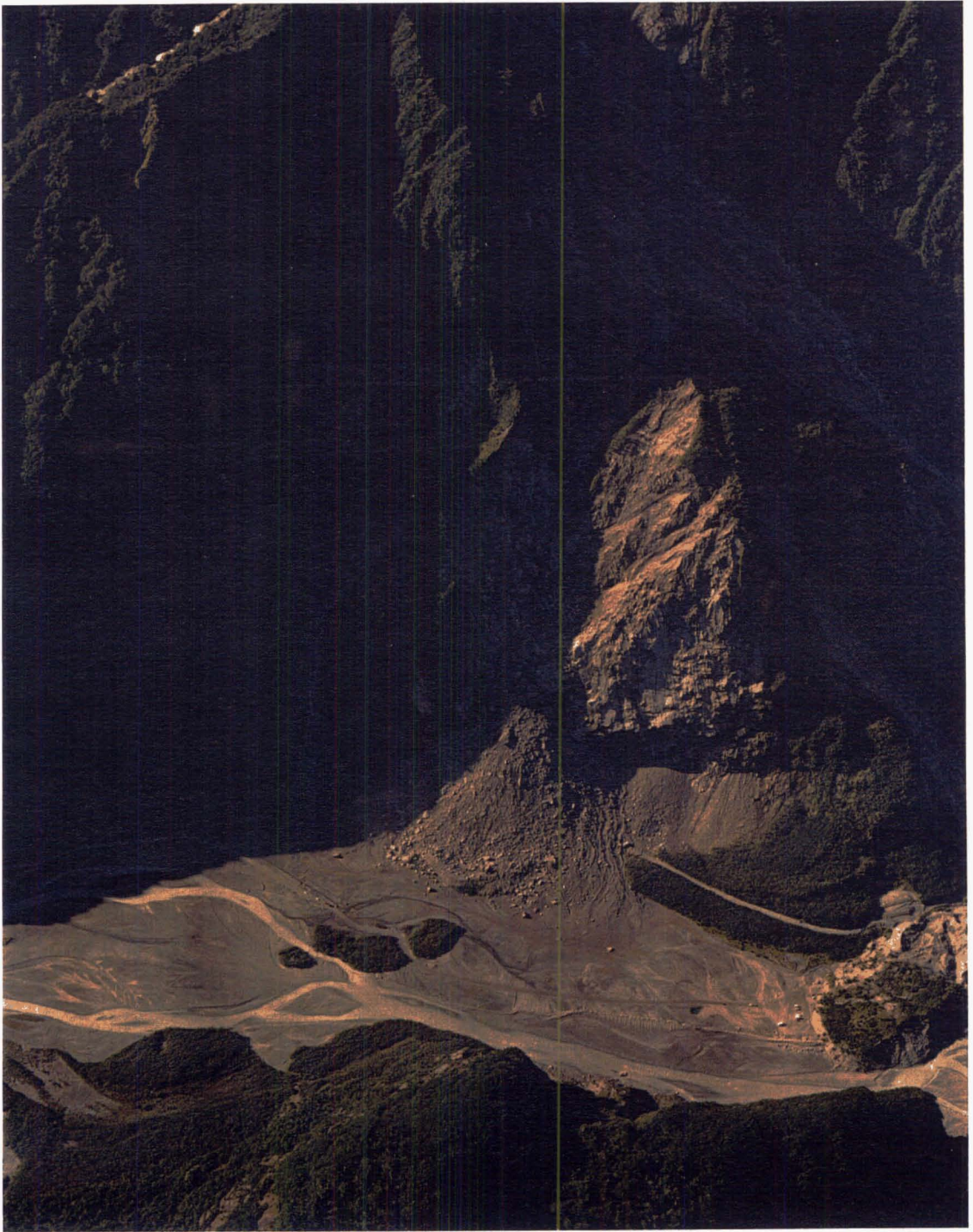


Photo 1-1: Aerial view of Undercite Creek fan after the January 1994 rockfall.

Note the closure of the North bank access road, and the temporary access road through the river bed. (*Photo by Lloyd Homer*).

1.3 Aim and Objectives

As stated earlier, the rockfalls at Fox Glacier need to be analysed to assess the potential hazard from rockfalls to the glacier visitors using the access road. A detailed analysis of rockfalls has to be carried out at the site to check the potential hazard from rockfalls to the glacier visitors using the access road. Rockfall analysis is usually carried out either by *in situ* tests, physical or computer modelling. Computer modelling of rockfalls was chosen as a means of rockfall analysis in this thesis as it has become an easy and economical means of rockfall analysis and to get the rockfall statistics (number, height above ground, and velocities of boulders reaching the road), which help in the prediction of rockfalls in the future.

To do this, first of all six computer simulation programs will be compared to see which program is the best for rockfall analysis in general. The best program (or a modified version of the program, if necessary) will then be used to analyse rockfalls at Fox Glacier. Next an assessment of the rockfall hazard at Fox Glacier will be carried out. An attempt will also be made to perform laboratory tests to find any easy means of determining the coefficient of restitution, which is an important parameter governing rockfall phenomenon. This coefficient of restitution (defined in section 2.2.1) plays an important role in simulating the bounce mode (rebound of the boulder after an impact with ground) of the rockfall.

Thus, the main aim of the research is:

“to review rockfall problems on the access road to Fox Glacier using computer simulation, and to assess the rockfall hazards”.

There are three main objectives of the research. They are:

1. to compare rockfall simulation programs to see which is the best (for a detailed rockfall analysis) and to modify the best program, if necessary.
2. to use the best simulation program to analyse rockfalls at Fox Glacier and to assess the rockfall hazard to the access road to the glacier.
3. to perform laboratory tests to find out an easy means of obtaining coefficient of restitution.

1.4 Thesis Structure

Chapter 2 discusses the rockfall phenomenon in detail and reviews the research work done on this topic to date. Chapters 3 and 4 move on to comparing five different rockfall simulation programs and modifying the best program, thus addressing the first objective. Chapters 5 and 6 concentrate on detailed rockfall analysis at the Undercite Creek and assessment of rockfall hazard to the access road addressing the second objective of the research. Chapter 7 describes the laboratory tests to the coefficient of restitution. In Chapter 8, the conclusions from all the chapters are integrated and cumulative conclusions are drawn based on the main objectives of the thesis, along with suggestions for future work.

Chapter 2

LITERATURE REVIEW

2.1 Introduction

This chapter first discusses the rockfall phenomenon and the parameters influencing rockfalls. The research work done to date to understand and predict rockfalls using *in situ* tests, physical and computer modelling, is then reviewed to draw some conclusions on the status quo of rockfall analysis and design. The rockfall stabilisation and protection methods, and hazard analysis systems will also be discussed in brief.

2.2 Rockfall Phenomenon

Rockfalls are generally triggered either by heavy rainfall, freeze-thaw cycles, or earthquakes. The initial velocity of the boulder thus depends on the triggering cause. Once the boulder leaves its place, it may either slide, roll or free-fall depending on the topography of the slope. If the boulder is dispatched from an overhang, the rock may free-fall until it impacts the ground. If the boulder is dispatched from the top of a slope (with slope angle $\leq 90^\circ$), it may either slide or roll. Once the boulder is in motion, it keeps on moving under the influence of gravity by rolling and bouncing (with both rotational and translational velocities) and there will be an enormous increase in its kinetic energy. The kinetic energy that is attained during the motion may be decreased by any kind of obstacles; such as trees, grass, surface roughness of the slope, debris underneath, and reverse slope in case of ditch. Once it reaches flat ground, the hardness/softness and friction of the ground surface helps retard the boulder velocities. Thus, the boulder keeps on moving until its kinetic energy becomes zero. Because the kinetic energy is retarded on a flat ground, or a reverse slope (in case of a catch ditch), the rockfalls pose more hazard where there is a road or a house immediately near the base of the slope.

The decrease in kinetic energy is influenced by hardness of the surface on which the boulder is moving. If the surface hardness is too low (e.g. river bed, or debris from earlier rockfalls or any other soft material), the kinetic energy of the boulder decreases instead of increasing. This hardness of the surface which influences rockfall motion is defined in terms of the coefficient of restitution defined in the following sub-section.

2.2.1 Rockfall Parameters

The following are the parameters influencing rockfalls:

- Normal and tangential coefficients of restitution;
- Tangential coefficient of friction;
- Slope roughness; and
- Coefficient of rolling friction.

These parameters are used in computer simulation of rockfalls and thus, discussion is included as to how these parameters are defined and used by the simulation programs.

Normal and tangential coefficients of restitution:

The coefficient of restitution is defined as the ratios of energies before and after impact, i.e.

$$\text{Restitution coefficient} = \text{Energy after impact} / \text{Energy before impact}$$

There will be two coefficients of restitution; normal and tangential, representing the energy loss in normal and tangential directions respectively. The ratio should lie between 0 and 1, as the energy after impact will always be less than the energy before impact. A value of 0 implies there is a total loss of energy and a value of 1 implies there is no loss of energy at all. These coefficients are then used to calculate the resultant velocity of a boulder after impact by reducing the velocities in the respective directions using the respective coefficients.

Tangential coefficient of friction

The tangential coefficient of friction is defined as the tangent of the angle of friction of the material in question. This coefficient is used by some of the authors of simulation programs in substitution to the tangential coefficient of restitution.

There is a major difference between the tangential coefficient of restitution and the coefficient of tangential friction. The values of these coefficients are the inverse of each other. For the same material, when the tangential coefficient of restitution is higher, the

coefficient of tangential friction is low. For example, the tangential coefficient of restitution for a smooth, hard bedrock can be around 0.6 - 0.7; whereas the coefficient of tangential friction for the same can be around 0.4. This is because to some extent the tangential coefficient of restitution depends upon the hardness of the material but, as the bedrock is smooth, the angle of friction will be low and so will the tangential coefficient of friction. Hence, these coefficients have to be clearly understood before the computer simulation of rockfalls is performed. Therefore, the authors of respective simulation programs have to specify clearly the definition of these parameters in their users guide to give a clear picture of the influence of these parameters on the simulation.

Slope roughness

In order to characterise the random behaviour of falling of boulders, slope roughness angle is used to randomise the inclination of the plane at the point of impact. This angle is used to represent, to some extent, the change in the angle of impact plane because of the undulations of the slope surface. Usually this angle is specified in degrees and the simulation program varies it randomly to simulate the uncertainty in impact angle. Some programs use a ratio for this purpose, which is the ratio of the slope angle between two coordinates of the slope surface to that of the angle of undulated surface. For example, if the slope angle is 30° and the angle of undulations is 10° , the ratio will be 0.3.

Rolling friction coefficient

The rolling friction coefficient is defined as the tangent of that angle at which the boulder, which is initially at rest, rolls off the surface without an external force. This rolling friction coefficient is used to reduce or increase the angular velocity of the boulder while in the process of rolling motion.

2.2.2 Definition of Terms Used in Rockfall Mitigation Design

The following are some of the terms used in rockfall mitigation design:

Catch Ditch

A catch ditch is a ditch that is provided to trap the boulders coming down the slope. This is usually dug at the base of the slope, between the slope and the road.

Fall Out Areas

Fall out areas are the flat grounds provided at the base of the slopes to help retard the boulder velocity.

Shoulders

Shoulders are flat areas provided on the slope to retard the boulders. These may be artificially made when there is access up to the slope. A few of these shoulders along with installed fences will help stop some boulders reaching the road.

Rockfall Fence

Fence is usually provided either to retard (if the fence is up the slope) or to stop the boulders (when the fence is installed at the base of the slope).

2.3 Research on Rockfalls

The earliest research into rockfall behaviour was not carried out until 1963, when Arthur M. Ritchie recognised the need to understand the actual rockfall process. He noted that there is a clear need for a means of predicting the stability of material on the surface of a rock cut, and thus he states in his paper (Ritchie 1963, p.18):

"So far, these factors remain elusive and many engineers approach the problem with apathy, as though walking up to a stone wall and half heartedly demanding that the wall give up its secrets and come under their slide rule".

After this early work, over 70 papers have been published on this topic during the past 30 years and considerable progress has been made in explaining rockfall behaviour. Most of the work was done in an attempt to stop boulders reaching transportation corridors like roads and railway lines.

Effective methods were developed and analysed to restrict boulders. For example, digging catch ditches, installing catch fences, or covering the whole slope with a net to stop rockfalls. Even though the basic rockfall phenomenon is understood in recent times, rockfalls pose problems because of their inherent random behaviour. As with other rock engineering problems, rockfall mitigation design is site-specific. Research to understand and analyse rockfall behaviour has been approached in two ways:

- Empirical methods; and
- Computer modelling.

Below is a brief outline of research carried out using these methods.

2.3.1 Empirical Methods

Empirical methods involve the study of rockfalls by means of *in situ* tests and physical modelling. *In situ* tests are conducted to understand the actual behaviour of rockfalls and boulder trajectories at a particular site. Physical modelling is an alternative method used to understand the rockfall behaviour compared to the *in situ* tests, because of the relative cost and risk involved with the *in situ* tests.

2.3.1.1 *In Situ* Tests

As stated above, the first ever published paper on rockfall was in 1963 by Arthur M. Ritchie (Ritchie, 1963). Ritchie performed *in situ* tests using slow-motion cameras to determine effective ditch sections and rock fences; and he performed these tests both on cliffs and talus slopes.

Ritchie (1963) found that though rockfall behaviour was random, effective use of fallout areas, ditches and fences would restrict rockfalls. The results from his study were used by Fookes and Sweeney (1976) to prepare a rocktrap design chart, which was further revised by Whiteside (1986). The following conclusions were drawn from Ritchie's studies:

- Fallout areas are useful to dissipate the enormous energy arriving at impact.
- Steep, off-shoulder slopes can be used to combat angular momentum of the rock generated after impact, thus providing a horizontal step on the steep slopes to slow down the boulder.
- Rock fences can be used as a flexible buttress and decelerating device to reduce the angular velocity.

Ritchie's (1963) work can be considered as a pilot study to understand rockfall behaviour. The use of fences and ditches to stop boulders were rather innovative at that time. Since then, his guidelines for catch ditch design have been extensively used for rockfall design. Although he suggested some ditch and fence dimensions, they are very conservative that is, they are designed for the worst case; these specifications give a large factor of safety, which is helpful for safety reasons but may not be desirable for a cost-effective design.

One of the few detailed studies on rockfall observations in the field has been reported by Mak and Blomfield (1986). The prime aim of the study was to obtain the rockfall statistics (number and velocities of boulders reaching the road) for design of rock traps. The work

involved releasing over 1,000 boulders on each of thirteen different pre-split slopes (i.e., a total of 13,000 boulders) ranging from 6 m to 12 m high and at angles of 55° to 70° . The ground at the toe of each slope was levelled and covered with a layer of compacted rockfill to provide consistent energy absorbing characteristics. Angular blocks of 100 to 300 mm were used but the experimental data did not indicate any significant difference in trajectories in relation to the specific block sizes. However, the angle and the height of the slope were found to have a major influence on boulder trajectory. Richards (1988) has summarised the data as follows: 1 and 1.5 m high barriers at 1.5 m from the slope toe will trap 95% and 100% respectively of all the boulders falling from slopes up to 12 m high in the range of 55° to 70° . Whiteside (1986) has also noted that Mak and Blomfield's (1986) results show good correlation with Ritchie's (1963) data.

Though Mak and Blomfield (1986) conducted extensive field tests involving rolling of around 13,000 boulders, the data cannot be generalised for rockfall design. Most of the tests were conducted using the same type of rock, which is strong to very strong, dark grey granite, and thus cannot be applied to other types of rock. The rock trap designs suggested are applicable only for relatively small pre-split slopes with detachable boulders up to 300 mm diameter. Also, Mak and Blomfield did not attempt to find the coefficient of restitution using the recorded data.

Chan, Chan and Au (1986) performed some field tests to study rockfall trajectories for fence design purposes. They rolled around 70 boulders, from 30 kg to over a tonne, down two 30° slopes; one slope having rock outcrops and thin vegetation, the other being more disintegrated with boulder deposits. The boulders were mainly rolling, with little or no bouncing or free flight. They found that there is no great difference in the measured boulder velocities on these two different slopes, both giving average velocities in the range of 5 to 8 m/sec. Chan, Chan and Au (1986) compared field data with the predicted boulder velocity using a mathematical model with octagonal prisms. They found that the actual velocities were less than predicted, which they attribute to the effects of uneven slope surfaces, vegetation cover and existing boulder deposits.

Chan, Chan and Au (1986) gave no information on how the computer simulation was done, and whether or not they used the coefficient of restitution, roughness, and friction angle for the simulation. The research work carried out by these authors was mainly to see whether

or not the rock traps designed by them would sustain actual rockfalls. Hence, their work can be considered applicable specifically for the site, with a good evaluation of rock fences.

The latest and most comprehensively studied *in situ* tests were reported in 1995, by Azzoni and de Freitas (1995) who conducted these tests to calibrate the computer program *CADMA* for rockfall analysis. Another aim of the tests was to study coefficient of restitution, rolling friction coefficient, dispersion of trajectories, effect of block geometry on its fall, and efficiency of ditch. The tests were conducted on two slopes at a quarry site in Italy: one with limestone and fine angular debris; the other with medium and fine angular debris. For both the slopes, the debris at the bottom of the slope was dry and loose. The blocks used were of different shapes and volumes ranging from 0.1 m³ to 2 m³. The falls were recorded using several video cameras and the recordings were digitised to calculate the velocities and heights of bounces for each boulder. The following conclusions were drawn by the authors:

- Coefficient of restitution: An assessment of the relationship between coefficient of restitution and the type of material on which the block impacted is possible by careful recording and analysis of *in situ* test data. The coefficient value ranges between 0.51 - 0.92 and 0.32 - 0.65 for the rock and debris respectively.
 - Rolling friction coefficient: The values of the coefficient determined lie between the theoretical upper and lower boundaries given by Statham (1979). These upper and lower boundaries were based on the angle of dynamic friction and the ratio of the size of particles on the slope to that of the falling boulder. Further explanation can be found in Azzoni *et al.* (1995).
 - Effects of block shape and dimensions on the rolling velocity: The authors noted that usually spheroidal blocks move faster than discoidal or tabular ones and the velocity achieved by bigger blocks is higher than that of smaller ones on the same slopes.
 - Lateral dispersion of the trajectories: The authors observed that the longer the slope the greater is the distance between extreme fall paths (extreme fall paths are the left-most and right-most trajectories). The dispersions measured were in the range of 10% to 20%, regardless of the length of the slopes, and generally the steepest slopes have the smallest dispersions.
 - Effect of ditch on fall trajectories: The authors concluded that the Whiteside's rock trap chart (made using Ritchie's (1963) data) is accurate but generally conservative.
-

The research work done by Azzoni and de Freitas (1995) is very helpful and informative for any proposed *in situ* tests in the future. Digitising recorded data with the available modern techniques will be very helpful in finding out the necessary coefficients for the input to the computer simulation programs. However, the conclusions drawn by Azzoni and de Freitas (1995) about the calculated coefficients for rock cannot be applied for every rock as the values depend on the type and strength of rock. Most of the conclusions were drawn from *in situ* tests at a quarry, which cannot be directly applied to some natural slopes. This is because the rockfall parameters that control the rockfall behaviour will be different for a quarry site compared to a natural slope. For example, since the quarry is an artificial cut slope, the slope roughness may not vary through the surface as compared to that of a natural slope with some vegetation.

2.3.1.2 Physical Modelling

Most comprehensive scale modelling of rockfall problems to date is the work carried by ISMES in Italy in 1976 by Fumagalli and Camponuovo. A detailed three dimensional model of the mountain St.Martino in Italy was constructed to a scale of 1:160, with a model height of about 4.5 m. The paper by Camponuovo (1976) describes the problems involved in achieving a mechanical similitude between the model and the prototype. The model was constructed as a true replica of the mountain. The main purpose of the study was to understand rockfall behaviour at all the important sections of the mountain. The authors attempted to simulate the crushing of boulders when coming down the slope, by cementing (with low mechanical resistance) small pebbles together to represent the lithoclase system of the rock. Several model rocks of these types were rolled along the model slope at different sections to study rockfall behaviour. The model results were calibrated against the *in situ* test results reported by Broili (1977). The following conclusions were drawn by the authors:

- The dynamic similitude was possible in the model after some corrections to deformability, compactness and roughness of the slope.
 - The model experiments made it possible to ascertain the ability of larger rock masses to heap up on the scree slope without causing failure of equilibrium of the stability of scree slope.
 - Model experiments were helpful in deciding the right design and dimensions of protective works.
-

- The scree slope is the most efficient protective device at nature's disposal to stop rolling blocks that are about the same size as debris accumulated earlier on the scree slope.
- The available modelling techniques represent an effective tool in the analysis of rockfall problems.
- When the scale ratios of the model are around 1:20 to 1:30, good mechanical similitude and satisfactory reliability of model results can be achieved.

The research carried out at ISMES using physical modelling techniques is a landmark in rockfall research history, and remains the only detailed physical modelling of rockfalls. As Fumagalli and Camponuovo (1976) concluded that modelling is helpful only when the scale is too low, it will be too expensive to model large slopes. The dynamic similitude between the original phenomenon and the model is very hard to achieve using modelling techniques.

The cost of carrying out these physical model tests (compared to computer models) and the difficulty in achieving dynamic similitude are the main reasons why no further attempt has been made to construct physical models of rockfalls. The biggest advantage of physical modelling would be a better representational study of rockfalls compared to that of analytical and computer modelling. The disadvantage would be the consumption of time and money involved in modelling in three dimensions, as a low scale has to be used for more accuracy. Hence, physical modelling can be useful for small slopes which are essentially three-dimensional, as computer simulation cannot be used effectively in these cases.

In comparison with physical modelling, the cost of *in situ* tests are more since the setup and other expenses (like artificial triggering of rocks, obtaining a resource consent, and stopping the traffic during the tests) make them more expensive. However, with respect to performance, the *in situ* tests will be preferable in comparison with physical modelling as the data obtained will be truly representative of the actual behaviour of rockfalls.

2.3.2 Computer Modelling of Rockfalls

Until the last decade, rockfall design was mostly carried out on an empirical basis using *in situ* tests and physical modelling techniques, which involve high cost and risk. With a better understanding of rockfall behaviour through physical modelling and *in situ* tests,

computer simulation of rockfalls has become a cheap and efficient alternative. In general, it is no longer necessary to perform expensive *in situ* tests to predict rockfall behaviour and for effective mitigation design. Since the computer is efficient for simulation of both random and repeatable behaviour of rockfalls, it has emerged as a preferable method of rockfall analysis for design of efficient protective structures.

The computer simulation of rockfalls can be used to get the rockfall statistics required for design of protective structures, like the range of energy of the boulders, boulder heights above ground, velocities and the possible trajectories. The key inputs for simulation of rockfalls are the coefficients of restitution. These coefficients are usually determined from the suggested values by some authors (e.g. Richards, 1988; Pfeiffer and Bowen, 1989; Azzoni *et al.*, 1995; Elliott, 1992; and Hungr and Evans, 1984), and adjusting them for the *in situ* conditions. Other methods include performing some *in situ* tests and recording the rockfall trajectories, from which the coefficients can be obtained (Azzoni *et al.* 1995). Sometimes, a back analysis is performed to get the coefficients using these simulation programs. The back analysis method is discussed in Chapter 5.

2.3.2.1 Simulation Methods

According to Hungr and Evans (1988), computer simulation of rockfalls has been approached in two ways :

- Rigorous method; and
- Lumped mass method.

a) The Rigorous Method:

The rigorous method was pioneered by Cundall (1971) and has been extended into three dimensions by Descoedres and Zimmermann (1987). Actual shape and dimensions of the boulder are assumed and all motions of the boulder are considered. While in the air, the fragment moves in a ballistic trajectory, rotating. Upon contact with slope surface, both translational and rotational momenta are transferred by an impact. The impulse of the impact changes both quantities according to a very complex set of conditions, depending upon the shape of the contact corner, the precise rotation angle at the point of contact, slope surface roughness, and normal and frictional deformations. At the present time it is difficult, if not possible, to calculate all these conditions and so, various simplifying

assumptions must be made. Consequently, because of these difficulties in simulation, very few programs are written using this method.

b) Lumped Mass Method:

In the lumped mass approach, the boulder is considered as a single point with mass m and velocity v . The point moves on a ballistic trajectory while in the air. Upon contact with the slope the normal component of velocity is reversed and reduced by a coefficient R_n and the tangential velocity component is reduced by a coefficient R_t . No attempt is made to keep track of the rotational momentum. The two restitution coefficients are taken as bulk measures of all the impact characteristics, incorporating deformational work, contact sliding and transfer of rotational to translational momentum and vice-versa. As a result, coefficients must depend upon fragment shape, slope surface roughness, momentum and deformational properties, and to a large extent on the chance of certain conditions prevailing in a given impact. The first model of this type was developed by Piteau and Clayton (1977), followed by Azimi *et al.* (1982), Shie-Shin Wu (1986), Hoek (1987), Spang and Rautenstrauch (1988), Hungr and Evans (1988), Pfeiffer and Bowen (1989), Elliott (1992), Chen, Chen and Huang (1994), and Azzoni *et al.* (1995).

Most popular (and available) programs used by geotechnical engineers for rockfall design in recent times are the ones developed by Hoek (1981), Hungr and Evans (1988), Pfeiffer and Bowen (1989), Elliott (1992), and Azzoni *et al.* (1995). Each of these programs were calibrated with some field tests carried out either by respective authors, or by other contributors.

2.4 Protection Measures

Considerable progress towards the mitigation design for rockfall problems has been made by various authors. Martin (1988) provides a convenient summary of the relevant stabilisation, protection and warning methods that are applicable to slopes with rockfall problems. These are shown in Table 2-1.

Stabilisation methods are used either to permanently reduce the rockfall hazard or to improve the stability of slope. Protection methods are relatively inexpensive compared to stabilisation methods, but they require an ongoing commitment to maintenance. The use of

warning methods is generally restricted to railways or other controlled access systems (Martin 1988). The treatment of slopes with rockfall problems are discussed in detail in the following references; Chan, Chan and Au (1986), Dubin *et al* (1986), Fookes and Sweeney (1976), Hoek (1981), Kirsten *et al* (1986), Mearns (1976), Peckover and Kerr (1976, 1977), Peckover (1975), Piteau and Peckover (1978), Rochet (1979, 1980), and Spang (1987). Discussion of stabilisation and protection methods in detail is beyond the scope of the thesis.

Table 2-1: Classification of remedial measures for rock slopes (Martin 1988).

Stabilisation Methods	Protection Methods	Warning Methods	Monitoring systems
Excavation Scaling and trimming	Relocation Tunnels and rock sheds	Patrols and signs Electric fences and wires	Precise surveys Extensometers, inclinometers tilt meters, load cells.
Ground water control and drainage	Interception ditches and shaped ditches	Warning lights and sirens	Systems in combination with protection
Rock reinforcement and rock support	Interception berms and shaped berms		
• Shotcrete and mortar	Catch walls		
• Dental treatment	Draped and pinned mesh		
• Rockbolts, dowels, rock anchors	Catch fences and catch nets		
• Buttresses and bulk heads			
• Retaining walls and tie back walls			
• Anchored beams and strapping			
• Beam and cable walls			
• Cable nets, lashing and chains			

Rockfall mitigation measures involve two types of methods:

- Active methods; and
- Passive methods.

The following is a brief review of these methods.

2.4.1 Active Methods

Active methods involve stabilisation measures designed to prevent boulders becoming detached, rather than stopping the boulders reaching road. This method is particularly applicable when the slope is not deteriorating fast. The size of slope to be treated by these measures influences the cost-effectiveness of this method. This method was discussed in detail by Peckover (1975), Fookes and Sweeney (1976), Peckover and Kerr (1977), and Piteau and Peckover (1978). The active method involves one or more of the measures described under column “Stabilisation Methods” in Table 2-1. This method proves effective for nearly vertical slopes where provision of a catch ditch is almost impossible.

2.4.2 Passive Methods

Passive methods include the measures stated in the column named “Protection Methods” in Table 2-1. Passive methods are relatively inexpensive compared to active methods, because of the ease of installation of these protective structures. The placement and dimensions of these protective structures are critical for efficient control of rockfalls. This method was discussed in detail by Ritchie (1963), Chan, Chan and Au (1986), Peckover (1975), Peckover and Kerr (1977), and Piteau and Peckover (1978).

2.5 Rockfall Hazard Analysis Systems

Several authors have reported risk rating systems for rockfalls and slope stability. Hunt (1992) reported risk mapping of slope failure. He proposed two ways of dealing with slope problems: either provide complete stability of all cuts and fills; or accept some risk of failure stabilising only those slopes with potential failure. His approach was qualitative with a scale of 1 to 5 for very high to low risk respectively. Romana (1985, 1988, 1991) used Bieniawski’s (1976) rock mass rating (RMR) classification of rocks to develop a Slope Mass Rating (SMR). Cancelli and Crosta (1993) suggested a risk mapping technique for rockfalls using relative risk rating for different conditions with respect to characteristics of rockfalls. The Rockfall Hazard Rating System (RHRS) was developed by Pierson *et al* (1990) at Oregon State Highway Division for ranking of rockfall hazards at a site. This system of hazard analysis seems to be widely acceptable among the geotechnical community, and has hence been used for this project. The hazard rating system is discussed in detail in Chapter 6.

2.6 Conclusions

The rockfall analysis and design can be carried out using computer simulation of programs as a tool. This conclusion can be drawn from the numerous published papers demonstrating the successful use of these programs.

Even though considerable progress has been made towards understanding and predicting rockfall behaviour, there are some gaps in the understanding and determination of some rockfall parameters used in computer simulation.

One such gap is obtaining the coefficient of restitution values for various types of rock, debris, and other material like asphalt and mud. Some authors have attempted to determine the coefficients for different material. However, the suggested values of the coefficients of restitution by these authors cannot be used directly for computer simulation of rockfalls. This is because some of the tests were performed on artificial cuts, the description of the tests were not detailed, and some of the tests were not representative, as the boulders were rolling most of the times without bouncing. Also, no attempt has been made to find out an easy means of determining the restitution coefficient, other than doing some field tests. As the coefficients of restitution are the key inputs for all the simulation programs, it is essential to explore any empirical relation between the index values for rock (e.g. compressive strength) and these coefficients, to find out easy means of obtaining the value. Apart from the relation between rock mass properties and the coefficient of restitution, the influence of jointing pattern, foliation, clay infillings, and weathering, and / or the rock mass classification on this coefficient can also be explored.

Due to the wide range of computer programs available for rockfall analysis it is difficult to choose which program to use as the simulation logistics used are different for various programs. Almost every program available in the market has been calibrated with some *in situ* tests, but no attempt is made (until now) for a comprehensive comparison of these programs with each other to find out relative advantages and disadvantages.

Fragmentation of rocks while coming down the slope has been extensively neglected in the literature. It is one of the interesting and important phenomenon involved with rockfalls, as these small fragments tend to travel faster than the original rock, and pose immediate

hazard to the rockfall victims. Rockfall simulation programs in the future should include the consideration of fragmentation of rocks, while coming down the slope to simulate rockfalls more accurately.

2.7 Summary

A literature review was carried out regarding the research work done by various authors using *in situ* tests, physical modelling, and computer simulation of rockfalls. The review further confirms the need for exploring an easy means of obtaining the restitution coefficient and to compare the rockfall simulation programs, which are two of the three main objectives stated in Chapter 1.

Chapter 3 goes on to the comparison of five different rockfall simulation programs to see which is the best program to use for a detailed rockfall analysis.

Chapter 3

COMPARISON OF SIMULATION PROGRAMS

3.1 Introduction

In chapter 2, it was concluded that there is a need to compare various rockfall computer simulation programs as it is difficult to decide upon which is the best one to use. Hence, in this chapter, a comprehensive comparison of five simulation programs is carried out to see the relative advantages and disadvantages of each. This will help to decide upon which program is the best to use for a detailed analysis of rockfalls at Fox Glacier.

3.1.1 Assumptions

Before the computer modelling of rockfalls is discussed, it is useful to know the basic assumptions considered in developing these models. The basic general assumptions considered for all the computer programs discussed here are:

- The effect of air friction on the movement of the boulder is negligible;
- For two dimensional models, lateral movement of the boulder is negligible;
- There are no break-ups of rocks while coming down the slope.

In addition to these general assumptions, other specific assumptions are used for individual programs.

3.1.2 Computer Simulation of Rockfalls

Ritchie (1963) suggested an analytical model which was a simple algorithm to calculate the velocity and path of a rockfall, starting with a free fall and bouncing into trajectory after impact with the slope surface. Ritchie did not use restitution coefficients in his model. After Ritchie, the first simulation program was announced by Piteau and Clayton (1977)

introducing the use of restitution coefficients. After Piteau and Clayton's first model, several programs were developed by various authors (Azimi *et al.* 1982, Shie-Shin Wu 1986, Hoek 1987, Spang and Rautenstrauch 1988, Hungr and Evans 1988, Pfeiffer and Bowen 1989, Elliott 1992, Chen, Chen and Huang 1994, and Azzoni *et al.* 1995) in an attempt to develop a computer program as an efficient tool for the analysis of rockfalls. It is some of these more recent programs which are compared here.

3.1.2.1 The General Algorithm

Although the simulation logistics used by authors differ from each other, the basic algorithm is the same. Figure 3-1 shows the flow chart showing the general algorithm used for computer simulation of rockfalls.

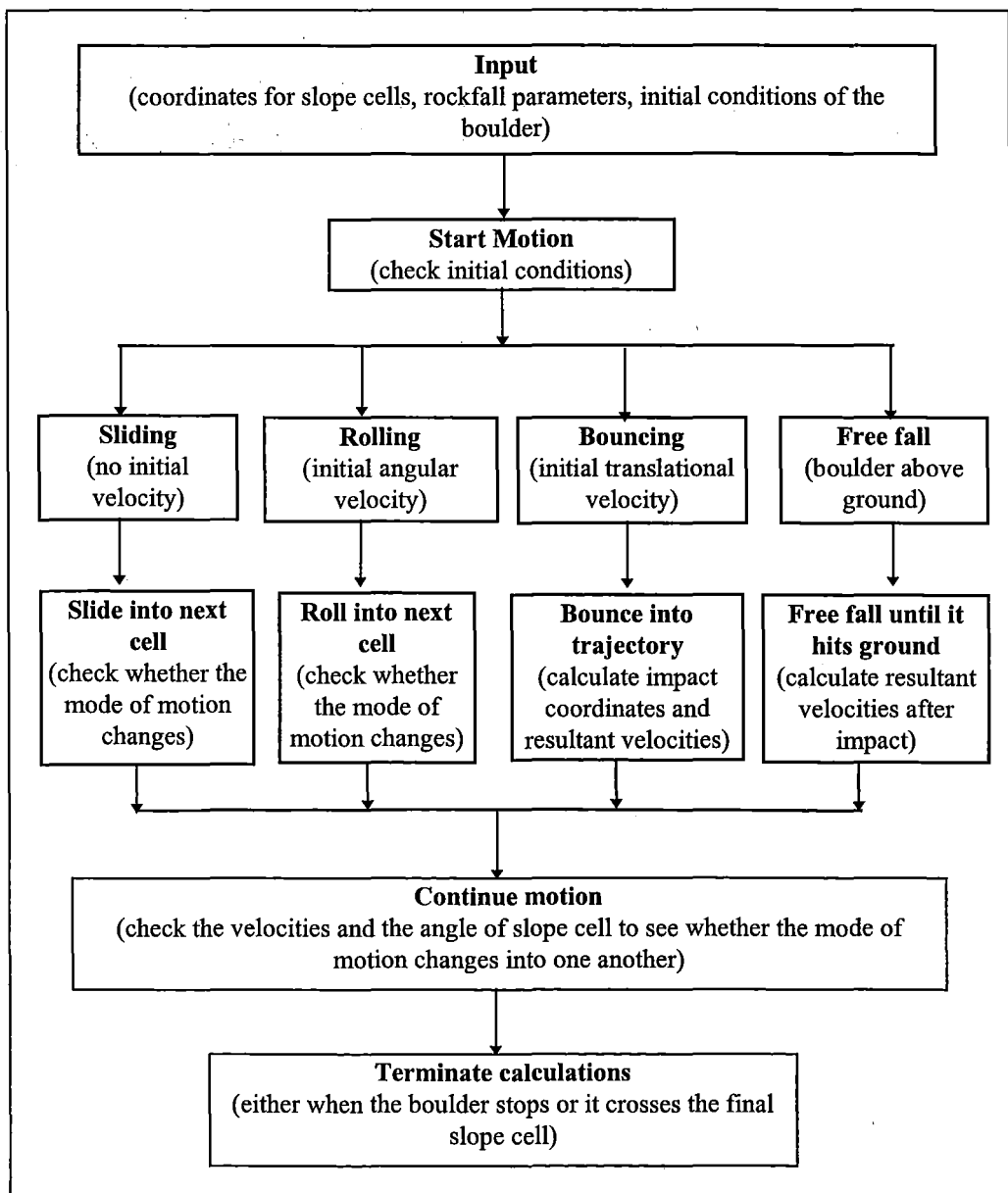


Figure 3-1: Flow chart showing the general algorithm for computer simulation of rockfalls.

3.2 Comparison of Simulation Programs

The programs used for comparison in this study are:

- *Rockfall* (Developed by Hoek, 1987).
- *CRSP* version 2 (Colorado Rockfall Simulation Program, developed by Pfeiffer, 1989).
- *Rockfal2* version 2 (Developed by Elliott, 1992).
- *RF* version 1.3 (Developed by Hungr, 1992).
- *CADMA* version 1.1 (Developed by Azzoni, 1995).

Among these programs, *CRSP*, *Rockfal2*, *RF* and *CADMA* have been calibrated with some *in situ* tests, and the authors found that the results were satisfactory. However, the authors of the above programs did not give the exact percentage accuracy of simulation of actual rockfalls. The reader may refer to the respective papers for the details of validation of the programs.

3.2.1 Assumptions for Comparison

For comparison of the simulation programs, some assumptions have to be made. The reader should note in particular, that the author is not trying to *validate* the programs, but is only comparing them with each other¹. These are the assumptions implicit:

- Each of the programs has been validated to simulate actual rockfalls.
- The calibration results reported by respective authors are true.
- The programs used for comparison simulate actual rockfalls, within their limitations.

3.2.2 Criteria for Comparison

The rockfall simulation programs are compared based on the following criteria:

1. Input parameters;
2. Simulation logistics;
3. Probabilistic analysis; and
4. Overall performance of the program in terms of user-friendliness, and relevance of the output for a detailed analysis of rockfalls.

The comparison details are discussed under each sub-heading.

¹ The reader may refer to the papers published by respective authors for calibration and validation of the respective programs.

3.2.3 Input Parameters

Usual input parameters for rockfall simulation include:

- Boulder information;
- Initial conditions of the boulder ie, initial velocities if any;
- Properties of the slope; and
- Coordinates for slope cells.

3.2.3.1 Boulder Information

Information about the boulder includes the size of the boulder and density of the rock material. Size is specified as the diameter for spherical boulders. For ellipsoidal boulders, axial ratios are specified. Table 3-1 shows the summary of boulder specifications for respective computer programs. As one can see in Table 3-1, the program *CADMA* is the only program which facilitates the dimensional variation of the boulder and which uses a three dimensional boulder.

Table 3-1: Summary of boulder details to be specified for each program

	<i>Rockfall</i>	<i>CRSP</i>	<i>Rockfal2</i>	<i>RF</i>	<i>CADMA</i>
Shape	Spherical	Spherical	Spherical	Spherical	Ellipsoid
Size (specified as)	Diameter	Diameter	Diameter	Cannot be specified	Axial ratios and volume
Mass	Density	Density	Density	Weight	Density
Solid	✘	✘	✘	✘	✓
Dimension variability	✘	✘	✘	✘	✓

✘ = No, ✓ = Yes.

3.2.3.2 Initial Conditions of The Boulder

Initial conditions of the boulder include specification of any initial horizontal, vertical or angular velocities, and the position of the boulder. Some programs may also require specification of orientation of the velocity vector (angle) with respect to the global cartesian system. Table 3-2 summarises the initial conditions to be specified for each program. Table 3-2 shows that only the programs *RF* and *CADMA* have a facility of varying the initial starting position of the boulder. This facility is very important in the simulation of rockfalls for a detailed probabilistic analysis to get the rockfall statistics of the rocks that originated from different places.

Table 3-2: Summary of initial conditions of boulder to be specified for each program

	<i>Rockfall</i>	<i>CRSP</i>	<i>Rockfal2</i>	<i>RF</i>	<i>CADMA</i>
Horizontal velocity	✓	✓	✓ ¹	✗	✓
Vertical velocity	✓	✓	✓ ²	✗	✓
Angular Velocity	✗	✗	✓	✗	✗
Position ³	(x,y) of first slope cell	Anywhere	Anywhere	Anywhere	Anywhere
Orientation of the velocity vector	✗	✗	✓	✗	✓
Variation of starting X	✗	✗	✗	✓	✓

✗ = No, ✓ = Yes.

3.2.3.3 Properties of Slope

Properties of the slope like restitution and rolling friction coefficients are used to simulate various types of motions of the boulder. To incorporate some randomness in the simulations, the Monte Carlo method is used to calculate a random coefficient from the specified mean and standard deviation values of the coefficients. Slope roughness is specified to simulate the undulations for some slopes, which is also varied each time using the Monte Carlo method. It should be noted that different programs define and vary slope roughness differently. Table 3-3 summarises the details of specifying slope properties for the respective programs. The definitions of the parameters can be found in section 2.2.1.

Table 3-3 shows that the programs *CRSP* and *Rockfal2* use the coefficient of tangential friction instead of the coefficient of tangential restitution. As discussed in section 2.2.1, these two coefficients are the inverse of each other. Hence, the user of these programs has to know this very important difference. Also, it is to be noted that almost all of the programs use and define the slope roughness quite differently to each other (see last row of Table 3-3). Another important point to note from Table 3-3 is that the program *CRSP* randomises only the slope roughness, whereas all other programs (except *Rockfall*) randomises the coefficients as well.

3.2.3.4 Coordinates of Slope Cells

Coordinates of slope cells are input in the form of x and y coordinates which need not start from (0,0). For some programs there is a restriction on the maximum number of slope cells that can be specified. This disables the user from using a slope with detailed profile

² For the program *Rockfal2* translational velocity is specified along with the angle of the velocity vector.

³ For all programs, the boulder should not be placed before the X - coordinate of the first slope cell.

coordinates, or very large slopes. For example, the programs *Rockfall* and *RF* use only 20 and 50 slope cells respectively, whereas for all others number of slope cells are usually 100.

Table 3-3: Summary of specifying slope properties in each program

	<i>Rockfall</i>	<i>CRSP</i>	<i>Rockfal2</i>	<i>RF</i>	<i>CADMA</i>
Properties can be input for each cell	✓	✓	✓	✓	✓
Normal coefficient of restitution	✓	✓	✓	✓	✓
Tangential coefficient of restitution	✓	✗	✗	✓	✓
Coefficient of tangential friction	✗	✓	✓	✗	✗
Rolling friction coefficient	✗	✗	✓	✓	✓
Monte Carlo simulation	✗	✓ ⁴	✓	✓	✓
Friction coefficient	✓	✗	✗	✗	✗
Slope roughness	✗	✓	✓	✗	✓
Slope roughness defined as	Not used by the program	Maximum perpendicular variation from an average plunge line over a distance equal to the radius of the rock. Angle is varied from 0 to maximum	Angle of variation of the slope cell angle. The angle is varied around 0 to \pm specified angle of variation	Not used by the program	Angle of variation of the slope cell angle. The angle is varied depending on the ratio (variation of slope angle) / (slope angle)

✗ = No, ✓ = Yes.

3.2.4 Simulation Logistics

Simulation logistics are the most important criteria for comparison of rockfall simulation programs. Although the basic algorithm is same for most of the programs, there is a substantial difference between the logistics used for simulation. This difference between the simulation logistics used by various programs is because the theory of impact mechanics is still under evolution. It is not known exactly what happens (in terms of the magnitude of energy dissipation and slippage of rock during impact) when a boulder

⁴ *CRSP* uses Monte Carlo simulation *only* for the variation of slope roughness angle.

impacts bed rock or any other material (e.g. road, debris). This section discusses in detail the difference between logistics used by each program. Please note that the details provided for simulation logistics are summarised from the papers published by respective authors. The derivations of the logistics used are included to clearly differentiate the approach used by various authors.

The simulation logistics will be compared based on the following criteria :

- Initial movement of the boulder;
- Free falling;
- Impact and bouncing;
- Transformation from bouncing to rolling;
- Rolling and sliding; and
- Stopping.

3.2.4.1 Initial Movement of The Boulder

The initial movement of the boulder depends upon the specified initial conditions of the boulder. If the boulder is given zero velocity, the initial start of the boulder is influenced by gravitational force, orientation and position of the boulder, and for the program *Rockfall*, by friction angle. If the boulder is given an initial velocity, the impact coordinates of the boulder are calculated using physical laws of motion and the equations of projectile motion. Table 3-4 summarises the starting conditions used by each program. From Table 3-4, one can see that the program *RF* does not use any starting velocities and it is only the program *Rockfal2* which allows specification of initial rotational velocity.

3.2.4.2 Free Falling

Free falling is simulated by each of the programs. The programs simulate a free fall of motion when the boulder is falling down a vertical or overhanging cliff, or when the boulder is positioned above the ground. The only force considered in free fall is gravitational force. The final velocity of the boulder is calculated using the physical laws of motion, using initial velocity of the boulder before it actually starts the free fall. If the initial velocity of the boulder is zero, the boulder descends vertically downwards. If the initial velocity is specified, the boulder follows a trajectory. Each of the programs considered for comparison simulates free fall in the same way.

Table 3-4: Summary of boulder starting conditions for each program.

	<i>Rockfall</i>	<i>CRSP</i>	<i>Rockfal2</i>	<i>RF</i>	<i>CADMA</i>
For zero velocity ⁵	Check the friction angle	Check the position of the boulder	Check the position of the boulder	Not used by the program	Check the position of the boulder
For specified translational velocities ⁶	Boulder starts by throw and impact coordinates are calculated	Boulder starts by throw and impact coordinates are calculated	Boulder starts by throw and impact coordinates are calculated	Not used by the program	Boulder starts by throw and impact coordinates are calculated
For specified rotational velocity	Not used by the program	Not used by the program	Boulder starts rolling ⁷	Not used by the program	Not used by the program
Friction angle	If friction angle > slope angle, boulder slides ⁸	Not used to start boulder	Not used to start boulder	Not used by the program	Not used to start boulder

3.2.4.3 Impact and Bouncing

Impact and bouncing conditions are simulated by using the coefficients of restitution (section 2.2.1). The coefficients of restitution are used in their respective directions to reduce the resultant velocities after an impact occurs. An impact occurs when the boulder is already in flight; either by free fall or by preceding impact and bounce. The following steps are generally followed by the programs to simulate impact and bouncing:

- The velocities in x and y direction before the boulder impacts ground are used to calculate the exact impact coordinates;
- The impact conditions are then simulated by decreasing the velocities in x and y directions using the normal and tangential coefficients of restitution for that particular slope cell;
- The velocities in x and y directions calculated from the above step are checked for bounce, roll or stop;
- If the boulder starts to bounce, the next impact coordinates are calculated and the impact conditions are simulated again. Alternatively, if the boulder rolls, the conditions for rolling are used to proceed the calculations;

⁵ If the position of the boulder is above ground, boulder starts by free fall, otherwise, boulder starts to roll (not applicable to program *Rockfall*, as initial position is first slope cell).

⁶ Impact coordinates are calculated using laws of motion and equations of projectile motion.

⁷ If the initial translational velocity is zero, boulder starts rolling; otherwise, boulder starts in a throw with rotational velocity.

⁸ Boulder slides if the translational velocity is zero.

Below are the details of simulation methods used by each program for impact and bouncing.

3.2.4.3.1 Calculation of Impact Coordinates

The method of calculation of impact coordinates is similar for all the simulation programs. The boulder impacts the ground surface when the trajectory intersects the slope surface. The method followed by Hoek in his program *Rockfall* is outlined here. Few changes are made by other authors, with the baseline remaining the same.

Each cell is assumed to be a part of a plane represented by the equation:

$$y = qx + p \quad \dots\text{Equation 3-1}$$

where p is the intercept of the line with the Y axis, and q is the slope of the line representing the plane. If the initial velocity components at the start (x_0, y_0) of any parabolic trajectory are defined by V_x and V_y , then the X coordinate of the point of impact with a plane defined by Equation 3-1 is:

$$x_i = x_0 + B \pm (B^2 - 2.V_x^2.C/g)^{1/2} \quad \dots\text{Equation 3-2}$$

where:

$$B = V_x^2 (V_y/V_x - q) / g, \quad C = p + qx_0 - y_0 \quad \text{and } g = \text{acceleration due to gravity.}$$

The positive sign in Equation 3-2 is used when $V_x > 0$. The impact point coordinate y_i is calculated from Equation 3-1. After getting the impact point coordinate, points along the parabolic trajectory are calculated at some intervals to find the exact point of intersection of the trajectory with the slope surface.

3.2.4.3.2 Calculation of Reflected Velocities

Calculation of reflected velocities after the impact of boulder with the ground is performed using the normal and tangential coefficients of restitution. The method followed by each of the programs is outlined here in detail.

Rockfall (Hoek)

After the rock impacts the ground, the impact velocity components V_{ix} and V_{iy} are altered to reflected velocity components V_{rx} and V_{ry} by the normal and tangential coefficients of restitution R_n and R_t . The reflected velocities are calculated from:

$$V_{rx} = D_n \sin \theta + D_t \cos \theta \quad \dots \text{Equation 3-3}$$

$$V_{ry} = D_n \cos \theta + D_t \sin \theta \quad \dots \text{Equation 3-4}$$

where

$$D_t = R_t(V_{ix} \sin \theta + V_{iy} \cos \theta)$$

$$D_n = R_n(V_{iy} \cos \theta - V_{ix} \sin \theta)$$

and θ is the slope angle of the cell on which the rock impacts.

CRSP (Pfeiffer and Bowen)

After establishing the impact angle, incoming velocity (V_i) is resolved into velocity components tangential (V_{it}) and normal (V_{in}) to the impacted surface. A new tangential velocity V_{rt} is calculated using the equations shown below using the law of conservation of energy:

$$(1/2 I \omega_i^2 + 1/2 m V_{it}^2) f(F) SF = 1/2 I \omega_r^2 + 1/2 m V_{rt}^2$$

Where:

m = rock mass

r = radius of the boulder

I = rock moment of inertia = $2mr^2/5$

ω_i = initial rotational velocity

ω_r = final rotational velocity

V_{it} = initial tangential velocity

V_{rt} = final tangential velocity

$$f(F) = \text{friction function} = f(F) = \frac{R_t - (1 - R_t)}{((V_{it} - \omega_i r) / 10^2) + 1.5}$$

$$SF = \text{scaling factor} = R_t / ((V_{in} / 50)^2 + 1)$$

Letting $V_{rt} = \omega_r r$:

$$V_{rt} = \sqrt{\frac{r^2 (I \omega_i^2 + m V_{it}^2) f(F) SF}{I + m r^2}} \quad \dots \text{Equation 3-5}$$

The new normal velocity V_{rn} is calculated using the coefficient of restitution and a velocity dependent scaling factor to modify the initial normal velocity V_{in} :

$${}^9V_m = \frac{V_{in}R_n}{1 + (V_{in}/30)^2} \quad \dots\text{Equation 3-6}$$

Rockfal2 (Elliott)

The trajectory of a boulder in flight is assumed to be parabolic. The position of the boulder at any time, (t), after the boulder takes to flight is defined in x,y coordinates using:

$$x_t = V_o \cos(\alpha_o)t + x_o \quad \dots\text{Equation 3-7}$$

$$y_t = V_o \sin(\alpha_o)t - 1/2 gt^2 + y_o \quad \dots\text{Equation 3-8}$$

Where V_o = initial velocity of the boulder

α_o = initial angle of the flight trajectory

The vertical (V_y) and horizontal (V_x) velocity components of the boulder, at time (t) are found by differentiating the position coordinates with respect to time, giving:

$$V_x = V_o \cos \alpha_o$$

$$V_y = V_o \sin \alpha_o - gt$$

From these velocity components, the actual velocity V_t and direction α_t of travel of the falling boulder at any time t are then calculated using:

$$V_t = \sqrt{V_x^2 + V_y^2} \quad \text{and} \quad \alpha_t = \tan^{-1} \left(\frac{V_x}{V_y} \right)$$

The x, y coordinates at the point of impact are calculated using equations 3-7 and 3-8 after first calculating the elapsed time till impact. The elapsed time till impact with a straight section of slope having end coordinates (x_1, y_1) and (x_2, y_2) , is the largest root of the following equation:

$$\frac{1}{2}gt^2 + At + B = 0$$

where

$$A = mV_o \cos \alpha_o - V_o \cos \alpha_o$$

$$B = m(x_o - x_1) - (y_o - y_1)$$

$$m = \frac{y_2 - y_1}{x_2 - x_1}$$

⁹ Detailed explanation of derivation of formulae can be found in Pfeiffer and Bowen's paper (1989).

The angle of impact relative to the ground surface, (β_i), the rotational velocity, (ω_i), and the impact velocity components, (V_{in}) and (V_{it}), normal and tangential to the ground surface respectively, at the time of impact are calculated using:

$$\beta_i = \alpha_t - \theta$$

$$\omega_i = \omega_o$$

$$V_{in} = V_t \sin(\beta_i)$$

$$V_{it} = V_t \cos(\beta_i)$$

where θ , the local inclination of the rock surface at the point of impact, equals the average slope angle plus the local slope roughness angle. The rebound velocity components, V_m and V_{rt} , normal and tangential to the ground surface respectively, and the rebound rotational velocity, ω_r , are calculated on the basis of energy balance considerations using empirical relationships for the energy lost during impact derived by Pfeiffer and Bowen (1989).

$$V_{rt} = \sqrt{\frac{r^2 (I\omega_i^2 + mV_{it}^2) F_1 F_2}{I + mr^2}} \quad \dots\text{Equation 3-9}$$

$$V_m = \frac{V_{in} R_n}{1 + \left(\frac{V_{in}}{30}\right)^2} \quad \dots\text{Equation 3-10}$$

$$\omega_r = \frac{V_{rt}}{r} \quad \dots\text{Equation 3-11}$$

where:

$$F_1 \quad \text{is a friction function defined by: } F_1 = R_t + \frac{400(1 - R_t)}{(V_{it} - \omega_i r)^2 + 480}$$

$$F_2 \quad \text{is a scaling function defined by: } F_2 = \frac{250^2 R_n^2 R_t}{V_{in}^2 + 250^2 R_n^2}$$

The actual rebound velocity, V_r , and the flight directions, β_r and α_r , relative to the ground surface and the x, y coordinate system, respectively, are then determined using:

$$\beta_r = \tan^{-1}\left(\frac{V_{rn}}{V_{rt}}\right), \alpha_r = \beta_r + \theta$$

$$V_r = \sqrt{V_{rn}^2 + V_{rt}^2}$$

RF (Hungr)

The details of simulation method for impact and bouncing were not given by the authors in their published work (Hungr and Evans 1988). However, the authors discussed the change of energy after the impact.

After the impact, the velocity component normal to the path is reduced by a ratio R_n and the tangential velocity component by R_t . It can be shown that the resulting incremental loss of energy (δE) is:

$$\delta E = \frac{V^2}{2g} \left[\left(\frac{R_t^2 + R_n^2 \tan^2 \theta}{1 + \tan^2 \theta} \right) - 1 \right] \quad \dots \text{Equation 3-12}$$

where V is the velocity and θ is the angle of incidence prior to the impact. Thus, the kinetic energy is reduced in each impact by a ratio ranging from R_t^2 for very flat trajectories, through $(R_t^2 + R_n^2)/2$ for 45° impacts, to R_n^2 for steep trajectories approaching the perpendicular. When the ratio $\delta E/\delta L$ (δL is the trajectory length) is less than the tangent of the slope angle, the fragment accelerates continuously and the energy line rises above the path. When the ratio becomes greater than the slope gradient, the fragment decelerates and the trajectories rapidly become shorter.

CADMA (Azzoni)

CADMA uses the principle of conservation of angular momentum to simulate impact conditions. It primarily assumes that the effect of internal forces are greater than external forces, and that the law of conservation of momentum is applicable by assuming that the contact point P is an infinitesimal area.

Applying the principle of the conservation of angular momentum over the infinitesimal time interval, before and after the impact (Figure 3-2), the following relation can be written:

$$I \cdot \omega_i + V_{ix} \cdot d_y - V_{iy} \cdot d_x = I \cdot \omega_r + V_{rx} \cdot d_y - V_{ry} \cdot d_x \quad \dots \text{Equation 3-13}$$

where:

$d_y = y_G - y_P$ and $d_x = x_G - x_P$ (G is the centre of mass, P is the contact point)

$V_{ix}, V_{rx} = x$ components of velocity before and after impact.

$V_{iy}, V_{ry} = y$ components of velocity before and after impact.

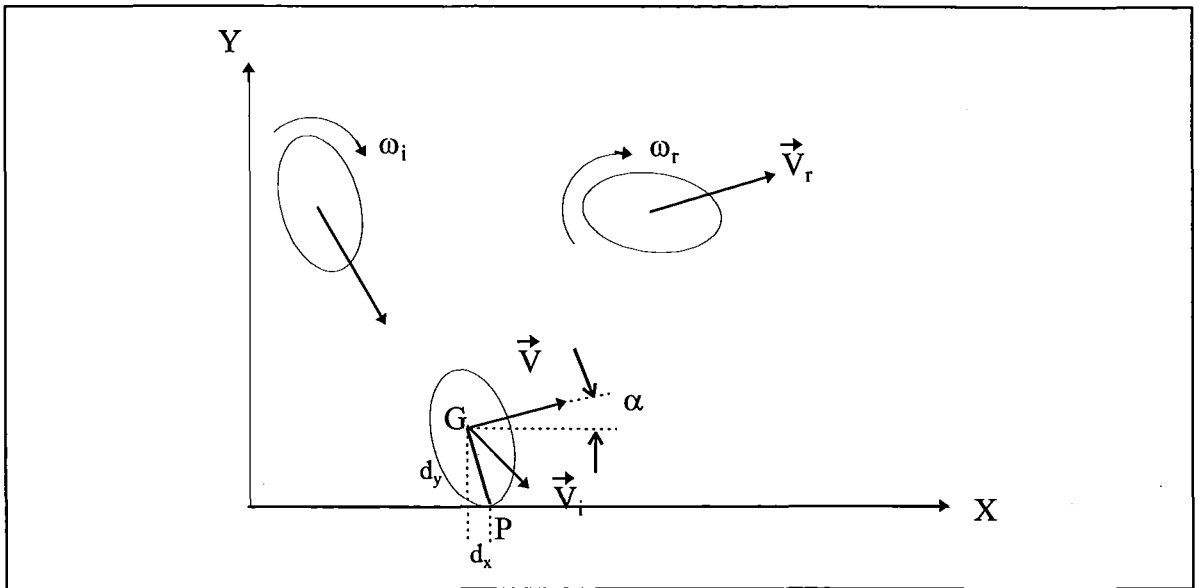


Figure 3-2: Configuration of the block before and after the impact (Azzoni *et al.* 1995).

Assuming that a rotational motion about the contact point P takes place after the impact, the velocity of the centre of mass can be obtained as follows:

$$V_r = \omega_r \times r = \omega_r \times PG$$

Since $\omega_r = 0 \cdot i + 0 \cdot j - \omega_z \cdot k$ and $PG = (x_G - x_P) \cdot i + (y_G - y_P) \cdot j + 0 \cdot k$

$$V_r = \omega_r \times PG = \begin{vmatrix} i & j & k \\ 0 & 0 & -\omega_z \\ (x_G - x_P) & (y_G - y_P) & 0 \end{vmatrix}$$

$$= \omega_z \cdot (y_G - y_P) \cdot i - \omega_z \cdot (x_G - x_P) \cdot j$$

Then: $V_{rx} = \omega_z \cdot dy$...Equation 3-14

$V_{ry} = -\omega_z \cdot dx$...Equation 3-15

assuming $\omega_r = \omega_z$: $V_r = \omega_r \cdot d_y \cdot i - \omega_r \cdot d_x \cdot j = V_{rx} \cdot i + V_{ry} \cdot j$...Equation 3-16

Since $y_G > y_P$ is always the case, then V_{rx} is always greater than zero. As for d_x , it could be less than, equal to, or greater than zero, depending on the centre of mass, G, with respect to the contact point P (Figure 3-3). Three different possibilities can occur :

1. $x_G > x_P \Rightarrow d_x > 0 \Rightarrow V_{ry} < 0$ (Figure 3-3 (a))
2. $x_G = x_P \Rightarrow d_x = 0 \Rightarrow V_{ry} = 0$ (Figure 3-3 (b))
3. $x_G < x_P \Rightarrow d_x < 0 \Rightarrow V_{ry} > 0$ (Figure 3-3 (c))

Obviously, if $V_{ry} \leq 0$ bounces cannot occur. In this case, the possibility of second impact has been introduced. In this way, the block assumes a symmetric position with respect to the previous position, and thus V_{ry} becomes positive.

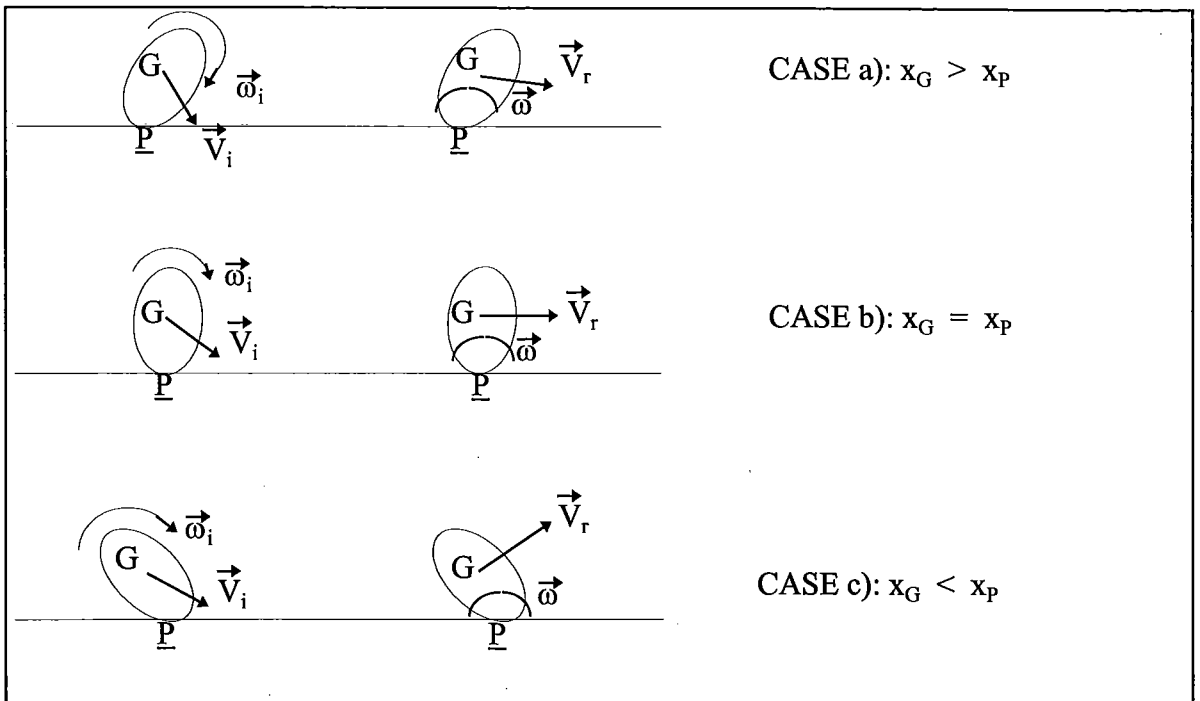


Figure 3-3: Different possibilities for the block at the impact (Azzoni *et al.* 1995).

Substituting Equations 3-14 and 3-15 into the right hand side of Equation 3-13, the following equation can be obtained:

$$\omega_r = \frac{I \cdot \omega_i + V_{ix} \cdot d_y - V_{iy} \cdot d_x}{I + d_x^2 + d_y^2} \quad \dots \text{Equation 3-17}$$

The components of the velocity after the impact can be determined by substituting the value of ω_r , calculated from Equation 3-17, into the Equations 3-14 and 3-15. The total kinetic energy for the unit mass after the impact K_r can be calculated by the following equation:

$$K_r = 1/2 \cdot (I \cdot \omega_r^2 + V_{rx}^2 + V_{ry}^2) = 1/2 \cdot \omega_r^2 \cdot (I + d_x^2 + d_y^2) = 1/2 \cdot \omega_r^2 \cdot (I + r^2)$$

Therefore, it is possible to evaluate a coefficient of restitution of energy ε with the following relation:

$$\varepsilon = \frac{K_r}{K_i} = \frac{Q_i^2}{2 \cdot K_i \cdot (I + r^2)} = \frac{\omega_r^2}{2 \cdot K_i} \cdot (I + r^2) = \frac{\omega_r \cdot Q_i}{2 \cdot K_i} \quad \dots \text{Equation 3-18}$$

within ($0 \leq \varepsilon < 1$) where:

$$Q_i = I \cdot \omega_i + V_{ix} \cdot d_y - V_{iy} \cdot d_x;$$

$$r^2 = d_x^2 + d_y^2; \text{ and}$$

K_i = total kinetic energy before impact.

As it is possible for the calculated ε to be greater than the one observed experimentally ε_{\max} , the latter is considered as the upper boundary of the range of the calculated ε ; in this case, angular momentum is not conserved, and thus gives:

$$K_r = \varepsilon_{\max} * K_i = 1/2 \omega_r^2 (I + r^2)$$

$$\Rightarrow \omega_r = \sqrt{\frac{2\varepsilon_{\max} K_i}{(I + r^2)}} \quad \dots \text{Equation 3-19}$$

As one must have observed from the above sub-sections for each program, the simulation logistics used by different authors for bounce mode of motion are totally different from each other. Hoek (1987) used the restitution coefficients in a very simple manner to reduce the final velocities (Equations 3-3 and 3-4) for the program *Rockfall*. Pfeiffer and Bowen (1989) used some empirical relationships and scaling factors in combination with the law of conservation of energy to calculate the final velocities (Equations 3-5 and 3-6) for the program *CRSP*. Elliott (1992) used the empirical relationships derived by Pfeiffer and Bowen (1989) and modified the friction function and scaling factor to calculate the final velocities (Equations 3-9 to 3-11) for the program *Rockfal2*. Hungr (1988) reduced the final velocities by simply multiplying the initial velocities by the coefficients of restitution in respective directions to calculate the energy loss in each bounce (Equation 3-12) for the program *RF*. Azzoni (1995) uses the calculated (ε) (Equation 3-18) and experimentally calculated restitution coefficient (ε_{\max}) (Equation 3-19) to calculate the final velocities after an impact for the program *CADMA*. However, it is unclear as to how the program uses the tangential and normal coefficients of restitution to reduce the final velocities, and what is the range of values of ε_{\max} .

3.2.4.4 Transition from Bounce Mode to Roll Mode

The transition from bounce mode to roll mode is usually made by the simulation programs when the velocity is less than or equal to a threshold velocity. The criterion used by each program is given in Table 3-5.

Table 3-5: Summary of criteria used to simulate transition from bounce mode to roll mode

	<i>Rockfall</i>	<i>CRSP</i>	<i>Rockfal2</i>	<i>RF</i>	<i>CADMA</i>
Criterion used to simulate transition from bounce mode to roll mode	Information not provided	If the distance the rock travels between bounces is less than its radius	If rebound velocity V_m is less than a critical velocity V_{cri} ¹⁰	When the ratio $\delta E/\delta L$ becomes greater than the rolling friction coefficient.	If the normal component of velocity $V_y < V_y^e$ (experimentally assessed V_y)

3.2.4.5 Rolling and Sliding

The condition of rolling is simulated by all the programs. The boulder starts rolling if the velocity is not high enough to put the boulder into a bouncing trajectory. The boulder keeps on rolling until it either stops or until it flies into trajectory again (if the next slope cell is steep). Below are the logistic details for each program.

Rockfall (Hoek)

The conditions of rolling or sliding is simulated only for the initial start of the boulder, that is the boulder either rolls or slides only in the first slope cell. After the boulder starts and crosses over the first slope cell, only the bouncing mode is simulated. The condition of rolling or sliding is simulated using the basic physical laws of motion based on the friction angle specified.

CRSP (Pfeiffer and Bowen)

The rolling mode is simulated as a series of short bounces, using the method described in the section 3.3.4.3.2 under the heading *CRSP*.

Rockfal2 (Elliott)

The acceleration/deceleration of a rolling boulder when rolling down/up an inclined plane can be determined from the following energy balance equation:

$$\frac{mV_i^2}{2} + \frac{I\omega_i^2}{2} + C m g dh = \frac{mV_r^2}{2} + \frac{I\omega_r^2}{2} + L\Delta$$

where: C = constant that equals +1 if the roll is downhill, and equals -1 if the roll is uphill;

¹⁰ The critical velocity is defined as the velocity of a boulder directed vertically upward required to lift the boulder a distance equal to one twentieth of the boulder radius and is calculated as $V_{cri} = (gr/10)^{1/2}$; where g is the acceleration due to gravity and r is the radius of the boulder.

dh = elevation gained or lost during the roll, which can be calculated using:

$$dh = r\Delta \sin(\theta)$$

where r = effective radius of the boulder;

Δ = elapsed angular displacement during the roll; and

θ = angle of inclination of the plane;

and L = torque provided by rolling friction at the boundary of the sphere, which is given by: $L = (\lambda m g \cos(\theta)) r$

where λ = coefficient of rolling friction.

It is assumed that the coefficient of rolling friction acts on the rolling sphere in a similar way that the coefficient of tangential friction, R_t , acts on the bouncing sphere. When $R_t = 1$, the rebound tangential velocity equals the impact tangential velocity (ie. no tangential speed is lost during the impact). Conversely when $R_t = 0$, the rebound tangential velocity is zero (ie. all the tangential speed is lost). When a sphere is rolling on a flat plane, no linear velocity (tangential velocity) is lost if $\lambda = 0$, whereas the sphere is brought to a halt in the shortest distance if $\lambda = \infty$.

On this basis it is hypothesized that:

$$\lambda = \frac{1 - R_t}{R_t} \quad \dots \text{Equation 3-20}$$

Rearranging the energy balance equation using Equation 3-20 provides the governing equation for a rolling sphere:

$$\omega_r^2 = \omega_i^2 - \frac{g\Delta}{0.7r} \left(\frac{1 - R_t}{R_t} \cos(\theta) - C \sin(\theta) \right) \quad \dots \text{Equation 3-21}$$

Using this equation, it can be shown that the sphere is accelerating when:

$$\frac{1 - R_t}{R_t} < \tan(\theta) \quad \dots \text{Equation 3-22}$$

The coefficient of rolling friction is therefore equal to the tangent of the maximum inclination of a plane on which an initially stationary sphere fails to start rolling. It can also be shown that the angular displacement, Δ , required to bring the sphere to a halt on a plane of constant grade is given by:

$$\Delta = \frac{0.7r \omega_i^2}{g \left(\frac{1 - R_t}{R_t} \cos(\theta) - C \sin(\theta) \right)}$$

Roll mode calculations are carried out for increments of 1 radian of rotation ($\Delta = 1$), thereby allowing local slope roughness to be incorporated. One radian of rotation corresponds to one radius of linear travel along the slope, which should be the gauge length used to characterize surface roughness of the slope for a given boulder size. The x,y coordinates of the boulder at the end of the roll increment are calculated using:

$$x_r = x_i + r \Delta \cos(\theta)$$

$$y_r = y_i + r \Delta \sin(\theta)$$

with $\Delta = 1$. The angular velocity at the end of the roll increment is found using Equation 3-21, and the linear velocity at the end of the roll increment is found using:

$$V_r = \omega_r r$$

The direction of travel at the end of the roll increment, α_r , is set equal to the local inclination of the rock surface for the roll calculation, this being the sum of the slope angle plus the local slope roughness angle.

RF (Hungt)

The authors did not provide any information regarding the logistics involved in simulating roll mode, but use of rolling friction coefficient has been indicated.

CADMA (Azzoni)

The dynamic equilibrium equations of the rigid body, in the assumed reference frame (Figure 3-4) are as follows¹¹:

$$0 = N - m \cdot g \cdot \cos\alpha \quad \dots\text{Equation 3-23}$$

$$m \cdot \ddot{x}_G = m \cdot g \cdot \sin\alpha - T \quad \dots\text{Equation 3-24}$$

$$I \cdot \frac{d^2\theta}{dt^2} = T \cdot r - N \cdot \ddot{u} \quad \dots\text{Equation 3-25}$$

Equation 3-25 can be written as:

$$I \frac{\ddot{x}_G}{r} = T \cdot r - N \cdot \ddot{u}$$

$$T = \frac{I}{r^2} \cdot \ddot{x}_G + N \cdot \frac{\ddot{u}}{r}$$

From Equation 3-23, $N = m \cdot g \cdot \cos\alpha$ then:

¹¹ The dots on top of the letters indicate the degree of differentiation with respect to time.

$$T = \frac{I}{r^2} \cdot \ddot{x}_G + m \cdot g \cdot \cos\alpha \cdot \frac{\ddot{u}}{r}$$

Substituting this equation into Equation 3-24:

$$\ddot{x}_G = \frac{m}{m + \frac{I}{r^2}} \cdot g \cdot \left(\sin\alpha - \cos\alpha \cdot \frac{\ddot{u}}{r} \right) \quad \dots\text{Equation 3-26}$$

Defining

$$A = \frac{m}{m + \frac{I}{r^2}}$$

and $\mu_r = \ddot{u}/r = \tan \phi_d$ is defined as the rolling friction coefficient. Equation 3-26 can be rewritten as follows:

$$\ddot{x}_G = A \cdot g \cdot \cos\alpha \cdot (\tan\alpha - \tan \phi_d) \quad \dots\text{Equation 3-27}$$

The integration of above Equation 3-27 gives:

$$\ddot{x}_G(t) = A \cdot g \cdot \cos\alpha \cdot (\tan\alpha - \tan \phi_d) \cdot t + \ddot{x}_G(t_0) \quad \dots\text{Equation 3-28}$$

Further integrating, $\dot{x}_G(t) = 1/2 (A \cdot g \cdot \cos\alpha \cdot (\tan\alpha - \tan \phi_d) \cdot t^2) + \dot{x}_G(t_0) \cdot t + x_G(t_0)$

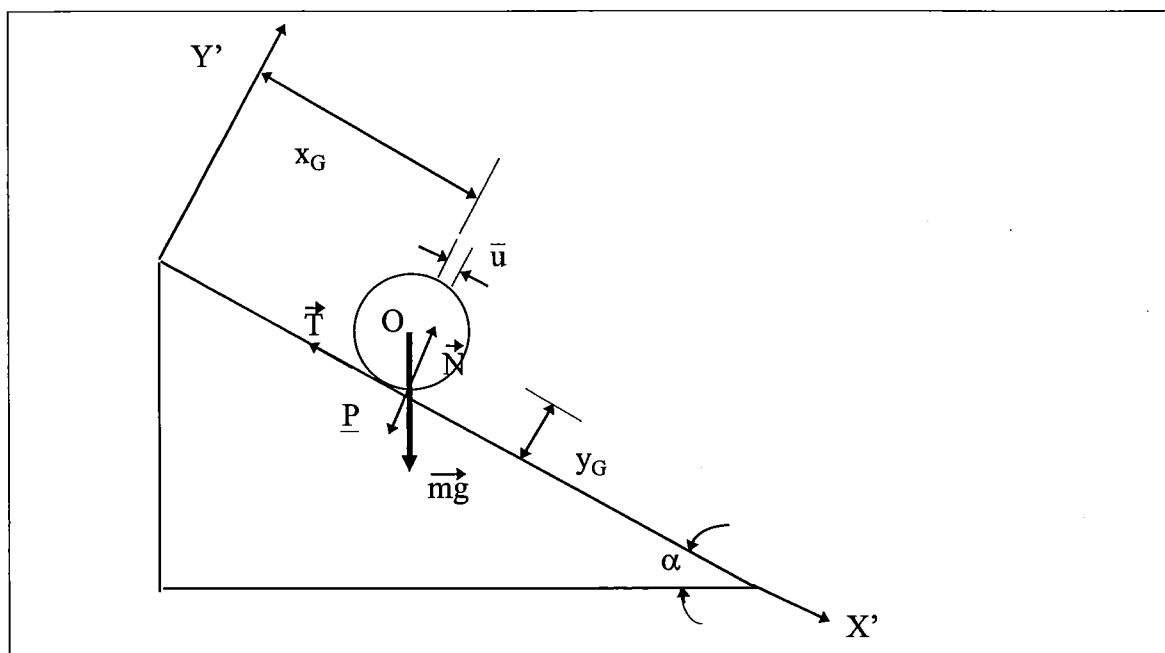


Figure 3-4: Definition of rolling problem in the assumed OX'Y' reference frame.

Equation 3-27 shows that three different situations can be possible:

1. $\ddot{x}_G = 0$ When $\tan \phi_d = \tan \alpha \Rightarrow$ uniform rolling motion with constant velocity.
2. $\ddot{x}_G < 0$ When $\tan \phi_d > \tan \alpha \Rightarrow$ uniformly decelerated rolling motion.
3. $\ddot{x}_G > 0$ When $\tan \phi_d < \tan \alpha \Rightarrow$ uniformly accelerated rolling motion.

Obtaining t from Equation 3-28:

$$t = \frac{\ddot{x}_G(t) - \ddot{x}_G(t_0)}{A \cdot g \cdot \cos \alpha \cdot (\tan \alpha - \tan \phi_d)} \quad \dots \text{Equation 3-29}$$

Substituting Equation 3-29 into 3-28, the velocity of the block during the rolling or sliding motion can be determined with the following equation:

$$\ddot{x}_G = \sqrt{2 \cdot A \cdot g \cdot \cos \alpha \cdot (\tan \alpha - \tan \phi_d) \cdot [x_G(t) - x_G(t_0)] + \ddot{x}_G^2(t_0)} \quad \dots \text{Equation 3-30}$$

From the above equation, the rolling friction coefficient can be determined as :

$$\mu_r = \tan \phi_d = \tan \alpha - \frac{\ddot{x}_G^2(t) - \ddot{x}_G^2(t_0)}{2 \cdot A \cdot g \cdot \cos \alpha \cdot [x_G(t) - x_G(t_0)]} \quad \dots \text{Equation 3-31}$$

The above sub-sections for each program demonstrated the difference between the simulation logistics used by different programs for the roll mode. Pfeiffer and Bowen (1989) use the same simulation logistics used for bounce and simulate rolling mode as a series of short bounces for the program *CRSP*. Hoek (1987) simulates roll mode only at the initial movement of the boulder for the program *Rockfall*. Elliott (1992) uses the conservation of energy by assuming that the rolling friction coefficient can be derived from the coefficient of tangential friction for the program *Rockfal2* (Equation 3-21). Azzoni (1995) uses the dynamic equilibrium equations to determine the velocity (Equation 3-30) and the rolling friction coefficient (Equation 3-31) at any time.

3.2.4.6 Stopping

Table 3-6 shows the stopping criterion used by the respective programs.

Table 3-6: Criteria used to terminate calculations.

	<i>Rockfall</i>	<i>CRSP</i>	<i>Rockfal2</i>	<i>RF</i>	<i>CADMA</i>
Criterion for stopping the boulder	¹² If $V_m > (V_{rx}^2 + V_{ry}^2)^{1/2}$	No information provided	If velocity becomes zero	No information provided	If the specified limit velocity is reached

3.2.4.7 Summary of Logistics Comparison

Table 3-7 below summarises comparison of *all* the simulation logistics used by the respective programs. It is evident from the table and the previous sections that the simulation logistics used by various authors are very different from each other.

Every author has stated and justified his own reasons for the use of the logistics, but considering the information provided regarding the logistics, the programs *CADMA* and *Rockfal2* can be recommended. This is because of the following disadvantages of the other programs in terms of simulation (from the available information from their published papers):

- The program *Rockfall* does not simulate rolling mode after the initial movement of the boulder.
- The program *CRSP* assumes that the rolling mode can be simulated as a series of short bounces which is not true in the practical world.
- The program *RF* uses the restitution coefficient to directly reduce the resultant velocities for the bounce mode which is not the true way of dissipating the energy during an impact.

3.2.5 Probabilistic Analysis

Since rockfalls involve intrinsic randomness by default, the simulation programs should incorporate some kind of randomness to imitate the intrinsic randomness involved in actual rockfalls. For this reason, almost all the programs considered for comparison use Monte Carlo simulation methods to incorporate some kind of randomness. The parameters varied during the execution of program (for each program considered) are different. Table 3-8 shows the summary of randomness incorporated in each program. From the table, it is evident that the program *Rockfall* does not use any means of randomisation. Another

¹² V_m is specified minimum velocity and V_{rx}^2 and V_{ry}^2 are the velocities in x and y direction respectively.

important point to note here is that the program *CRSP* randomises only the slope roughness and does not vary the restitution coefficients.

Table 3-7: Comparison of *all* of the simulation logistics used by respective programs.

	<i>Rockfall</i>	<i>CRSP</i>	<i>Rockfal2</i>	<i>RF</i>	<i>Cadma</i>
Initial start ¹³	Check the friction angle and velocity of the boulder	Check the position and velocity of the boulder	Check the position, velocity and orientation of velocity	Check the position and velocity of boulder	Check the position, velocity and orientation of velocity
Free fall	Not simulated at the start	When the position of boulder is above ground	When the position of boulder is above ground	When the position of boulder is above ground	When the position of boulder is above ground
Impact and bounce ¹⁴	Uses the angle of slope to reduce the reflected velocities	Uses law of conservation of energy in combination with empirical formulae	Uses law of conservation of energy in combination with empirical formulae	Uses energy loss calculated using the reduced velocities	Uses law of conservation of momentum
Transition ¹⁵	Details not available	If the distance the rock travels between bounces < it's radius	If the rebound velocity < critical velocity $V_{cri} = (gr/10)^{1/2}$	When the ratio $\delta E/\delta L >$ rolling friction coefficient	If the normal component of velocity $V_y < V_y^e$ (exp. assessed V_y)
Rolling and sliding	Simulated only at the start	Simulated as a series of short bounces	Uses rolling friction coefficient and law of conservation of energy	Details not available.	Uses the dynamic equilibrium equations of the rigid body
Stopping	If the velocity \leq specified minimum	Details not available	If velocity becomes zero	Details not available	If the velocity \leq specified minimum

Table 3-8: Randomness incorporated in respective programs.

	<i>Rockfall</i>	<i>CRSP</i>	<i>Rockfal2</i>	<i>RF</i>	<i>CADMA</i>
Uses Monte Carlo Simulation	✘	✓	✓	✓	✓
Randomises restitution coefficients	✘	✘	✓	✓	✓
Randomises rolling friction coefficient	✘	✘	✓	✓	✓
Randomises slope roughness	✘	✓	✓	✘	✓
Randomises size and shape of boulder	✘	✘	✘	✓	✓
Randomises starting coordinates of the boulder	✘	✘	✘	✓	✓

✓ = Yes, ✘ = No

¹³ Boulder follows a ballistic trajectory, if the initial velocity is specified.

¹⁴ All the programs use the restitution coefficients to reduce the reflected velocities after impact.

¹⁵ Transition from bounce mode to roll mode.

3.2.6 Overall Performance

Overall performance of the programs will be compared by modelling rockfalls on an actual slope. The section and the properties used for simulation will remain same for all programs to make a compatible comparison. Because of the restrictions of particular programs, the initial conditions are not exactly identical.

3.2.6.1 Simulation Details

The section used for the analyses is from a hill site in Hong Kong, with the geology consisting of Hong Kong Granite. The height of the slope is about 67 m, and the width of the hill is around 46 m (Figure 3-5). The boulder diameter of one metre is kept constant for all the programs; where there is no possibility of specifying boulder size, an equivalent mass of the boulder was used assuming the mass density to be around 0.027 MN/m^3 . The values of the parameters used are shown in Table 3-9.

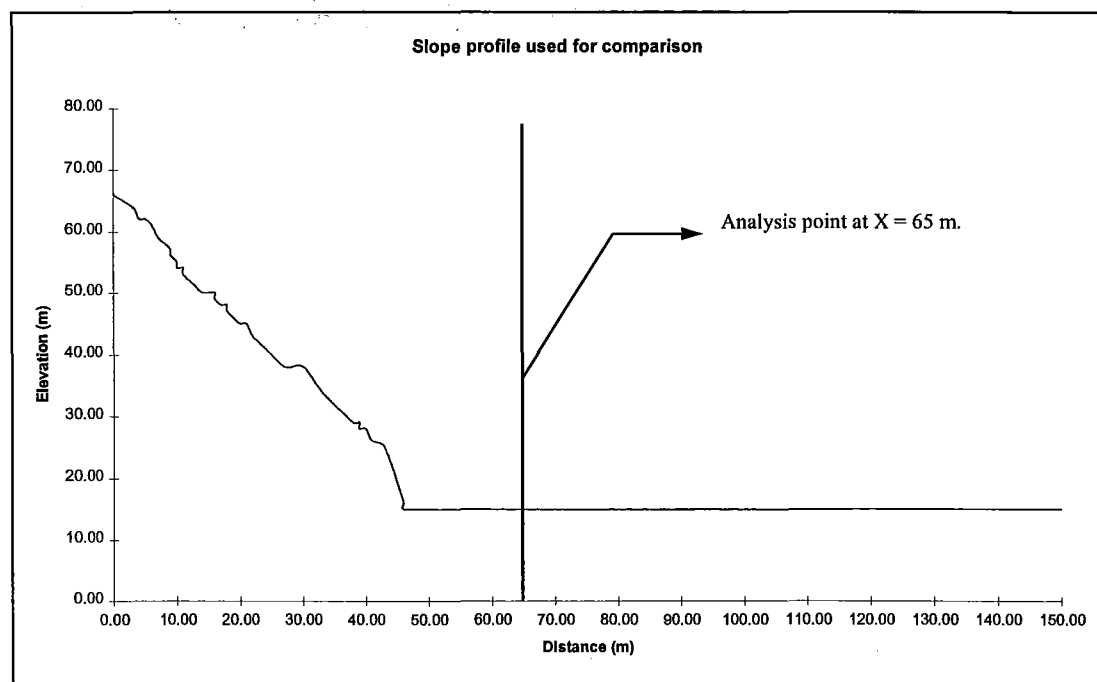


Figure 3-5: Profile of the slope used for overall comparison of simulation programs.

The analysis was carried out to find the boulder velocities, height of boulders above ground, and the percentage of boulders reaching the horizontal coordinate of 65 m (see Figure 3-5). The analysis point is where the road starts from and hence it is helpful to get the above rockfall statistics at this point, so that a catch ditch and/or fence design can be carried out. One hundred simulations were carried out using each of the programs which provide facility for multiple simulations.

Table 3-9: Parameter values used for the rockfall simulation.

Parameter	Value
Diameter (d) - m	1
Mass density (γ) - MN / m ³	0.027
Gravitational acceleration (g) - m / sec ²	9.81
Normal coefficient of restitution (R_n) {slope}	0.36
Normal coefficient of restitution (R_n) {road}	0.30
Tangential coefficient of restitution (R_t) {slope}	0.85
Tangential coefficient of restitution (R_t) {road}	0.75
Slope roughness (angle) {slope}	11
Slope roughness (angle) {road}	1
Angle of friction (ϕ) - degrees	20
Initial horizontal velocity (V_x) - m / sec	0
Initial vertical velocity (V_y) - m / sec	0

3.2.6.2 Simulation Results

Results of the simulation are presented here for each program. The graphical output from the respective programs is included so as to give an idea how the output actually looks like, and to check whether the output is sufficient for a detailed rockfall analysis.

Rockfall (Hoek)

The program *Rockfall* allows only up to 20 slope cells to be specified. For this reason, most of the coordinates specifying minute changes in slope are neglected. Figure 3-6 shows the simulation result from the program *Rockfall*, showing the trajectory of the boulder. The program was giving an error for the starting condition of zero velocities and executed only when either a horizontal velocity of $V_x = 7$ m / sec or an angle of friction of zero is specified. The boulder stopped at $x = 66$, $y = 15$. It is not possible to perform 100 simulations using this program as the starting position of the boulder cannot be specified. Only the velocities, and the friction angle can be varied in this program.

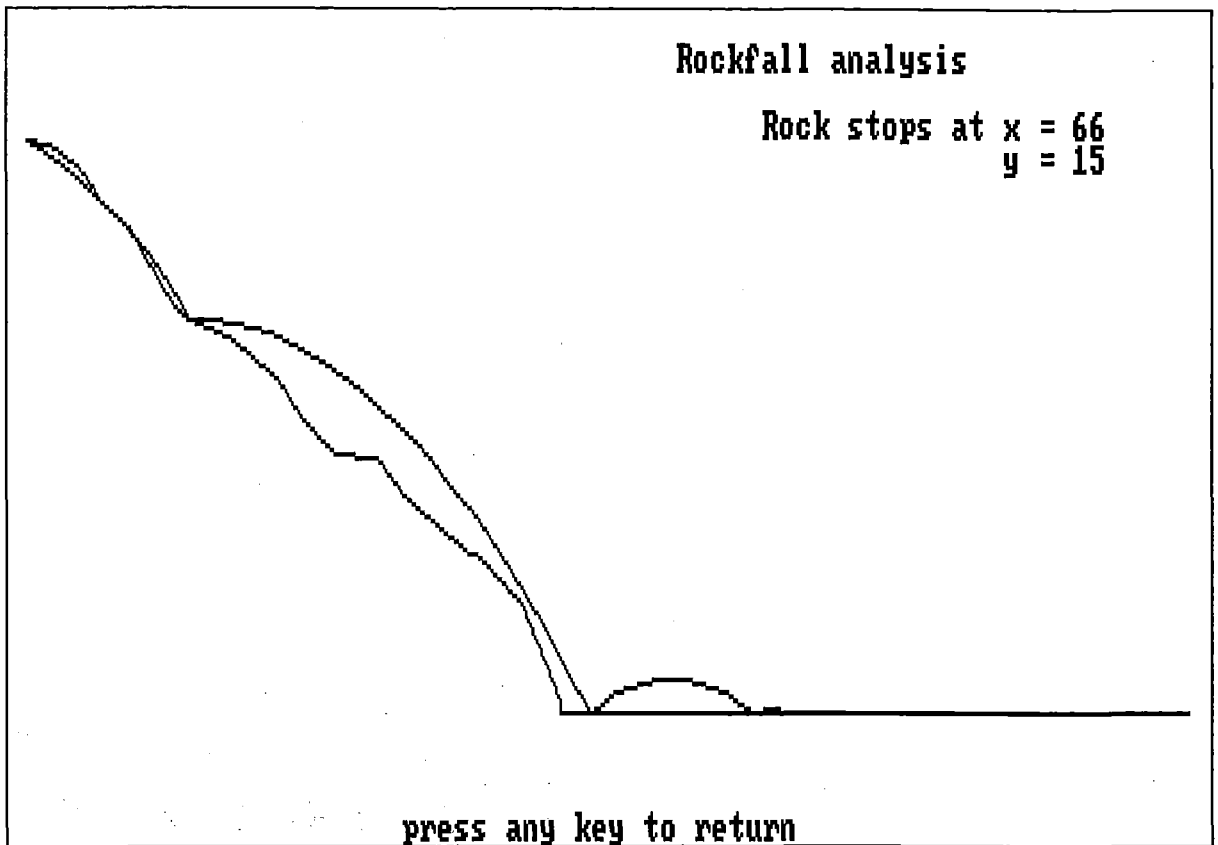


Figure 3-6: Boulder trajectory (*Rockfall*).

Results

- Boulder stops at $x = 66$, $y = 15$.

CRSP (Pfeiffer and Bowen)

This program also did not have any restrictions as per the number of slope cells. One of the major difference between this program and other programs is the need to use FPS (Foot, Pound, Second) system of units. This program also had some problems to simulate with the vertical slope cells. The program did not execute until all the vertical faces had been changed to nearly-vertical faces ($< 90^\circ$). Also, the program required a minimum initial velocity of 1 ft / sec, to simulate rockfalls. Figures 3-7 to 3-10 below show the results from this program. Please note that the graphs show the plots for FPS system of units.

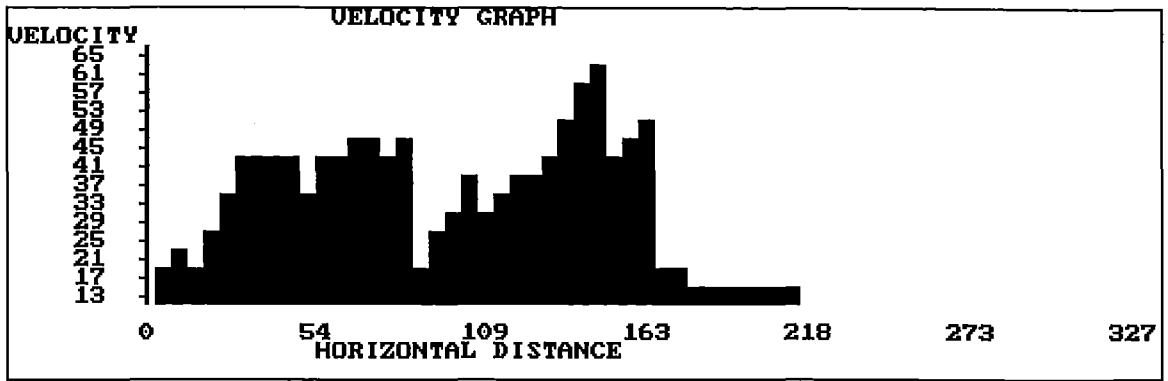


Figure 3-7: Velocity graph for the whole slope (*CRSP*).



Figure 3-8: Velocity distribution at analysis point (*CRSP*).

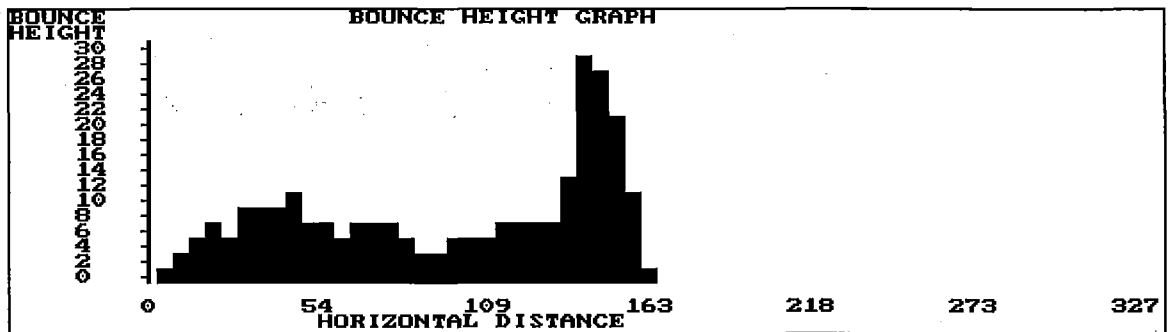


Figure 3-9: Bounce height graph for the whole slope (*CRSP*).

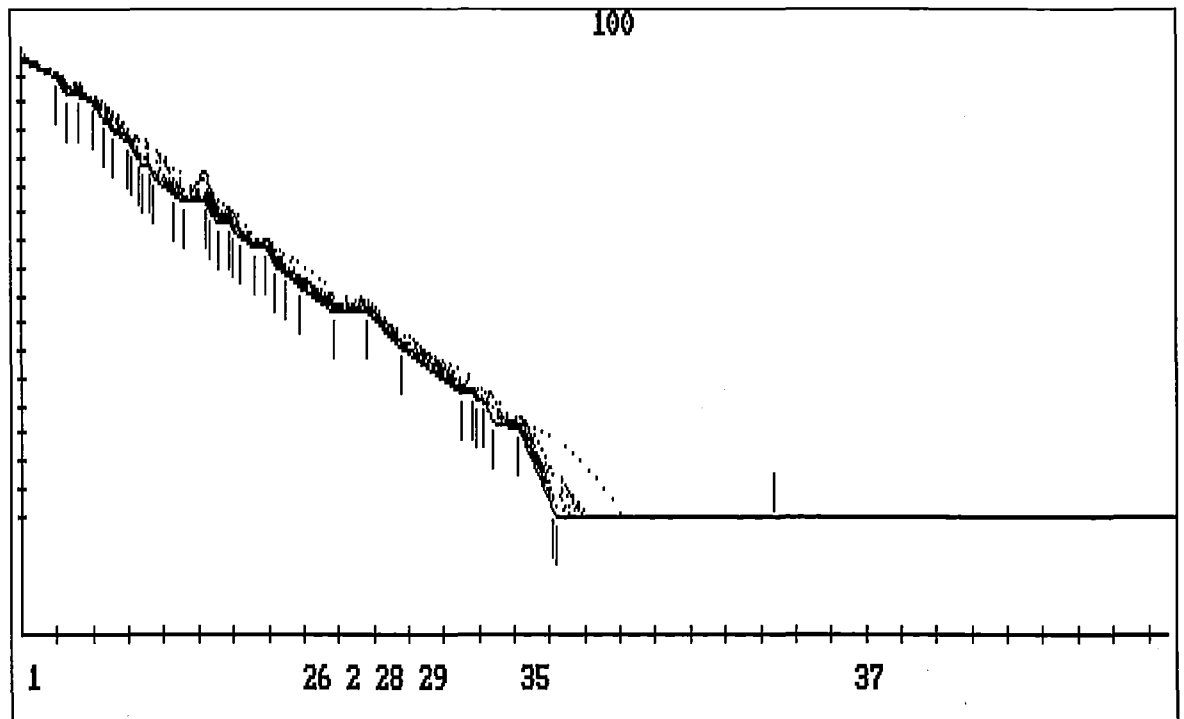


Figure 3-10: Boulder trajectories simulated by the program *CRSP*

Results

- 10% of the boulders crossed $x = 214$ ft or 65 m.
- Average velocity = 10 ft / sec i.e., 3 m / sec (min = 1.2, max = 4.6 m/sec).
- Bounce height at analysis point = 0 ft i.e., 0 m.
- Maximum kinetic energy at analysis point = 80540 ft lb i.e., 1113.5 KNm.

Rockfal2 (Elliott)

The program *Rockfal2* did not have any restrictions as per the maximum number of slope cells that can be specified. The initial conditions that can be varied are boulder position and velocities. One hundred simulations were performed using the same boulder position and velocity. The results are shown in the Figures 3-11 to 3-16 below.

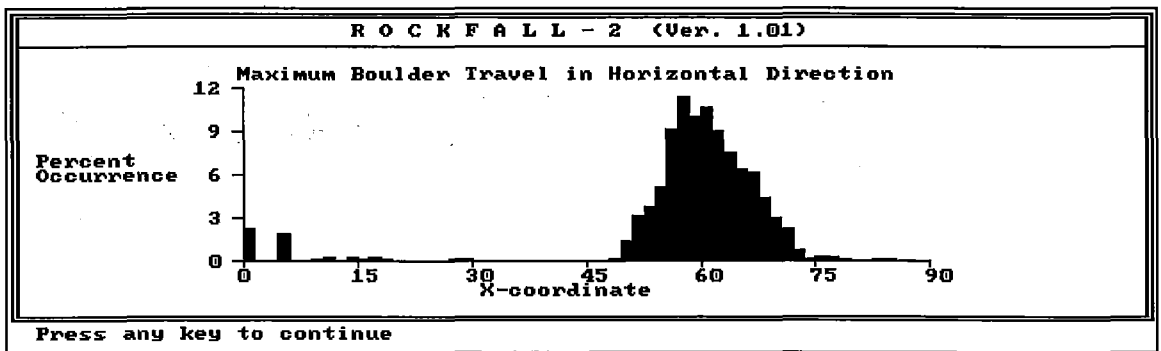


Figure 3-11: Maximum boulder travel in horizontal direction (*Rockfal2*).

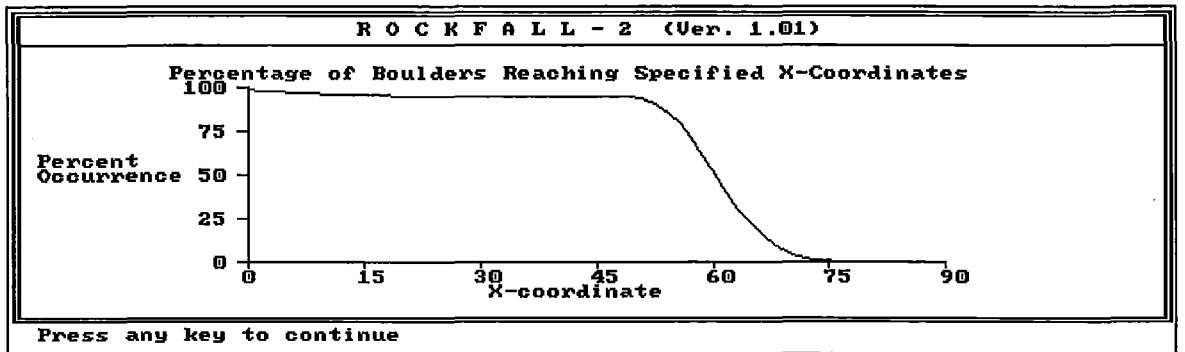


Figure 3-12: Percentage of boulders reaching specified X-coordinates (*Rockfal2*).

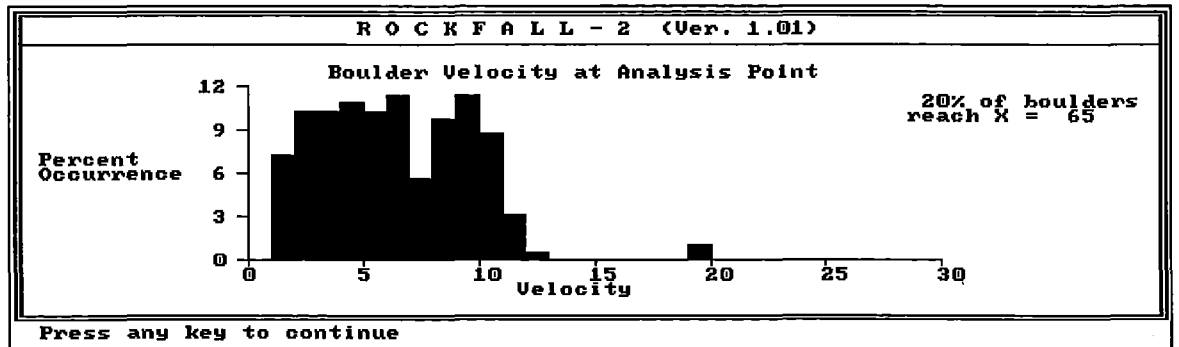


Figure 3-13: Boulder velocity at analysis point (*Rockfal2*).

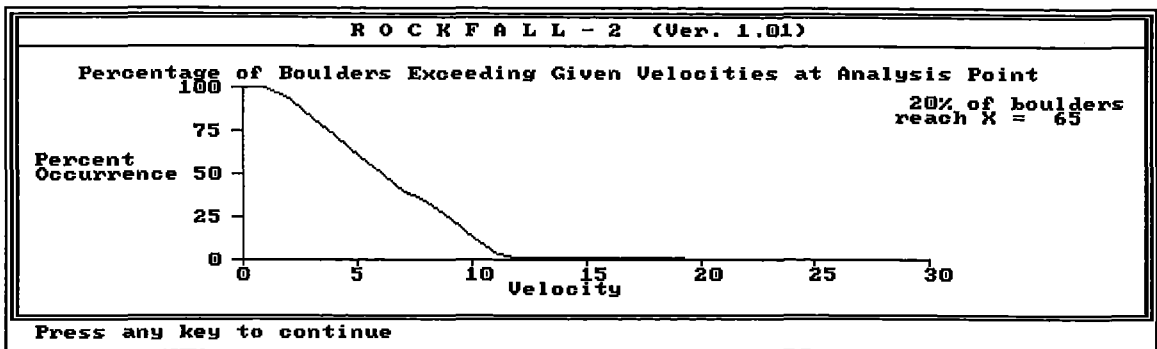


Figure 3-14: Percentage of boulders exceeding given velocities at analysis point (*Rockfal2*).

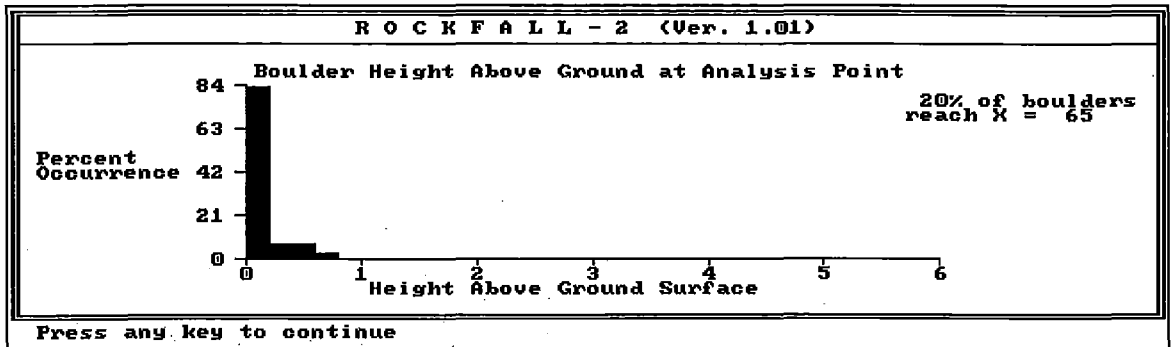


Figure 3-15: Boulder height above ground at analysis point (*Rockfal2*).

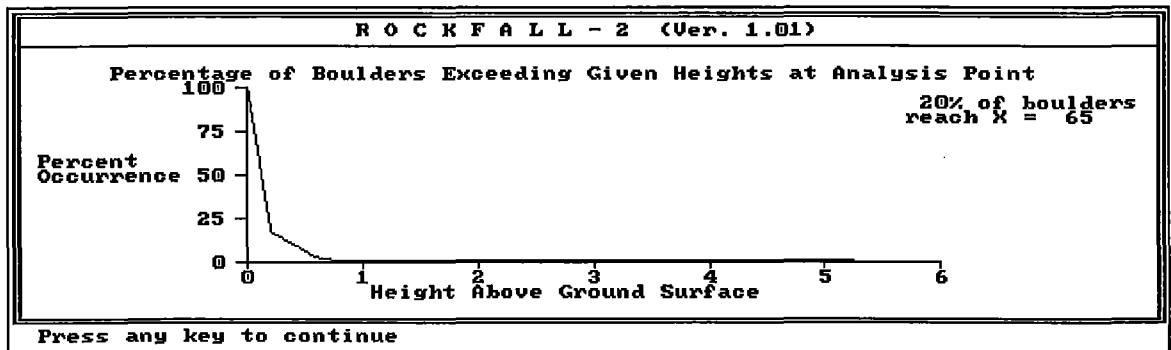


Figure 3-16: Percentage of boulders exceeding given heights at analysis point (*Rockfal2*).

Results

- 20% of boulders reach the coordinate $x = 65$ m.
- All the boulders are below 1.5 m height at this point.
- 66.8% of the boulders cross this point below a height of 0.05 m.
- Average boulder height at this point is about 0.03 m.
- Minimum velocity of the boulders crossing this point is 0.75 m / sec.
- Maximum velocity of boulders at this point is about 21 m / sec.
- Average boulder velocity at this point is 1.3 m / sec.

RF (Hungr)

The program *RF* allows us to specify around 50 slope cells as the input. The program allows the user to specify a range of boulder weights and position, and the analysis point. The simulation was performed by specifying a small range of weights and the boulder position (as it is one of the requirements of the program while performing multiple simulations), to make a compatible comparison. Figure 3-17 shows the trajectories of the boulders.

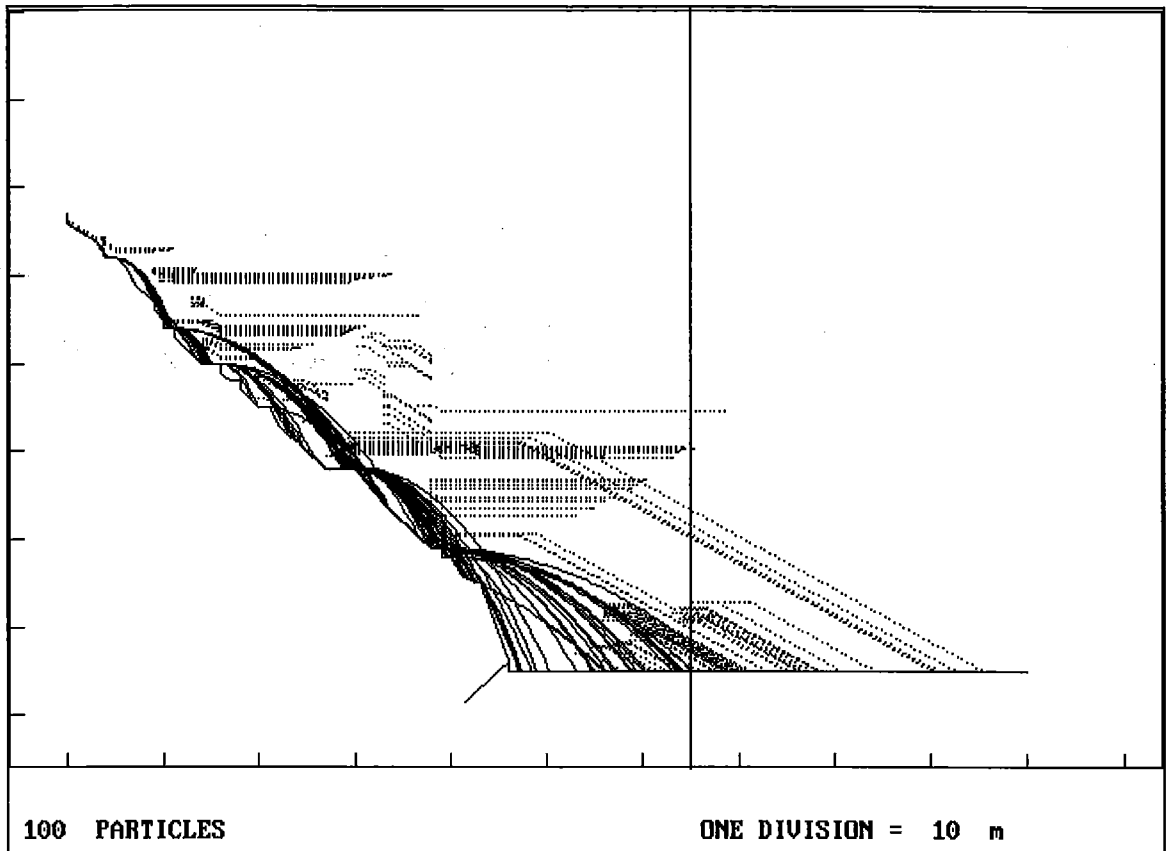


Figure 3-17: Trajectories of the boulders (*RF*).

Results

- 41% of particles passed the observation point at 65 m.
- Mean arrival time = 10 seconds.
- Average velocity = 10.68 m / sec (min. = 2.97, max. = 22.78).
- Average height of flight above ground surface = 0.11 m (min. = 0.00, max. = 3.15).

CADMA (Azzoni)

For the program *CADMA*, there is no restriction as per the number of slope cells. The difficulty with this program is that it gives an error when a slope roughness is specified on

a part of slope where there is vertical/near vertical face. This is probably because the program cannot accept a reverse slope generated by the variation of roughness angle on a vertical face. For this reason, zero slope roughness was specified on all vertical/near vertical faces. Figures 3-18 to 3-22 below show the results from the program.

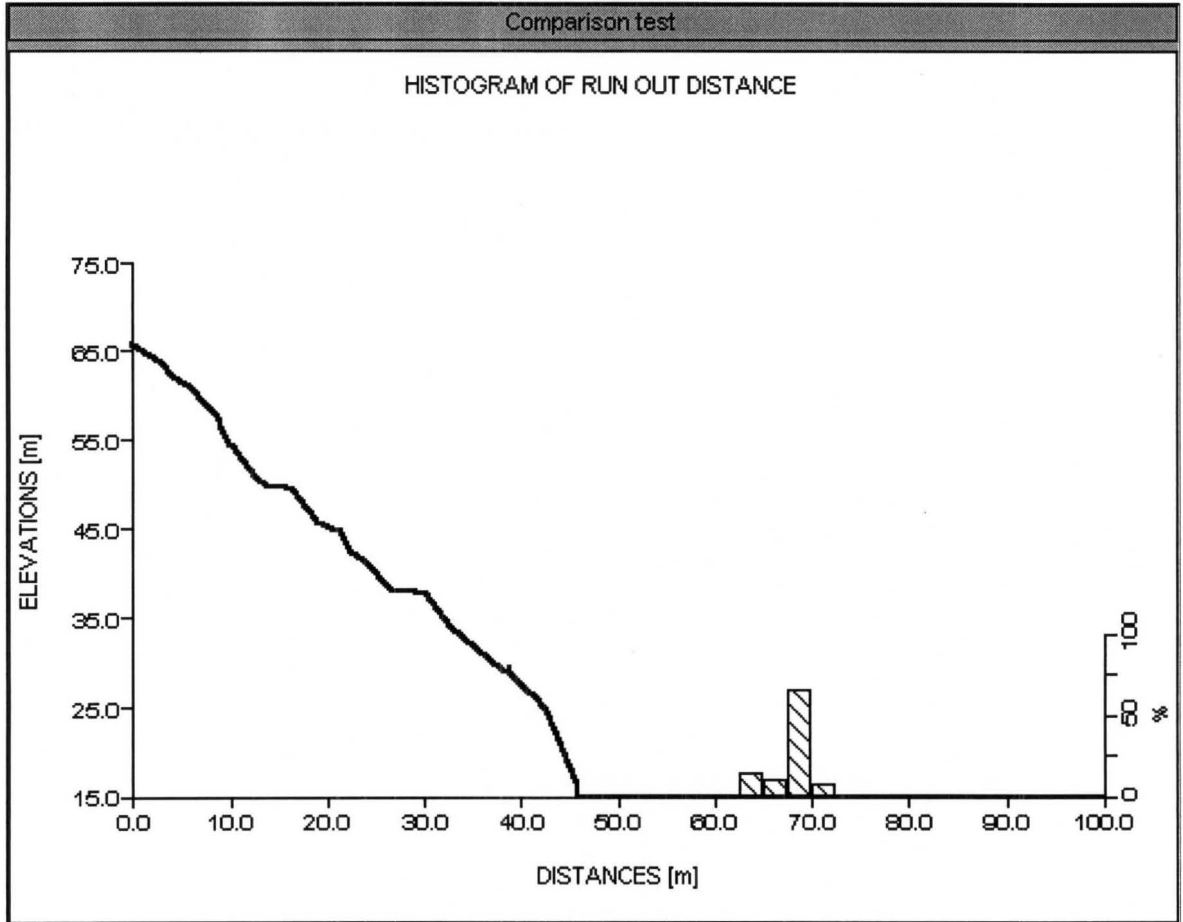


Figure 3-18: Plot showing the histogram of run out distances (*CADMA*).

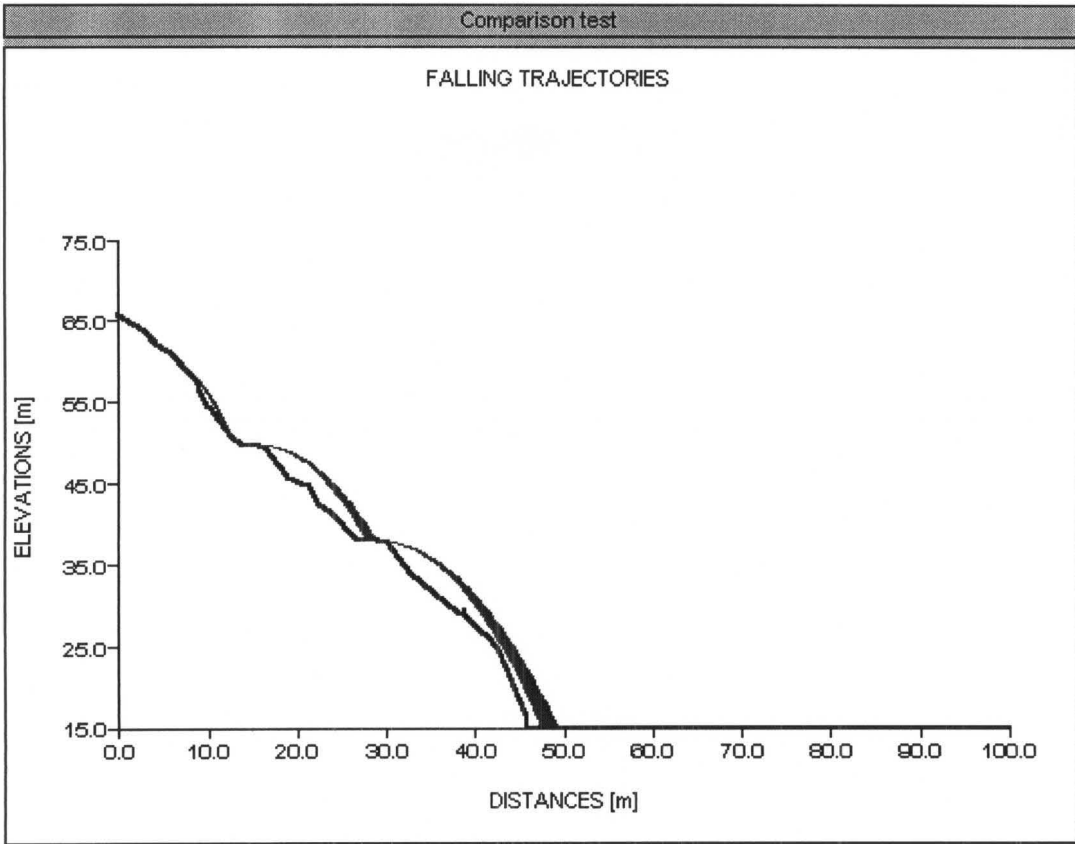


Figure 3-19: Boulder trajectories (CADMA).

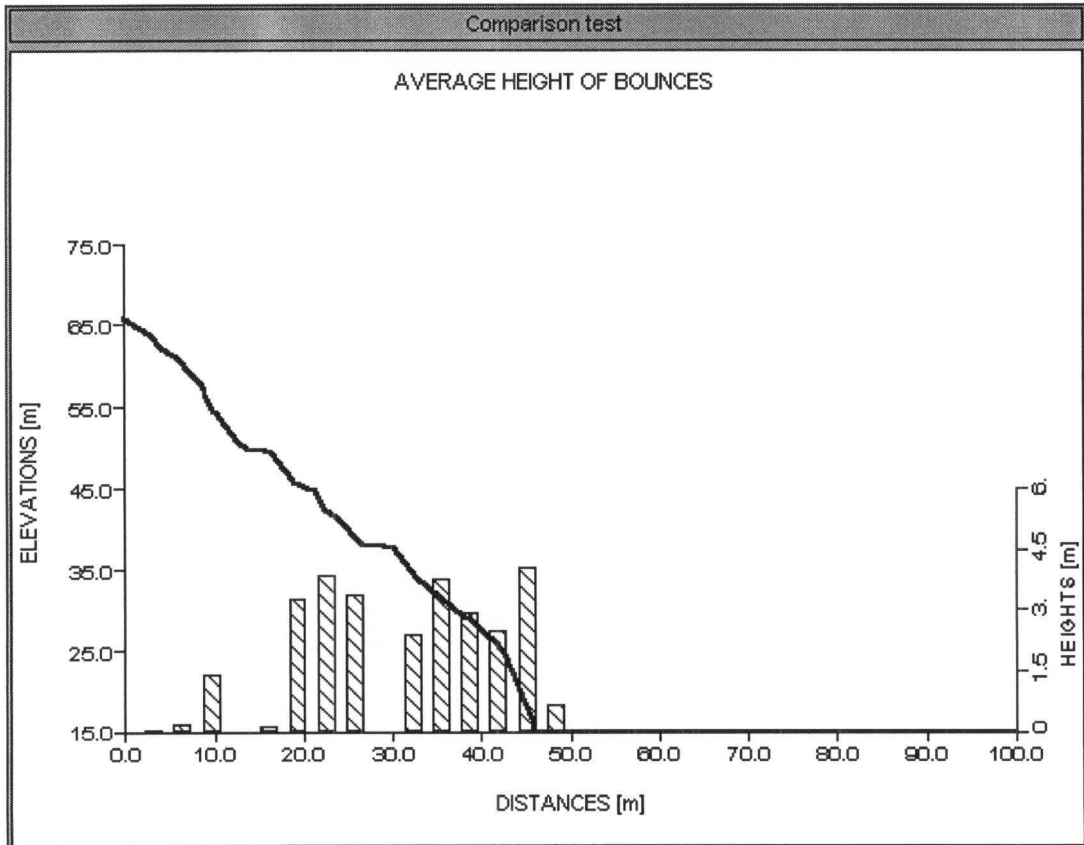


Figure 3-20: Average bounce heights at particular distances (CADMA).

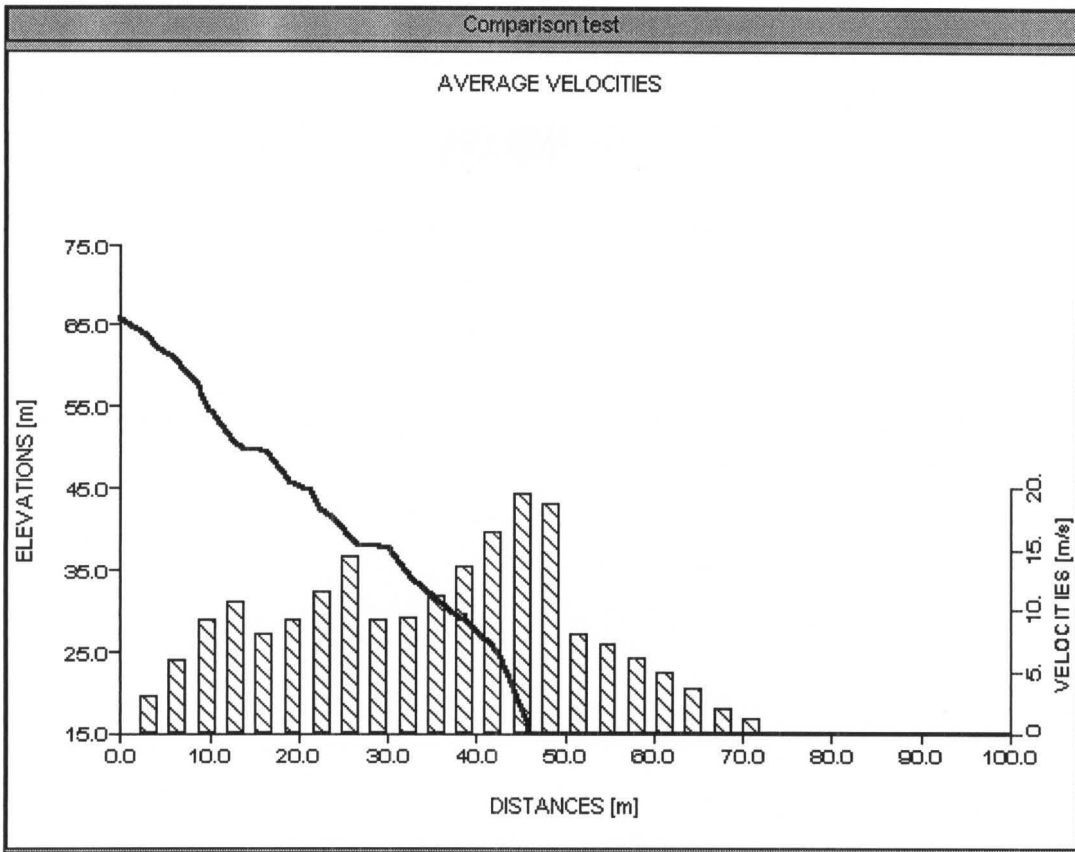


Figure 3-21: Average velocities at respective distances (CADMA).

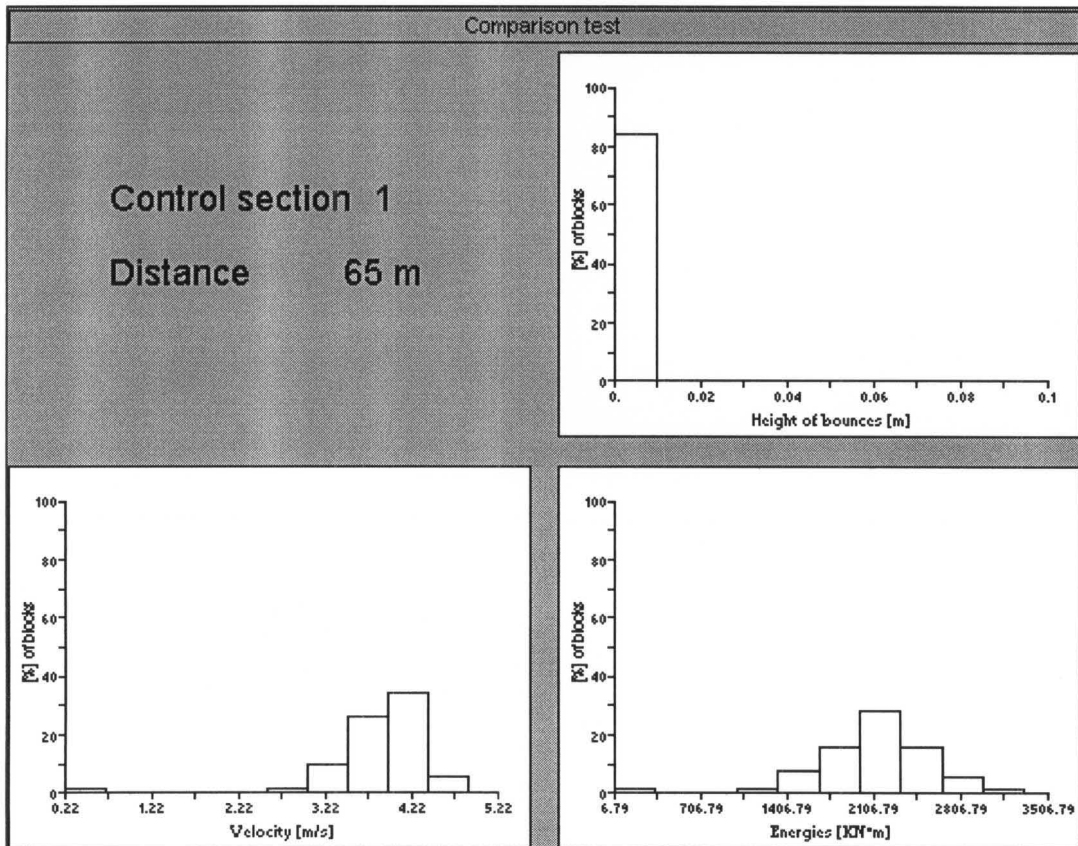


Figure 3-22: Plots showing the statistics at analysis point (CADMA).

Results

- 26% of the boulders reached $x = 65$ m. (% is not included in the output).
- Average height of bounces at the analysis point = 0.01 m.
- Average velocity = 3.7 m/sec. (min = 0.94, max = 5.41).
- Average energy = 1997 KNm. (min = 124, max = 4070).

3.2.6.3 Summary of Results

Table 3-10 gives the summary of results at the analysis point from all the programs.

Table 3-10: Summary of results at the point of analysis

Program	Results			
	Ave. boulder height (m)	% of boulders passing	Ave. boulder velocity (m/sec)	Time taken to simulate 100 boulders (sec)
<i>Rockfall</i>	NA	NA	NA	NA
<i>RF</i>	0.11	41	10.68	40
<i>Rockfal2</i>	0.03	20	1.3	20
<i>CADMA</i>	0.0	26	3.7	200
<i>CRSP</i>	0.0	10	3.0	20

As one can see, there is no consistency among the results. To some extent, this can be attributed to the changes made in the input parameters for respective programs to carry out the simulations. The program *RF* has over-predicted the rockfalls compared to others. The material constants specifying the state of elasticity of the material is influencing the run-out distances of the boulders for the program *RF*, for which there is no information available as to what these constants represent and the units used.

On the other hand, the program *CRSP* seems to be under-predicting the rockfalls. Kuantsai Lee (1997) came up with an explanation for this which is explained below.

CRSP and *Rockfal2* use the restitution coefficients for “velocities” which are used to directly reduce the resultant velocity of a boulder after an impact. On the other hand, *CADMA* uses the coefficient of restitution for the “energy loss” during a bounce. This coefficient ϵ is related to the tangential and normal restitution as follows (slightly manipulated from Azzoni *et al.* 1995):

$$\varepsilon = \frac{I\omega_o^2 + m(R_n^2 V_{no}^2 + R_t^2 V_{to}^2)}{I\omega_{1o}^2 + m(V_{no}^2 + V_{to}^2)} \quad \dots \text{Equation 3-32}$$

where ω_o , V_{no} , V_{to} are the angular, normal and tangential velocity at impact, ω_1 is the angular velocity at rebound, and I and m are the moment of inertia and mass of the boulder, respectively. From Equation 3-32, it can be seen that the energy restitution coefficient cannot be easily converted into the velocity restitution coefficients because of the involvement of normal and tangential velocities. Because of the use of different restitution coefficients, different models produce different results. Consider the extreme, but unrealistic case of a rock dropping vertically onto a hard surface. In this case, both the angular and tangential velocities are zero and thus the above equation reduces to:

$$\varepsilon = R_n^2$$

Using Azzoni's (1995) recommended (based on *in situ* tests) value of ε of 0.75, the corresponding R_n would have been about 0.87. This is more than twice the value suggested by Pfeiffer and Bowen (1989) which is 0.37 to 0.42 for hard surfaces. In other words, under the extreme case illustrated, the rebound velocity predicted by *CADMA* will be twice that of value predicted by *CRSP*. This leads to the conclusion that the program *CRSP* produces results that are considerably less than *CADMA*.

Finally, only the programs *CADMA* and *Rockfal2* make similar predictions for rockfalls.

From the simulation results we can conclude that no two simulation programs predict rockfalls identically. This can be linked to the difference in simulation logistics used by the respective authors. The simulation logistics used by the authors were based on some scientific facts and, in some cases, on empirical assumptions.

3.3 Conclusions and Recommendations

The following sections provide conclusions for each program based on the comparison performed in the earlier sections and recommendations are made as to which program is the best to use for a detailed analysis of rockfalls.

3.3.1 Conclusions for Each Program

Based on the comparison performed in the earlier sections and the results from the overall performance, following conclusions can be drawn for each program:

Rockfall

- This program is sensitive to initial conditions. The program did not perform the simulation until either a horizontal velocity of 7 m / sec was specified or the angle of friction has been reduced to zero.
- The number of slope cells that can be specified (20) is not sufficient for large slopes or even for detailed specifications of small slopes.
- The output from the program is not sufficient for analysis and design of remedial works.
- The probabilistic analysis of rockfalls cannot be performed using this program as the user have to change the initial conditions each time the simulation is performed.
- The program has no facility to specify the analysis point.
- Time taken for simulation of 1 boulder is 2 seconds.

CRSP

- There is no restriction on the number of slope cells.
- This program has also some problems associated with vertical faces. The program did not simulate until the vertical faces have been changed to nearly vertical faces¹⁶.
- There is a need to convert the input parameters into FPS system of units, which is not very helpful to use in most of the countries which use International System (SI) of units.
- The assumption that rolling can be simulated as a series of short bounces has to be changed and the rolling friction coefficient should be used to simulate the rolling mode of motion.
- The output from the program is sufficient for a detailed analysis, but it should be improved so that the images can be included in reports.
- The program does not incorporate sufficient randomness to study the effects of all the parameters influencing the rockfalls at a particular site. Only slope roughness is varied by the program which is not enough to randomise the bounce characteristics of a boulder.
- Time taken for simulation of 100 boulders is 20 seconds.

¹⁶ However, the program works in some cases.

Rockfal2

- There is no restriction on the number of slope cells that can be specified.
- Output from the program is sufficient for a detailed rockfall analysis, but can be improved so that the images can be included in a report.
- Good facility for stochastic modelling (incorporates Monte Carlo simulation).
- The program allows the specification of the analysis point to get the boulder velocities and heights at the point which can be used for the design of remedial works.
- There is no facility to specify a range of initial conditions to simulate most probable starting positions and velocities for a particular site.
- There is no facility to plot the trajectories of boulders.
- Time taken for simulation of 100 boulders is 20 seconds.

RF

- The number of slope cells that can be specified (43) is not sufficient for large slopes or even for detailed specifications of small slopes.
 - The program uses some material properties like contact yield limit, initial contact stiffness, and the stiffness reduction ratio for which there is no information as to what the range of values and the units are. With some experimentation, it was found that by the use of these parameters, the elasticity of the material can be clearly specified. For example, a contact yield limit value of 0 means the material is perfectly elastic. These material properties does have a large influence on the rockfall simulation, with the number of rocks reaching the analysis point being maximum when the material is perfectly elastic.
 - There is no facility for specification of any initial velocities in this program. Hence, this program is not suitable for the slopes where there could be some initial velocities (e.g. from freeze-thaw cycles of the ice, water pressure from fissures and seismic activity).
 - Output from the program is sufficient for a detailed analysis of rockfalls.
 - There is facility to specify a range of boulder weights and positions to simulate most probable starting conditions for the probabilistic studies. However, change of weight of the boulder does not affect on the final position of the boulder.
 - The trajectory plots and velocity profile of the boulder are provided by the program, which are essential for a detailed analysis of rockfalls.
 - There is a facility to specify the analysis point to get the boulder velocities and heights at the point which can be used for the design of remedial works.
-

- There is no facility to get histogram plots or any kind of graphs, as we can get from the program *Rockfal2*. However, the text output includes the energy, time taken to reach, velocity, and height of the boulders above ground.
- Time taken for simulation of 100 boulders is about 40 seconds.

CADMA

- There is no restriction as per the number of slope cells that can be input.
- Good facility to draw or modify the slope.
- A minimum limit normal velocity is required to perform the simulation.
- The program gives an error for a slope with vertical faces as sometimes, the program does not perform simulation for slopes with vertical faces¹⁷. Hence, this program is not suitable for slopes with overhanging faces.
- Output from the program is sufficient for a detailed analysis. The results can be printed out or can be captured using a graphic program.
- Incorporates all sorts of randomness required for detailed analysis, including variation of the shape of ellipsoidal boulders.
- There is no facility to save the graphic output from the program. The program has to be run again if you forget to print the results before exiting.
- Time taken for simulation of 100 boulders is around 200 seconds.

3.3.2 Recommendations

Based on the comparison performed in the earlier sections and the conclusions drawn for each of the programs, this work recommends the programs *CADMA* and *Rockfal2* for simulations and analysis of rockfalls¹⁸. However, as only the program *Rockfal2* is free of any errors in the simulation (e.g. *CADMA* is unable to handle vertical faces for some slopes), it can be concluded that *Rockfal2* is the best program to use for a detailed rockfall analysis.

Although the program *Rockfal2* is one of the best programs to use for simulation and analyses of rockfalls, the program should be modified to give an improved output. Also,

¹⁷ Experimentation showed that the program is not giving errors for every slope with vertical faces.

¹⁸ Please note that the author is in no way involved in development or marketing of these programs.

additional randomness needs to be incorporated to vary initial starting position and velocity of the boulder. These modifications will be explained in detail in Chapter 4.

Finally, although the rockfall phenomenon has been thoroughly investigated in recent times, it is almost impossible (with the present standard of knowledge) to simulate the actual behaviour of rockfalls with accuracy. The simulation of rockfalls does help the engineer to design rockfall protection, but he/she should not rely completely on computer predictions. Hence, the rockfall simulation programs have to be used only as an aid for the design of rockfall protection structures. Thus, the design of rockfall protection barriers has to be carried out in combination with engineering judgement.

3.4 Summary

A comprehensive comparison of five rockfall simulation programs has been carried out based on the criteria discussed in section 3.2.2. Comparison of the simulation logistics showed that various authors adapted different simulation logistics for simulation of the mode of motions (rolling and bouncing). Comparison of the overall performance of the programs indicated that neither of the programs simulate rockfalls identically, which must be because of the difference in simulation logistics used. Finally, it was concluded that the program *Rockfal2* is the best program to use for a detailed analysis of rockfalls at Fox Glacier.

Chapter 4 goes on to modifying the program *Rockfal2* by incorporating more randomness and improving the aesthetics of the program (so that the output graphs can be included in the technical reports).

Chapter 4

Modification of The Program *Rockfal2*

4.1 Introduction

From the comparison performed in Chapter 3, it was concluded that the best program to use for a detailed analysis of rockfalls is the program *Rockfal2*. It was also concluded that improved randomness and graphic output is needed for this program (section 3.3.1). Hence, it was decided to modify the program *Rockfal2* so it can be used for a detailed analysis of rockfalls at Fox Glacier discussed in Chapter 5.

In this chapter, details of the modifications made to the original program *Rockfal2* are discussed. A comparison is performed between the outputs from both the programs *Rockfal2* and the modified version *WinRock* to make sure that the output is same as the basic simulation logistics are unchanged in the modified version. Comparison is also performed among the trajectory plots generated by *CADMA*, *RF* and *WinRock*. Finally, the problems involved with the modified program *WinRock* are discussed.

4.2 Modifications Made to The Program

The original program by Gordon Elliott in 1992 was written using GWBASIC and hence it is a DOS based menu-driven program. The simulation logistics and calculation sequence involved in the program *Rockfal2* are discussed in detail in Appendix A. The program first prompts the user to specify the input parameters. After the input parameters are specified, the user will be able to save the input file and perform the rockfall simulation. The output can be viewed in terms of graphs that give statistical information of number of boulders, distribution of boulder heights, and velocities at analysis point. Although the output can be

viewed, it cannot be printed and hence the image has to be captured by a “grabbing” software. The text output from the program can also be saved so it can be reviewed by the analyser at a later time. Based on the present standards of the application softwares that are available in the market, it was decided to incorporate the following technical and aesthetical changes:

- Randomising the starting position of the boulder
- Randomising the starting velocity
- Generating 20 representative boulder trajectories
- Improving the aesthetics of the program by “window-ising” the program.

4.2.1 Randomising Starting Position and Velocity of The Boulder

Randomisation was carried out using the Monte Carlo method already available in the core program. The changes made for starting position and velocity were done by enabling the user to specify mean and standard deviation values for the parameters, which are used by the program to vary starting position and velocity of every boulder using the Monte Carlo method. The Monte Carlo method assumes a normal distribution of the values between mean plus standard deviation and mean minus standard deviation. Hence, the starting position and/or velocity of the boulder are initially specified as mean and standard deviation. For every run of the rockfall, the program selects a particular value using the specified mean and standard deviation values. If the user decides not to use the varied positions and velocities of the boulders, a value of zero can be specified for the standard deviation.

The randomisation of initial position and velocities enables the user to check the effects of a “range” of boulders that have the potential to get dispatched from a “range” of starting positions with different velocities, instead of the same starting position and velocity for all the boulders. For example, in a typical rockfall area, the boulders may not initiate from the same point and with the same velocity every time; instead, they can get despatched from a range of heights and locations with varying velocities. Hence, these changes are made to incorporate more randomness to the simulations and thus make simulation more realistic.

4.2.2 Generating 20 Representative Boulder Trajectories

The original program *Rockfal2* does not show the boulder trajectories. The generation of boulder trajectories is important for analysis of rockfalls to get a pictorial view of how the

boulders are actually coming down the slope. Hence, it was decided to add generation of boulder trajectories to the program. The modification to generate 20 trajectories is an artificial one and does not effect the simulation.

The generation of trajectories will be carried out by storing every position (x,y), of the boulder when it is coming down the slope, whether it is bouncing, or rolling. The original program calculates only the impact points when the boulder is bouncing. Hence, additional programming was required to generate intermediate points between two impact points. As the storage of trajectory points of each boulder consumes a lot of memory space in the computer, it was decided to generate only 20 representative trajectories of the rockfalls simulated. Hence, no matter how many boulders are simulated, the program generates trajectories for only 20 boulders. For example, if 100 simulations are performed, the program will generate a trajectory for every fifth boulder.

4.2.3 Improving The Aesthetics of The Program

As stated earlier, the program *Rockfal2* was originally written using GWBASIC, and is a menu-driven DOS based program. As there is no facility to print the program output, and the “appearance” of captured images is not aesthetically good enough to be included in technical reports, it was decided to re-write the program in a windows based environment. After considering different ways of “window-ising” the program, it was decided to use MSEXCEL for the following reasons:

- Facility to input parameters in a tabular form and also to edit, cut, and paste
- Very widely used and available program
- Facility to plot graphs, and also to cut and paste the graph to be included in a technical report
- Facility to use the Visual Basic programming as a Macro. This is very helpful as the core program was written in BASIC language and only a few changes and additional programming is required for adaption of the program in MSEXCEL.

4.3 “WinRock”-The Modified Program of The Original *Rockfal2*

The modified program is about 22 full A4 sized papers. The logistics of the program were not altered, but the additional programming required was for adaption of the program in MSEXCEL, generation of trajectories, and additional randomisation incorporated. As the

program occupies 22 pages, it was decided to include the program on a floppy disk attached to the thesis, instead of increasing the bulk of thesis. The program can be found in one of the spreadsheets (named "Rockfall Program") of the EXCEL file *WinRock* available on the floppy. The program for the generation of the trajectories is included in another spreadsheet (named "Plot Trajectories") of the same EXCEL file *WinRock*. Figure 4-1 shows the layout of the modified program "WinRock". The program is simply an EXCEL spreadsheet file. The user can open the file in EXCEL and work as he/she works on a normal EXCEL spreadsheet. It is assumed that the user is familiar with MSEXCEL. The buttons named as "Run" and "Plot Trajectories" were created for the use of program. The user should press the button "Run" for simulation after entering all the required input. It is generally recommended to save every modified file (in terms of input data) under a different name to avoid confusion and also to save the original file *WinRock* from any mistakes of mis-entry.

The screenshot displays the Microsoft Excel interface for the 'Rockfall Simulation Program'. The main window title is 'Microsoft Excel - COMPARE.XLS'. The menu bar includes File, Edit, View, Insert, Format, Tools, Data, Window, and Help. The toolbar shows various icons for file operations and formatting. The worksheet area is titled 'Rockfall Simulation Program' and contains the following sections:

- Run Identification :**
 - Run Title :
 - Description :
 - Run Number :
- Boulder Information:**
 - Diameter :
 - Density :
 - Gravitational acceleration :
- Initial Conditions :**
 - X - Starting position :
 - Y - Starting position :
 - Trajectory :
 - Rotational Velocity :
- Simulation Details :**
 - Enter Number of Simulations to be performed:
 - Enter X - Coordinate of Analysis point :
 - Number of simulations to be completed :
 - (Need not input anything in this cell. Look for the countdown)

Two buttons are present: 'Plot Trajectories (Click once only after Run)' and 'Run'. The status bar at the bottom shows 'Ready' and 'NUM'.

Figure 4-1: Layout of the main sheet of the program *WinRock*.

4.3.1 Input for The Program *WinRock*

Figure 4-1 shows the sheet named as “Main”, which is the main sheet of the program where all the input for the rockfall simulation is entered. All the facilities that are available in EXCEL are obviously available for this program as well. Figure 4-2 shows the window in the same sheet to input the slope information. About 100 slope cells (coordinates) can be input.

4.3.1.1 Run Identification

The first part of the input is the identification of the rockfall simulation; like run title, and description. The box shown on the other end of the sheet named “Run Number” (cell G5) is the number of times the simulation has been carried out for the same input. To start with, the user has to input “1”. This is the identification number for the number of runs the user carries out, which will be used by the program for plotting graphs and trajectories later, during simulation. The user need not change the “Run Number” for every rockfall simulation for the same slope, as it will be automatically changed by the program. The user has to remember to input number “1” only when starting with a new slope or on a fresh start of the simulation for a new slope.

4.3.1.2 Boulder Information

This part of the input is for the information about the boulder that is to be simulated. As the program assumes a spherical shape of the boulder, the input parameters for the boulder will be diameter (cell B10), density (cell B11) and the acceleration due to gravity (cell B12). As the user can specify the value of acceleration due to gravity, it can be used for any type of measurement of units. For example, if the user wants to use FPS system of units, he/she can specify the gravity as 32.2 ft/sec, whereas, for SI units, 9.81 m/sec. The only thing the user has to remember is to maintain consistency of units.

4.3.1.3 Initial Conditions

Initial conditions of the boulder include starting position (cells B16, B17 and B19), initial velocities (rotational (cell B21) and translational (cells B17 and C17)), and the trajectory angle (cell B20) of the boulder relative to the absolute horizontal. The X-coordinate of the starting position and velocities can be varied using Monte-Carlo methods, assuming a normal distribution using the mean and standard deviation values. Hence, the translational velocity and the X-coordinate of the starting position can be given mean and standard

deviation values. If the user decides not to use the “range” of starting positions and velocities, a standard deviation of zero can be specified. This will disable the random variation of input parameters.

4.3.1.4 Simulation Details

Simulation details to be input are the total number of simulations that the user intends to perform (cell G16), and the X-coordinate of the analysis point (cell G17). The analysis point is important for the analysis of rockfalls to check the boulder height distribution, velocity distribution and the total number of rocks reaching. This, in turn, can be used for design of protection structures such as height of fence and depth of catch ditch. The cell besides the box named “Number of simulations to be completed” (cell G18) is the cell where the user can see the countdown of the number of simulations that are yet to be performed, while simulating rockfalls. Hence, the user need not input anything in this cell, and is shaded with green colour to distinguish it from input cells.

Microsoft Excel - COMPARE.XLS

File Edit View Insert Format Tools Data Window Help

Times New Roman 12 B I U

G5 2

22 Slope Information :

23

24 (Coordinates for The Slope) [Coeff. of Normal Restitution] [Coeff. of Tangential Friction] (Slope Roughness)

	X	Y	Mean	Std.Dev	Mean	Std.Dev	Std.Dev
26	0.00	66.00	0.36	0.050	0.85	0.050	11.00
27	3.00	64.00	0.36	0.050	0.85	0.050	11.00
28	4.00	62.00	0.36	0.050	0.85	0.050	11.00
29	5.00	62.00	0.36	0.050	0.85	0.050	11.00
30	6.00	61.00	0.36	0.050	0.85	0.050	11.00
31	7.00	59.00	0.36	0.050	0.85	0.050	11.00
32	8.00	58.00	0.36	0.050	0.85	0.050	11.00
33	9.00	57.00	0.36	0.050	0.85	0.050	11.00
34	9.00	56.00	0.36	0.050	0.85	0.050	11.00
35	10.00	55.00	0.36	0.050	0.85	0.050	11.00
36	10.00	54.00	0.36	0.050	0.85	0.050	11.00
37	11.00	54.00	0.36	0.050	0.85	0.050	11.00
38	11.00	53.00	0.36	0.050	0.85	0.050	11.00
39	13.00	51.00	0.36	0.050	0.85	0.050	11.00
40	14.00	50.00	0.36	0.050	0.85	0.050	11.00
41	16.00	50.00	0.36	0.050	0.85	0.050	11.00
42	16.00	49.00	0.36	0.050	0.85	0.050	11.00
43	17.00	48.00	0.36	0.050	0.85	0.050	11.00
44	18.00	48.00	0.36	0.050	0.85	0.050	11.00
45	18.00	47.00	0.36	0.050	0.85	0.050	11.00

Chart 1 - 6 Trajectory data 1 Output data1 Trajectory plot 1 Main Rockfall Program Plot Trajectories

Ready NUM

Figure 4-2: EXCEL sheet showing the input for slope.

4.3.1.5 Slope Information

Figure 4-2 shows the input required for the slope information which starts from the row number 26. Input about the slope includes the coordinates for each slope cell (columns A and B), coefficient of normal restitution (columns C and D), coefficient of tangential friction (columns E and F), and slope roughness (degrees) (column G). The normal coefficient of restitution and coefficient of tangential friction are specified as mean and standard deviation values, but the slope roughness is specified as the standard deviation value only. For each simulation of rockfall, the program checks the position of the boulder and thus determines the slope cell which it is presently in. According to this information, the program uses the mean and standard deviation values of the coefficients (for that particular slope cell) to generate a random value for these coefficients. The slope roughness is determined by varying the angle between zero and the standard deviation value. The three parameters can be specified for each slope cell so that they can be altered down slope wherever required.

4.3.2 Rockfall Simulation Using The Program *WinRock*

Once the input for the program has been entered, the user can proceed on to the simulation of rockfalls. To do this, he/she should simply press the button named "Run", which enables the execution of the simulation program. The rockfall simulation is then carried out according to the logistics discussed and following the calculation sequence detailed in Appendix A. After the program executes and creates six different graphs and writes the statistical output on a separate sheet, the program returns back to the sheet named "Main". If the user wants to look at the trajectories of the boulders that have come down the slope, he/she should press the button named "Plot Trajectories" to enable the program to plot the trajectories that are stored in the sheet named "Trajectory Data". It should be noted that the user has to press the button to plot trajectories *once* and *only* after each simulation of rockfalls. The program then gives the output of the simulation in the form of graphs and tables discussed in the following section.

4.3.3 Output from The Program

As an example of simulation, the slope used for the comparison of rockfall simulation programs in Chapter 3 has been analysed. Figures 4-3 to 4-10 shows the output from the program *WinRock*. The program output includes the following:

- For each rockfall simulated, (Figure 4-3) (sheet name = “Output data n¹”)
 - X-coordinate of the position where the boulder has stopped (Xmax, column A).
 - Y-coordinate of the position where the boulder has stopped (Y@Xmax, column B).
 - translational and angular velocities of the boulder at the analysis point (Va & Wa, columns C & E).
 - height of the boulder at analysis point (Ha, column F).
 - angle of the boulder at analysis point (Aa, column D).
- Statistical data giving, (Figure 4-4) (sheet name = “Output data n”)
 - the X-coordinate interval and the total percent of boulders stopping and crossing the interval.
 - the velocity interval and the percent stopping and crossing the interval at the analysis point.
 - the height interval and the percent stopping and crossing the velocity interval at the analysis point.
 - Total percentage of boulders reaching the analysis point.
- Six different graphs showing
 - maximum boulder travel in horizontal direction (Figure 4-5) (sheet name = “Chart n-1”).
 - percentage of boulders reaching specified X-coordinates (Figure 4-6) (sheet name = “Chart n-2”).
 - boulder velocity at analysis point (Figure 4-7) (sheet name = “Chart n-3”).
 - percentage of boulders exceeding given velocities at analysis point (Figure 4-8) (sheet name = “Chart n-4”).
 - boulder height above ground surface at analysis point (Figure 4-9) (sheet name = “Chart n-5”).
 - percentage of boulders exceeding given heights at analysis point (Figure 4-10) (sheet name = “Chart n-6”).
- Coordinates for the trajectory followed by 20 of the total rockfalls simulated (Sheet name = “Trajectory data n”).
- Trajectory plot showing 20 representative boulder trajectories (Figure 4-11) (sheet name = “Trajectory plot n”).

¹ n is the simulation run number for that particular simulation.

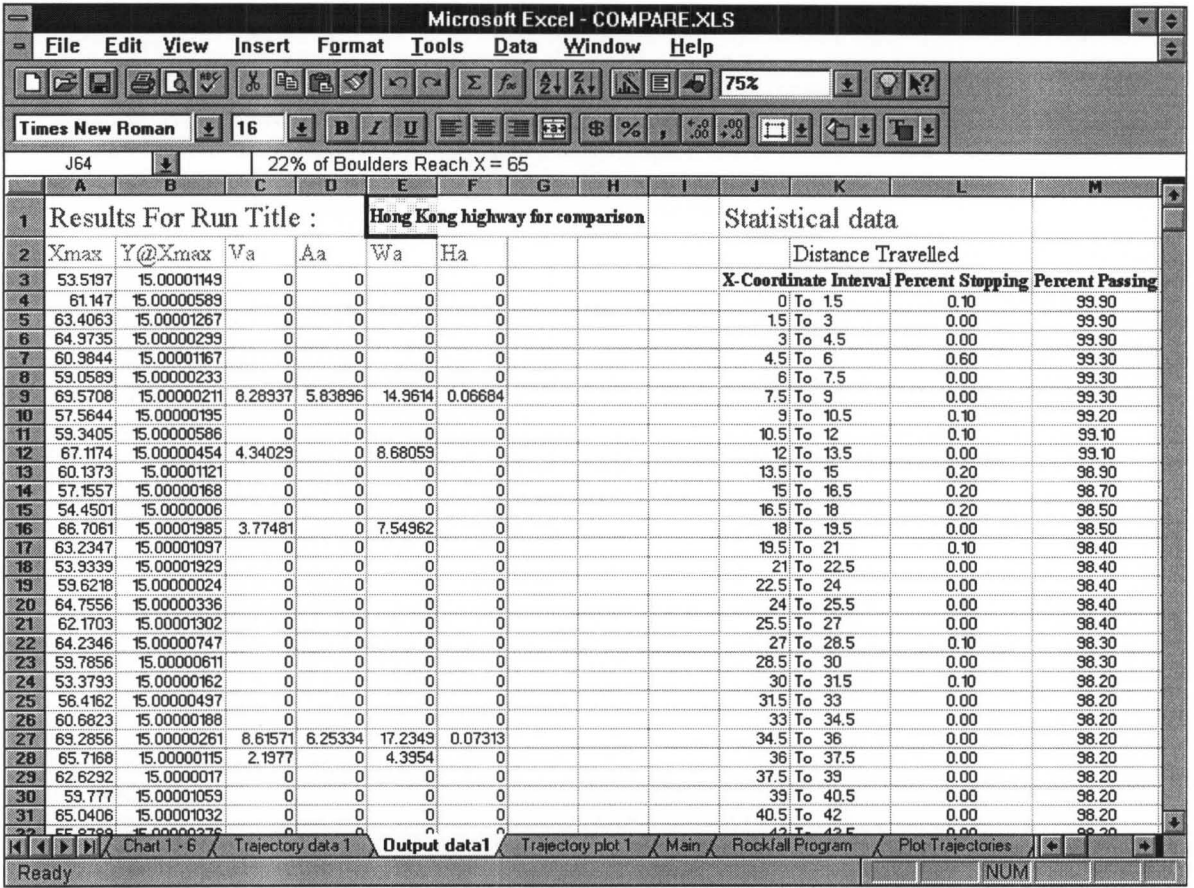


Figure 4-3: Output data from the program WinRock.

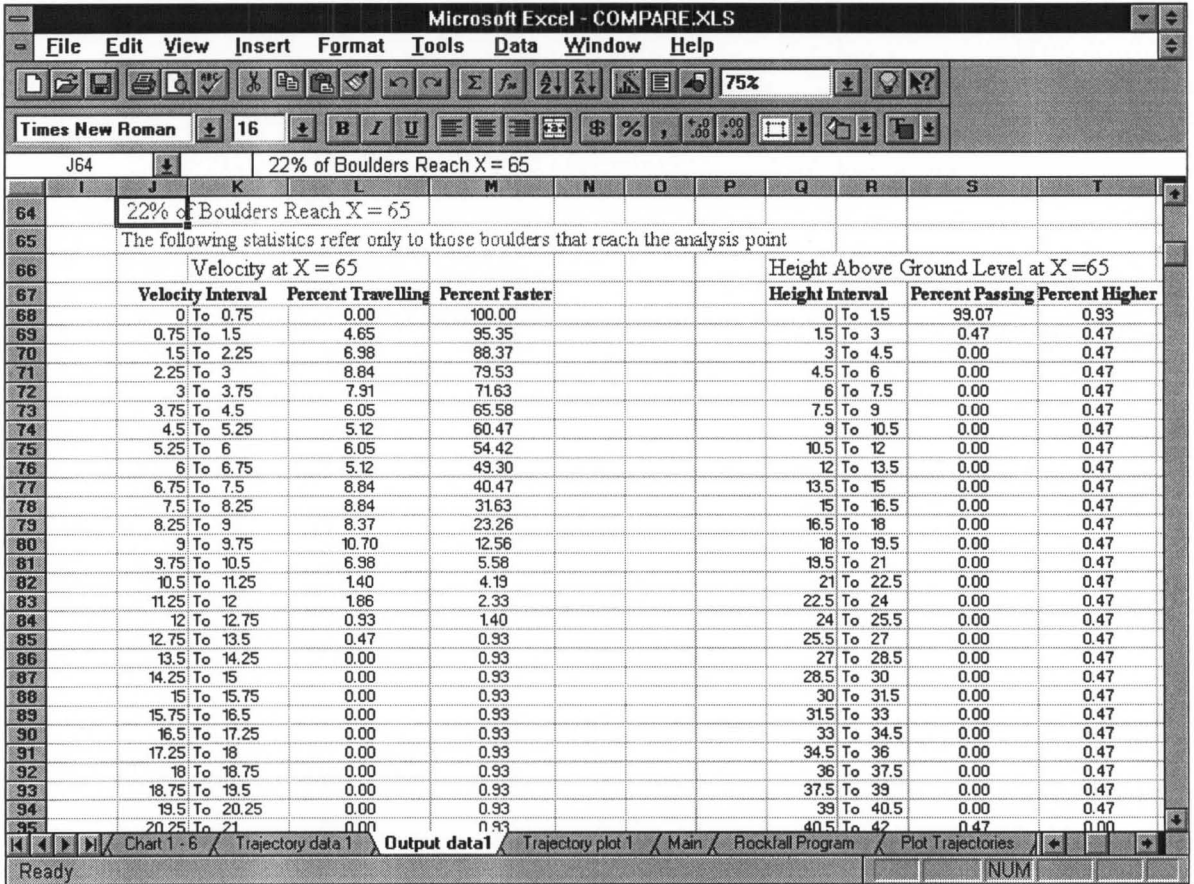


Figure 4-4: Statistical output data from the program WinRock.

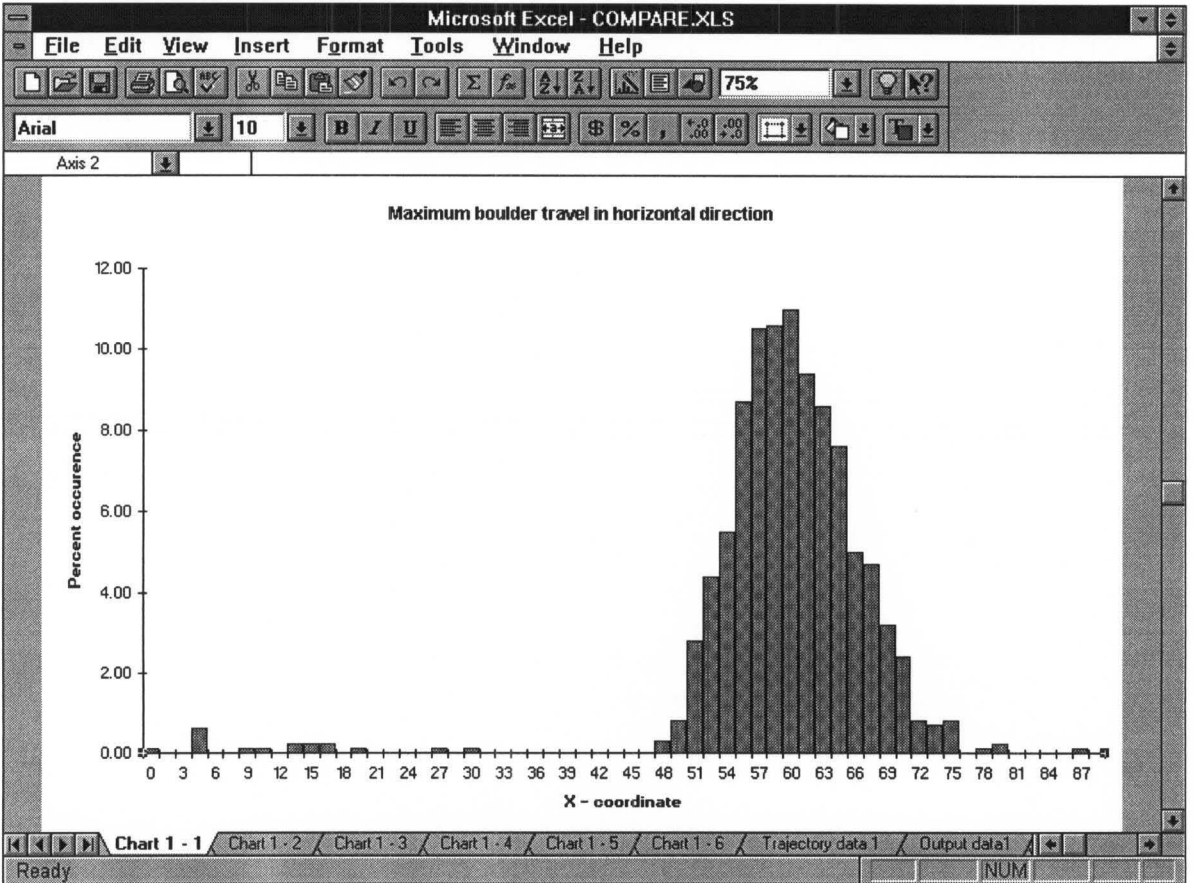


Figure 4-5: Maximum boulder travel in horizontal direction (*WinRock*).

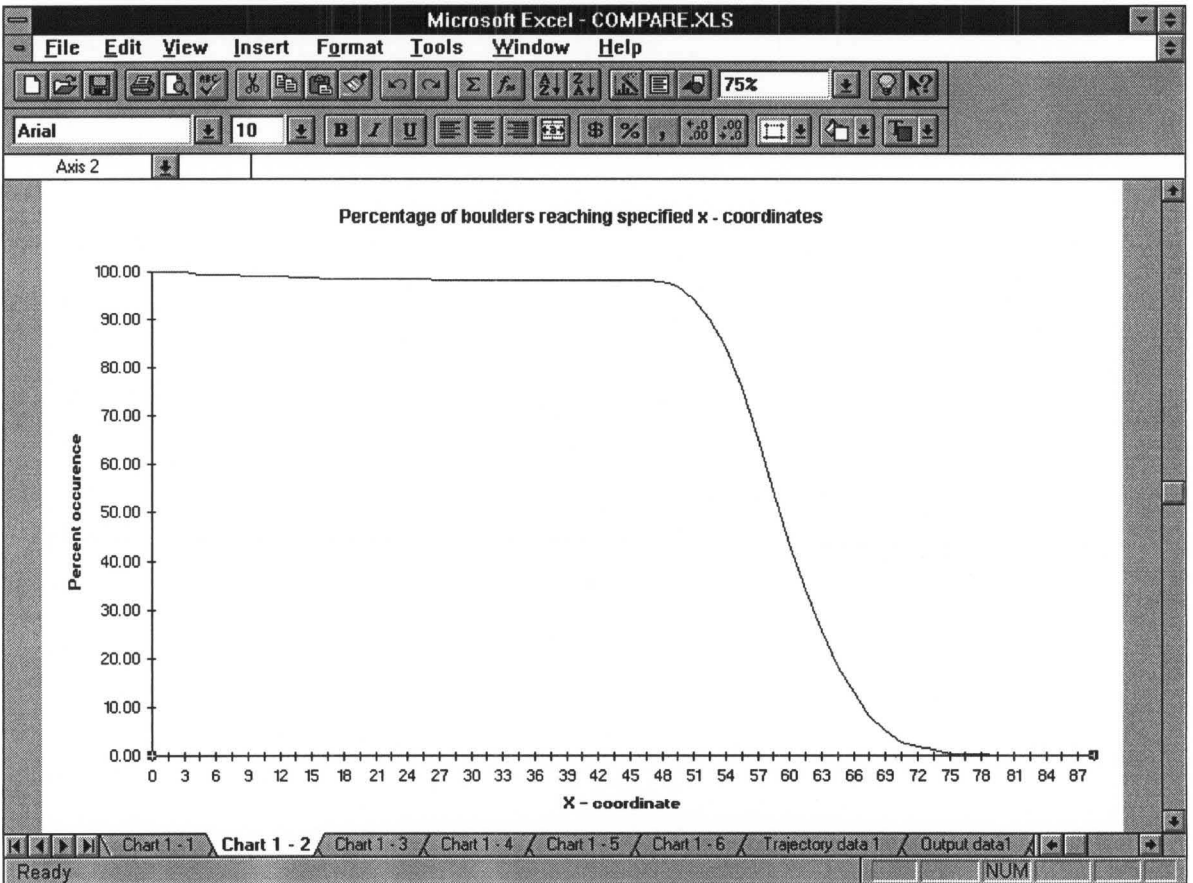


Figure 4-6: Percentage of boulders reaching specified X-coordinates (*WinRock*).

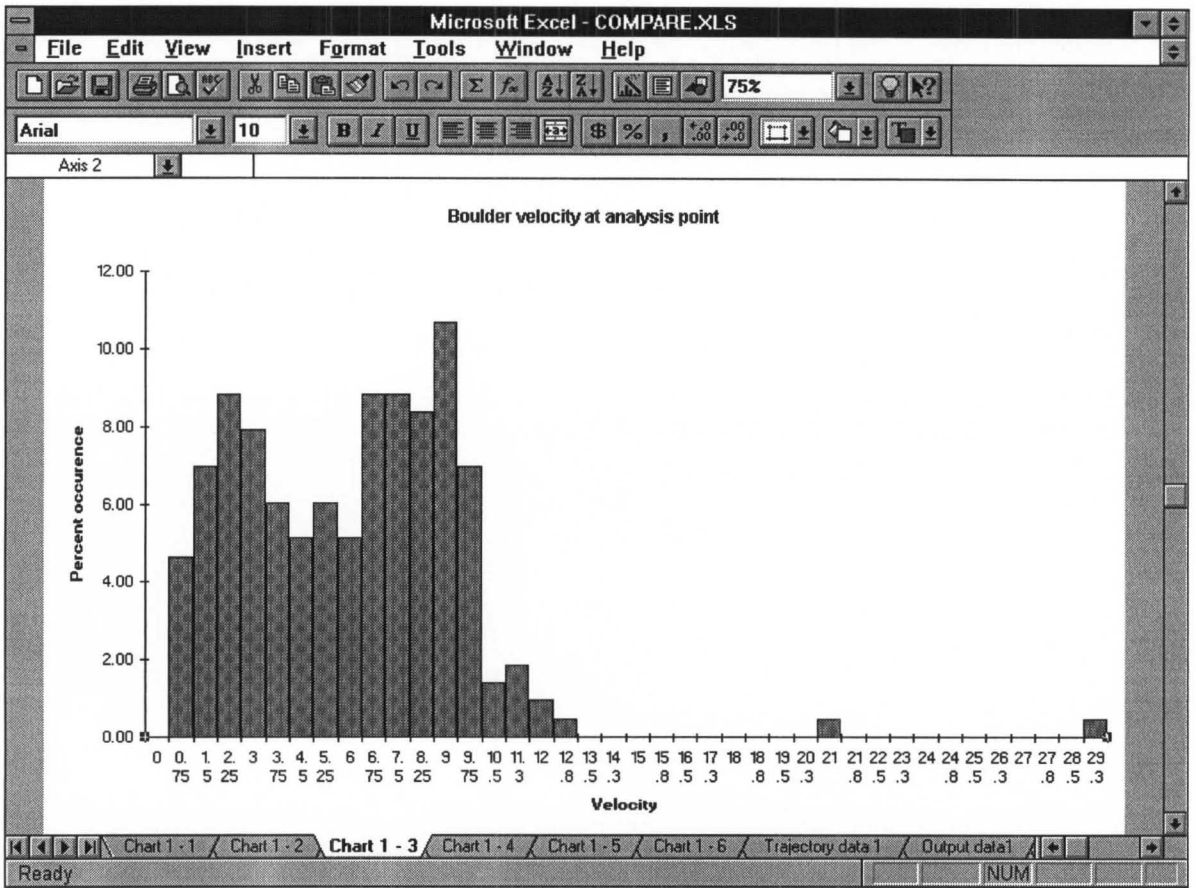


Figure 4-7: Boulder velocity distribution at analysis point (*WinRock*).

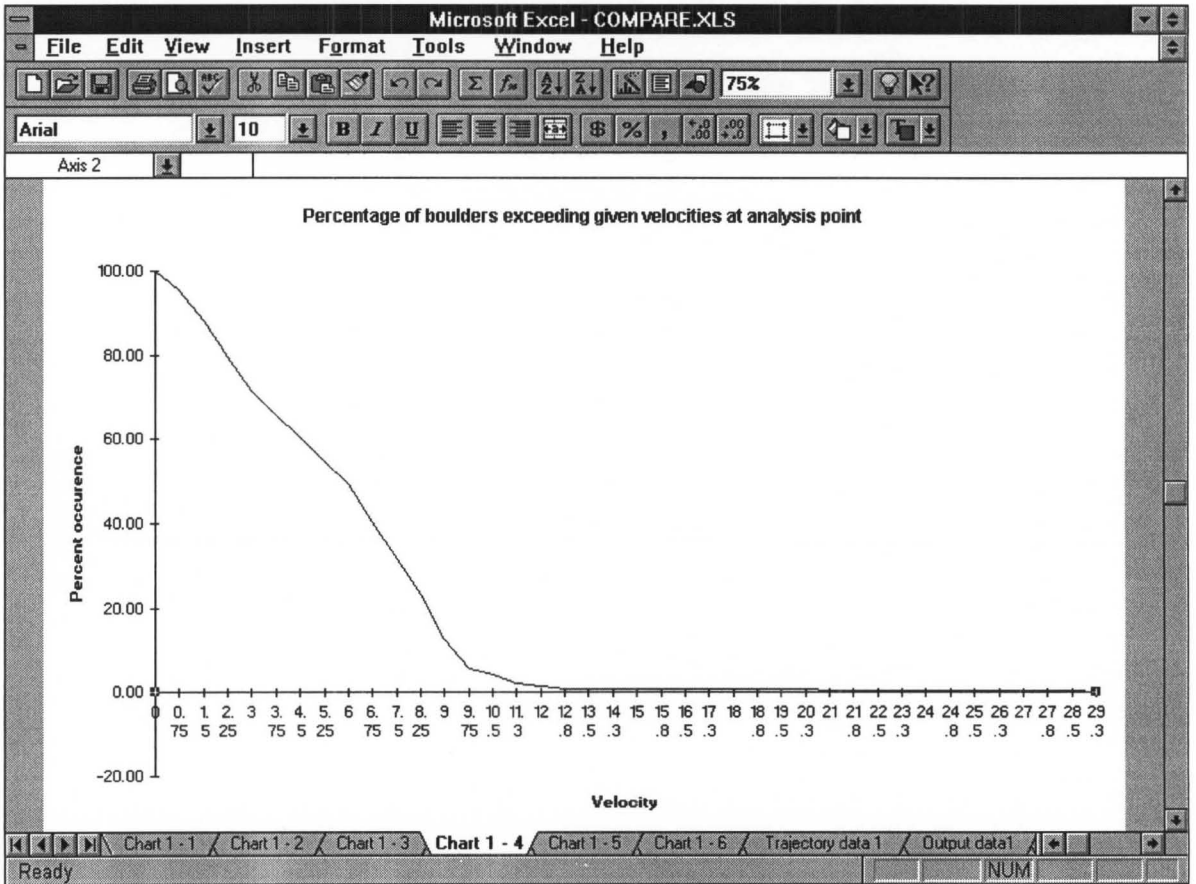


Figure 4-8: Percentage of boulders exceeding given velocities at analysis point (*WinRock*).

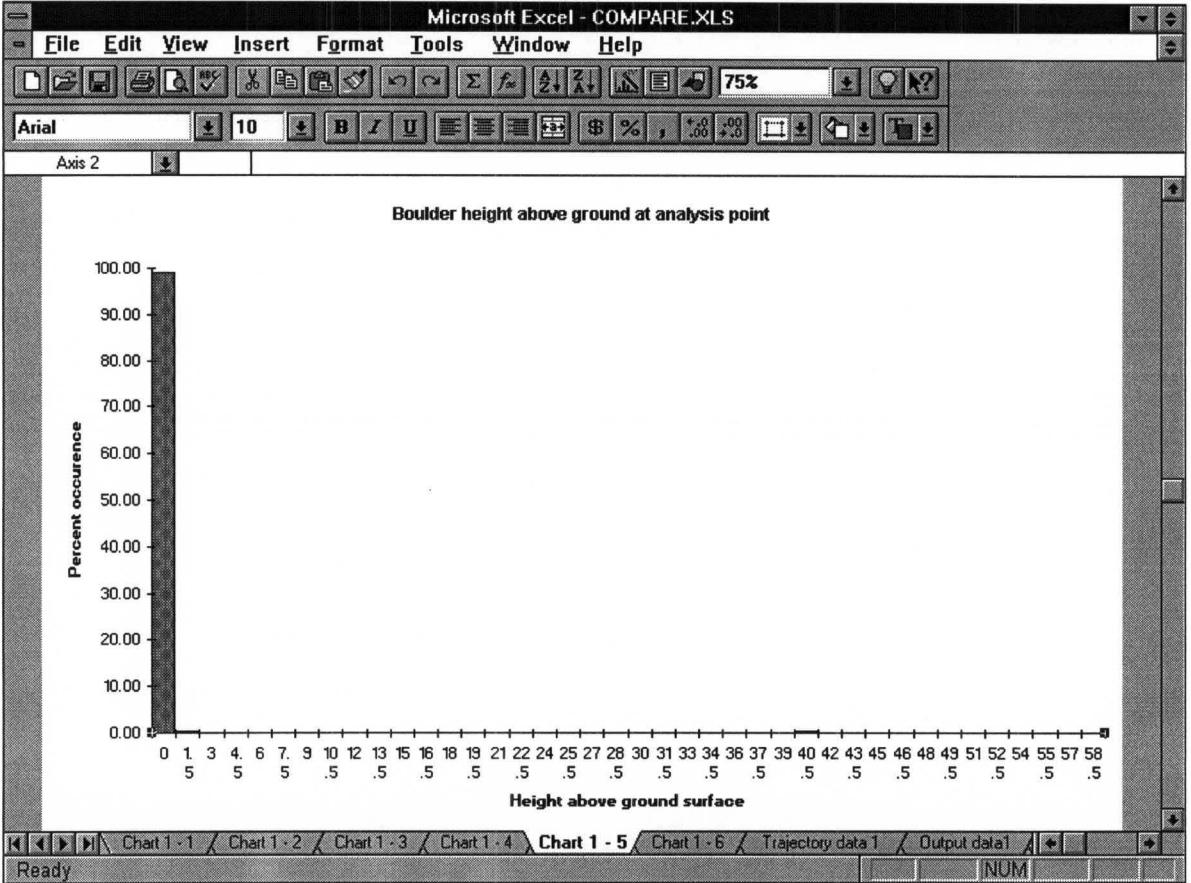


Figure 4-9: Boulder height above ground surface at analysis point (*WinRock*).

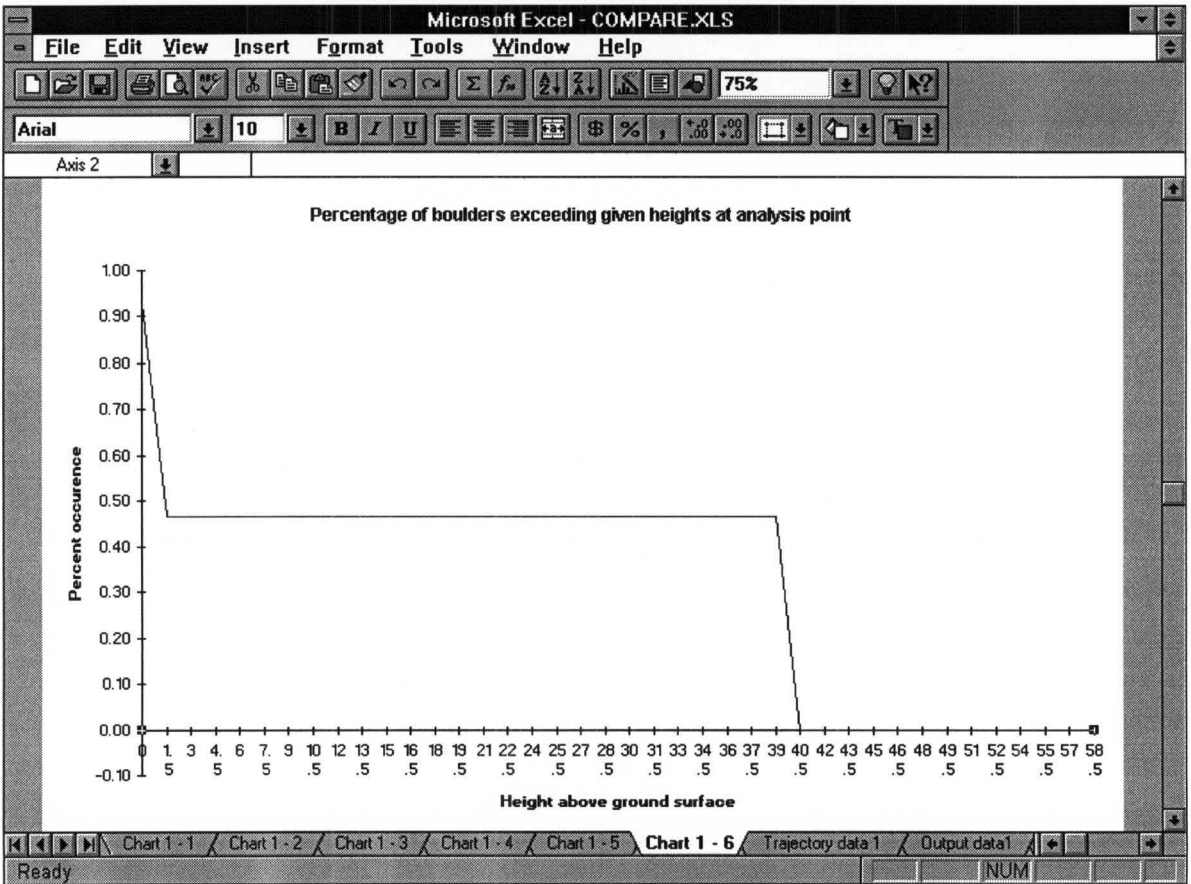


Figure 4-10: Percentage of boulders exceeding given heights at analysis point (*WinRock*).

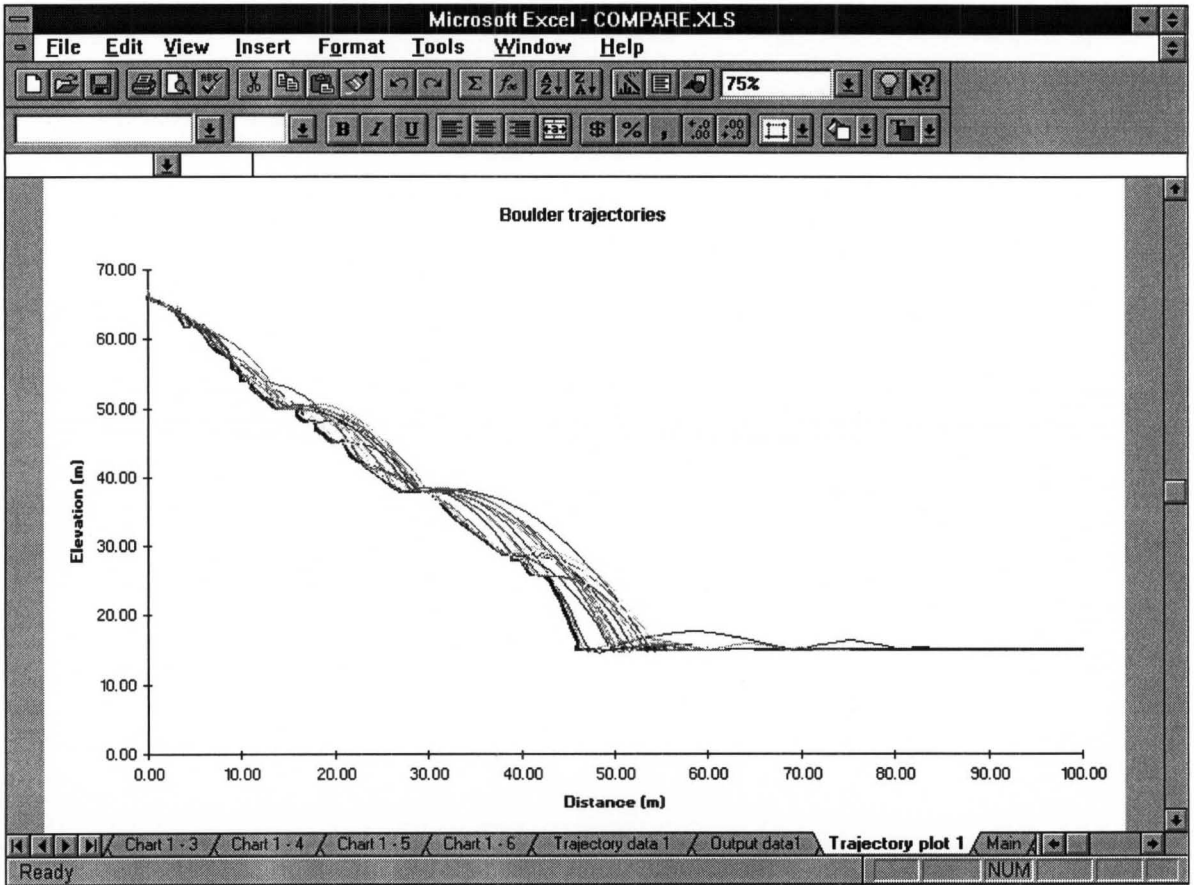


Figure 4-11: Boulder trajectories for the slope analysed (*WinRock*).

4.4 Comparison of Program Output from *Rockfal2* and *WinRock*

The input data used for comparison of rockfall simulation programs (section 3.2.6.1) has been used for this purpose. This check is essential to see if the simulation and output data are exactly the same for both *Rockfal2* and *WinRock*.

Using *WinRock* the total percentage of boulders that have reached the analysis point of 65m is 22, which is almost the same as for *Rockfal2* (considering the variance generated in the output pertaining to the randomisation of parameters). Comparison of all the graphical and text output from *Rockfal2* (Figures 3-11 to 3-16) with those from *WinRock* (Figures 4-5 to 4-10) confirmed that there is no change in output of the program *WinRock*. The comparison also proves the aesthetic changes of the program².

² Please note that the images shown are captured images, but they can be printed out neatly on to separate sheets from the EXCEL file if necessary.

4.5 Advantages of *WinRock* Over *Rockfal2*

The major advantages of *WinRock* over *Rockfal2* are listed below:

- Windows based program which provides a user-friendly interface.
- Improved aesthetics of the graphical output to be included in technical reports.
- Generation of trajectories to get a pictorial view of how the boulders actually come down the slope.
- Improved randomisation by variation of starting velocity and initiating point of rockfall.
- Allows user to browse through the output data from earlier simulations as all the output data will be saved in the same file. This is particularly helpful while performing iteration analysis of rockfalls.

4.6 Comparison of Trajectories from *WinRock* With Those from *CADMA* and *RF*

Figures 4-11, 4-12 and 4-13 show the boulder trajectory trends from *WinRock*, *CADMA*, and *RF* respectively. From the figures, it can be seen that generation of trajectories look similar for *RF* and *WinRock* in terms of randomisation. The program *CADMA* does not seem to have used sufficient randomness while simulating rockfalls for this slope. This is evident from Figure 4-12 as all the boulders seem to have come down the slope following a similar trajectory with bouncing at almost the same point.

The trajectory output from the program *WinRock* shows some trajectories at the flat ground which seem to be unusually long jumps. This would indicate that there is an error in the program, but as can be seen, the trajectory that is projecting a long jump is starting from a bounce which has come down from 25 m up the hill. The velocity by which it is impacting the flat ground may be very high and hence, there is a possibility of long jump. Also, it is to be noted that a normal coefficient of restitution of 0.3 (Table 3-10) has been specified for the ground which is sufficient to keep the rock bouncing.

Overall, it is evident that 85% of the boulder trajectories generated by *WinRock* are similar to those from the programs *CADMA* and *RF*. However, the user should remember that the trajectory plot in the program *WinRock* is sometimes erroneous which is further explained in the following section.

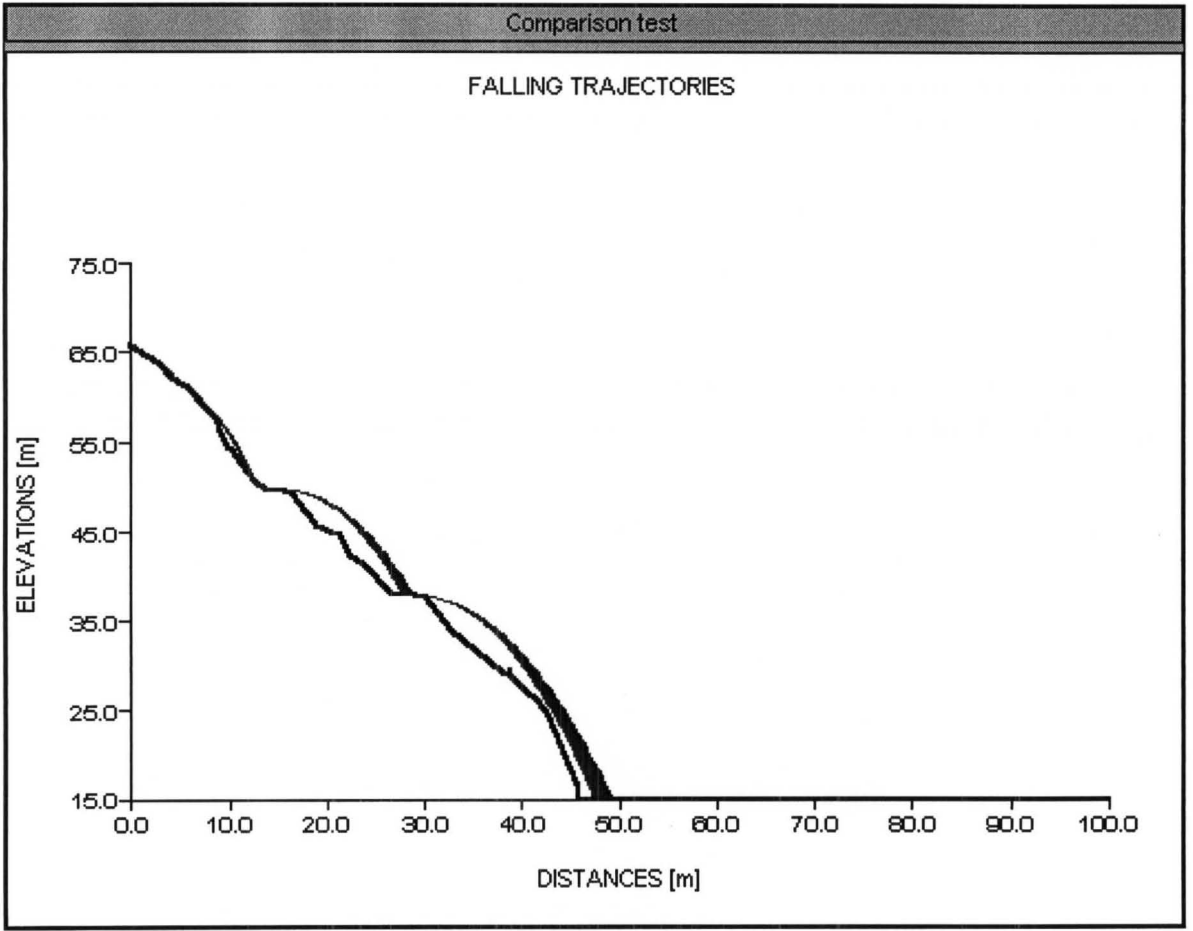


Figure 4-12: Boulder trajectories (*CADMA*).

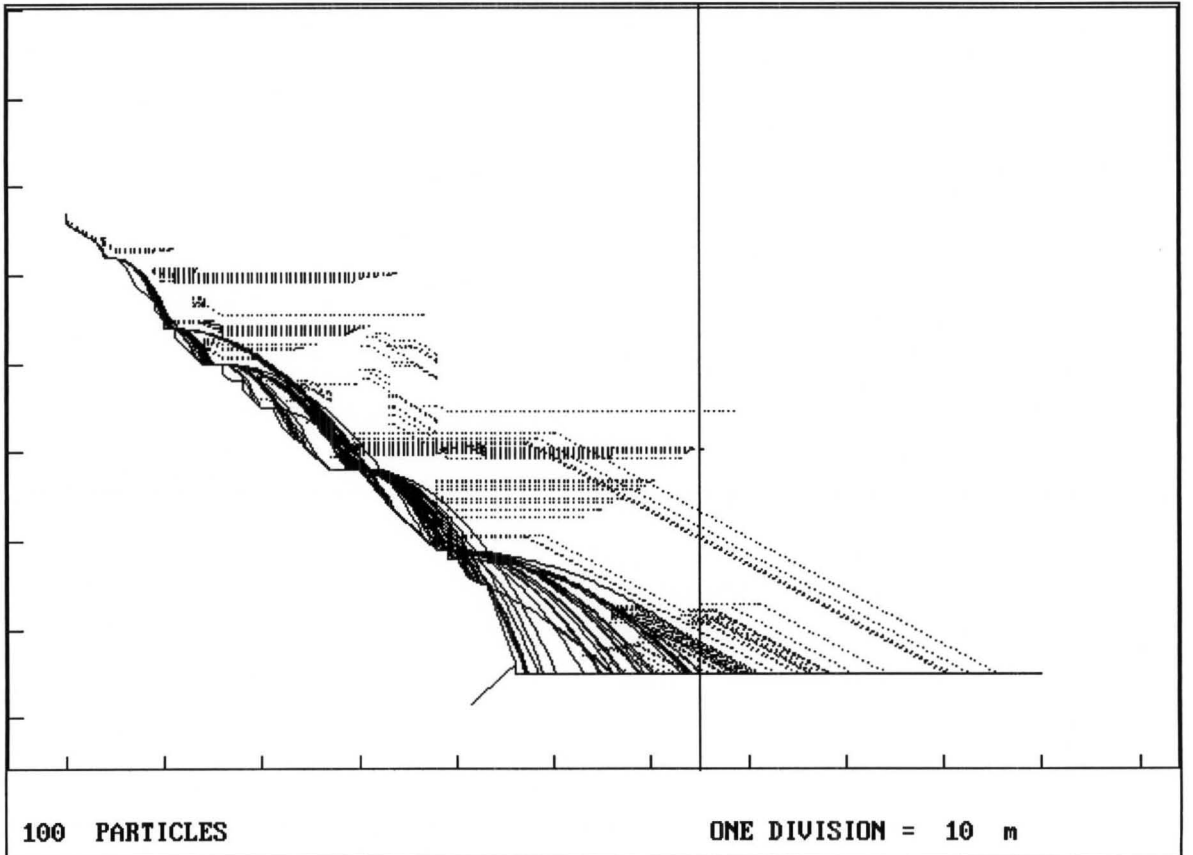


Figure 4-13: Boulder trajectories (*RF*).

4.7 Bugs and Rules of The Program *WinRock*

As the program has been rewritten in MSEXCEL, some unavoidable bugs have been introduced. Following are the main problems associated with the program and some of the rules to be followed while simulating rockfalls using *WinRock*:

- There are no error traps for the input of the program. For example, the user should remember to enter the right number in right cell. To make it more clear, if the user inputs a value of 11 for restitution coefficient which is totally invalid, the program does not check the number and prompt the user to use the right number. Hence, the user should remember to input the right number for the right parameter.
 - As the program reads the data input from pre-assigned cells, the user should enter the input in the assigned cells only. If a cell is left empty, a value of zero is assigned to it.
 - If the user likes to specify a range of starting positions, he/she should specify the mean and standard deviation values so that the boulder will not start from behind the first coordinate of the first slope cell. This is because the Monte Carlo method assumes a normal distribution of values. For example, if the first X-coordinate is 0, and the user wants to specify a range of boulders starting from 0 to 10, the mean and standard deviation values can be 5 and 5 respectively.
 - The user should remember to maintain consistency in the usage of the units of measurement.
 - It is always better to keep the original file as it is, and save the modified file as a different EXCEL file.
 - For the purpose of plotting the boulder trajectories, the program generates six trajectory points between every bounce of the boulder, using the general projectile motion formulae which are dependent on velocity and time of flight. As the original program calculates only the bounce and impact points, the trajectory points are generated for the purpose of plotting trajectories *only*. Thus, sometimes the points will be generated in a very haphazard manner. For example as the boulder always comes down, the trajectory should be a parabola starting from a point at the top of the slope and coming down. As the trajectory points are generated using the initial and final velocities, the generation may instead give rise to coordinates of a trajectory followed by a ground to air missile, because of using a wrong sign (+ve or -ve) for velocities. However, the user should particularly note that the generation of trajectory points is *independent* of the rockfall simulation that is carried out to simulate bounce mode by the program. Hence the
-

haphazard boulder trajectories plotted *does not* mean that the program is simulating rockfalls inaccurately.

- Another point to remember while specifying the slope cells is that the user should specify another point very near to the point where there is a steep change in the slope. This is because the slope is plotted on a normal EXCEL chart and hence, the EXCEL program tries to round-up the curve. For example, if the slope consists of only two cells with a 70° bed rock slope joining the flat ground, the user should specify another point (in addition to the point where the bed rock intersects the ground) just after the intersection of the slope and the flat ground surface. It should also be remembered that this is only for the purpose of plotting and *does not* effect the rockfall simulation.
- While performing multiple simulation (e.g. by changing initial conditions) of rockfalls for the same slope, the user should remember to write a comment in the cell for “Run Title” as it will be copied onto the sheet “Output data”. This is helpful for later verification of the output.

4.8 Summary

The original program *Rockfal2* has been rewritten as a macro in an EXCEL file. This improved the aesthetics and user-friendliness of the program with the added advantages of user interface. Additional randomness has been incorporated to vary the initial translational velocity and the starting position of the boulder. Comparison of the output from the program *WinRock* with that from *Rockfal2* confirmed that the simulation logistics are unchanged.

Chapter 5 goes on to the application of the program *WinRock* for a detailed rockfall analysis for the Undercite Creek at Fox Glacier.

Chapter 5

Rockfall Analyses at Undercite Creek, Fox Glacier

5.1 Introduction

The modified program *WinRock* developed in Chapter 4 will be used in the present chapter for analysis of rockfalls at the Undercite Creek, Fox Glacier, to check the potential hazard of rockfalls reaching the new access road. First, a back-analysis of rockfalls is carried out to determine the parameters influencing the rockfall trajectory at the site using the position of the boulders that rolled down the slope in the past rockfalls. The parameters that are determined using the back-analysis are then used to predict rockfalls in the future and to determine the roll-out distance of the boulders. Conclusions are then drawn as to potential future hazards to a new access road from rockfall.

5.2 Rockfall History at Undercite Creek

In October-November 1992, the Department Of Conservation (DOC) closed a section of the northern access road to the Fox Glacier because of the damage of the road, and the safety hazard created by rockfalls at Undercite Creek (see map in Figure 1-2). Since this period, slope failure has escalated, necessitating re-location of the access road along the flood plain of the Fox River, away from the base of unstable slopes. In January 1994, heavy rockfalls occurred and about one million cubic metres of material came down the slope, closing the North Bank access road completely. After this incident, DOC re-located the access road further south onto the flood plain of the Fox River. Occasional roll-out of boulders onto the access road was reported during 1995, which required a further re-location of the access road away from the rockfall debris. Photo 5-1 shows the previous and present locations (1995 and 1996-97) of the access road.

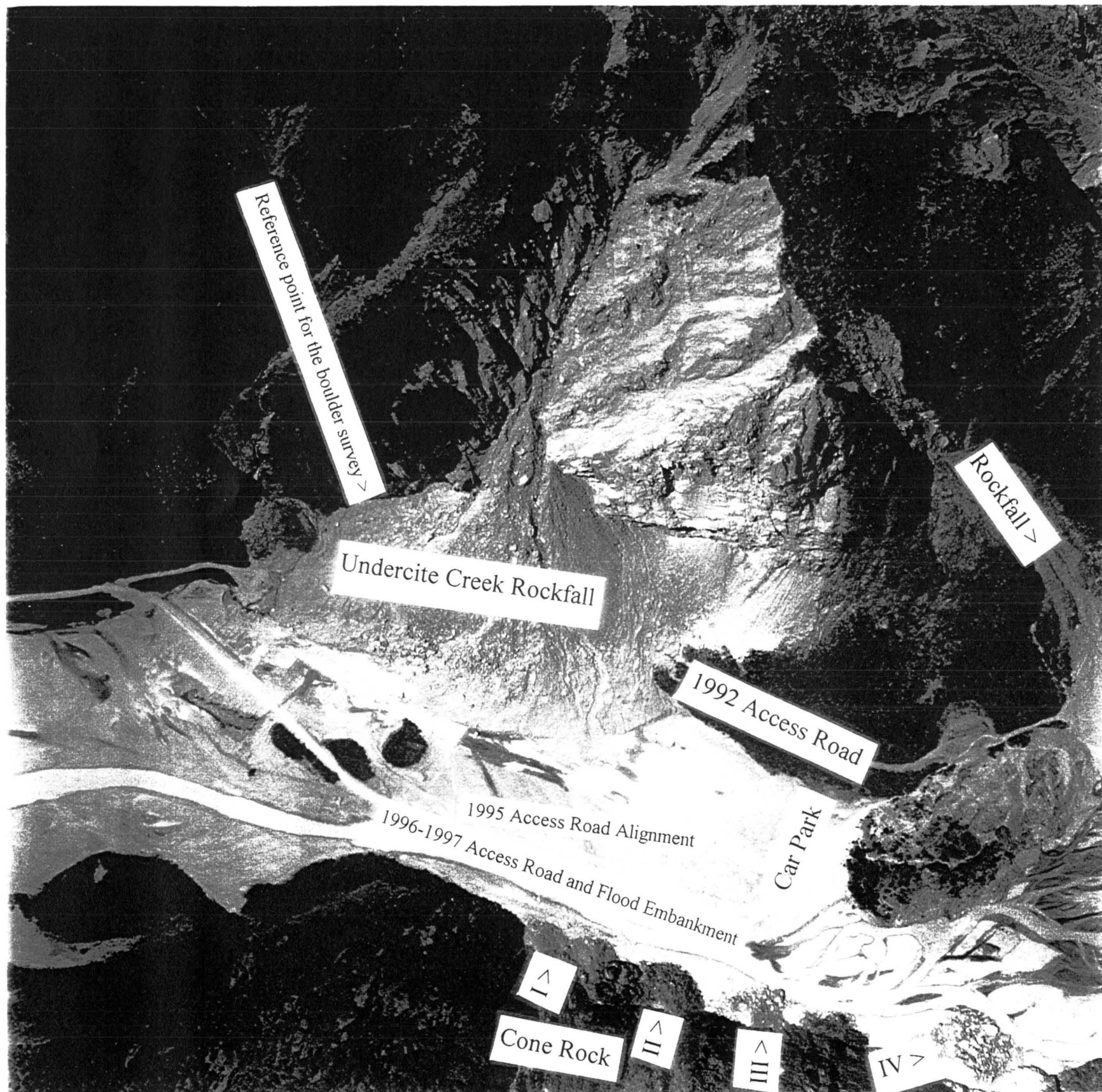


Photo 5-1: Vertical aerial photograph of the site taken by DOC during January 1997 showing the locations of rockfalls (courtesy: Brian Paterson) (Scale: 1: 5400)

5.3 Site Description

This section describes the location, geology and geomorphology and the environment of the Fox valley.

5.3.1 Location

The main slope failure is located on the north-eastern side of the Fox River valley, 3.2 km along the northern access road from State Highway 6, and approximately 1.5 km downstream from the glacier terminus. Photo 5-2 shows a recent photograph of Undercite Creek taken in April 1997.

5.3.2 Geology and Geomorphology

Paterson (1994) describes the Fox valley as a typical broad, U-shaped glacial valley, containing glacial till, glaciofluvial deposits, and alluvial fans deposited by tributary streams. Yellow Creek has formed a large alluvial fan which extends well across the Fox valley, forcing the river against the true left bank. On the north-eastern side of the valley, steep rock slopes on either side of Undercite Creek and First Creek were undercut by the Fox glacier as recently as 1955 (Sara 1979). It is generally believed that the retreat of the glacier terminus has made the valley unstable, ie when the ice is removed from the valley, the over-steepened walls tend to rebound.

The main feature of the geology is the Alpine Fault which forms a boundary between mountainous terrain to the east, and areas of low relief to the west (Figure 1-2). Southeast of the Alpine Fault the rock consists of highly indurated Alpine Schist - a hard foliated and jointed rock. Northwest of the Alpine Fault, near-surface materials consist of alluvium and glacial deposits. Detailed geological mapping by Hanson *et al.* (1990) revealed three sets of faults in the area, two of which are dominant in the Fox valley. One set crosses the valley in a north-easterly direction parallel to foliation (mineral layering/cleavage) in the schist (Figure 5-1), and to the Alpine Fault. A second set is parallel to the main valley downstream of the glacier terminus (Gunn 1960). These features have an important influence on the location and development of slope failures in the study area (Paterson 1994). Faulting in Undercite Creek consists of a series of low angle ($30-40^{\circ}$) faults which strikes across the ridge between Yellow Creek and the Fox valley, and dip towards the north.

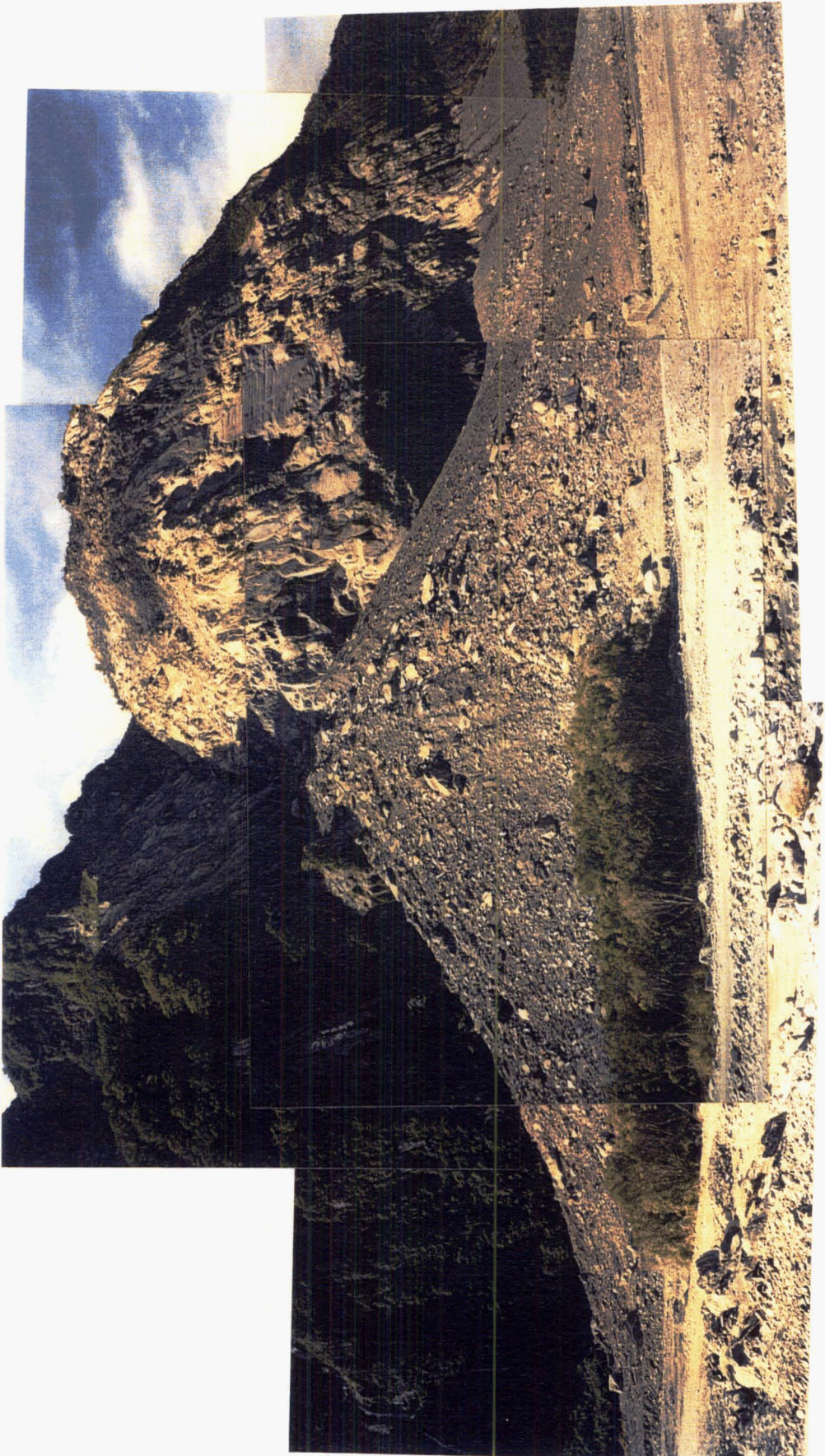


Photo 5-2: Photograph taken from the ground showing the whole slope of Undercite Creek.

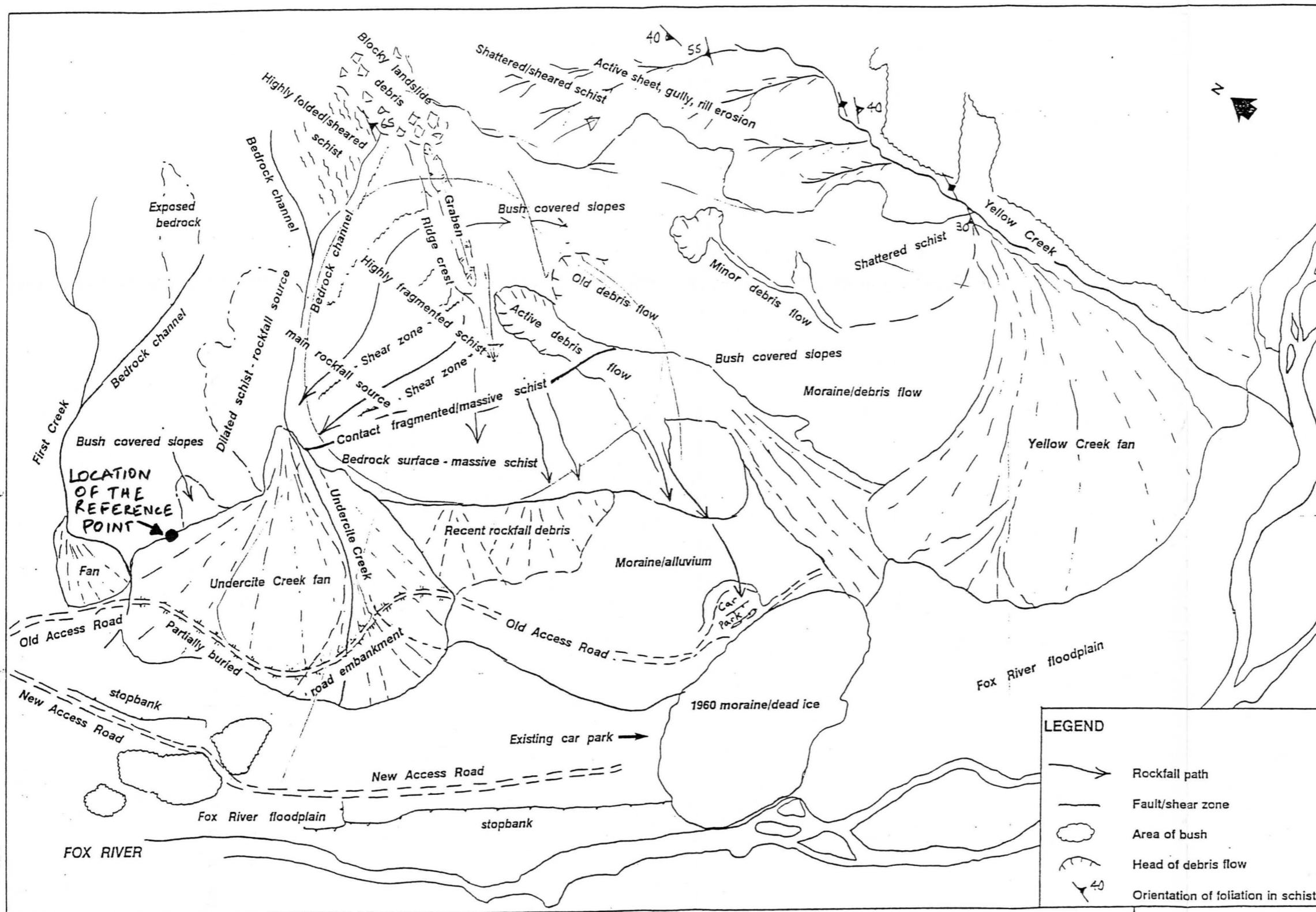


Figure 5-1: Map of Undercite Creek - Yellow Creek area showing geomorphic features and geologic structure (courtesy: Brian Paterson) (Scale: 1:5000).

These features are exposed only on the denuded rock face near the top of the ridge immediately south-east of Undercite Creek. The highly sheared rock mass within this fault zone is highly erodible and comprises the main potential source of rockfall and rock avalanche debris.

5.3.3 Environment

According to New Zealand Meteorological Service Publications (1983), the average daily range of temperature is -2.4 (min) to 9.5 (max) degrees Celsius. Hence, at certain times, there appears to be freeze-thaw cycles at the site. It is known that freeze-thaw cycles influence the triggering of rockfalls as the water in the fissures will freeze increasing the volume of the fissures forcing the rock to disintegrate. The annual average precipitation is around 5.6 m (NZ Met Service Publications 1983). The high precipitation at the site is linked to the history of rockfalls at the site. This conclusion is drawn from recorded rockfalls at the site by the DOC officials as the rockfalls usually occurred during or immediately after high rainfall.

5.4 Back-Analysis of Past Rockfalls

Back-analysis is a common method that is followed by rock engineers for the purpose of analysis and design. It is usually carried out when there is not much understanding of either the phenomenon under analysis, or the parameters involved in the process. Back-analysis of rockfalls is usually carried out as there are no easy means of determining the input parameters for rockfall simulation, such as the coefficients of restitution. The basic theory behind this is to use the observations of the actual recordings of rockfalls at the site to find the input parameters. The back analysis usually requires some assumptions but the results are generally much more reliable than data obtained from laboratory testing, as the program is calibrated against actual field observations. Although the method is crude, the back analysis at least provides some real data that makes the results practical. The usage of back analysis with proper assumptions combined with engineering judgement can prove to be a very helpful tool. Based on this analysis of the past rockfalls, predictions can be carried out for rockfalls in the future.

In this section, back-analysis of past rockfalls will be carried out to find the relevant values of the coefficients of restitution of bedrock, and debris. To do this, first of all a detailed site

investigation is carried out to plot the boulder distribution that has formed from the past rockfalls. Then this distribution is used to roll-out some assumed number of boulders (in the computer simulation program), so that the percentage of boulders that reach a certain point on the slope corresponds to the number of boulders that have actually reached the same point at the site. To carry out this analysis, the following assumptions have to be made for the boulders that are going to be used for the back-analysis:

- The boulders travel in two dimensions only, that is there is no lateral movement of boulders while coming down the slope.
- The boulders can be represented by an equivalent size of a spherical boulder.
- The boulders must have initiated from the same height on the top of the slope.
- The boulders rolled down the slope “individually” and not as a group interacting with each other.
- Although the distribution of boulders is concentrated “around” certain point on the base of slope, it will be assumed that they have all stopped at the same point.
- The average size of the boulders can represent all the boulders at the analysis point.
- There is no fragmentation of the boulders during motion.
- If the number of boulders used for back analysis is 10, it will be assumed that out of 100 boulders initiated from the top of the slope, only 10 reached the ground. Furthermore, it will be assumed that only 10%¹ of that size of boulders reach that point.

5.4.1 Field Investigation

Field investigation involved a survey to map the boulder distribution. While doing the survey, importance was given only to boulders of greater than 1m diameter.

The survey was carried out using an Electronic Distance Measurement (EDM) theodolite. A reference point was established at a safe (undisturbed) point (Photo 5-3) so that the site can be surveyed again in the future, if required. The boulder mapping was carried out using a single station of the EDM. All the measurements were taken with reference to the reference point. In the first part of the survey, the access road was established in the plot by plotting the edge of the road at relevant intervals where there is change in the shape of the boundary of the access road. The second part of the survey concentrated on establishing the

¹ Please note that this assumption is arbitrary and will be justified later in section 5.4.2.2.

existing boundary of the rockfall debris cone. This enables the distance between the boundary of the rockfall debris cone and the present access road to be measured.

The third and main part of the survey is to map the boulder distribution. Unfortunately, when the access road was re-located in 1996, the new road was laid using the rockfall debris that was lying near the access road. The re-location of the access road has thus contributed to the loss of boulders that have reached the vicinity of the access road. However, there are still many rocks that are near to the boundary of the rockfall debris, the distribution of which can be used for the back-analysis.

The position of each boulder was approximately measured by placing the reflector (part of EDM) around the centre position in front of the boulder on the ground (not on the boulder). After noting the location of the boulder, the boulder was numbered for the purpose of further investigation and future reference of the boulder. After noting the positions of the boulders, they were re-visited to measure the approximate size. In line with common practice, the size of each boulder was measured approximately by measuring the three significant dimensions of the boulder along with a sketch. These three measurements were then multiplied to get the approximate volume of each boulder. A total of 41 boulders were measured in the same way. Appendix B gives the results of the survey. For purposes of plotting, each boulder was assumed to be spherical and the boulders were plotted as circles with the diameter of an equivalent spherical boulder (Figure 5-2).



Photo 5-3: Photograph showing the reference point used for the survey.

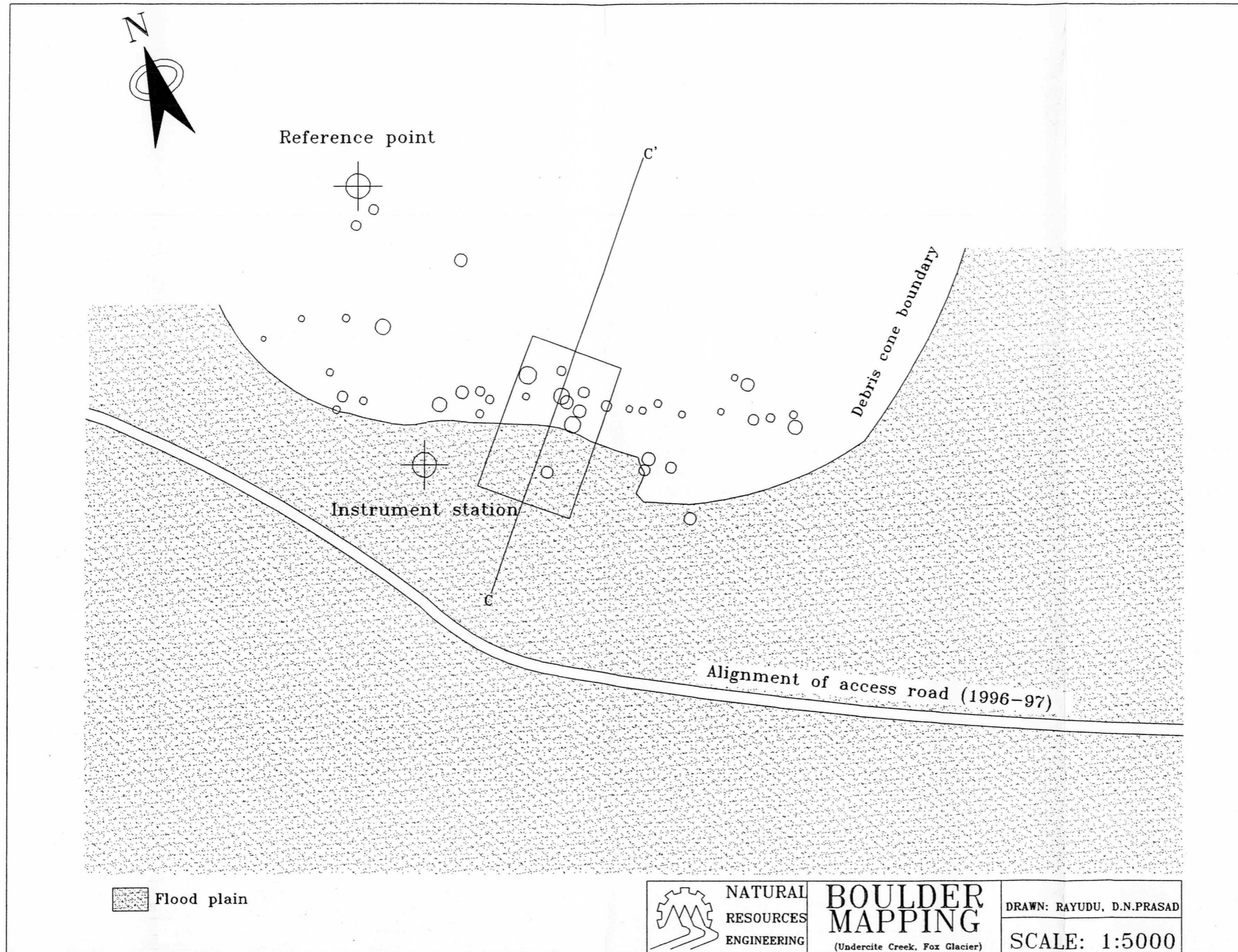


Figure 5-2: Boulder mapping at Undercite Creek, Fox Glacier.

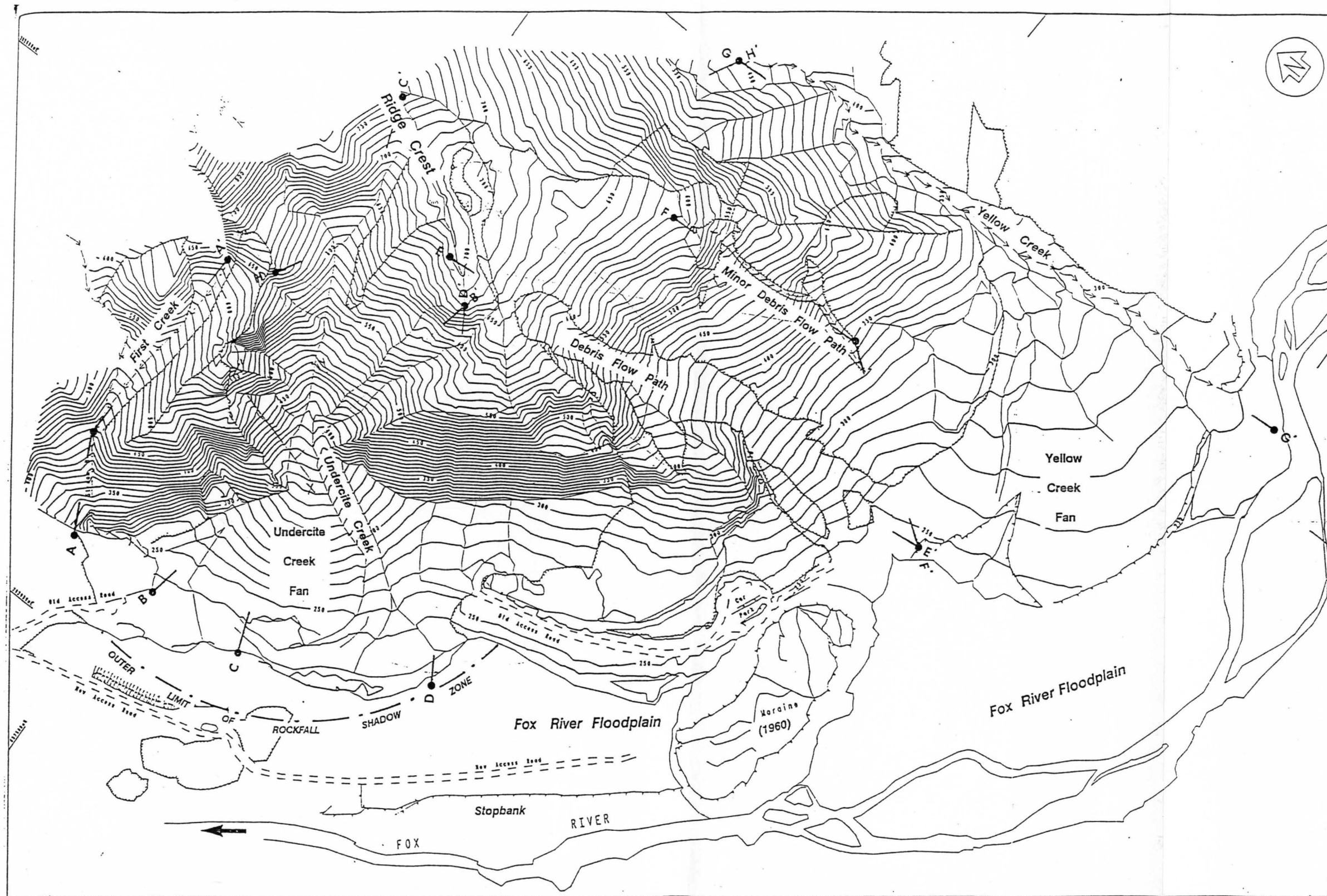


Figure 5-3: Topographic map of Undercite Creek - Yellow Creek area showing location of topographic cross-sections (courtesy: Brian Paterson) (Scale: 1:5000)

5.4.2 Computer Simulation

Figure 5-2 shows the boulder mapping at Undercite Creek. The distribution of the boulders is three dimensional; they do not appear to have come down through the same topographical cross-section of the slope. This is very typical of Undercite Creek and Photo 5-2 shows that the slope provides a three dimensional run-out alley for the boulders. The trajectory of the boulder depends heavily on the initial starting position. For example, if it starts on the south-east side, it may come down the bedrock following the chute in the south-east direction, and after reaching the top of the debris cone, it may turn into a north-south direction. However, an amateur video (supplied by DOC) taken during the time of active rockfalls in 1995 shows that the rocks starting from the top of the slope perpendicular to the present access road (at centre line of the debris cone), are essentially rolling down in two dimensions only; that is, there is very little lateral movement of boulders. Thus, the assumption that the boulders travel in two dimensions can be accepted at this particular cross-section of the slope.

Figure 5-3 shows the topography of Undercite Creek along with the location of topographic cross-sections used by Paterson (1994). Comparing the map with the boulder mapping in Figure 5-2, we can see that the cross-section C-C' partially coincides with the boulder concentration indicated in Figure 5-2 by a box. Also, this cross-section coincides with the centre line of the debris cone where the boulders were found to be rolling down with no lateral movement in the amateur video tape, as discussed earlier. Hence, this cross-section is chosen for the purpose of back-analysis and the boulders will be assumed to have released from the top of the slope. The computer simulation will be carried out in such a way that the total number of rocks that have reached the analysis point will be the same as found in the site. As 10 boulders are going to be used for the back analysis, about 10 % of boulders should reach the analysis point in the computer simulation. The simulation for the back-analysis will be carried out using the modified program *WinRock*.

5.4.2.1 Input Parameters

As discussed earlier, the cross-section that is used for the back-analysis is the section C-C', shown in the topographic map (Figure 5-3). As you can see from Figure 5-2, the exact number of boulders that fall in the cross-section C-C' is about 7. There are some other boulders that are sitting very near to this line C-C'. For the purpose of analysis, these boulders will be assumed to have come down through the same cross-section. Hence, the

total number of boulders that are used for the analysis is 10 (see the box indicating the boulders that were used for the analysis in Figure 5-2).

5.4.2.1.1 Boulder Information

As the program *WinRock* assumes the boulders to be spherical, the size of the boulder is specified as diameter, which will be the average of 10 boulders that lie around this cross-section. From the survey data, it is found that the average diameter is 7.3 m. The bulk density of the rock (schist) found in the laboratory is about 2680 kg/m^3 . This density has been determined without altering any moisture content of the specimen from the *in situ* value.

5.4.2.1.2 Initial Conditions

As discussed earlier, all the boulders will be assumed to have started off from the top of the cross-section. An estimated initial horizontal velocity of 0.5 m / sec will be used to account for velocities initiated from ice and / or water pressure in the rock fissures. No trajectory angle or the rotational velocity will be given in the initial conditions.

5.4.2.1.3 Simulation Details

The analysis point that is used for the analysis can be found from the topographic map (Figure 5-3) and the boulder mapping (Figure 5-2). The cross-section C-C' starts from the end of the debris cone that was existed in November 1994. As mentioned earlier, the new access road was laid using the debris from Undercite Creek. Hence, the present boundary of the debris cone may not coincide with the debris cone boundary that existed in November 1994. Thus, to get the starting point of the section C-C' from the present debris cone boundary, first of all, the distance from point C in the topography map (Figure 5-3) is measured along the extended line C-C'. Then the distance from the present access road to the access road in the past is determined from the scaled aerial photograph (Photo 5-1) along the same extended line C-C'. Both these measurements are then added to get the starting point C of the cross-section C-C' which is then used to locate the exact distance of the analysis point from the point C, using the boulder map (Figure 5-3).

The computer program assumes that the boulders are spherical, and so the rockfall statistics given will be on the conservative side, that is, more number of boulders reach the analysis point determined above as spherical blocks roll faster than angular ones. Hence, the

analysis point will be specified 20 m away from the original analysis point to account for this correction. To check the effect of shape on run-out distance, analysis was carried out using the program *CADMA* which uses ellipsoidal shape of boulders. From this analysis, it was found that the run-out distance of ellipsoidal boulders is less than those of spherical ones by 10 to 15 m. Since most of the boulders at Undercite Creek are angular, assumption of taking the analysis point 20 m away from actual point on the slope is justified. Also, the total number of boulders that reach the analysis point can be in the range of 15 ± 10 , keeping in mind the variance generated in the output by the random usage of input parameters by the program.

5.4.2.1.4 Slope Information

The most important part of input for the simulation is the slope information. As discussed earlier, the x, y coordinates used for the slope are obtained from the cross-sections provided in Paterson (1994). The cross-section was obtained from the surveyed topography (by Elliott and Sinclair Ltd.) in 1994. Figure 5-4 shows the cross-section of the slope used for the back-analysis.

5.4.2.2 Iterations to Find The Values of The Coefficients

The initial values that are used for the back-analysis were selected from the suggested values by various authors (Richards 1988, Pfeiffer and Bowen 1989, Azzoni *et al.* 1995, Elliott 1992, and Hungr and Evans 1984), and adjusting the values for the present site conditions. The following initial values were used for the purpose of back-analysis:

- R_n (Bed Rock) = 0.35
- R_t (Bed Rock) = 0.85
- R_n (Scree) = 0.10
- R_t (Scree) = 0.78
- Roughness (Bed Rock) = 8 degrees
- Roughness (Scree) = 20 degrees

The initial values specified above were first used (specifying the standard deviation of coefficients to be zero) to check the total number of boulders that reached the analysis point, which was found to be 19%. This percentage is acceptable in comparison of the total number of boulders (10) used for the back analysis, keeping in mind the variance generated by using the standard deviation of slope roughness.

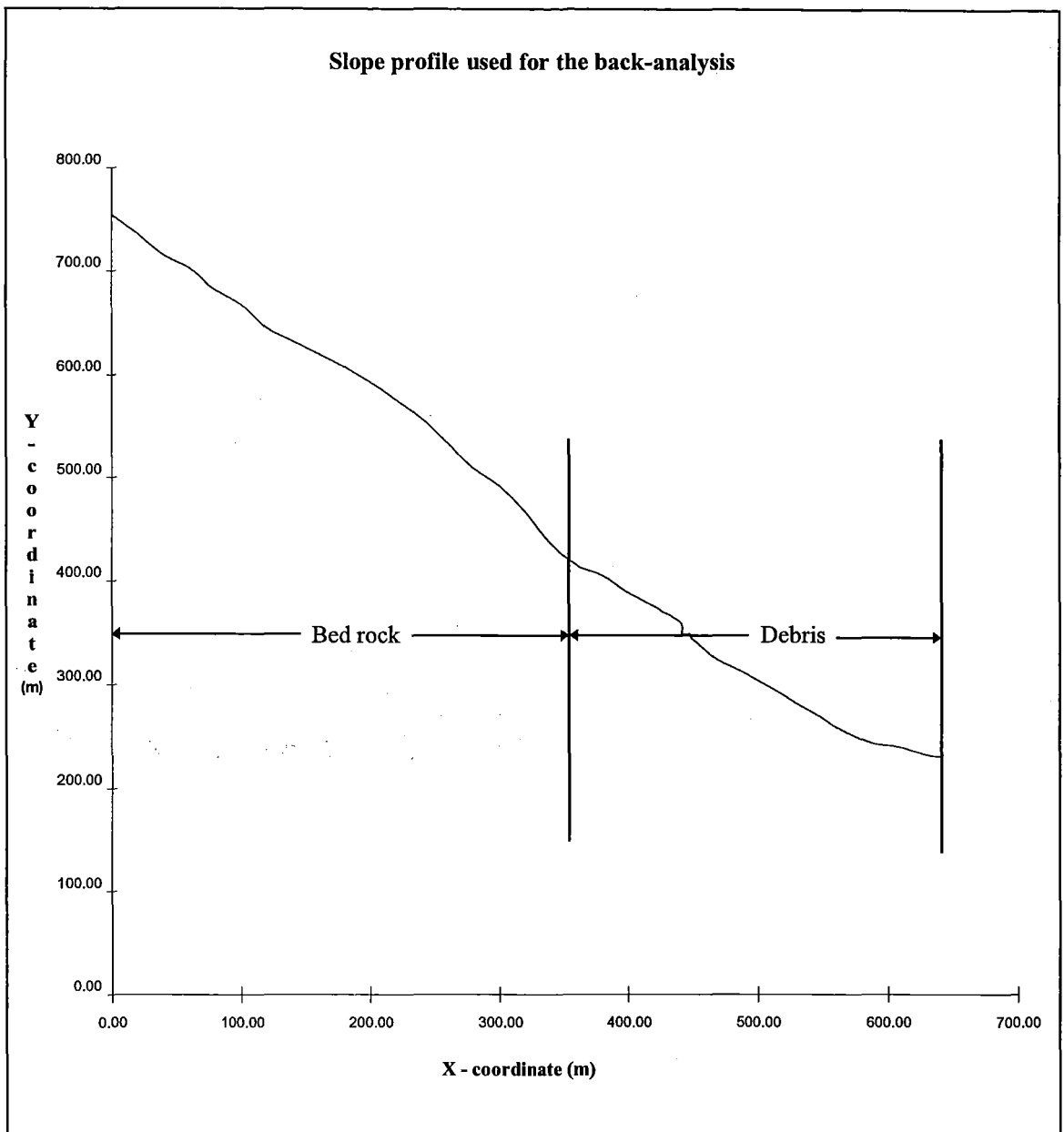


Figure 5-4: Slope profile used for the back-analysis (cross-section C-C').

After the above simulation was completed, several simulations were carried out changing each of the values (except roughness values for both bed rock and the scree²), keeping all other parameters constant, to see the effect of the parameter on total percentage of boulders that reach the analysis point. For example, the normal coefficient of bed rock was varied, keeping all others constant. A standard deviation of zero was specified during all of these simulations to reduce the effect of randomisation of the parameter values. As there are four coefficients that can be varied, the following cases will be considered for the iteration:

² The slope roughness was not varied in the iteration, assuming that the effect of the roughness will be very low on the total percentage of boulders that reach the analysis point.

- R_n (bed rock) changing, all others constant.
- R_t (bed rock) changing, all others constant.
- R_n (scree) changing, all others constant.
- R_t (scree) changing, all others constant.

Table 5-1 provides the summary of the iterations carried out.

Table 5-1: Summary of iterations carried out to find the parameter values.

R_n (Bed Rock) changing, all others constant				
R_n (Bed Rock)	R_t (Bed Rock)	R_n (Scree)	R_t (Scree)	% of boulders
0.35	0.85	0.10	0.78	24.00
0.30	0.85	0.10	0.78	09.00
0.25	0.85	0.10	0.78	07.00
0.20	0.85	0.10	0.78	04.00
0.40	0.85	0.10	0.78	19.00
0.45	0.85	0.10	0.78	26.00
0.50	0.85	0.10	0.78	39.00
0.55	0.85	0.10	0.78	34.00
R_t (Bed Rock) changing, all others constant				
R_n (Bed Rock)	R_t (Bed Rock)	R_n (Scree)	R_t (Scree)	% of boulders
0.35	0.85	0.10	0.78	18.00
0.35	0.80	0.10	0.78	06.00
0.35	0.75	0.10	0.78	08.00
0.35	0.70	0.10	0.78	07.00
0.35	0.65	0.10	0.78	00.00
0.35	0.60	0.10	0.78	00.00
0.35	0.90	0.10	0.78	36.00
0.35	0.87	0.10	0.78	21.00
0.35	0.88	0.10	0.78	29.00
R_n (Scree) changing, all others constant				
R_n (Bed Rock)	R_t (Bed Rock)	R_n (Scree)	R_t (Scree)	% of boulders
0.35	0.85	0.10	0.78	17.00
0.35	0.85	0.15	0.78	51.00
0.35	0.85	0.05	0.78	02.00
0.35	0.85	0.11	0.78	26.00
0.35	0.85	0.12	0.78	26.00
0.35	0.85	0.13	0.78	31.00
0.35	0.85	0.08	0.78	08.00
R_t (Scree) changing, all others constant				
R_n (Bed Rock)	R_t (Bed Rock)	R_n (Scree)	R_t (Scree)	% of boulders
0.35	0.85	0.10	0.78	21.00
0.35	0.85	0.10	0.83	95.00
0.35	0.85	0.10	0.82	80.00
0.35	0.85	0.10	0.81	63.00
0.35	0.85	0.10	0.80	45.00
0.35	0.85	0.10	0.79	24.00
0.35	0.85	0.10	0.77	08.00
0.35	0.85	0.10	0.76	00.00

After these iterations were completed, only those values of the coefficients were picked up as the *right* ones for which the total number of boulders that reached the analysis point were between 5 - 25 %. Even though the number of boulders that lie near this cross-section is only 10, the above range was used to cover the variance generated by the random usage of slope roughness by the program. Using the above method of iteration, the following range of values for the coefficients can be suggested for Undercite Creek:

- R_n (Bed Rock) = 0.25 - 0.45
- R_t (Bed Rock) = 0.70 - 0.87
- R_n (Scree) = 0.08 - 0.12
- R_t (Scree) = 0.77 - 0.79

The normal coefficient of restitution obtained is comparable with the value obtained using the laboratory tests in Chapter 7 ($R_n = 0.77$) considering the fact that the laboratory tests involved bouncing a “steel ball” on to the clamped rock. Obviously when a rock impacts rock, the restitution will be less with the influence of amount of weathering and schistosity. Hence, the assumption that only 10% of the boulders reach the analysis point in back analysis (page 85 in section 5.4) is justified.

5.5 Prediction of Rockfalls at Undercite Creek

In this section, computer simulation will be carried out to predict rockfalls in the future. The recorded rockfall history obtained from the DOC showed some evidence of the typical rockfall paths at Undercite Creek. Figure 5-5 shows the zoning for the rockfall slip zones and the deposit zones that were used to record the rockfalls at the site.

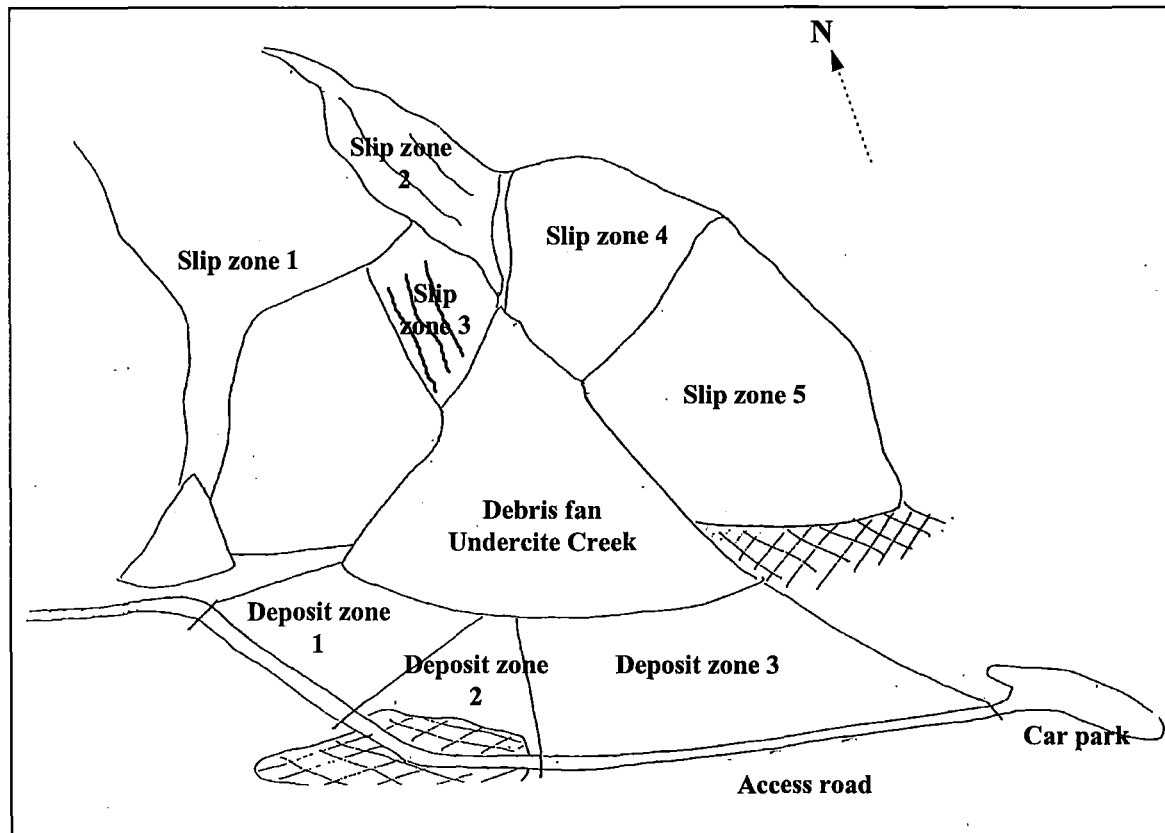


Figure 5-5: Hand-drawn map of the zoning used by the Department Of Conservation for recording rockfalls (courtesy: DOC).

Most of the rockfalls that reached the access road were in deposit zone 2. Also, from the recordings, it can be concluded that the rockfalls that occur from slip zones 2, 3, and 4 are the ones that come down to deposit zone 2. Hence, from these recordings, it can be concluded that the most hazardous part of the rockfall slope is deposit zone 2. This conclusion is further used for the analysis of rockfalls to check the rockfall statistics at the new access road.

5.5.1 Sections Used for The Analysis

As mentioned earlier, the boulders at Undercite Creek come down following typical rockfall paths. For example, if the boulders start from slip zone 2, they follow the chute in the zone until they reach the debris cone, from where they turn around and start rolling or bouncing down the debris cone. As the rockfall paths are typically three dimensional (that is, the boulders do not come down following the same cross section), the path is divided into two sections for the purpose of the present analysis. For example, the simulation of rockfalls from slip zone 2 will be carried out to see the average velocities of the boulder at the point where it reaches the debris cone (X-X' in Figure 5-6). Then these average velocities are used as the starting velocities for the section starting from the end point of the earlier section to get the rockfall statistics at the present access road (X'-C' in Figure 5-6). Figure 5-7 illustrates the sections used for analysis. Appendix C provides the cross-section layouts of the sections used along with some boulder trajectories.

The simulation of rockfalls will be carried out using the parameter values obtained through the back-analysis in section 5.4.2.2. The boulder size used for the prediction is the average of the maximum size of the boulders surveyed, that is 7.5 m (Appendix B). Even though the size of boulders at the site vary from 20 cm to 10 m diameter, 7.5 m was used for the analysis to represent this range. The detachment zone of the rocks has been specified as a range, as the modified program allows the user to specify a range of starting locations for the boulders.

5.5.2 Simulation Results

The following are the results of the simulation carried out for the cross-sections shown in Figure 5-6. The reader may refer to Figure 5-6 for the location of points along the cross-sections used.

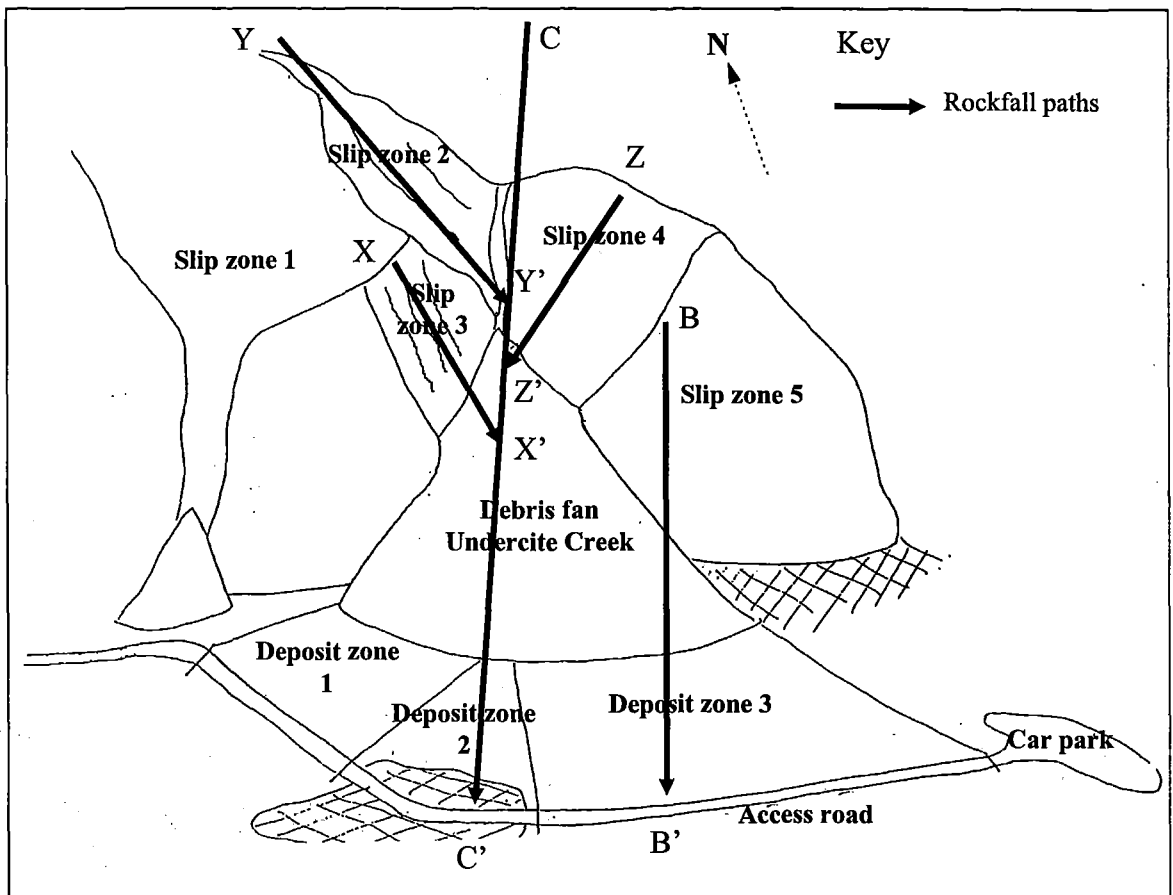


Figure 5-6: Sections showing the rockfall paths used for the prediction of rockfalls.

Rockfall path C-C':

- About 2 % of the boulders reach the new access road in the deposit zone 2, if the rockfalls initiate from the top of the section C-C'. The percentage of boulders reaching the access road remains the same, even for the rocks initiating from the zone of intersection between slip zone 2 and 4.
- The average velocities of the boulders that reach the new access road is about 2 m / sec.
- The average height of boulders that reach the new access road is about 0 - 0.1 m above ground.

Rockfall path X-X'-C':

- About 80 % of boulders reach the point X'.
- The average velocity of the boulders is around 4.97 m / sec at point X'.
- Average height of the boulders is about 4.94 m above ground at point X'.
- Overall, about 0.8 % of the boulders reach the new access road if they start from the top of slip zone 3. This means, there is a chance of 1 in 100 where a boulder initiated from the slip zone 3 can reach the access road at the deposit zone 2.

- The average velocities of those reaching the road is 0.033 m / sec.
- The average height of boulders reaching the road is 0 m above ground.

Rockfall path Y-Y'-C':

- 100 % of boulders reach the point Y'.
- Average velocity at point Y' is about 38.9 m / sec.
- Average height of boulders at point Y' is about 4.94 m above ground.
- Overall, 13 % of the boulders released from the top of the slip zone 2 will reach the new access road.
- The average velocity of the boulders that reach the new access road is about 2.75 m / sec.
- Average height of boulders that reach the new access road is about 3.5 m above ground.

Rockfall path Z-Z'-C':

- About 95 % of the boulders released from slip zone 4 reach the point Z'.
- The average velocity of the boulders at the point Z' is about 10.23 m / sec.
- The average height of boulders at the point Z' is about 0.46 m above ground.
- Overall, about 15 % of the boulders reach the new access road.
- The average velocity of the boulders that reach the new access road is about 0.048 m/sec.
- The average height of boulders that reach the new access road is 0 m.

Rockfall path B-B':

- No rocks dispatched from the top of the section B-B' reach the new access road.

5.6 Conclusions

The following conclusions can be drawn from the rockfall analyses carried out for the Undercite Creek:

- The most probable hazard from rockfalls for the new alignment of access road, is at the deposit zone 2 shown in Figure 5-5. This conclusion is basically drawn from the recorded rockfalls by DOC. Also, the typical layout (Photo 5-2) of the whole slope shows that the boulders that follow the rockfall path through the centre line of the debris cone are the most hazardous and have potential to reach the access road.
-

- The maximum velocity of the boulders that are reaching the new access road is less than 3 m / sec that is, 11 km / hr. Although this velocity is enough for potential hazards, considering the decision sight distance (refer to Appendix D for definition) available at the site, there should be no occurrence of fatalities. In other words, there will be enough time for the driver to manoeuvre his vehicle to avoid a possible hit with the boulder. However, it should be remembered that the potential hazard may increase in the event of poor visibility (e.g. fog or heavy rain) and / or inactiveness of the driver.
 - Deposit zone 3 is safe under present conditions of slope erosion and the alignment of access road. This can be concluded from the simulation results of the section B-B' shown in Figure 5-6. Although there is evidence showing a strong potential for toppling failure at the top of this section, it can be confirmed that there is no threat to the access road at this location as the rocks will not reach the access road.
 - As expected, the debris cone is helping to retard and stop most of the boulders from reaching the access road. This is because the roughness of the debris with small and big rocks lying on the top of the cone will help to stop the rocks that are smaller than those that are already sitting there. However, there is a chance that big boulders will roll down further as the effect of roughness will be negligible. Hence, the potential threat to the access road is mainly from the big boulders.
 - During the research, the height of the debris cone was increasing indicating that only small rocks and surface material are getting detached from the bed rock. This conclusion is drawn from general observation of the debris cone during 5 visits made between June 1995 and April 1997. It is not known exactly how much higher the debris cone has grown during the research period. However, it is worth noting that in an unlikely event of a rock avalanche at the site, the spread of the debris cone will increase and hence the potential threat from rockfalls reaching the access road. This is because, the so-called outer limit of rockfall shadow zone shown by Paterson (1994, pp.20), which was determined from the methods suggested by Evans and Hungr (1993), will move further into the valley. Hence, a need may arise to shift the access road further into the valley or increase the relative height of the road creating a catch ditch, if the spread of the debris cone increases. This particular conclusion is applicable to all three deposit zones.
 - The total number of rocks that can reach the new access road is about 30 % of the boulders that are detached from the slip zones 2, 3 and 4. It should be noted that the average diameter of the boulders used for the analysis is about 7.5 m. As there will be numerous rocks that are smaller than 7.5 m diameter, rockfall simulations were carried
-

out using smaller diameters of the boulders to check whether they reach the new access road. Figure 5-7 shows the graph showing the relation between boulder diameter and the run-out distance for the cross-section C-C'. From the figure it is clear that the boulder diameter needs to be at least 5.5 m to reach the new access road. Hence, it can be concluded that any boulder which has an equivalent diameter smaller than 5.5 m will have limited potential to reach the new access road no matter where they initiate from. This also indicates that the larger rocks have more potential to reach the access road.

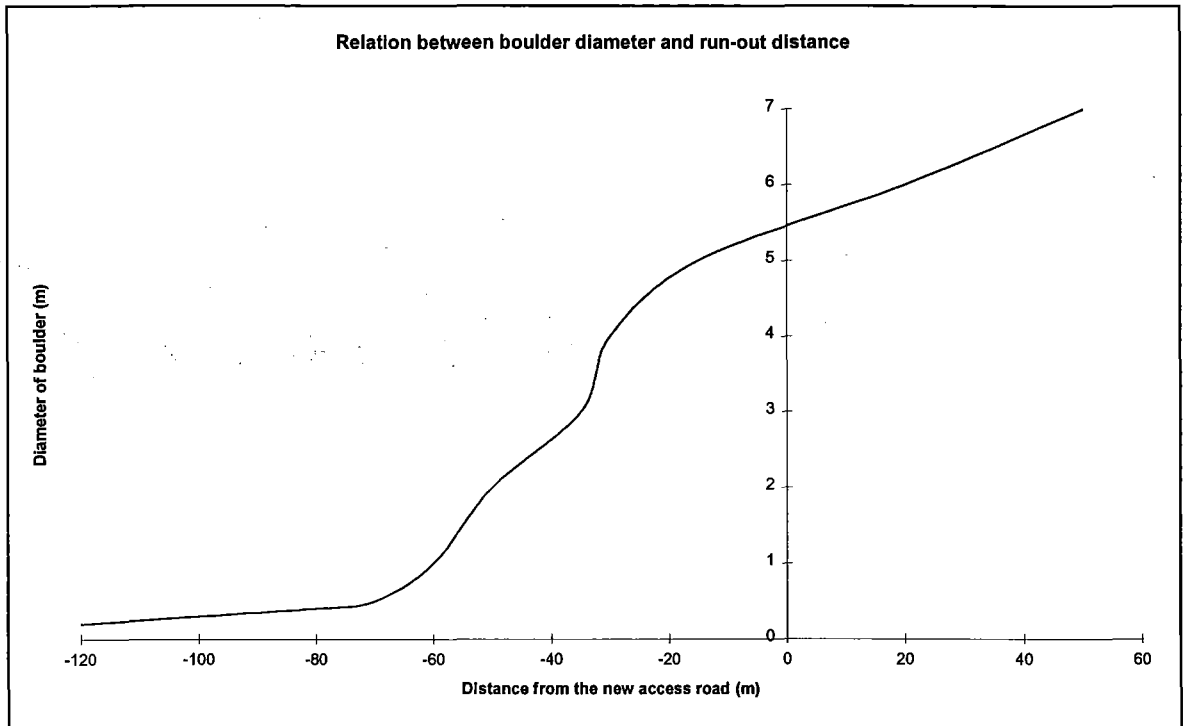


Figure 5-7: Graph showing the relation between boulder diameter and run-out distance.

5.7 Summary

Using the modified program *WinRock* developed in Chapter 4, a detailed analysis of rockfalls at Undercite Creek has been carried out. The parameter values obtained from the back analysis were used to predict rockfalls in the future, which indicated that potential hazard from rockfalls is at the deposit zone 2 (Figure 5-6). Deposit zone 3 is under no threat from rockfalls.

Chapter 6 goes on to assessing the rockfall hazards at Fox Glacier using the risk analysis techniques.

Chapter 6

Assessment of Rockfall Hazard to The Access Road at Fox Glacier

6.1 Introduction

In Chapter 5 an analysis of rockfalls at Undercite Creek was carried out. It was concluded that the rockfalls at Undercite Creek do not pose immediate threat to the access road. When the site was re-visited on 1st April 1997, it was observed that the occurrence of rockfalls has increased on the true left bank of the river, at Cone Rock. There were also some big boulders which have reached the walking track at Yellow Creek.

Since the hazard of rockfalls is not restricted to Undercite Creek, it was decided to assess the rockfall hazard to the access road from all the degrading slopes in the valley. In this chapter, a complete rockfall hazard analysis will be carried out for the access road, using the Rockfall Hazard Rating System (subsequently referred to as RHRS), developed by the United States Department Of Transportation (USDOT). This enables the rockfall hazard to the access road to be quantified, which in turn will be helpful to determine the alignment of the access road in the near future, if re-location becomes essential. Finally, a semi-quantitative risk analysis will be carried out for the access road to find the probability of accidents that may happen with the present alignment of the road. The calculated risks are then compared with allowable risks around the world.

6.2 Rockfall Hazard Rating System (RHRS)

The RHRS is a process that allows agencies to actively manage the rock slopes along their highway system. It provides a rational way for an agency to make informed decisions on

where and how to spend construction funds. The six steps generally followed in the process are summarised below :

1. Slope inventory - Creating a geographic database of rockfall locations.
2. Preliminary rating - Grouping the rockfall sites into three broad, manageably sized categories; A, B, and C slopes.
3. Detailed rating - Prioritizing the identified rockfall sites from the least to the most hazardous.
4. Preliminary design and cost estimate - Adding remediation information to the rockfall database.
5. Project identification and development - Advancing rockfall correction projects toward construction.
6. Annual Review and Update - Maintaining the rockfall database.

Among the steps described above, steps 1, 2 and 3 will be carried out in this chapter to rate the rockfall hazards at Fox Glacier. Detailed description of the methodology of the rating system can be found in RHRS participant's manual (1993).

6.2.1 Slope Inventory

This part of the rating system concentrates on the recognition of the slopes that have the potential for rockfall hazards. It is essential first of all, to establish a database of all the rockfall locations at the site. As the access road under investigation is only about 2 km long, establishment of a rockfall location database in this case is very simple. The site was visited to note the rockfall locations that have the potential for rockfall hazard on the access road and walking tracks. The rockfall locations were updated every time the site was re-visited. From the latest observation on 1st April 1997, the following locations were identified (see map in Figure 1-2 for the locations)¹ :

- Undercite Creek.
- Yellow Creek.
- Four small rockfalls at Cone Rock.

Among the above sites, the rockfalls at Undercite and Yellow Creek are the major ones. Photo 5-1 shows a vertical aerial photograph taken on 29th January 1997. From the photo, we can see the extent of rockfalls occurring at the site and also the distance of the sites

¹ The rating is only with respect to rockfalls.

from the present access road. Photo 6-1 shows a boulder that rolled down to the walking track at Yellow Creek.



Photo 6-1: Photo showing a boulder that rolled down on to the walking track at Yellow Creek.

6.2.2 Preliminary Rating

- Preliminary rating is carried out to further categorise the rockfalls into three, broad categories (A, B, and C slopes). This evaluation is a critical step in the RHRS process, especially where large numbers of slopes are involved, as it helps to prioritise the importance for performing detailed rating of the slopes. The criteria used in the preliminary rating to categorise sections as A, B or C slopes are shown in Table 6-1.

Table 6-1: Preliminary rating system.

Criteria	Class		
	A	B	C
Estimated potential for rockfall on roadway	High	Moderate	Low
Historical rockfall activity	High	Moderate	Low

According to these criteria, following ratings are given for the slopes at Fox Glacier:

- Undercite Creek - A
- Yellow Creek - B
- Cone Rock - C

This preliminary rating is helpful to prioritise the slopes according to rating, for large areas with rockfalls. In the case of Fox Glacier, as there are only a total of 3 main rockfall locations to perform the hazard analysis, it was decided to do the detailed rating for all 3 slopes.

6.2.3 Detailed Rating

The purpose of the detailed rating is to numerically differentiate the risk at the identified sites. Once rated, the sites can be sorted and prioritised on the basis of their scores. These lists are then used to help make decisions on where safety projects should be initiated.

The detailed rating shown in Table 6-2 includes 12 categories by which slopes are evaluated and scored. A detailed explanation of all these categories can be found in the RHRS participant's manual (1993). These 12 categories represent the significant elements of a rockfall section that contribute to the overall hazard. The four columns of benchmark criteria to the right correspond to logical breaks in the increasing risk associated with each category. The categories scores are then totalled and the slopes with higher scores present the greater risk. The scoring system is explained in detail in the RHRS Participant's manual (1993).

6.3 Detailed Rating for the Slopes at Fox Glacier

Detailed rating for the slopes at Fox Glacier was carried out using the RHRS participant's manual (1993), and therefore explanation of the complete method of rating is not necessary here. However, a brief explanation is given for the Undercite Creek slope in Appendix D for illustration purposes. Table 6-3 provides the summary of rating for the slopes at Fox Glacier, in which the column value refers to the value of the parameter (e.g. slope height value = height in metres) . The reader may refer to Photo 5-1 for the location of rockfalls.

Table 6-2: Summary sheet of the rockfall hazard rating system

Category		Rating criteria and score				
		Points 3	Points 9	Points 27	Points 81	
Slope height		25 feet*	50 feet	75 feet	100 feet	
Ditch effectiveness		Good catchment	Moderate catchment	Limited catchment	No catchment	
Average vehicle risk		25 % of the time	50 % of the time	75 % of the time	100 % of the time	
Percent of decision sight distance		Adequate sight distance, 100% of low design value	Moderate sight distance, 80 % of low design value	Limited sight distance, 60 % of low design value	Very limited sight distance, 40 % of low design value	
Roadway width including paved shoulders		44 feet	36 feet	28 feet	20 feet	
Geological character	a s e 1	Structural condition	Discontinuous joints, favourable orientation	Discontinuous joints, random orientation	Discontinuous joints, adverse orientation	Continuos joints, adverse orientation
		Rock friction	Rough, irregular	Undulating	Planar	Clay infilling, or slickensided
	a s e	Structural condition	Few differential erosion features	Occasional differential erosion features	Many differential erosion features	Many differential erosion features
		Difference in erosion rates	Small difference	Moderate difference	Large difference	Extreme difference
Block size Volume of rockfall/event		<u>1 foot</u> 3 cubic yards	<u>2 feet</u> 6 cubic yards	<u>3 feet</u> 9 cubic yards	<u>4 feet</u> 12 cubic yards	
Climate and presence of water on slope		Low to moderate precipitation; no freezing periods; no water on slope	Moderate precipitation of short freezing periods or intermittent water on slope	High precipitation or long freezing periods or continual water on slope	High precipitation and long freezing periods or continual water on slope and long freezing periods	
Rockfall history		Few falls	Occasional falls	Many falls	Constant falls	

* Please note that the FPS system of units is used here, because the RHRS was developed in the U.S.A.

Table 6-3: Rockfall hazard rating for slopes at Fox Glacier.

	Undercite Creek		Yellow Creek		Cone Rock I		Cone Rock II		Cone Rock III		Cone Rock IV	
	Value	Score	Value	Score	Value	Score	Value	Score	Value	Score	Value	Score
Slope height (m)	600	100	650	100	500	100	500	100	500	100	500	100
Ditch effectiveness		3		50		9		9		9		1
Slope length (m)	200		100		50		50		75		75	
Average vehicle risk %	11.47	1			11.45	1	11.45	1	11.45	1	11.45	1
Sight distance (m)	182				182		182		182		182	
Percent sight distance	149	1			149	1	149	1	149	1	149	1
Roadway width (m)	12.5	5			12.5	5	12.5	5	12.5	5	12.5	5
Geology Structure		81		27		50		50		50		50
Rock friction		52		9		27		27		27		27
Block Size (m)	1	27	2	81	2	81	2	81	2	81	2	81
Climate		81		81		81		81		81		81
Rockfall history		20		20		20		20		20		20
Total		371		378		375		375		375		367

Although there is not much difference among the scores, they indicate that Yellow Creek poses the most immediate threat and relevant action has to be taken. For example, as the Yellow Creek poses threat only to pedestrians, the regional authority may shift the access track as far away from the reach of Yellow Creek as possible.

The scores also indicate that the next priority has to be given to the Cone Rock rockfalls I, II, and III. To reduce the rockfall hazard in this area, the access road may be re-located towards the Undercite Creek as (apparently) the hazard from rockfalls at this part of the slope is lesser.

The slope to be considered next is Undercite Creek. To reduce hazard in this area, the regional authority may increase the height of the road by creating an embankment, thereby,

creating a catch ditch. Also, constant surveillance of the slope for any possible rockfalls can be carried out so that the road can be closed in an event of rockfall reaching the road.

6.4 Risk Assessment of Rockfalls at Fox Glacier

Bunce (1994) used a methodology for rockfall risk assessment suggested by Canadian Standards Association (CAN/CSA 1991). He chose the “Methods of Analysis of Engineering systems” (CAN/CSA 1991, pp.21-24) for the quantification of risk posed by rockfalls on a highway. According to the Canadian Standards Association (CAN/CSA 1991), all risk analyses should include six stages in the following order (CAN/CSA 1991, p.15):

1. Scope definition.
2. Hazard identification.
3. Risk estimation.
4. Documentation.
5. Verification.
6. Analysis update.

Stages 1, 2 and 3 will be carried out in the present research.

6.4.1 Criteria for Detailed Risk Analysis

At the outset, consideration should be given to the risk analysis requirements. CAN/CSA (1991) suggests that level of analysis be related to the severity of the outcome of the hazard by using Table 6-4. As the rockfall hazard history for the access road at Fox Glacier comes under the category “Occasional - Major”, a semi-quantitative risk analysis will be carried out in the following sections. The reader may refer to CAN/CSA (1991) for exact definitions of the terms used in the table.

Table 6-4: Frequency severity matrix and action guide

Frequency	Severity			
	Catastrophic	Major	Minor	Negligible
Frequent	A	A	A	C
Probable	A	A	B	C
Occasional	A	B	B	D
Remote	A	B	C	D
Improbable	B	C	C	D

A - detailed quantitative, B- semi-quantitative, C- qualitative, D- not required.

6.4.2 Scope Definition

The objective of a risk analysis for the slopes at Fox Glacier is to determine the level of risk from the hazard of rockfall that vehicle occupants place themselves in when using a specific section of the access road to the Fox Glacier. The risk calculations will be carried out to check the probability that a fatal accident can occur. Documentation, verification, and the analyses update may be carried out by the regional authority.

6.4.3 Hazard Identification

The hazard identification has been carried out in section 6.3 using the RHRS. This has enabled us to decide upon which slope poses the immediate hazard to the access road at Fox Glacier. After the hazard identification stage, the risk estimation and calculation will be carried out for only those slopes which poses an immediate threat.

6.4.4 Risk Estimation and Calculation

Risk estimation for rockfall includes several topics such as frequency and consequence analysis, selection of qualitative or quantitative analysis methods, determination of required data, statement of assumptions, and estimation of the risks with their sensitivity or uncertainty (Bunce 1994). Where data is unavailable, information of a representative or generic nature, or expert judgment, should be used.

Frequency analysis investigates the hazard sources to determine the likelihood and nature of the hazard event. Using historical data (if available), it determines the frequency with which rockfalls have occurred in the past and then makes a judgment as to the frequency of their occurrence in the future, or estimates event frequency using a technique such as event tree analysis described below in section 6.4.4.1.

Consequence analysis involves estimating the impact on adjacent people, property or the environment should the undesired event (rockfall) occur (CAN/CSA 1991, p.23). Consequence analysis consists of estimating the probability of people being in the proximity of a rockfall when it occurs, and how they will be effected by the rockfall. As this analysis comes under detailed quantitative analysis and as it was decided to perform only a semi-quantitative analysis for the site, it was decided not to perform the consequence analysis in this research.

6.4.4.1 Event Tree Analysis

An event tree considers the range of possible events that lead to specific outcomes. Russell (1976) provided an example of an event tree for a slope stability problem in a mine and is used in this research to determine the probability of fatalities at Fox Glacier. Figure 6-1 shows an event tree analysis for rockfalls at Undercite Creek due to rainfall resulting in a probability of someone being impacted. For each event tree there are a set of outcomes that can have probabilities assigned to them.

Initiating event (annual)	Rockfall	Vehicle impacted by or impacts rock	Impact results in fatality	Number of occupants impacted	Probability		
Rain 4%	no 98%	-----			0.392		
		yes 2%	no 99.9%	-----			7.99×10^{-2}
	yes 0.1%		no 40%	-----			3.20×10^{-5}
			yes 60%	one 10%	-----	4.80×10^{-6}	
					two 50%	-----	2.40×10^{-5}
					three or more 40%	-----	1.92×10^{-5}
Annual probability of a single fatality			$= (0.48+2.4+1.92) \times 10^{-5}$		$= 4.80 \times 10^{-5}$		
Annual probability of two fatalities			$= (2.4+1.92) \times 10^{-5}$		$= 4.32 \times 10^{-5}$		
Annual probability of three or more fatalities			$= 1.92 \times 10^{-5}$		$= 1.92 \times 10^{-5}$		

Figure 6-1: Event tree analysis for Undercite Creek.

The following assumptions were made in deriving the event tree shown in Figure 6-1:

1. The probability of occurrence of rain heavy enough to initiate rockfall events at Fox is estimated at 14 days per annum or 4%.
2. The probability of a rockfall being triggered by heavy rain, based upon the rockfall history of the slope, has been estimated as 2%.

3. As the traffic density is only 150 cars per day (75 cars per lane per day), and the access road is quite away from normal reach of rockfalls, the probability of a vehicle being hit is estimated as every one in thousand or 0.1%.
4. As the boulders that reach the access road are usually large (more than 1m diameter), it is estimated that impact results in fatality 60% of the time.
5. As the access road is used by tourists most of the time, the number of vehicle occupants impacted by a rockfall has been estimated at between 1 and 3 or more.

The calculated risks above will be compared with the level of acceptable risks from other major civil engineering projects in Section 6.5.

6.4.4.2 Risk Calculation

The final step in the risk analysis is the calculation of the risk. The methodology used in this research considers only the hazards associated with a vehicle being hit by a falling rock, or hitting a fallen rock. All additional hazards which may result from a moving vehicle interacting with other elements of the road or other traffic will not be considered. As a result, only the first vehicle to encounter a fallen rock is considered. If a vehicle-rock impact occurs, the assessment of the resulting risks to other highway users is beyond the scope of this research. The risk values calculated will be applicable only for the present alignment of the access road.

The calculation of rockfall hazard is a quantitative expression of the expected return period of a vehicle/rockfall accident. Three different hazards should be considered while calculating the risk for rockfalls:

1. Falling rock hitting a moving vehicle.
2. Falling rock hitting a stationary vehicle.
3. Moving vehicle hitting a fallen rock.

Among the above categories, category 2 can be eliminated as the warning sign posts “No Stopping” are already in their positions at the access road. Hence, risk calculation will be carried out only for categories 1 and 3 assuming no cars will stop on the access road.

As there were no reported rockfalls that have reached the road at Cone Rock to date, risk calculation will be carried out only for the access road at Undercite Creek.

6.4.4.2.1 Moving Vehicle / Falling Rock

The computation of the hazard of a vehicle being hit by a falling rock while moving is completed by considering the number, size and speed of the vehicles and the estimated number of rockfalls that reach the road per year for a given length of road. The following assumptions have been made while deriving the expression (Bunce 1994):

- a) The vehicle speed is the posted limit.
- b) The average length of a vehicle can be used to represent all vehicles.
- c) The temporal distribution of traffic is uniform throughout a 24 hr period. In the case of Fox Glacier, the access road is used only for 12 hours a day on an average, as it is used only to view the Glacier in the day time.
- d) The spatial distribution of rockfalls within a cut is uniformly distributed.
- e) The timing of each rockfall is assumed to be an independent event and therefore a uniform temporal rockfall distribution is assumed.
- f) The traffic flow and rockfall are independent.

When the rockfall occurs on to the highway, two cases must be considered. If the length of road, L_{rf} , effected by a rockfall is less than the average length of the road occupied by vehicles, then the probability of a spatial impact given a rockfall occurs, $P(S:H)$, equals the fraction of the highway occupied by a vehicle, F_v . If L_{rf} is greater than the length of road occupied by vehicles then $P(S:H)$ is the fraction of a cut effected by the rockfall. Therefore:

$$\begin{aligned} P(S:H) &= L_{rf} / L_c && \text{for } L_{rf} > F_v * L_c \\ P(S:H) &= F_v && \text{for } L_{rf} < F_v * L_c \\ &= N_v * L_v / 24 / V_v && \dots\text{Equation 6-1} \end{aligned}$$

where N_v is the number of vehicles at risk which is the traffic volume in vehicles per day, L_v is the average vehicle length in kilometres, L_c is the length of the rock cut and V_v is the average vehicle speed in kilometres per hour.

In the present situation, since the access road is assumed to be used only 12 hrs per day, the formula for the average fraction of the highway occupied by a vehicle F_v will be:

$$F_v = N_v * L_v / 12 / V_v \quad \dots\text{Equation 6-2}$$

Following the above procedure,

$N_v = 150$ vehicles per day (estimated by DOC, using four month recording of vehicles crossing the road), $L_v = 4$ m (0.004 km) and $V_v = 50$ km/hr.

$$\begin{aligned} F_v &= N_v * L_v / 12 / V_v \\ &= 150 * 0.004 / 12 / 50 \end{aligned}$$

$$= 1 * 10^{-3}.$$

Hence $F_v * L_c = 0.001 * 459 = 0.459$ m which is less than $L_{rf} = 542$ m. Hence, using the criteria described above in equation 6-1,

$$P(S:H) = F_v = 1 * 10^{-3}.$$

Morgan (1990) and Morgan *et al.* (1992) used the reciprocal of the return period as the probability of hazard, P(H). This method is not applicable to multiple or frequent events where the probability of a given result is not the sum of the probabilities of each individual event. This is illustrated by the case of an object being thrown at two targets, A and B. If one object is thrown, the chance of hitting the target A is 0.50. If two objects are thrown independently, the probability of hitting A is not 1.00 (the sum of two trials) but rather $(1 - 0.5^2)$ or 0.75. This is an application of binomial probability. Applying the binomial formula (Benjamin and Cornell 1970) to calculate the probability that a rock hits a vehicle, P(S) of N_a vehicles being hit by falling rocks,

$$P(S, N_a) = \frac{N_r!}{N_a! (N_r - N_a)!} P(S:H)^{N_a} \{1 - P(S:H)\}^{(N_r - N_a)} \quad \dots \text{Equation 6-3}$$

where N_a is the number of vehicles hit by falling rocks and N_r is the number of rockfalls per year. If N_a is zero, then the above equation provides the probability that no vehicles are hit by a given number of rockfalls. Substituting $N_a = 0$ into the above equation and remembering that factorial of zero is unity by definition, the equation reduces to:

$$P(S, N_a = 0) = \{1 - P(S:H)\}^{N_r}$$

The probability that one or more vehicles are impacted by a rockfall, $P(S, N_a \geq 1)$ is one minus $P(S, N_a = 0)$. For convenience, P(S) will always be considered for $N_a \geq 1$. Therefore, the probability of at least one vehicle occupying the location of rockfall is:

$$P(S) = 1 - \{1 - P(S:H)\}^{N_r} \quad \dots \text{Equation 6-4}$$

In the present case, for the Fox Glacier, N_r was estimated using the recorded rockfalls that have reached the access road. Hence:

$$\begin{aligned} P(S) &= 1 - \{1 - 0.001\}^{2.2} \\ &= 2.19 * 10^{-3}. \end{aligned}$$

Since a moving car is always occupied by one or more occupants and F_v of a cut is occupied all the time, the probability of temporal occupancy of a cut, P(T:S) is unity. The

probability of at least one accident, P(A) is the product of P(S) and P(T:S). Therefore, P(A) = P(S) in this case.

The probability of an individual's vehicle being in an accident, PAV, can also be calculated. The probability of a rock hitting a single vehicle, P(S:H), is equal to the fraction of a cut occupied by the vehicle. Therefore,

$$\begin{aligned} P(S:H) &= F_v \\ &= L_v / L_c \end{aligned}$$

P(S) is same as calculated above. The probability that a vehicle is in a cut when a rockfall occurs, P(T:S) is equal to the fraction of the year the vehicle is in a cut. Using a single pass through a cut as a standard

$$P(T:S) = t / 4380 \text{ (where } 4380 = 12 \text{ hrs} * 365 \text{ days).}$$

where t is the time at risk which is the travel time through a cut in hours. The travel time,

$$t = L_c / V_v \text{ (} L_c \text{ in kilometres)}$$

Therefore $P(T:S) = L_c / V_v / 4380$

and $PAV = P(S) * P(T:S)$...Equation 6-5

For the Fox situation,

$$\begin{aligned} P(T:S) &= 0.459 / 50 / 4380 \\ &= 2.09 * 10^{-6}. \end{aligned}$$

and $PAV = (2.19 * 10^{-3}) * (2.09 * 10^{-6})$
 $= 4.57 * 10^{-9}.$

6.4.4.2.2 Moving Vehicle / Fallen Rock

The computation of the probability of a moving vehicle hitting a fallen rock is dependent on several factors and, as a result, there are at least four subsets of this event.

1. First, the rock must be of sufficient size to affect a vehicle, otherwise the driver may drive around or over the rockfall debris. Therefore, only larger rocks than some minimum will be considered. For the present situation at Fox, the average size of the rocks that have rolled on to the road was one metre.
2. The rockfall may occur outside or within the driver's decision sight distance (DSD). If the rock falls outside the DSD, the driver should be able to stop or avoid the rock on the road. If the rock falls inside the driver's DSD, the probability that the vehicle will impact the rock is increased. The faster the vehicle velocity, the greater the DSD and the

higher the probability that a rock falls within the DSD. Therefore, in this case, faster travel increases risk.

3. Due to road conditions, if the sight distance is less than the decision distance, the probability of the vehicle impacting the rock increases with the decrease of sight distance. For the access road at Fox, the sight distance was found to be more than the required DSD.
4. If the volume of the traffic is high, the sight distance for a rock on the road will be reduced due to the vehicle spacing. The traffic volume is not very high, and hence this condition is eliminated for the access road at Fox Glacier.

For the access road at Fox Glacier, only the condition where the rock falls within the DSD without the reference to sight distance will be considered for the risk calculation. The assumptions a), c), d), e), f) and g) from section 6.4.4.2.1 have been made for the derivation of the expression. In addition to those, the following assumptions were also considered:

- h) If the first vehicle that encounters the rock is able to avoid the collision with the rock, then it is assumed that all other vehicles will be able to do so. As a result, the analysis is independent of the time it takes to clear the debris from the roadway.
- i) The rockfall events that pose hazards to vehicles include only those rocks large enough to affect the performance of a vehicle. To pose a hazard to the vehicles the diameter of a rockfall must be 15 cm diameter or larger. This is the clearance of an average passenger vehicle ie, the distance between ground and underneath of the vehicle.
- j) The effective vehicle length is assumed to be half the DSD for the posted speed limit. The hazard posed by a rock falling on the road increases with proximity to the front of the vehicle. Assuming zero hazard for the rock falling within DSD in front of the vehicle, and a hazard probability of unity of the rock falling immediately in front of the vehicle, setting the effective length to half the sight distance will result in an average hazard for this condition.

The fraction of a road occupied by half the driver's DSD, F_v , can be calculated. Again using Equation 6-1 substituting L_{dsd} for L_v :

$$\begin{aligned}
 P(S:H) &= F_v \\
 &= N_v * L_{dsd} / 24 / V_v
 \end{aligned}$$

where N_v is the number of vehicles at risk which is the traffic volume in vehicles per day, $L_{d_{sd}}$ is the length of the DSD in kilometres, and V_v is the average vehicle speed in kilometres per hour. Therefore, a driver's DSD occupies F_v of the road at any given time.

For the access road at Fox Glacier, $N_v = 150$ per day, $V_v = 50$ km/hr, and for the posted speed limit of 50 km/hr, the DSD is $L_{d_{sd}} = 122$ m (0.122 km) (AASHTO² 1990, Table III-3). Hence:

$$\begin{aligned} P(S:H) &= N_v * L_{d_{sd}} / 24 / V_v \\ &= 150 * 0.122 / 24 / 50 \\ &= 1.52 * 10^{-2}. \end{aligned}$$

$P(S)$ can be calculated using the Equation 6-4:

$$P(S) = 1 - \{1 - P(S:H)\}^{N_r}$$

where N_r includes only those rocks larger than 15 cm diameter which is the same as N_r used in section 6.4.4.1 as the reported average diameter of rocks is around one metre.

For the access road at Fox Glacier:

$$\begin{aligned} P(S) &= 1 - \{1 - 0.0152\}^{2.2} \\ &= 3.32 * 10^{-2}. \end{aligned}$$

As in section 6.4.4.2.1, the probability of an individual's vehicle being in an accident is calculated for this case. The probability of a vehicle hitting a rock, $P(S:H)$, is equal to half the fraction of a cut occupied by the driver's DSD. Therefore:

$$\begin{aligned} P(S:H) &= F_v \\ &= L_{d_{sd}} / 2 / L_c \end{aligned}$$

For the access road at Fox Glacier, $L_{d_{sd}} = 122$ m (0.122 km) and $L_c = 459$ m (0.459 km) and thus:

$$\begin{aligned} P(S:H) &= 0.122 / 2 / 0.459 \\ &= 1.32 * 10^{-1}. \end{aligned}$$

² American Association for State Highway and Transportation Officials.

Then equation 6-4 gives the P(S):

$$\begin{aligned}
 P(S) &= 1 - \{1 - P(S:H)\}^{Nr} \\
 &= 1 - \{1 - 0.132\}^{2.2} \\
 &= 2.67 * 10^{-1}.
 \end{aligned}$$

The probability that the vehicle is in the cut when a rockfall occurs, P(T:S), is equal to the fraction of a year the vehicle is in the cut. Using a single pass through the cut as a standard:

$$P(T:S) = t / 4980$$

where t is the time at risk which is the travel time through the cut in hours. The travel time,

$$t = L_{dsd} / V_v$$

Therefore:

$$\begin{aligned}
 P(T:S) &= L_{dsd} / V_v / 4980 \\
 &= 0.122 / 50 / 4980 \\
 &= 4.89 * 10^{-7}.
 \end{aligned}$$

Then using Equation 6-5:

$$\begin{aligned}
 PAV &= P(S) * P(T:S) \\
 &= 2.67 * 10^{-1} * 4.89 * 10^{-7}. \\
 &= 1.3 * 10^{-7}.
 \end{aligned}$$

Table 6-5 provides the summary of the calculated risks from rockfalls for the access road at Undercite Creek. The probability of an accident occurring is the probability that any accident can occur to any vehicle and the probability of an individual's vehicle being in an accident is the probability that a particular individual can have an accident assuming one trip per year. These values are compared with the acceptable risks in other major civil engineering projects in the following section.

Table 6-5: Summary of calculated probabilities of fatalities and accidents at Undercite Creek.

Type of accident	Probability of an accident	Probability of an individual's vehicle being in an accident
Moving vehicle/falling rock	$2.19 * 10^{-3}$	$4.57 * 10^{-9}$
Moving vehicle/fallen rock	$3.32 * 10^{-2}$	$1.30 * 10^{-7}$

6.5 Comparison Between Assessed Risk and Acceptable Risk

The estimated annual probabilities of fatalities from rockfalls, discussed in the previous sections, have little meaning unless they are compared with published and proposed acceptable risk guidelines worldwide. As there is no published or proposed acceptable risks

for rockfalls, it was decided to compare the hazard with those of “Major Civil Engineering Projects”. The hazard posed by rockfalls can be compared with the hazards posed by major civil engineering projects because both of these come under “occasional major risks”.

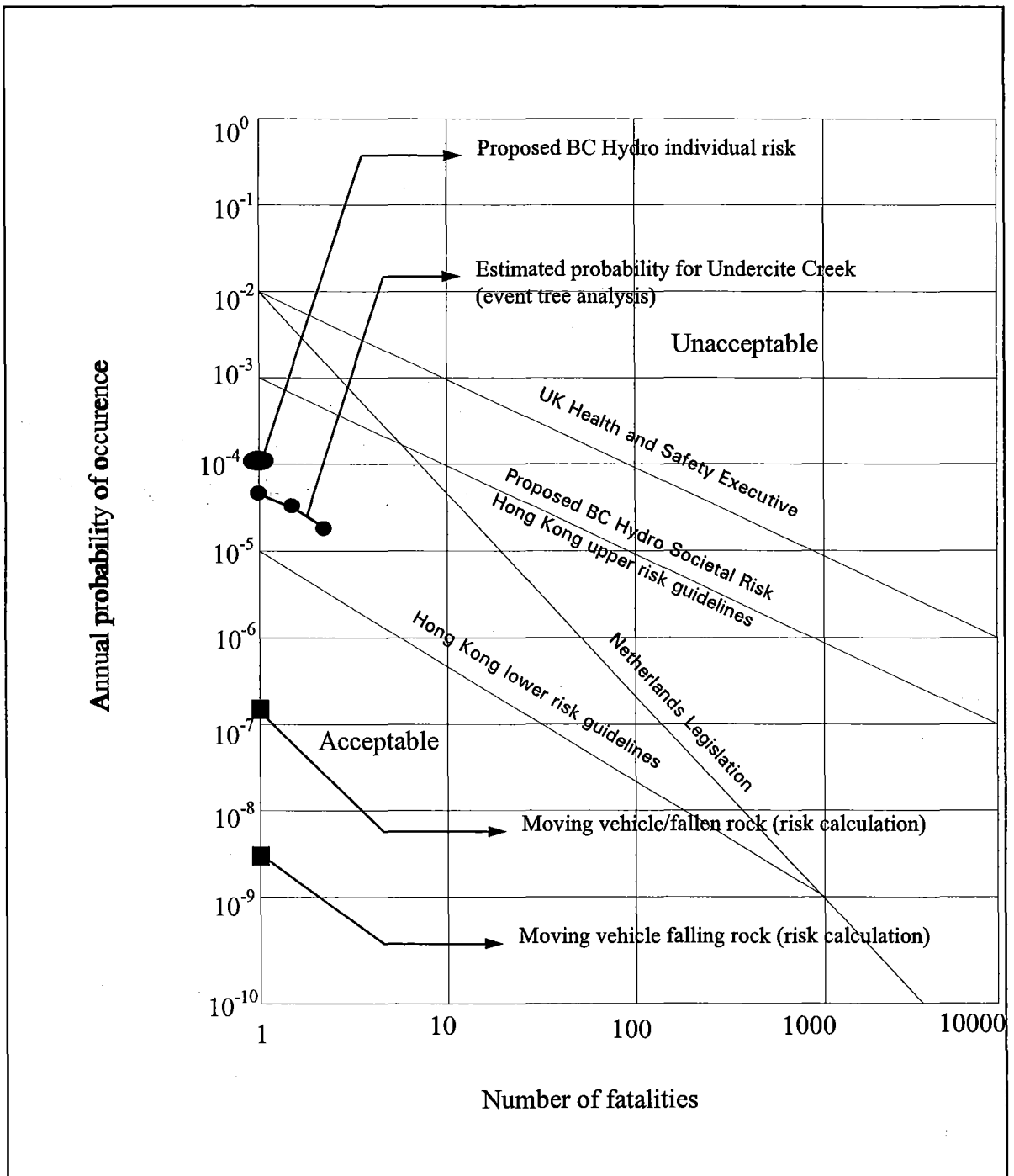


Figure 6-2: Comparison between risks of fatalities due to rockfalls with published and proposed acceptable risk criteria.

Figure 6-2, based on a graph published by Neilsen *et al.* (1994), summarises published and proposed guidelines for tolerable risk. The line marked ‘Proposed BC Hydro Societal Risk’

is particularly interesting since this defines an annual probability of occurrence of fatalities due to dam failures as 0.001 lives per year or 1 fatality per 1000 years. The risk from rockfalls can be compared to the risks from dam failures by assuming that both (dam and rockfalls) come under “Major Civil Engineering Projects” for which the risks to the public must be reduced to acceptable levels. The so-called “acceptable levels” may vary for different countries based on their respective guidelines.

Another point to be noted in Figure 6-2 is that marked ‘Proposed BC Hydro Individual Risk’. This annual probability of fatalities of 10^{-4} (1 in 10,000) is based upon the concept that the risk to an individual from a dam failure should not exceed the individual ‘natural death’ risk run by the safest population group (10 to 14 year old children). Consensus is also developing that the annual probability of fatality of 10^{-4} defines the boundary between voluntary (restricted access to site personnel) and involuntary (general public access) risk (Nielsen *et al.*, 1994).

The calculated probabilities of fatalities from event tree analysis and risk calculation methodology for rockfalls have been plotted in Figure 6-2. These plots show that the estimated risk for Undercite Creek from both the methods is well under the 0.001 lives per year line. Also, the levels are under the acceptable individual risk from hydro projects of 10^{-4} . This indicates the level of risk at Undercite Creek is under “acceptable level” according to the published and proposed acceptable levels around the world (except Hong Kong’s lower risk guidelines). However, it has to be remembered that the risks were compared with hydro projects and also, the acceptable level of risk may be different according to New Zealand guidelines.

6.6 Conclusions and Discussion

The Rockfall Hazard Rating System (RHRS) and the risk calculations, discussed in the previous sections are very crude tools which can only be regarded as semi-quantitative. However, when the trends indicated by these tools are considered together with common sense engineering judgment, they suggest that the risk of fatalities due to rockfalls at Undercite Creek are under the acceptable levels. However, this does not mean that the regional authority can consider the access road and pathway to be “safe”, as the risk calculation involved some estimated parameters. Hence, the regional authority should

continue to monitor rockfall activity at the site so that relevant action can be taken in an event of increase of rockfall activity.

The RHRS developed by the USDOT was used to rate the slopes at Fox Glacier to identify the most hazardous slopes. Application of the RHRS required to assume many things, and the ratings given to a particular unmeasurable category (e.g. geology) is dependent on the rater himself. Hence, allowance should be given for the variance in category scoring for the scores calculated. The following conclusions can be drawn considering the overall rockfall analyses at the site:

- Undercite Creek does not pose any immediate threat to the access road users. However, it should be remembered that the rockfall hazard may increase due to earthquakes and/or a rain storm. Although no rockfalls have been recorded for the past sixteen months, there is sufficient evidence that the slope is further degrading and there is a chance for toppling failure. In an event of increase in rockfall activity, the regional authority may provide a catch ditch by increasing the embankment of the road.
 - Yellow Creek rockfalls pose relatively more danger and an immediate threat to the pedestrians. Rockfalls at Yellow Creek recently reported include a boulder of approximately 4 m diameter (Photo 6-1). Hence, extreme caution should be given to the pathway users about the situation of rockfalls, and if possible, the pathway should be re-located away from the reach of rockfalls from Yellow Creek. Analysis of rockfalls at Yellow Creek using the program *WinRock* suggests the pathway should be shifted at least 20 m away from the base of talus slope.
 - Cone Rock rockfalls show a potential threat to the access road if the degrading of the slopes increases. The degrading of the slopes at parts of the Cone Rock is inevitable considering the orientation of the foliation, and the steepness of the slopes (almost 90°). If rockfall activity at these slopes increases in the near future, it will be better to consider re-location of the access road away from the vicinity of the rockfall debris in order to avoid roll-out of the boulders onto the access road. This conclusion follows the conclusions from previous chapter that deposit zone 3 at Undercite Creek (Figure 5-6) is not under any immediate threat from rockfalls. Coincidentally, the Cone Rock rockfalls occur just opposite to the deposit zone 3 of Undercite Creek. This means that for the present situation, the access road in the deposit zone 3 of Undercite Creek can be safely re-located towards the Undercite slope to avoid rockfalls from Cone Rock. However, the
-

re-location should not be considered in an event of rock avalanche or a major rockfall in deposit zone 3.

Risk assessment carried out for the access road followed a methodology for predicting risks resulting from rockfalls on highways, based on the CAN/CSA (1991) guidelines and Bunce (1994).

Knowledge of the frequency of rockfalls is essential for the accurate assessment of risk. Records of rockfall incidents acquired from the Department Of Conservation (DOC) are incomplete and insufficient. Hence, the estimate of rockfall frequency from the acquired information is an estimated figure. Monitoring of vehicular traffic was not started by the DOC until April 1997, and hence the average daily traffic used to calculate the risk is also an estimated figure. The following conclusions can be drawn from the risk assessment carried out for the access road at Undercite Creek, Fox Glacier:

- The calculated probability of fatalities are under the acceptable levels compared to published and proposed risk guidelines for major civil engineering projects worldwide.
- The probability that an individual's vehicle being in a fatal accident can occur is higher for the moving vehicle hitting a fallen rock than moving vehicle hitting a falling rock. Hence, the local authority may continue to concentrate more on clearing off the rockfall debris than working on effective mitigation of rockfalls.

It has to be remembered that the above conclusions are drawn using estimated values for some parameters and they should, therefore, be used within those limitations. Also, the conclusions drawn are in relative sense, ie comparing one risk to another in case of RHRS rating. The risk assessment did not consider any consequential accidents after the first accident. For example, a vehicle impacts a rock and blocks road; then the immediate vehicle following it will definitely be involved in an accident. The chance that an accident may occur immediately after the first accident increases with poor visibility conditions, panic, and inability of a driver to think that another rock may come down soon. These are only some of the situations where consequential fatal accidents may occur. However, detailed risk assessment considering all of these conditions is beyond the scope of the thesis.

6.7 Summary

RHRS (1993) and CAN/CSA (1991) guidelines have been used in this chapter to perform a semi-quantitative assessment of rockfall hazard at Fox Glacier. The assessment showed that the calculated risks are under the acceptable levels of risk for civil engineering projects worldwide.

Chapter 7 goes on to carrying laboratory tests in an attempt to find out an easy means of determining the coefficient of restitution used in the computer simulation of rockfalls.

Chapter 7

Laboratory Tests To Find The Coefficient of Restitution

7.1 Introduction

The coefficient of restitution is usually determined from *in situ* tests that are very expensive and risky. A need is identified for finding out a safe and less expensive method of determining these coefficients. Hence, in this chapter an attempt is made to find an easy means of determining the normal coefficient of restitution.

Two different methods of obtaining the coefficient of restitution will be discussed in this chapter: to use Schmidt hammer (to obtain an empirical relation between Schmidt number and restitution coefficient), and to use a steel ball impacting a rock slab tightly clamped on to the ground (by finding a correlation between steel-rock impact restitution and rock-rock impact restitution).

7.1.1 Importance of The Restitution Coefficients

Richards (1988) explains the importance of the restitution coefficients for the computer simulation of rockfalls. In his paper, Richards (1988) showed the influence of the coefficients of restitution on the calculations of maximum trajectories of falling rocks (Figures 7-1 and 7-2). The trajectories were simulated using the program *Rockfall*. From Figures 7-1 and 7-2, one can see that a slight change in the value of the coefficients of restitution result in totally different trajectories. This explains the importance of obtaining the coefficients of restitution as accurately as possible, so that the computer simulation of rockfalls carried out is more realistic to the natural environment.

Research on rockfalls has in the past been concentrated either on the understanding of the phenomenon and performing some *in situ* tests, or developing a computer model. No research has been carried out to attempt find the coefficients of restitution by laboratory methods. Although these coefficients can be obtained with fair accuracy by means of *in situ* tests, no relation has been explored between these coefficients and material constants of rocks.

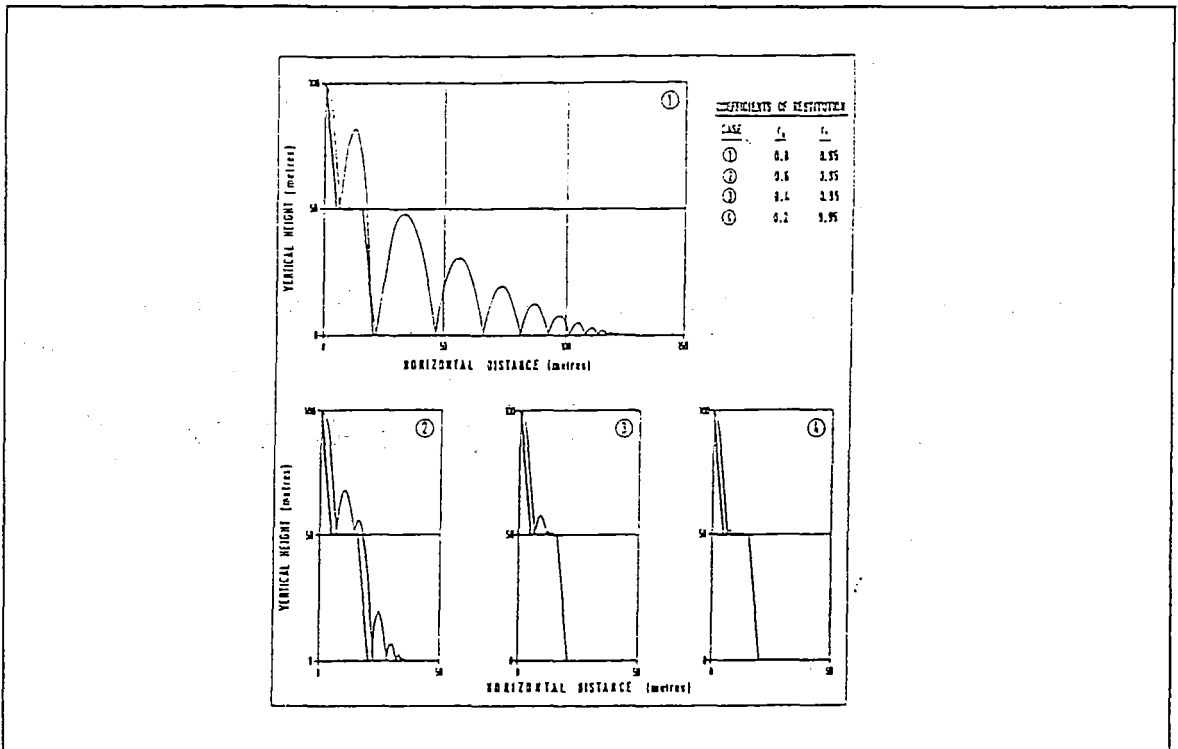


Figure 7-1: Example of effect of varying R_n on rockfall trajectory (Richards 1987).

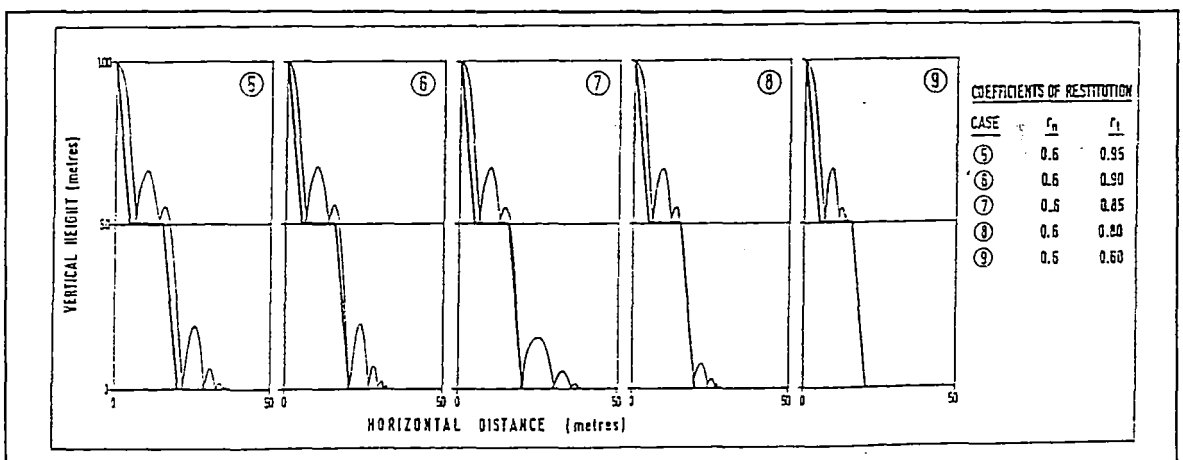


Figure 7-2: Example of effect of varying R_t on rockfall trajectory (Richards 1987).

7.2 Background on Restitution Coefficients

The restitution coefficients were first discussed by Isaac Newton in the 17th century. Newton introduced these coefficients while discussing impact mechanics. According to Newton, there will be some loss of energy during the impact of two rigid bodies which can be obtained using mass, initial velocities and final velocities of the impacting bodies. A literature search on these coefficients of restitution indicate many attempts to derive a better understanding of the mechanics involved in the impact of two rigid bodies, especially because the coefficients are of interest to many industries (e.g. pharmaceutical, manufacturing etc.).

Smith (1992) writes that there are three types of restitution coefficients to be considered in rigid body impact problems: coefficient of restitution (work); coefficient of restitution (velocities); and the coefficient of restitution (momentum). While defining these coefficients, Smith (1992) divided the impact system into two phases: compression phase and restitution phase. The duration between initial contact and the instant at which the normal component of the velocity difference between the impacting bodies reaches zero is called the “compression phase” and the remainder of the period of contact is called the “restitution phase”. The definition of the restitution coefficients are (Smith 1992):

- Coefficient of restitution (momentum): is the ratio of impulse in the restitution phase to that of compression phase.
- Coefficient of restitution (velocities): is the ratio of velocity difference between the impacting bodies at the instant the contact ends, to that of the velocity difference before the impact.
- Coefficient of restitution (work): is the square root of the ratio of the work done during restitution to that during compression.

Smith (1992) states that although these three coefficients are stated to be different depending upon the impact characteristics, they are of same value in some circumstances. Smith (1992) did not mention any particular situations where these three coefficients can be similar. For the purpose of rockfall simulation, apparently these coefficients were assumed to be the same, as different authors (Elliott 1992, Pfeiffer and Bowen 1989, Azzoni 1995, and Hungr and Evans 1988) used different coefficients for restoring velocities. For example, Azzoni (1995) used momentum restitution coefficient whereas

Elliott (1992), Hungr and Evans (1988) and Pfeiffer and Bowen (1989) used the velocity restitution. The definitions given above for the three types of restitution implies that the restitution coefficient found using the velocities will be the best to use as the coefficient is further used by the program to reduce the resultant velocities after an impact occurs.

The coefficient of restitution was found in the past either by bouncing a spherical boulder in the laboratory (Campanuovo 1977) or by means of *in situ* tests (Azzoni *et al.* 1995). The *in situ* tests are found to be more reliable as the bounce characteristics are those of original scale. Using rock spheres in the laboratory is not a good method as often there are breakage of rocks dropped from a height of 1 to 1.2 m. The coefficients found in the laboratory also need to be adjusted for the site-specific conditions, considering the rock characteristics, strength and amount of weathering.

7.3 Obtaining a Relation Between The Schmidt Number and Restitution Coefficient

As a first attempt to find an easy means of determining the restitution coefficient, experimentation will be carried out to check whether a correlation exists between Schmidt number and the restitution coefficient. The Schmidt hammer is widely used in the construction industry (and in rock engineering) as a non-destructive means of determining the rebound hardness of a test material.

As the Schmidt hammer is widely available and as the principle involved is based on impact, it was decided to investigate any correlation between the Schmidt number and the restitution coefficient for rock. An experimental setup was used to find the normal coefficient of restitution by vertically dropping a steel ball onto a clamped rock surface. The following sections describe the experimental procedure and setup used to find the restitution coefficient and the Schmidt number in the laboratory.

7.3.1 Experimental Procedure To Find The Restitution Coefficient

The procedure used to find the restitution coefficient is very simple. A steel ball (hardened ball bearing type, with diameter 4cm) is dropped vertically onto the rock slab which is tightly clamped to the floor (concrete). The rock slab used was cut to make it smooth and flat on both sides. The height from which the steel ball is released (h) and the height to

which it rebounds (h') are both recorded. Then the restitution coefficient can be found using (Spang and Reutentsrauch 1988):

$$R = \sqrt{\frac{h'}{h}} \quad \dots\text{Equation 7-1}$$

The above equation has been derived from the original definition of the restitution coefficient which is the ratio of energy after and before impact. In this particular case, as the steel ball is released for a free fall, the ratio is of kinetic energies, which finally reduces to the Equation 7-1.

A levelling staff was used to measure the bounce heights of the steel ball. Only the first bounce was used for the recordings. A high speed camera, which is capable of recording up to 200 frames per second is used to record every bounce of steel ball on rock. The following section describes the complete experimental setup used for the purpose. The steel ball is dropped 10 times for each type of rock in order to get statistically significant results. The restitution coefficient will be the average of all these values.

7.3.1.1 Experimental Setup To Find The Restitution Coefficient

Photo 7-1 shows the experimental setup used to find the restitution coefficient of an impact between a steel ball and a rock. A mechanical magnet is attached to a tripod stand which was used to stick the steel ball so that the steel ball can be released from a known vertical point. This also eliminates human errors involved in releasing the ball by hand. The rock slab on to which the steel ball impacts is clamped tight on to the ground (concrete floor) so as to imitate an immovable bed rock (Photo 7-2). The clamping of the rock slab is essential so that the restitution coefficient obtained is not effected by the non-uniform transfer of impact force (from steel ball to rock slab) that may arise if the rock slab was sitting on the floor without being clamped.

A black and white high speed camera was used to record every drop of ball onto the rock slab. The camera is able to record up to 200 frames per second and the recorder is capable of replaying the recording using frame by frame, thus enabling precise identification of the bounce height. However, a normal camera can also be used for simplicity.

The height of the drop and rebound were measured by using a levelling staff for only the first bounce of each drop. All drops were from the same height of 1 m.

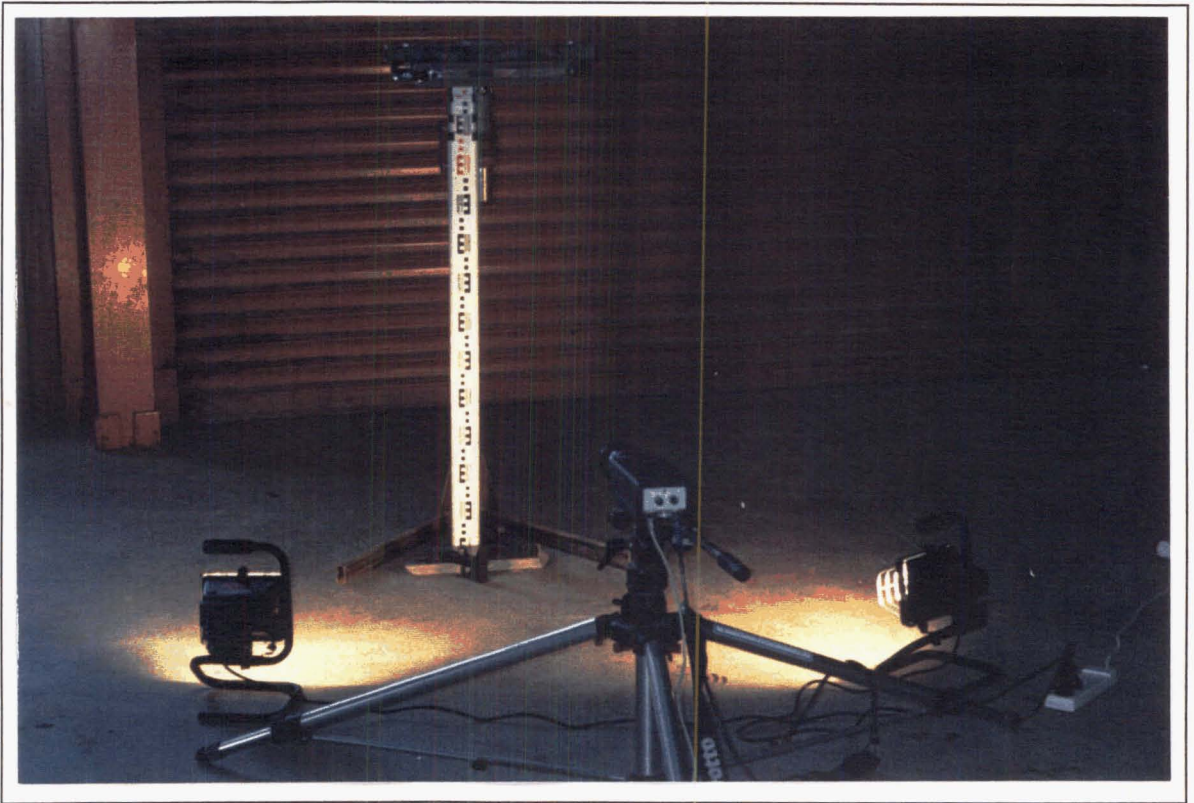


Photo 7-1: Experimental setup to find the coefficient of restitution.

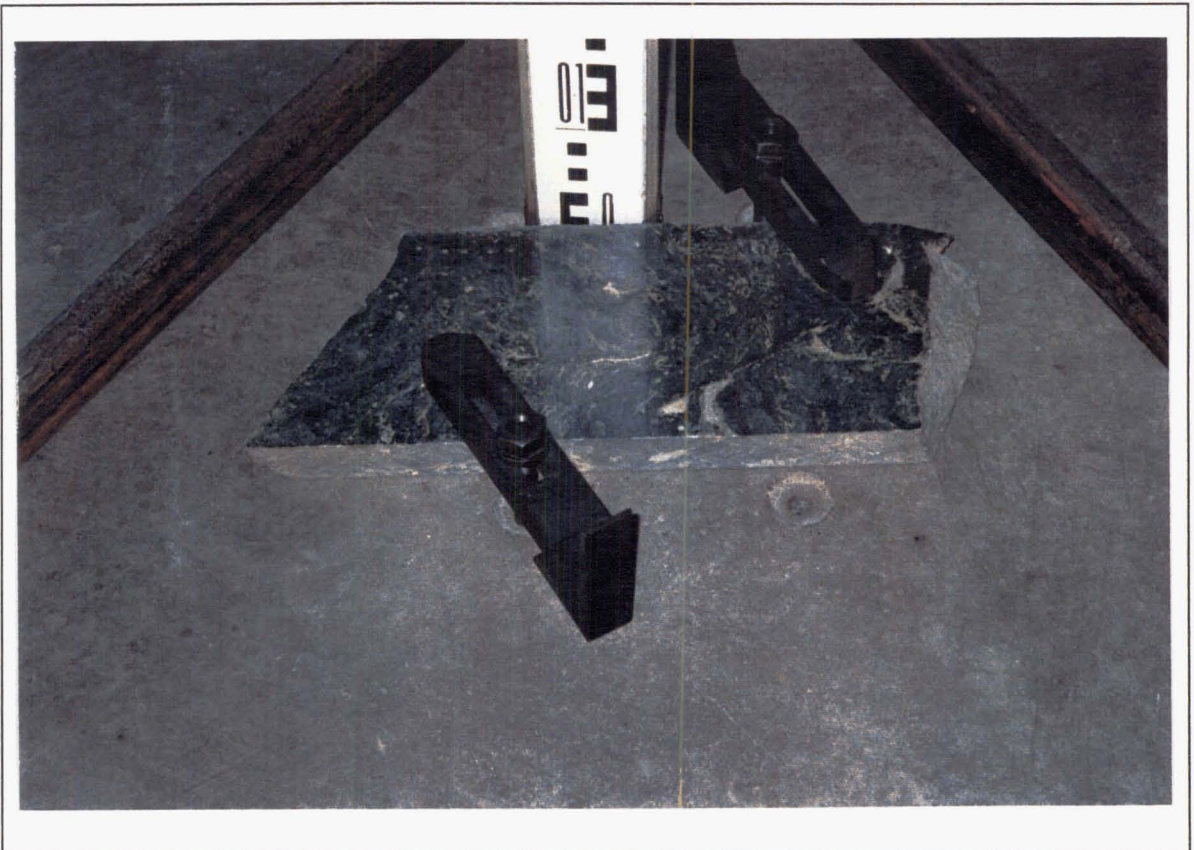


Photo 7-2: Method of clamping the rock slab tight to the ground.

7.3.2 Method of Finding The Schmidt Number of Rock

The Schmidt hammer is usually used to determine the rebound hardness of a test material (Photo 7-3). The plunger of the hammer is placed against the specimen and is depressed into the hammer by pushing the hammer against the specimen. Energy is stored in a spring which automatically releases at a prescribed energy level and impacts a mass against the plunger. The height of rebound of the mass is measured on a scale and is taken as the measure of hardness. The device is portable and may be used both in the laboratory and field.

The Schmidt hammer used in this research is of type L whose impact energy is 0.735 Nm. The Schmidt number obtained for the rock specimens comply with the ISRM (International Society for Rock Mechanics) suggested methods (Brown 1981). The Schmidt number will be obtained at least 10 times for the same rock specimen as per the ISRM recommendations. The average of these 10 values will be the Schmidt number for that particular rock.

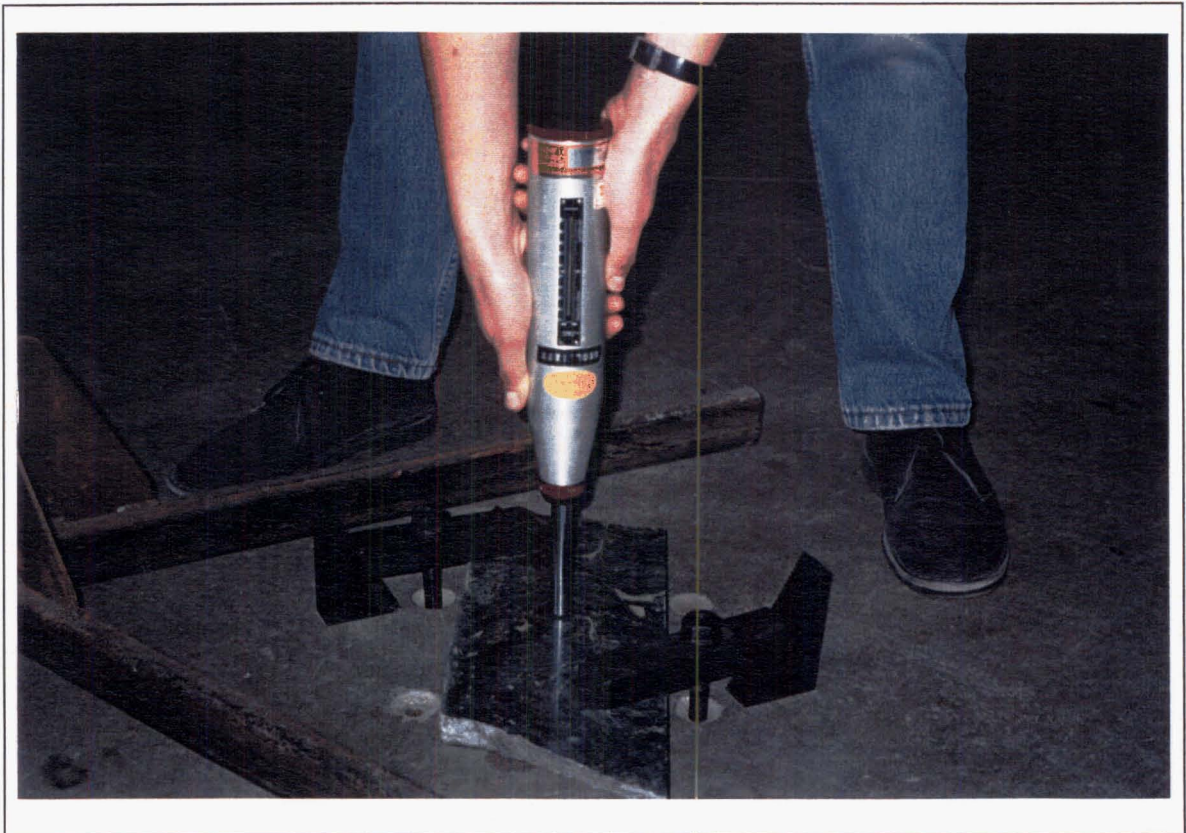


Photo 7-3: Schmidt hammer used for the experiments (Type L).

7.3.3 Correlation Between Schmidt Number and Restitution Coefficient

In order to get good statistical analysis, it was decided to use a large number of different types of rocks for this purpose. A total of 14 different types of rock specimens were obtained (from the library of rocks in the Geology Department at University of Canterbury), covering all major types of rocks: igneous, metamorphic, carbonates and sedimentary. Table 7-1 shows the list of rock specimens used for the experiment. All of these rocks were tested to find the restitution coefficient and the corresponding Schmidt number using the method described above.

Table 7-1: Types of rock specimens used for the tests.

Igneous	Carbonates	Metamorphic	Sedimentary
Granite	Travertine	Serpentinite	Berrina Sandstone
Trachyte	Carrara marble	Narrandera quartzite	Piles Creek Sandstone
Basalt	Classico marble	Welsh Slate	Maroubro Sandstone
			Joadja Sandstone
			Fox Schist

Table 7-2: Schmidt number and restitution coefficients of different types of rocks.

Rock type	Schmidt Number	Restitution Coefficient
Granite	59.17	0.77
Trachyte	51.33	0.72
Basalt	63.33	0.78
Travertine	44.67	0.53
Carrara	30.67	0.54
Classico	29.17	0.33
Serpentinite	38.83	0.55
Narrandera Quartzite	50.83	0.70
Welsh Slate	46.67	0.70
Berrina Sandstone	42.67	0.60
Piles Creek Sandstone	33.00	0.51
Maroubro Sandstone	41.83	0.62
Joadja Sandstone	26.67	0.51
Fox Schist	49.83	0.68

Table 7-2 shows the average values of the restitution coefficients and the corresponding Schmidt numbers for different rock types. From the table, it is clear that restitution coefficients for igneous rocks are the highest, as usually igneous rocks are the strongest and hence a high restitution coefficient. However, the restitution value depends on the weathered condition of the rock as well.

Figure 7-3 shows the graph for the correlation between restitution coefficient and Schmidt number. From the correlation analysis, an r^2 value of 0.793 and a correlation coefficient of 0.89 is obtained. This means that a good correlation exists between the Schmidt number and restitution coefficient. The equation relating the two parameters can be written as:

$$\text{Restitution coefficient} = 0.1734 + 0.0101 * \text{Schmidt number} \quad \dots \text{Equation 7-2}$$

Using the above empirical relation, the coefficient of restitution of a steel ball impacted on a rock can be obtained from the Schmidt number.

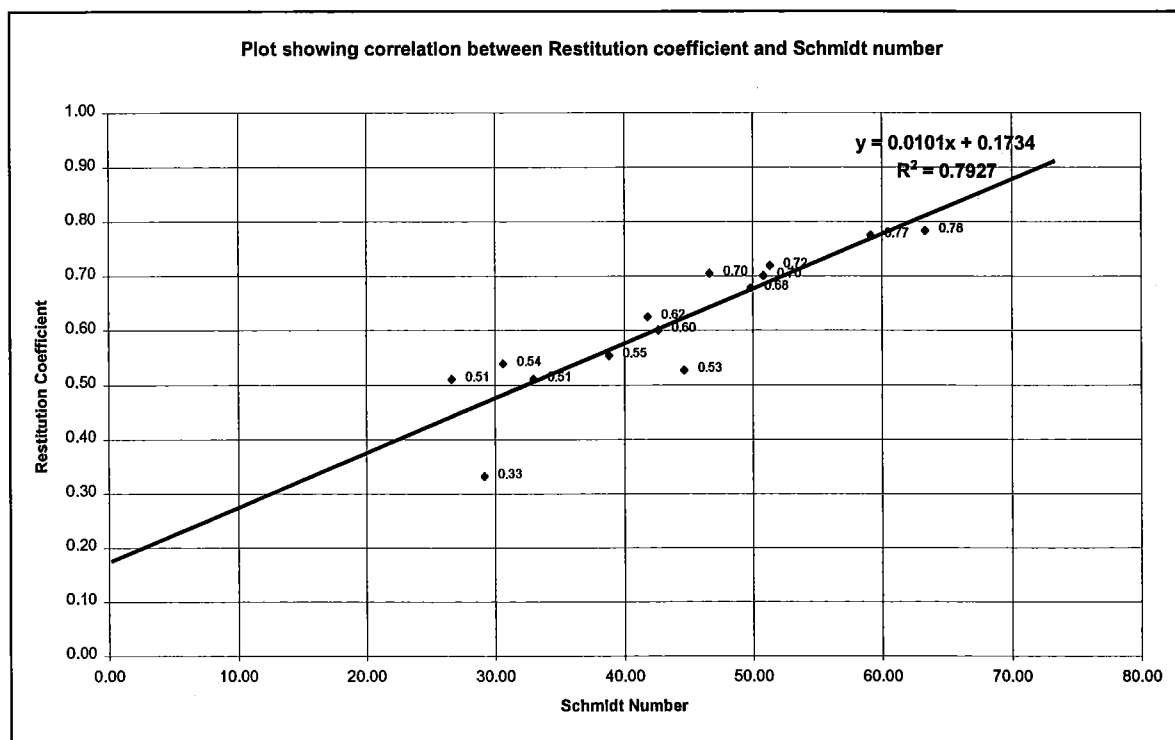


Figure 7-3: Plot showing the correlation between restitution coefficient and Schmidt number.

The r^2 and correlation coefficient values for restitution coefficients of various types of rocks (igneous, carbonates, metamorphic and sedimentary) and Schmidt number are shown in Table 7-3.

Table 7-3: r^2 and correlation coefficient values for different types of rocks.

	r^2	r
Total	0.79	0.89
Igneous	0.95	0.97
Carbonaceous	0.28	0.53
Metamorphic	0.86	0.93
Sedimentary	0.92	0.96

From the table, it can be seen that the correlation is high for igneous, metamorphic and sedimentary rocks but, for carbonaceous rocks the correlation is extremely low. This implies that the usage of Schmidt number to obtain a value of restitution coefficient for carbonaceous rocks is unreliable. The correlation coefficient for igneous, metamorphic and sedimentary rocks is high compared to the correlation coefficient for total (including carbonaceous). This in turn implies that the restitution coefficient can be obtained from Schmidt number for igneous, metamorphic and sedimentary rocks with reasonable accuracy. However, it should be remembered that the correlation for individual types of rocks is based on less than 5 specimens.

7.4 Obtaining The Coefficient of Restitution of Rock-Rock Impacts From Steel-Rock Impacts

When a steel ball is bounced on rock, the impact characteristics will be different to that of when a rock sphere bounces on rock. The restitution coefficient of rock-rock will be lesser than that of steel-rock, because the steel ball is more elastic than rock and hence bounces higher. For this reason, the coefficient of restitution determined above cannot be used in the computer simulation of rockfalls.

A second attempt to find an easy means of determining the coefficient of restitution is to obtain a relationship between restitution coefficients of steel-rock and rock-rock impacts. To achieve this, experiments can be carried out using rock spheres, of the same rock as the

impact surface. The coefficient of restitution can be found for both rock-rock and steel-rock by bouncing the steel ball and the rock sphere on the rock slab.

It can be suggested to use the steel ball and rock sphere with the same mass. This suggestion is made from bouncing two steel balls of different diameter (and mass, of course) from same height onto the same rock slab. From these tests, it was found that the steel ball with a smaller diameter and mass was bouncing higher. Using Equation 7-1, the coefficient for smaller steel ball was found to be higher than that of larger steel ball. Even though the effect of mass can be theoretically cancelled out while calculating restitution coefficient when a ball is released to impact a rock slab by free-fall, the mass does effect the rebound height. This can be explained by the ability of a sphere of larger mass to make a dent (permanent deformation) in rock. As the larger mass is able to make a permanent deformation on the rock slab, the dissipation of energy is obviously greater than that of when a smaller ball is impacted on the rock slab. Hence, by using spheres (steel and rock) of same mass to bounce on a rock slab, the variance of energy dissipation pertaining to the effect of mass can be eliminated.

When the restitution tests described above are performed on about 15 to 20 different types of rock, a relation can be obtained between steel-rock and rock-rock restitution coefficients. If a good correlation exists between restitution coefficients of steel-rock and rock-rock, the tests of bouncing a steel ball onto a clamped rock slab can be made a standard test for obtaining the restitution coefficient of rocks.

The experimentation for obtaining a relationship between the restitution coefficient of steel-rock and rock-rock impacts can be extended to explore the relation between restitution coefficient of rock-rock and the Schmidt number. This can be done using the procedure described in section 7.3. If a good correlation exists between Schmidt number and coefficient of rock-rock, it will be a spin-off in the rockfall simulation as the Schmidt number can be directly used to obtain the restitution coefficient.

Unfortunately, it was decided not to perform these tests in this research because of the financial (making rock spheres) and time constraints.

7.5 Conclusions and Discussion

The first attempt to find an empirical relation between Schmidt number and restitution coefficient showed good results. However, the relation was obtained for the restitution coefficient of a steel ball impacting rock surface. The attempt can be considered completely successful only if a good correlation is obtained between the Schmidt number and restitution coefficient of rock-rock impact. The following conclusions can be drawn from the experiments carried out in an attempt to use the Schmidt hammer to find the restitution coefficient:

- An r^2 value of 0.739 and the correlation coefficient of 0.89 has been obtained showing a good relation between Schmidt number and the restitution coefficient of a steel ball impacting rock slab.
- The empirical equation (Equation 7-2) can be used to obtain a restitution coefficient of a steel ball impacting rock using the Schmidt number of that rock.
- The correlation between steel-rock impact shows that a good correlation may also exist between rock-rock restitution and steel-rock restitution.

Because of the financial and time constraints, tests to obtain the relation between restitution coefficient for steel-rock and rock-rock impacts were not performed in this research. However, the author is optimistic that a good correlation exists between the two restitution coefficients.

7.6 Summary

For the first time in rockfall research, an attempt was made to find out an easy means of obtaining the coefficient of restitution. The experimentation showed that a good correlation ($r = 0.89$) exists between Schmidt number and restitution coefficient of a steel ball impacting rock surface.

Chapter 8 goes on to drawing cumulative conclusions based on the individual conclusions from previous chapters.

Chapter 8

Conclusions and Discussion

8.1 Introduction

In this chapter, conclusions from the previous chapters are integrated and discussed. Cumulative conclusions will be drawn regarding computer simulation of rockfalls, rockfall hazards at Fox Glacier and the coefficient of restitution, based on research carried out in this thesis. Finally, suggestions for future work in this area will be made.

8.2 Achieving Three Main Objectives

The three main objectives stated in Chapter 1 are achieved in Chapters 3, 4, 5, 6 and 7. Chapter 3 compared five simulation programs and concluded that the best program to use for a detailed analysis of rockfalls is *Rockfal2*. In Chapter 4, the program *Rockfal2* was modified to include facility to perform more probabilistic analysis of rockfalls. Thus achieving objective 1, in Chapter 5, the modified program of the original *Rockfal2*, *WinRock*, is used to analyse the rockfalls at Undercite Creek, Fox Glacier. Chapter 6 concentrated on assessment of rockfall hazard to the access road at Fox Glacier. Thus objective 2 achieved, in Chapter 7, an attempt was made to obtain a relation between Schmidt number and the coefficient of restitution to derive an easy way of obtaining the coefficient in future. Figure 8-1 provides a schematic diagram of how the three main research objectives were achieved along with the main conclusions of the respective chapters.

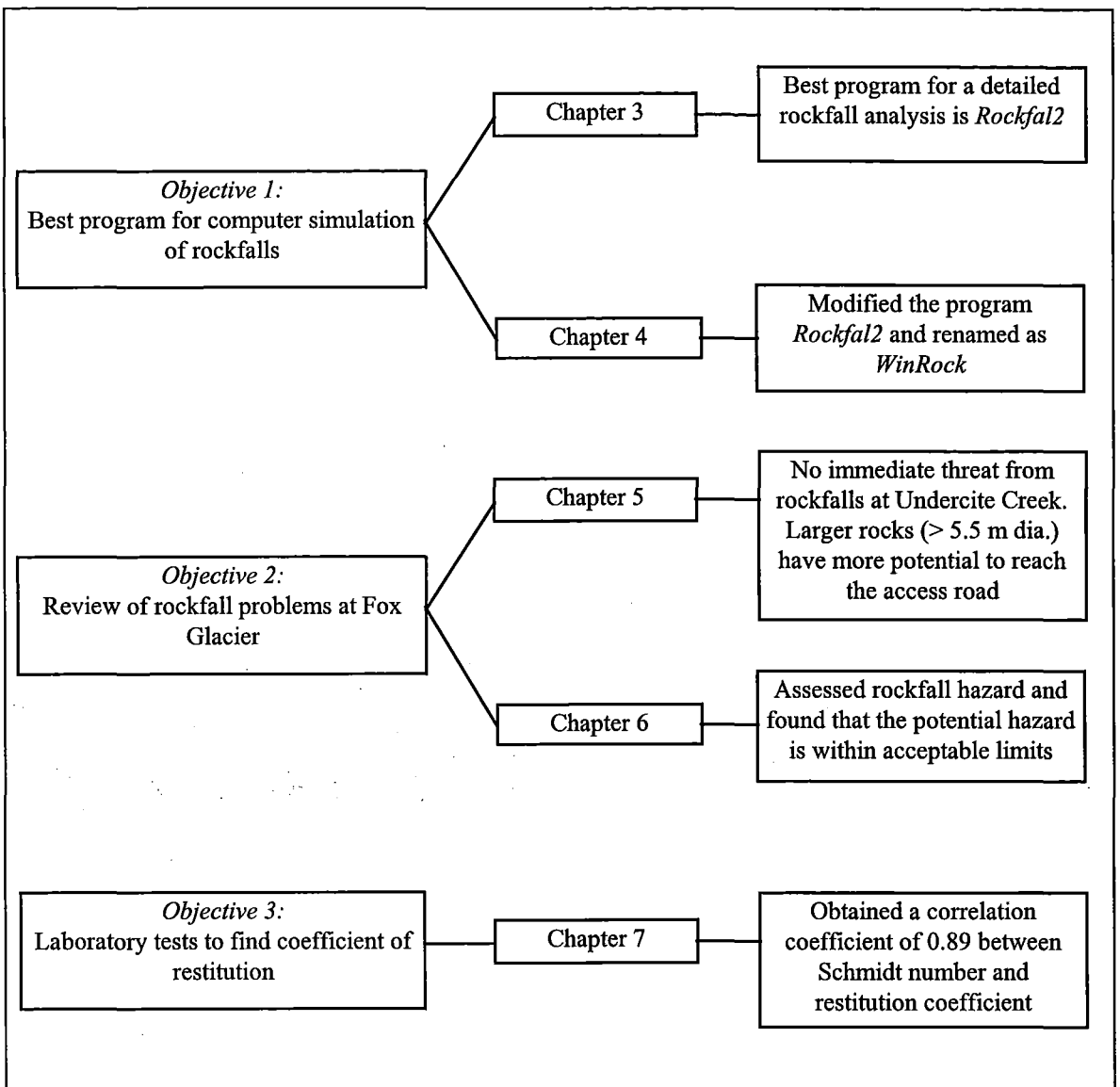


Figure 8-1: Schematic diagram showing the three main research objectives and the main conclusions from each chapter.

8.3 Overall Conclusions

In this section, conclusions are drawn and discussed under three main sub-headings: computer simulation of rockfalls; review of rockfall problems at Fox Glacier; and coefficient of restitution.

8.3.1 Computer Simulation of Rockfalls

The following are the main conclusions from Chapters 3 and 4:

- *Rockfall* - The program does not incorporate randomisation of rockfall parameters, which is the most important part of rockfall simulation.

- *CRSP* - The program randomises only the slope roughness of the slope and has problems handling vertical or overhanging slopes.
- *Rockfal2* - The program is capable of simulating rockfalls with sufficient output for a detailed analysis but lacks some randomisation and generation of boulder trajectories.
- *RF* - The program can handle only small slopes (up to 43 slope cells), lacks specification of initial conditions of the boulder, and uses some un-explained parameters governing the elasticity of the material.
- *CADMA* - The program incorporates sufficient randomness but is incapable of handling vertical or overhanging slopes.
- *WinRock* (modified program of the original *Rockfal2*) - The program uses the same simulation logistics as *Rockfal2* with an additional facility to randomise initial velocity and starting position of the boulder, along with developing boulder trajectories.

Comparison of five different programs written by various authors revealed a large difference between the simulation logistics adapted by them. This difference suggests that the understanding of the logistics involved in rockfalls is still under evolution, and hence various authors used their own assumptions for computer simulation of rockfalls.

8.3.2 Review of Rockfall Problems at Fox Glacier

The following conclusions are drawn from Chapters 5 and 6 regarding the rockfalls at Fox Glacier:

- Undercite Creek
 - There is no immediate threat from rockfalls in the deposit zones 1 and 3 (see Figure 5-6).
 - Deposit zone 2 is under threat from rocks larger than 5.5 m equivalent spherical diameter.
 - The calculated probabilities of fatalities are well under the published and proposed acceptable limits for major civil engineering projects worldwide.
 - In the event of increased rockfall activity, the regional authority may consider increasing the elevation of the road, thus creating a catch ditch.
 - In the event of occurrence of another major rockfall event or rock avalanche resulting in the spread of the debris cone, the site should be re-analysed.

- Yellow Creek
 - The regional authority should consider re-location of the access pathway at least 20 m away from the base of talus slope as there is a high potential for rockfall hazard in this area.
- Cone Rock
 - There is high potential for increase in the rockfall activity in this area considering the orientation of foliation and the steepness of the slope along with the recent increase in rockfall activity.
 - In the event of increase in the rockfall activity in this area, which may increase the potential hazard of rockfalls reaching the access road, the regional authority may re-locate the road towards the Undercite Creek *only* in deposit zone 3 (see Figure 5-6).

The hazard assessment has to be updated if the rockfall activity at the site increases in due course. To perform a detailed hazard assessment, the regional authority needs to maintain and update a complete database of rockfall activity at all the slopes. A systematic recording of rockfalls is essential for this purpose. The recordings may include the details of deposit zone and starting zone (if seen) of rock, approximate size and distance from the access road along with comments on weather of the previous and present day.

8.3.3 Coefficient of Restitution

The following are the main conclusions drawn from Chapter 7:

- A correlation coefficient of 0.89 was found between the Schmidt number and the coefficient of restitution of a steel ball impacting on a rock surface.
- The above conclusion indicates that a good correlation may also exist between the Schmidt number and the coefficient of restitution of a rock sphere impacting on the surface of the same rock type.
- Thus Schmidt number can be used to determine the restitution coefficient of rock to rock impact (once the relation has been found between the coefficient and Schmidt number) which eliminates the need of *in situ* tests in the future.

8.4 How helpful was this research?

The research carried out in this thesis is helpful for the computer simulation of rockfalls in general, and to draw some conclusions about the rockfalls at Fox Glacier.

The comparison of rockfall simulation programs has helped to decide upon the best program to use for a detailed analysis of rockfalls. The modified program *WinRock* can now be successfully used for a detailed probabilistic analysis of rockfalls. The comparison of programs also indicated that there is a large difference among the simulation logistics used by various authors because of lack of understanding of the impact characteristics and hence, there is a need to perform research in this area.

Detailed analyses and hazard assessment of rockfalls at Fox Glacier has been helpful to draw some valuable conclusions for the present and future hazards, which in turn will be helpful for planning and maintenance of the access road to the glacier in the future.

Experimentation carried out to find out an easy means of determining the coefficient of restitution for the first time in rockfall research history will be helpful to standardise the method of using Schmidt hammer to find the restitution coefficient.

8.5 Future Work

Although the phenomenon of rockfalls has been thoroughly studied in recent times and the approach of the engineers has been more technical, there is a need to upgrade the present level of understanding of and approach to the problem. Some future work which may help to do so is outlined below.

The work carried out in Chapter 7 to find the restitution coefficient in the laboratory indicates that a good correlation may exist between Schmidt number and the coefficient of restitution of rock on rock impact. Suggestions made in section 7.4 can be followed to achieve this. If this research is successful, there will be no need of performing expensive and risky *in situ* tests any more for this purpose.

The simulation of bounce mode in the rockfall simulation programs has to be upgraded to incorporate the present understanding of the rigid body impact problem. Research has to be carried out in this area so that the impact characteristics can be better simulated and brought as close to nature as possible. For example, the assumption that no slippage occurs during the impact in the simulation of rockfalls can be eliminated by including the coefficient of friction and the formulae given by Brach (1984). Also, attempt can be made

to simulate disintegration of rocks while coming down the slopes as the pieces of disintegrated rocks travel with increased velocity and hence pose more threat to the road users.

An attempt can also be made to compare rockfall simulation programs with some detailed *in situ* tests so that every program can be tested for accuracy of simulating rockfalls imitating nature. This will be helpful to draw a baseline and to show how accurate or inaccurate each program simulates actual rockfalls.

Appendix A

Logistics and Sequence of Calculation Steps Involved in The Program *Rockfal2*

A.1 Logistics Involved in The Program *Rockfal2*

This appendix describes the simulation logistics and the calculation steps used by the program *Rockfal2* in detail¹. The approach used herein to model rockfall behaviour is based on the equations of dynamics and the discussions of rockfalls published in Ritchie (1963), Descoudres and Zimmermann (1987), Spang (1987), Chan *et al.* (1986), Benitez *et al.* (1986), and Pfeiffer and Bowen (1989). The numerical solution presented here involves determining whether the motion of the boulder is in "bounce" or "roll" mode, and calculating the velocity at the end of the "bounce" or "roll" cycle. The algorithms used by the program for "bounce" and "roll" modes are first presented in sections A.1.1 and A.1.2 respectively. The calculation sequence used by the program is then presented in section A.2.

A.1.1 "Bounce" Mode Algorithms

The trajectory of a boulder in flight is assumed to be parabolic. The position of the boulder at any time, t , after the boulder takes to flight is defined in x, y coordinates using,

$$x_t = V_o \cos(\alpha_o)t + x_o \quad \dots \text{Equation A-1}$$

$$y_t = V_o \sin(\alpha_o)t - \frac{1}{2}gt^2 + y_o \quad \dots \text{Equation A-2}$$

where V_o is the initial velocity of the boulder

α_o is the initial angle of the flight trajectory

¹ This notes has been summarised from Elliott (1992).

- g is the acceleration due to gravity
 x_0 is the x-coordinate at the start of the trajectory
 y_0 is the y-coordinate at the start of the trajectory

The vertical and horizontal velocity components of the boulder, V_y and V_x , respectively, at time t are found by differentiating the position coordinates with respect to time, giving,

$$V_x = V_o \cos(\alpha_o) \quad \dots \text{Equation A-3}$$

$$V_y = V_o \sin(\alpha_o) - gt \quad \dots \text{Equation A-4}$$

From these velocity components, the actual velocity V_t and direction α_t of travel of the falling boulder at any time t are then calculated using:

$$V_t = \sqrt{V_x^2 + V_y^2} \quad \dots \text{Equation A-5}$$

$$\alpha_t = \tan^{-1} \left(\frac{V_y}{V_x} \right) \quad \dots \text{Equation A-6}$$

The time at which the boulder passes above some prescribed point on the slope having x-coordinate x_a can be determined by rearranging Equation A-1 as follows:

$$t_a = \frac{x_a - x_o}{V_o \cos(\alpha_o)} \quad \dots \text{Equation A-7}$$

The y-coordinate at this moment in time, y_a can then be found by substituting $t = t_a$ in Equation A-2. The height of the boulder above the slope can then be found by comparing y_a with the y-coordinate of the slope at $x = x_a$. For a linear segment of slope having end points (x_1, y_1) and (x_2, y_2) , the height of the boulder above the slope at $x = x_a$ can be found using:

$$h_a = y_a - \left(\frac{y_2 - y_1}{x_2 - x_1} \right) x_a - (y_1 x_2 - x_1 y_2) \quad \dots \text{Equation A-8}$$

At some point in time the boulder will impact the ground surface, and will rebound. The x , y coordinates at the point of impact are calculated using Equations A-1 and A-2 after first calculating the elapsed time till impact. These (x, y) coordinates will also define the start coordinates (x_o, y_o) for the next calculation cycle. The elapsed time till impact with a straight section of slope having end coordinates (x_1, y_1) and (x_2, y_2) , is the largest root of the following equation:

$$\frac{1}{2} g t^2 + At + B = 0 \quad \dots \text{Equation A-9}$$

where:

$$A = mV_o \cos(\alpha_o) - V_o \sin(\alpha_o)$$

$$B = m(x_o - x_1) - (y_o - y_1)$$

$$m = \frac{y_2 - y_1}{x_2 - x_1}$$

The rebound characteristics will depend on the impact velocities (directional and rotational) and angle relative to the ground surface, and the loss of kinetic energy on impact. The angle of impact relative to the ground surface, β_i , the rotational velocity ω_i and the impact velocity components, V_{in} and V_{is} , normal and tangential to the ground surface respectively, at the time of impact are calculated using:

$$\beta_i = \alpha_i - \theta \quad \dots \text{Equation A-9}$$

$$\omega_i = \omega_o \quad \dots \text{Equation A-10}$$

$$V_{in} = V_i \sin(\beta) \quad \dots \text{Equation A-11}$$

$$V_{is} = V_i \cos(\beta) \quad \dots \text{Equation A-12}$$

where q , the local inclination of the rock surface at the point of impact, equals the average slope angle plus the local slope roughness angle.

Generally, boulders in flight also tend to rotate, and pick up or lose rotational speed on each impact. Rotational speed is gained on each impact by virtue of the center of gravity of the boulder being offset from the periphery of the boulder at the point of impact. Hence at the moment of impact, the point coincident with the center of gravity has a tangential velocity component, while the point of impact on the periphery is momentarily brought to rest. The rebound velocity components, V_{rn} and V_{rs} , normal and tangential to the ground surface respectively, and the rebound rotational velocity, ω_r , are calculated on the basis of energy balance considerations, using empirical relationships for the energy lost during impact derived by Pfeiffer and Bowen (1989).

$$V_{rn} = \frac{V_{in} R_n}{1 + \left(\frac{V_{in}}{30}\right)^2} \quad \dots \text{Equation A-13}$$

$$V_{rs} = \sqrt{\frac{r^2 (I\omega_i^2 + mV_{is}^2) F_1 F_2}{I + mr^2}} \quad \dots \text{Equation A-14}$$

$$\omega_r = \frac{V_{rs}}{r} \quad \dots \text{Equation A-15}$$

where R_n is the coefficient of normal restitution;

r is the radius of the boulder;

- ω_i is the rotational speed before impact;
 m is the mass of the boulder;
 R_t is the coefficient of tangential friction;
 I is the moment of inertia of the boulder, which for a sphere is defined by:

$$I = \frac{2}{5} m r^2$$

- F_1 is a friction function defined by:

$$F_1 = R_t + \frac{400 (1 - R_t)}{(V_{is} - \omega_i r)^2 + 480}$$

- F_2 is a scaling function defined by

$$F_2 = \frac{250^2 R_n^2 R_t}{V_{in}^2 + 250^2 R_n^2}$$

The actual rebound velocity, V_r , and the flight directions, β_r and α_r , relative to the ground surface and the x, y coordinate system, respectively, are then determined using,

$$V_r = \sqrt{V_{rn}^2 + V_{rs}^2} \quad \dots \text{Equation A-16}$$

$$\beta_r = \tan^{-1} \left(\frac{V_{rn}}{V_{rs}} \right) \quad \dots \text{Equation A-17}$$

$$\alpha_r = \beta_r + \theta \quad \dots \text{Equation A-18}$$

(Note that the sign in Equation A-18 is positive because the impact and rebound velocities are treated as absolute values, and do not conform to the coordinate sign convention).

The transfer from "bounce" mode to "roll" mode has been defined in *Rockfal2* as the velocity of a boulder directed vertically upward required to lift the boulder a distance equal to one twentieth of the boulder radius. This velocity is calculated using:

$$V_{crit} = \sqrt{\frac{2gr}{20}} \quad \dots \text{Equation A-19}$$

If the rebound velocity V_m exceeds V_{crit} , V_r , α_r and ω_r then become V_o , α_o , and ω_o , respectively, for the next "bounce" calculation cycle. If the rebound velocity is less than or equal to V_{crit} the motion of the boulder is considered to have changed into "roll" mode.

A.1.2 "Roll" Mode Algorithms

The acceleration/deceleration that a rolling boulder gains when rolling down/up an inclined plane can be determined from the following energy balance equation

$$\frac{mV_i^2}{2} + \frac{I\omega_i^2}{2} + C m g dh = \frac{mV_r^2}{2} + \frac{I\omega_r^2}{2} + L\Delta \quad \dots\text{Equation A-20}$$

where: V_i, V_r are the linear velocities at the start and end of the roll respectively;

ω_i, ω_r are the angular velocities at the start and end of the roll respectively;

C is a constant that equals +1 if the roll is downhill, and equals -1 if the roll is uphill;

dh is the elevation gained or lost during the roll, which can be calculated using:

$$dh = r\Delta \sin(\theta)$$

where Δ is the elapsed angular displacement during the roll; and

θ is the angle of inclination of the plane;

and L is the torque provided by rolling friction at the boundary of the sphere, which is given by: $L = (\lambda m g \cos(\theta)) r$, where λ is the coefficient of rolling friction.

It is assumed that the coefficient of rolling friction acts on the rolling sphere in a similar way that the coefficient of tangential friction, R_t , acts on the bouncing sphere. When $R_t = 1$, the rebound tangential velocity equals the impact tangential velocity (ie. no tangential speed is lost during the impact). Conversely when $R_t = 0$, the rebound tangential velocity is zero (ie. all the tangential speed is lost). When a sphere is rolling on a flat plane, no linear velocity (tangential velocity) is lost if $\lambda = 0$, whereas the sphere is brought to a halt in the shortest distance if $\lambda = \infty$. On this basis it is hypothesized that:

$$\lambda = \frac{1 - R_t}{R_t} \quad \dots\text{Equation A-21}$$

Rearranging Equation A-21 provides the governing equation for a rolling sphere:

$$\omega_r^2 = \omega_i^2 - \frac{g\Delta}{0.7 r} \left(\frac{1 - R_t}{R_t} \cos(\theta) - C \sin(\theta) \right) \quad \dots\text{Equation A-22}$$

Using this equation, it can be shown that the sphere is accelerating when:

$$\frac{1 - R_t}{R_t} < \tan(\theta) \quad \dots\text{Equation A-23}$$

The coefficient of rolling friction is therefore equal to the tangent of the maximum inclination of a plane on which an initially stationary sphere fails to start rolling. It can also be shown

that the angular displacement, Δ , required to bring the sphere to a halt on a plane of constant grade is given by:

$$\Delta = \frac{0.7 r \omega_i^2}{g \left(\frac{I - R_t}{R_t} \cos(\theta) - C \sin(\theta) \right)} \quad \dots \text{Equation A-24}$$

Roll mode calculations are carried out for increments of 1 radian of rotation ($\Delta = 1$), thereby allowing local slope roughness to be incorporated. One radian of rotation corresponds to one radius of linear travel along the slope, which should be the gauge length used to characterise surface roughness of the slope for a given boulder size. The x, y coordinates of the boulder at the end of the roll increment are calculated using:

$$x_r = x_0 + r \Delta \cos(\theta) \quad \dots \text{Equation A-25}$$

$$y_r = y_0 + r \Delta \sin(\theta) \quad \dots \text{Equation A-26}$$

with $\Delta = 1$.

The angular velocity at the end of the roll increment is found using Equation A-22, and the linear velocity at the end of the roll increment is found using:

$$V_r = \omega_r r \quad \dots \text{Equation A-27}$$

The direction of travel at the end of the roll increment, α_r , is set equal to the local inclination of the rock surface for the roll calculation, this being the sum of the slope angle plus the local slope roughness angle.

If at the end of the roll increment, the calculated linear velocity along the slope is less than 0, the boulder is assumed to have stopped during the roll increment. The angular displacement to the stop point is calculated using Equation A-24, and the x, y coordinates of the stop point can then be calculated using equations A-25 and A-26.

During each "roll" calculation cycle, the end x-coordinate is checked to see whether the boulder has rolled past a prescribed reference point, or whether the boulder has rolled into the next linear segment of the slope geometry. In the case of the former, the angular displacement to the reference point is calculated using:

$$\Delta = \sqrt{\frac{(x_a - x_0)^2 + (y_a - y_0)^2}{r^2}} \quad \dots \text{Equation A-28}$$

where x_a , y_a are the coordinates of the reference point. The angular and linear velocities of the boulder at the reference point are calculated using equations A-22 and A-27 respectively. The height of the boulder above the ground will be zero and the direction of travel will equal α_r since the boulder travel is in "roll" mode.

A.2 Calculation Sequence

A complete rockfall simulation comprises a prescribed number of individual rockfall simulation runs. The size and location of the boulder, the initial velocities (linear and rotational) and direction of travel of the boulder at the start of each rockfall simulation run are set by the user and are the same for each run. A rockfall simulation run, in turn, consists of a large number of calculation cycles. The type of calculation carried out during each calculation cycle depends on the "mode" of travel determined at the end of the previous calculation cycle (eg., "roll" mode, or "bounce" mode). During each calculation cycle the position, time, and velocity at the end of the cycle are calculated, and checks are made to see whether any of several conditions have been met (eg. boulder travelled past analysis point, boulder travelled past end of line segment, or boulder travelled past end of geometry). Calculation cycles are repeated, using the conditions at the end of one cycle as the initial conditions for the next cycle, until the mode at the end of a calculation cycle is "stop". When a simulation run "stop"s, output data for the simulation run are stored, and another simulation run is initiated. The rockfall simulation stops when the prescribed number of rockfall simulation runs has been completed. The stored data for each rockfall simulation run are then processed, and the results can be reviewed.

The calculation sequence for each rockfall simulation starts with calculating the mass and moment of inertia of the boulder, the y-coordinate and inclination of the slope at the prescribed starting x-coordinate of the boulder, and the y-coordinate corresponding to the selected x-coordinate of the analysis point. The random generator is then seeded with the time of day.

The calculation sequence for each rockfall simulation run then starts by initialising x_o , y_o , V_o , α_o and ω_o using the prescribed starting conditions, and setting x_a , y_a , V_a , α_a , ω_a (the respective variables at analysis point) and the following tracking variables to zero:

- bounce time, the elapsed travel time since the start of a bounce;

- x_{\max} , the maximum x-coordinate travelled by the boulder; and
- y_{\max} , the y-coordinates on the slope at $x = x_{\max}$

The initial travel mode is determined according to the conditions shown in Table A-1.

Table A-1: Conditions for the initial travel mode for the program *Rockfal2*.

Condition	Travel Mode
boulder position is above the slope	"bounce"
boulder position is on the slope, and the initial velocity is zero.	"roll"
boulder position is on the slope, the velocity is non-zero and the direction of travel is parallel to the slope	"roll"
boulder position is on the slope, the velocity is non-zero and the direction of travel is not parallel to the slope	"bounce"

If the mode is "roll" and prescribed velocity is greater than the product of the prescribed rotational velocity and the radius, the initial rotational velocity is re-initialised to be consistent with the prescribed velocity. Conversely, if the prescribed velocity is less than the product of the prescribed rotational velocity and the radius, the initial velocity is recalculated to be consistent with the prescribed rotational velocity.

Having initialised the simulation run, the continuous loop of calculation cycles begins. The loop consists of:

- carrying out a bounce calculation of the mode = "bounce"
- carrying out a roll calculation if the mode = "roll"
- exiting the loop if the mode at the end of either a bounce or roll calculation is "stop"

Upon exiting the calculation cycle loop, x_{\max} , y_{\max} , V_a , α_a , ω_a , and h_a are stored for post-simulation processing. If at this point, the prescribed number of individual rockfall simulation runs have been completed, the rockfall simulation is terminated, and post-simulation processing of the results takes place. If the prescribed number of rockfall simulation runs has not been completed, a new rockfall simulation run is initiated.

The calculation sequence for a "bounce" cycle is as follows:

- calculate time in flight till impact with current line segment (Equation A-9) (endpoints of current line segment defined by x_1, y_1 and x_2, y_2)
- calculate coordinates of point impact with current slope segment (Equations A-1 and A-2)
- check if boulder passes analysis point before impact. If so:
 - calculate t_a (Equation A-7)
 - calculate y_a (Equation A-2)
 - calculate V_a the velocity of the boulder above the analysis point (Equations A-3, A-4, and A-5)
 - calculate α_a , the direction of travel of the boulder above the analysis point (Equation A-6)
 - calculate h_a (Equation A-8)
- check if the boulder has flown past end of the current line segment. If so:
 - initialise x_1, y_1 and x_2, y_2 using endpoints of next line segment
 - calculate slope angle for next line segment (Equation A-9)
 - repeat the bounce calculation cycle from the beginning.
- update x_{\max} and y_{\max} with coordinates of point of impact with slope.
- sample values for slope roughness angle, R_n and R_t from respective distributions.
- check values of R_n and R_t and:
 - if $R_t > 1$, set $R_t = 1$
 - if $R_t < 0$, set $R_t = 0$
 - if $R_n > 1$, set $R_n = 1$
 - if $R_n < 0$, set $R_n = 0$
- Calculate impact velocities and angle (Equations A-3 through A-6)
- Resolve impact velocities normal and parallel to the surface of the slope at the point of impact (Equations A-9 through A-12).
- Check if normal component of impact velocity is zero or if $R_n = 0$. If so, let mode = "roll", and proceed directly to a roll calculation without resampling the slope roughness angle, R_n or R_t .
- Calculate rebound velocity and direction (Equations A-14 through A-18)
- Check if the normal component of the rebound velocity is less than the critical value distinguishing "bounce" from "roll" modes (Equation A-19). If so set mode = "roll"

- re-initialise start variables for next calculation cycle and loop to the start of calculation cycle

The calculation sequence for a "roll" cycle is as follows:

- set bounce time = zero
- set $C = -1$ if roll uphill
- set $C = +1$ if roll downhill
- set $\Delta = 1$ (ie., allow boulder to roll one radian)
- calculate the coefficient of rolling friction (Equation A-21)
- calculate the angular velocity at the end of the roll (Equation A-22)
- check if boulder has stopped during roll. If so:
 - let mode = "stop"
 - calculate angle rotated to stop location (Equation A-24)
 - calculate x, y coordinates at stop location (Equations A-25 and A-26)
 - set rotational velocity to zero
- calculate the velocity at the end of the roll (= 0 if boulder has stopped)
- check whether boulder rolled past analysis point during roll. If so:
 - calculate rotational displacement at analysis point (Equation A-28),
 - calculate the rotation and linear velocity at analysis point (Equations A-22 and A-27).
- check if boulder rolls past the end of the line segment during the roll. If so:
 - reset the boulder coordinates to those for the start of the new line segment,
 - calculate the distance travelled to the end of the line segment (Equation A-28),
 - calculate the angular and linear velocities of the boulder at the end of the line segment (= end of roll) (Equations A-25 and A-26),
 - let mode = "bounce"
 - let mode = "stop" if end of line segment is last coordinate on slope.
- Update x_{\max} and y_{\max}
- if mode = "stop" then terminate the calculation cycle
- re-initialise start variables for next calculation cycle
- sample a new slope roughness angle, R_n and R_t
- change mode to "bounce"

- check compare new surface angle with boulder travel direction. If boulder is travelling into the new slope surface, proceed directly into the “bounce” calculation sequence at the point where the newly sampled values of R_n and R_t are being checked
- loop to start of calculation cycle.

Appendix B

Details of Survey Carried Out for Boulder Mapping

This appendix gives the details of survey carried out for boulder mapping on the debris cone of Undercite Creek at Fox Glacier.

Instrument Station Details:

Height of Instrument: 1.295 m

Height of reflector: 1.295 m

Reference Point:

Location : Left end of Undercite rockfall debris; Near to the slope.

Angle (with respect to True North):

Horizontal: 9 deg 10 min 10 sec

Vertical: 82 deg 2 min 50 sec

Horizontal distance: 173.048

Vertical distance: 24.177

Slope distance: 174.729

All measurements are taken with respect to the reference point.

Position of Boulders:

Boulder No. (Number)	Vert. angle (Deg Min Sec)	Hor. angle (Deg Min Sec)	Slope dist. (Metres)	Hor. dist. (Metres)	Vertical dist. (Metres)	Boulder volume (M * M * M)
1	83 07 20	06 50 05	151.509	150.419	18.145	4.67*1.99*3.9
2	81 43 00	11 25 55	158.745	157.088	22.872	5.5*2.5*2.6
3	84 34 00	05 05 45	87.472	87.079	8.284	8.6*3.5*4.67

4	86 15 30	354 12 35	101.062	100.847	6.596	3.6*1.65*2.72
5	87 23 05	342 07 00	116.603	116.482	5.322	3.25*1.67*1.8
6	88 55 25	330 25 50	125.428	125.404	2.357	2.15*1.76*1.3
7	88 16 00	336 53 20	80.994	80.957	2.450	2.79*2.1*2.35
8	88 43 20	332 03 15	65.331	65.315	1.457	2.93*2.42*6.4
9	89 40 35	324 40 35	63.807	63.806	0.360	3.59*1.9*2.67
10	87 42 45	338 43 40	54.223	54.180	2.164	4.64*1.69*2.1
11	76 54 20	33 28 35	127.553	125.235	28.899	8.2*2.2*4.5
12	84 34 40	37 32 35	37.681	37.492	3.559	6*4*4
13	84 12 50	51 17 35	49.777	49.523	5.018	6.5*4.5*2.6
14	84 53 50	61 13 00	56.494	56.270	5.025	2.15*4.84*3.1
15	85 53 45	69 08 40	56.81	56.664	4.066	3.1*3.2*2.45
16	86 37 35	71 34 30	46.357	46.277	2.728	1.7*3.8*3.1
17	86 57 35	80 01 10	75.547	75.441	4.007	4.3*2.1*1.4
18	84 13 35	73 00 20	84.364	83.936	8.487	8.3*2.6*8.8
19	85 24 35	79 25 40	102.167	101.839	8.177	3*2*5
20	88 21 55	87 03 00	94.384	94.346	2.694	5*5*6
21	88 39 10	89 57 00	95.777	95.751	2.253	4.5*8*2.4
22	89 33 25	98 23 50	94.808	94.805	0.734	11*5*3.1
23	88 44 10	94 39 40	101.348	101.323	2.236	8*3*3
24	85 47 15	89 07 55	108.131	107.839	7.944	3*3*5
25	86 35 30	95 40 15	118.002	117.793	7.016	3.2*4*3.6
26	86 28 25	98 05 05	131.224	130.977	8.053	1.9*3.1*5
27	87 06 50	99 31 55	138.688	138.512	6.984	3*3.8*1.2
28	86 59 10	98 56 50	148.837	148.631	7.827	2.6*2*3.5
29	87 18 15	102 10 45	161.746	161.567	7.610	3*1.6*2.6
30	88 52 20	111 49 55	138.408	138.381	2.725	5.96*4.83*2.9
31	89 46 20	116 32 15	76.223	76.222	0.303	3.22*5.1*3.79
32	89 20 45	114 32 30	135.876	135.867	1.552	6.85*1.87*3.9
33	88 45 20	113 57 50	151.944	151.908	3.302	4.7*3.1*3.31
34	89 40 50	124 12 25	166.926	166.923	0.933	5.7*4.6*2.57
35	87 32 00	107 27 35	229.728	229.515	9.891	4.46*4*5.95

36	87 00 45	105 38 50	229.635	229.323	11.972	3.84*2.46*1.9
37	87 02 40	105 36 40	215.322	215.036	11.105	2.55*4.83*2
38	86 55 35	105 31 30	204.773	204.478	10.983	2.77*3.6*4.59
39	85 18 05	99 33 30	205.601	204.909	16.845	4.3*3.9*4.61
40	84 25 10	97 59 10	199.058	198.332	16.987	1.9*1.94*2.9
41	86 48 20	103 03 40	185.952	185.663	10.364	2.5*2.35*1.9

Equivalent diameter of the boulder = boulder volume / volume of a sphere

Debris Boundary:

Point number (Number)	Vert. angle (Deg Min Sec)	Hor. angle (Deg Min Sec)	Slope dist. (Metres)	Hor. dist. (Metres)	Vertical dist. (Metres)
1	89 44 35	324 02 35	62.996	62.995	0.283
2	90 01 40	330 12 45	46.873	46.873	0.023
3	89 54 30	343 24 20	32.212	32.212	0.052
4	90 01 00	26 52 35	25.789	25.789	0.008
5	89 47 25	69 35 35	37.269	37.269	0.136
6	88 56 25	86 17 40	54.977	54.968	1.017
7	89 06 55	94 19 55	74.734	74.726	1.154
8	89 12 10	105 04 30	103.500	103.490	1.441
9	89 07 40	111 10 35	132.341	132.326	2.016
10	89 22 40	115 05 55	136.089	136.081	1.479
11	89 37 25	120 37 40	132.107	132.104	0.869
12	89 49 50	122 37 10	137.192	137.191	0.407
13	89 45 15	122 00 40	145.333	145.332	0.625
14	89 41 40	121 29 40	163.919	163.917	0.876

Details of Road Boundary:

Point Number (Number)	Vert. angle (Deg Min Sec)	Hor. angle (Deg Min Sec)	Slope dist. (Metres)	Hor. dist. (Metres)	Vertical dist. (Metres)
1	89 48 40	302 35 45	210.458	210.457	0.697
2	89 54 20	300 52 10	182.165	182.165	0.302
3	89 01 15	201 50 15	80.305	80.293	1.372
4	89 01 10	168 01 00	146.935	146.913	2.516

5	89 00 46	159 53 00	174.264	174.238	3.005
6	89 15 40	131 42 30	493.143	493.102	6.375

Appendix C

Sections Used for Rockfall Analysis at Undercite Creek

This appendix gives details of the sections used (along with the boulder trajectories) for the analysis of rockfalls at Undercite Creek, Fox Glacier. The initial conditions are the same for every section which are as follows:

- Boulder diameter = 7.5 m;
- Density of rock = 2680 kg/m^3 ; and
- Initial linear velocity = 0.5 m / sec

Section C-C':

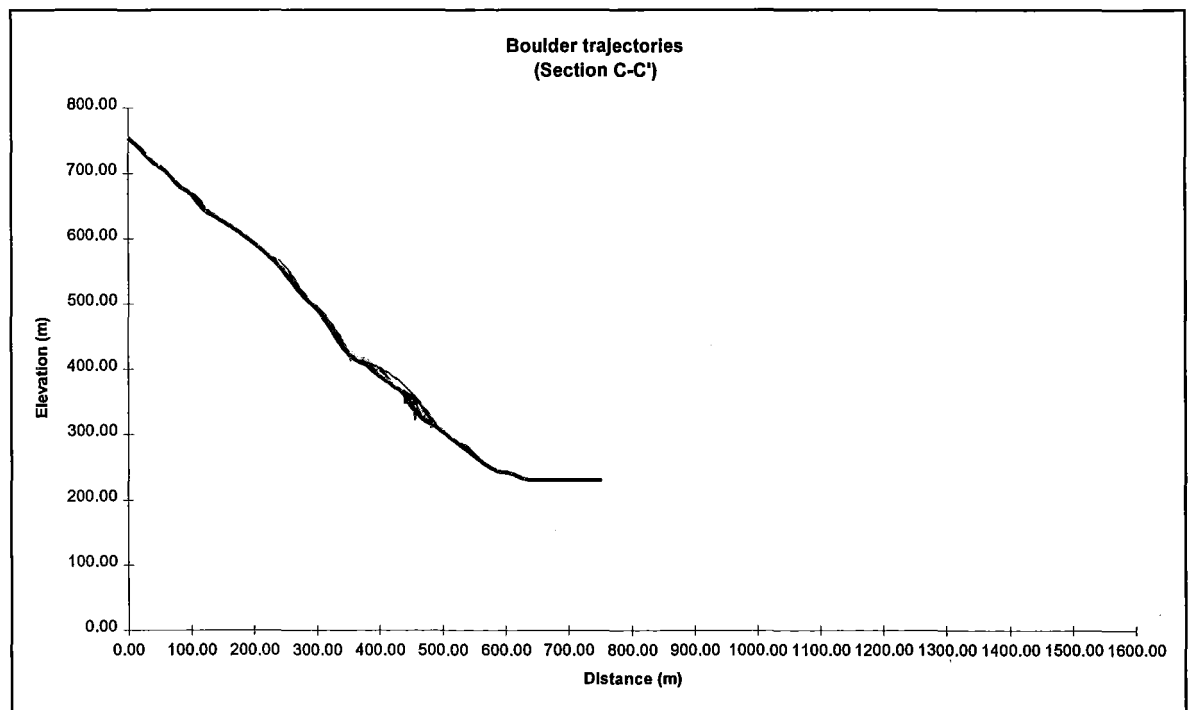
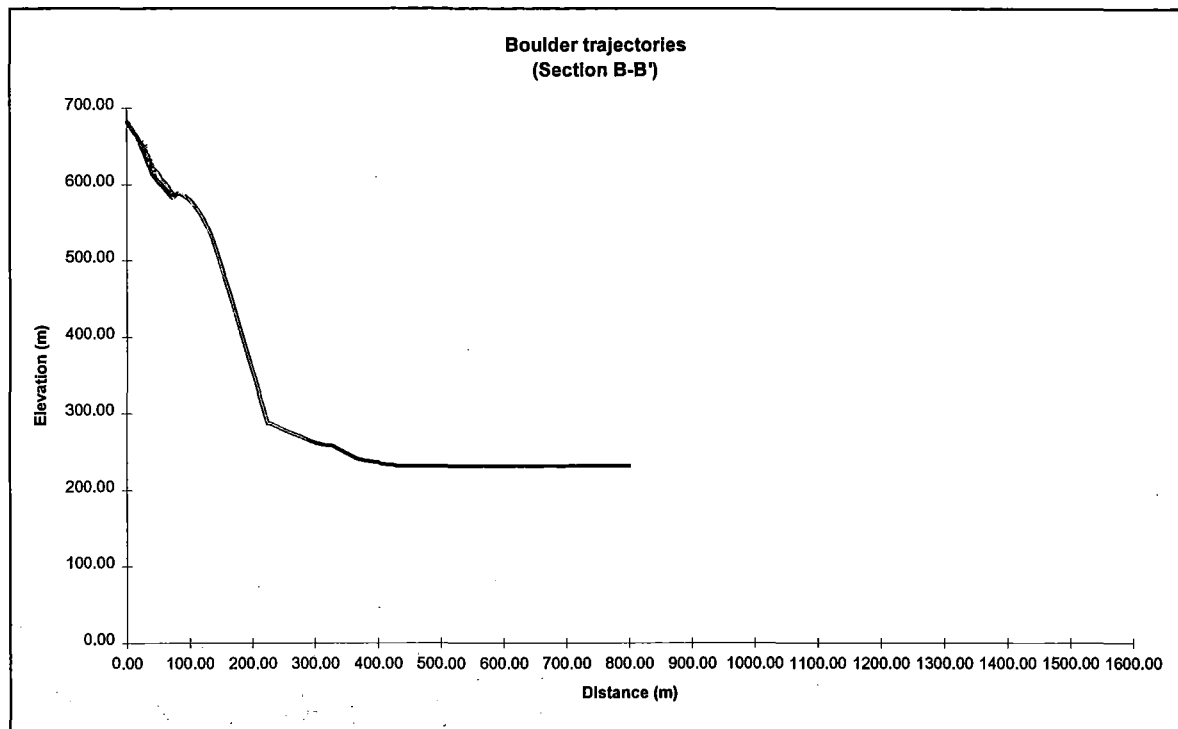
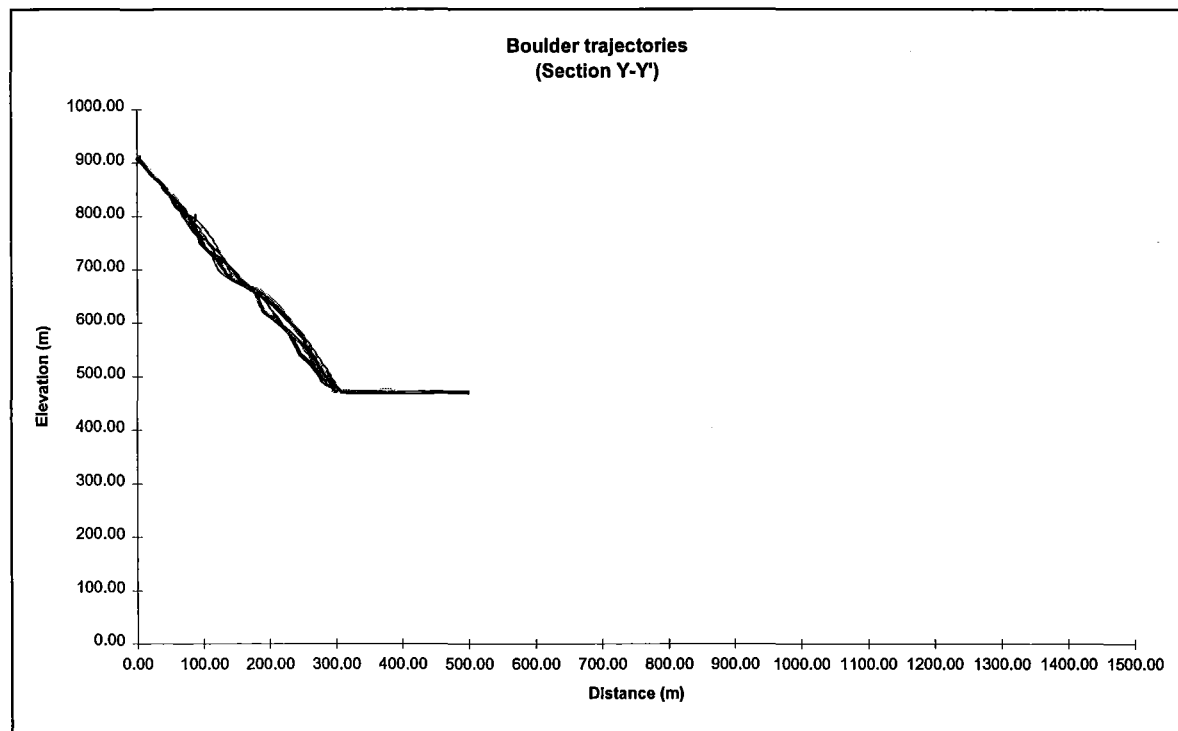
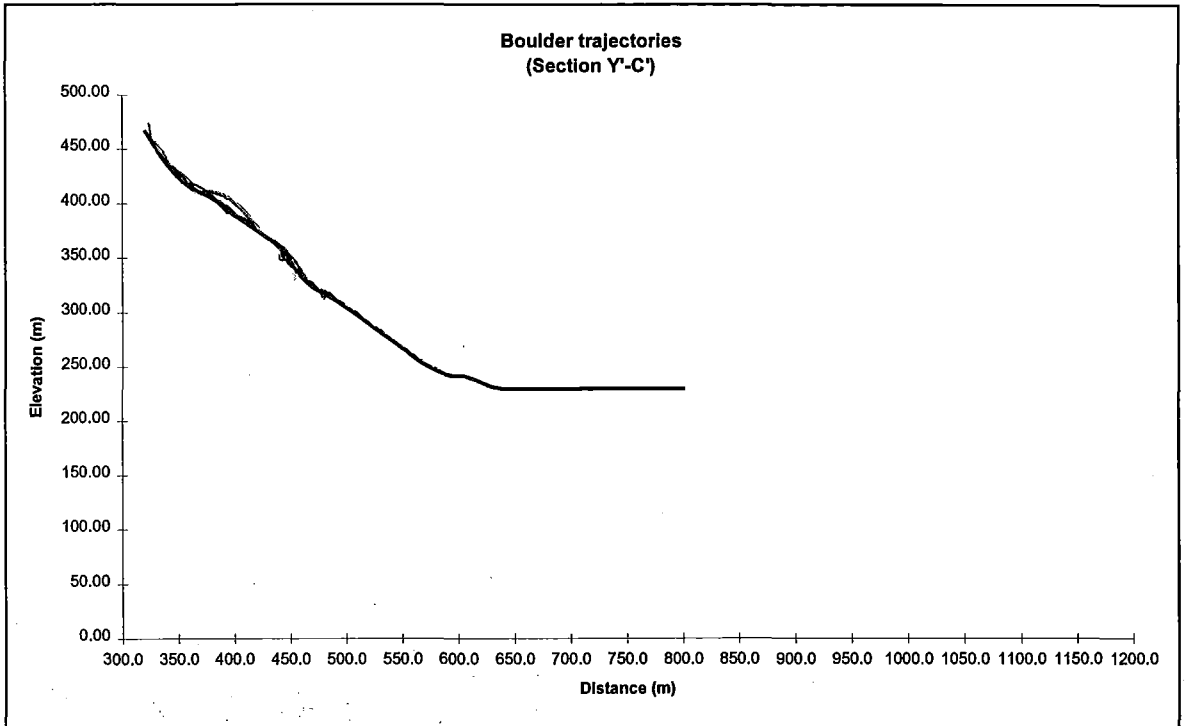
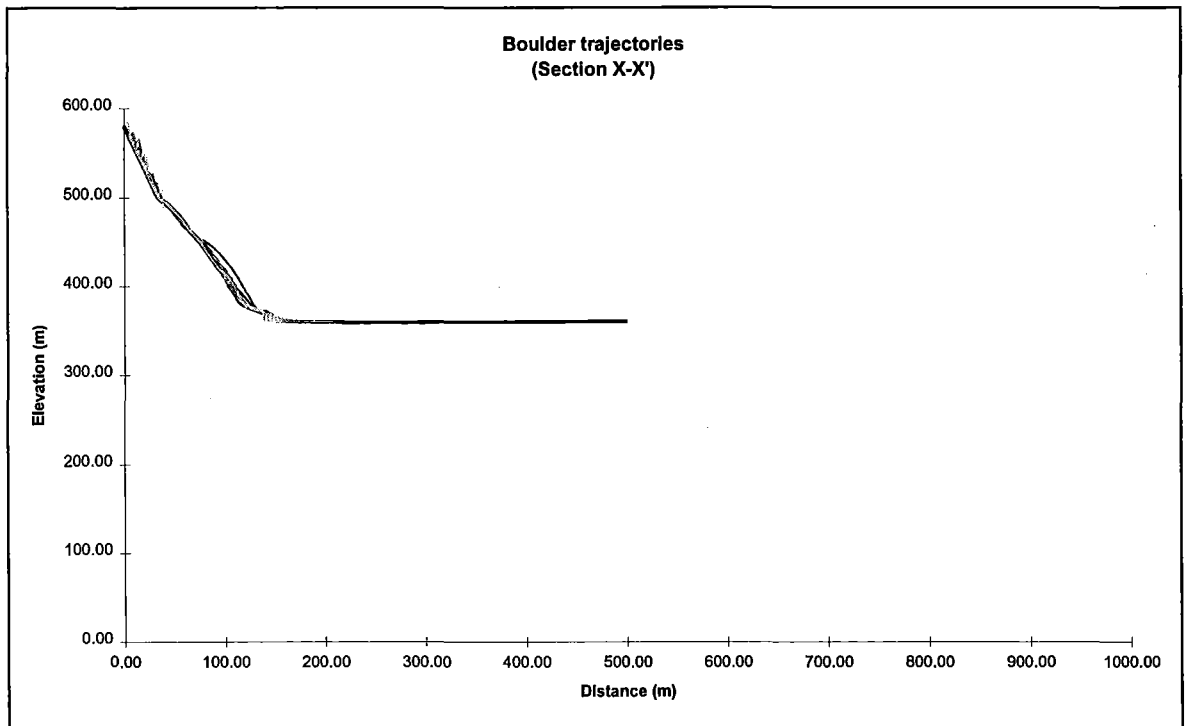
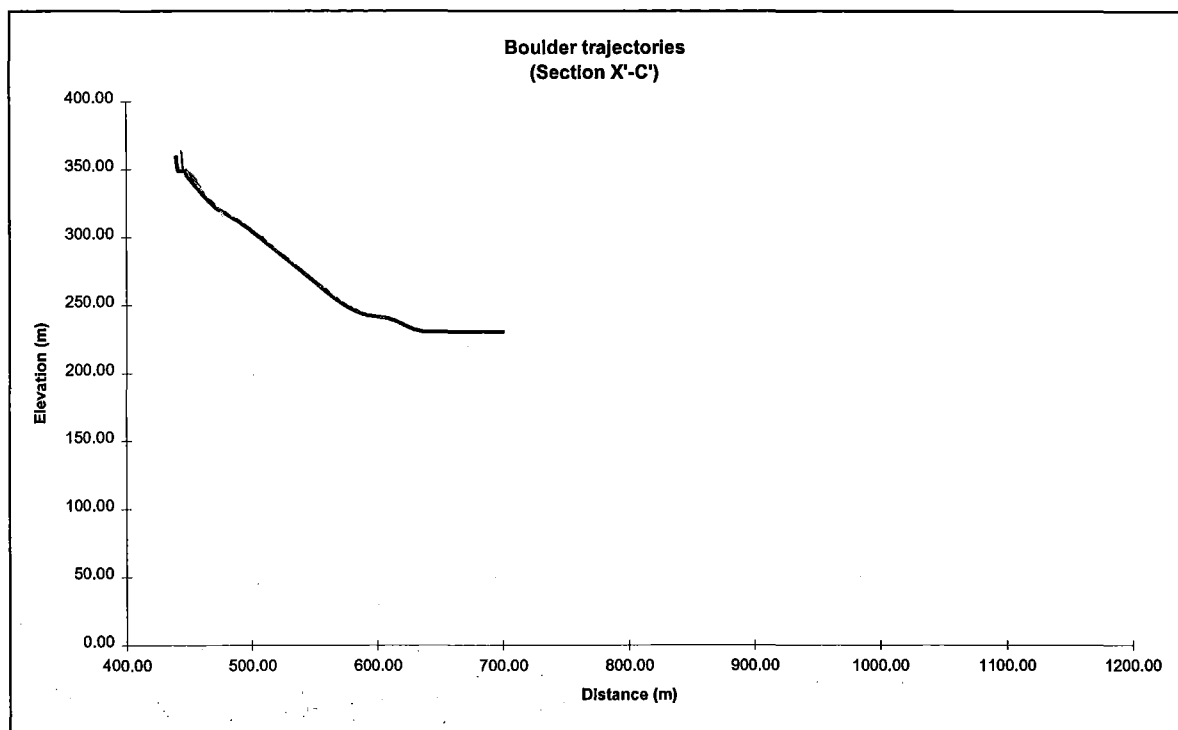
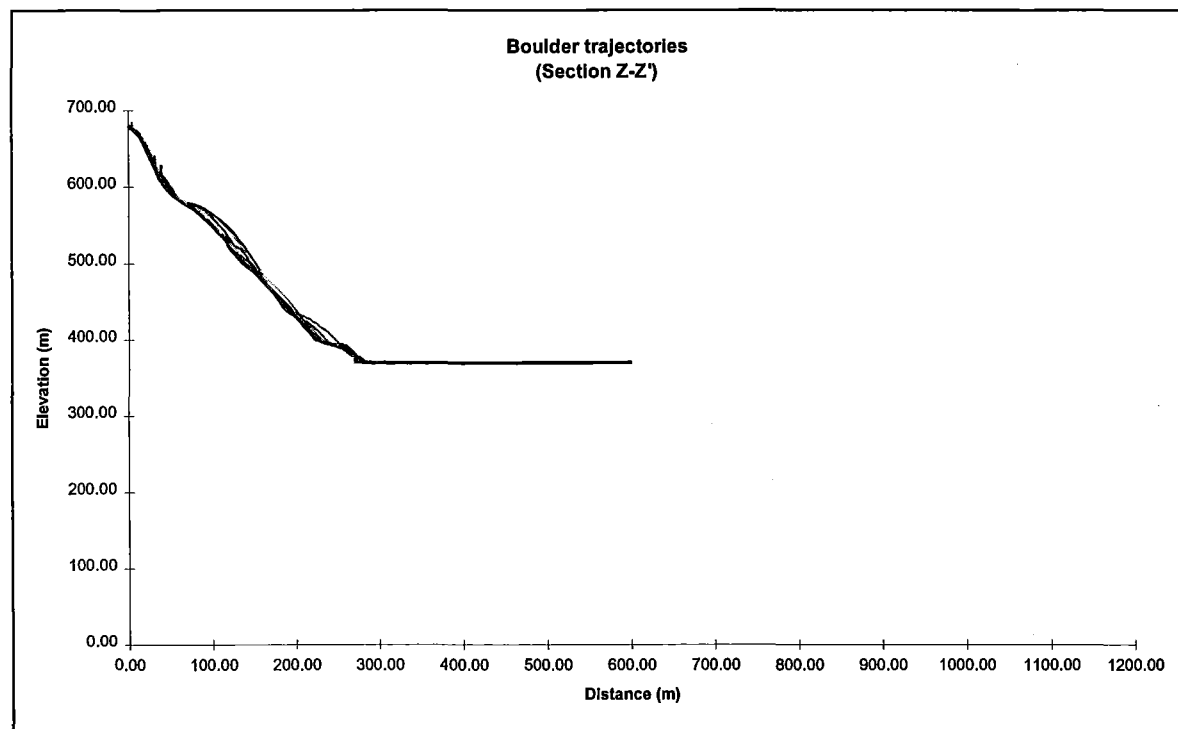


Figure C-1: Details of section C-C' along with some boulder trajectories (*WinRock*).

Section B-B':Figure C-2: Details of section B-B' along with some boulder trajectories (*WinRock*).Slip Zone 2 (Y-Y'):Figure C-3: Details of section Y-Y' along with some boulder trajectories (*WinRock*).

Section Y'-C':Figure C-4: Details of section Y'-C' along with some boulder trajectories (*WinRock*).Slip Zone 3 (X-X'):Figure C-5: Details of section X-X' along with some boulder trajectories (*WinRock*).

Section X'-C':Figure C-6: Details of section X'-C' along with some boulder trajectories (*WinRock*).Slip Zone 4 (Z-Z'):Figure C-7: Details of section Z-Z' along with some boulder trajectories (*WinRock*).

Section Z'-C':

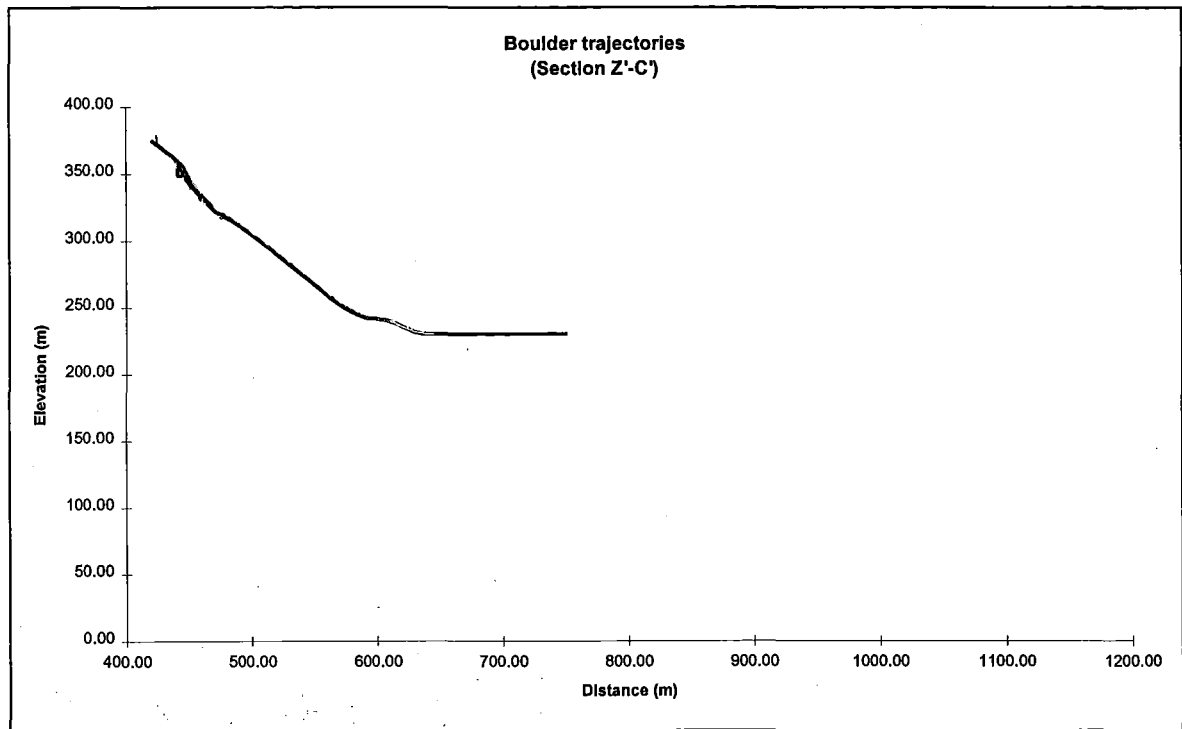


Figure C-8: Details of section Z'-C' along with some boulder trajectories (*WinRock*).

Appendix D

RHRS Rating for Undercite Creek

D.1 Detailed RHRS Rating for Undercite Creek at Fox Glacier

Detailed rating for the slope at Undercite Creek, Fox Glacier will be carried out in this appendix based on the 12 categories stated in Table 6-2, using the RHRS participant's manual (1993). Table D-2 shows the rockfall hazard field data sheet, which can be used when rating the slope.

D.1.1 Slope Height

The height of the slope at Undercite Creek is about 650 m (2132 ft). According to the rating table, any slope above 100 ft height gets the maximum points of 100.

- Hence, the slope height rate is 100.

D.1.2 Ditch Effectiveness

The effectiveness of ditch is measured by its ability to restrict falling rock from reaching the roadway. As you can see from Photo 5-1, the present alignment of the access road is quite far away from the debris cone of the Undercite Creek, and also, for the past 16 months, no rock was reported to have reached or crossed the present access road. As such, there is no defined catch ditch at the Undercite Creek, but a recent re-alignment of the access road was carried out, using the rockfall debris to raise the level of the road. According to the RHRS Participant's manual (1993), a good catchment ditch is the one in which all or nearly all falling rocks are retained in the catch ditch. For this reason, it can be concluded that the ditch at Undercite Creek provides a "good catchment".

- Hence, the rating for the ditch effectiveness is 3.

D.1.3 Average Vehicle Risk (AVR)

With the AVR category, the risk associated with the percentage of time a vehicle is present in the rockfall section is evaluated. The percentage is obtained by using the formula based on slope length, average daily traffic (ADT), and the posted speed limit at the site.

$$\text{AVR} = \frac{\text{ADT (cars/day)} \times \text{Slope length (km)} / 24 \text{ (hours/day)} \times 100 \%}{\text{Posted speed limit (km/hr)}}$$

The results are based on the benchmark criteria shown in Table 6-2.

Combining the ADT, the length of the rockfall section and the posted speed limit produces a category that represents the potential for a vehicle to be involved in a rockfall event. Another way of looking at this is that it shows how many vehicles are in the rockfall section at any one time.

The Average Daily Traffic at the Fox Glacier is around 150 per day. It is assumed that the average usage time for the access road at Fox Glacier is only 12 hrs/day as it is used only to view the glacier. Hence:

$$\begin{aligned} \text{AVR} &= \frac{\text{ADT (cars/day)} * \text{Slope length (km)} / 12 \text{ (hours/day)} \times 100 \%}{\text{Posted speed limit (km/hr)}} \\ &= \frac{150 * 0.459 / 12}{50} * 100 \% \\ &= 11.47 \% \end{aligned}$$

- From the score table in the RHRS Participant's manual (1993), the score for 11.47 % AVR is 1.

D.1.4 Percent of Decision Sight Distance (DSD)

The decision sight distance compares the amount of sight distances available through a rockfall section to the low design amount prescribed by the American Association of State Highway Transportation Officials (AASHTO). Sight distance is the shortest distance that a 15 cm object is continuously visible to a driver along a roadway. Decision sight distance is the length of the roadway required by a driver to perceive a problem and then bring a vehicle to a stop.

The actual decision sight distance is measured by placing a 15 cm object at the pavement of the road and walking along the pavement in the opposite direction to the traffic, until the object disappears at an eye height of 1.2 m. The required decision sight distances based on the posted speed limits, according to AASHTO standards, are shown in Table D-1.

Table D-1: Required decision sight distance according to AASHTO standards (1991).

Posted speed limit (mph)	Decision sight distance (ft)
25	375
30	450
35	525
40	600
45	675
50	750
55	875
60	1000
65	1050

Once the actual sight distance is measured and the recommended sight distance determined from the Table D-1, the two values can be used in the following formula to calculate the percent of Decision Sight Distance.

$$\% \text{ DSD} = \frac{\text{Actual sight distance}}{\text{Required decision sight distance}} \times 100 \%$$

For the Undercite Creek, the actual sight distance has been measured as 182 m. The posted speed limit for the access road is 50 km/hr (26.7 mph). From Table D-1, the required sight distance is found to be 400.5 ft (122 m).

Using the formula written above,

$$\% \text{ DSD} = \frac{182 \text{ m}}{122 \text{ m}} \times 100 \% = 149 \%$$

Hence, the percentage sight distance is 149 % of low design value. From the scoring table in the RHRS Participant's manual (1993), anything above 113 % of low design value gets 1 point.

- Thus, the percent of decision sight distance rate is 1 point.

D.1.5 Roadway Width

The roadway width is measured perpendicular to the highway, which doesn't include the unpaved shoulders, if any. If a driver notices rocks on the road, or rocks falling, it is possible for the driver to react and take evasive action to avoid them. The more room there is for manoeuvre, the greater the likelihood the driver will successfully miss the rock without hitting some other road side hazard or oncoming vehicle. After measuring the roadway width, the score can be calculated using the score table in the RHRS Participant's manual (1993).

The roadway width for the access road at Undercite Creek is measured to be 12.5 m (41 ft), including the paved width.

- From the score table in RHRS Participant's manual (1993), the appropriate score is 5.

D.1.6 Geologic Character

Since the conditions that cause rockfall generally fit into two categories, case one and case two rating criteria have been developed. Case one is for slopes where joints, bedding planes or other discontinuities, are the dominant structural features that lead to rockfall. Case two is for slopes where differential erosion or over-steepening is the dominant condition that controls rockfalls. Whichever case best fits the slope should be used for the rating. If both situations are present, and it is unclear which dominates, both are scored, but only the worst case (highest score) is used in the rating. The criteria for the two cases are shown in Table 6-2. The rockfalls at Undercite Creek fall into case one, as the toppling failure and structural discontinuities are most influential. Hence, scoring is done for case one.

D.1.6.1 Structural Condition

Rockfall from case one slopes occurs as a result of movement along discontinuities. The word "joint" as applied here, represents all possible types of discontinuities including bedding planes, foliations, fractures and faults. The term "continuous" refers to joints that are greater than 10 ft (3.05 m) in length. The term "adverse" applies not only to the joint's spatial relationship to the slope, but also to such things as rock friction angle, joint filling, and the effects of water, if present. According to the RHRS Participant's manual (1993), following are the benchmark criteria descriptions:

3 points	<u>Discontinuous joints, favourable orientation</u>	Slope contains jointed rock with no adversely oriented joints.
9 points	<u>Discontinuous joints, random orientation</u>	Slope contains randomly oriented joints creating a variable pattern. The slope is likely to have some scattered blocks with adversely oriented joints, but no dominant adverse pattern is present.
27 points	<u>Discontinuous joints, adverse orientation</u>	Rock slope exhibits a prominent joint pattern with an adverse orientation. these features have less than 10 ft (3.05 m) of length.
81 points	<u>Continuous joints, adverse orientation</u>	Rock slope exhibits a dominant joint pattern with an adverse orientation and a length greater than 10 ft (3.05 m).

The category that best describes the rockfall source will be “Continuous joints, adverse orientation”, as there is a high possibility of toppling failure.

- Hence, the score for the structural category of the geologic character, case one, is 81.

D.1.6.2 Rock Friction

The potential for rockfall by movement along discontinuities is controlled by the condition of joints. The condition of joints is described in terms of micro and macro roughness. This parameter directly affects the potential for a block to move relative to another. Friction along a joint, bedding plane, or other discontinuity is governed by the macro and micro roughness of the surfaces. Macro roughness is the degree of undulation of the joint relative to the direction of possible movement. Micro roughness is the texture of the surface. According to the RHRS Participant’s manual (1993), following are the benchmark criteria descriptions:

3 points	<u>Rough, irregular</u>	The surface of the joints are rough and the joint planes are irregular enough to cause interlocking.
9 points	<u>Undulating</u>	Macro rough but without the interlocking ability.
27 points	<u>Planar</u>	Macro smooth and macro rough joint surfaces. Friction is derived strictly from the roughness of the rock surface.
81 points	<u>Clay infilling, or slickensides</u>	Low friction materials separate the rock surfaces, negating any micro or macro roughness of the joint surfaces. Slickensided joints also have low friction angle, and belong in this category.

The best description of the rock friction at the Undercite Creek will be between “Planar” and “Clay infilling, or slickensided”.

- Hence, the score for the rock friction will be 52, using the exponential system of scoring.

D.1.7 Block Size or Volume of Rockfall Per Event

In some rockfall events, the failure is comprised of an individual block. In other cases, the event may include many blocks of differing sizes. Which ever type of event is typical is rated according to the benchmark criteria specified in Table 6-2.

From the history of rockfall event, we can see that there was a big event of rockfall of about a million cubic metres of material in January 1994. After this event, no such big event was reported again. The recent rockfall events reported in the area consisted mainly of single boulders running on to the access road in 1995-96. Hence, we can say that the individual block roll out will be the dominant case in this criteria for rating. The average size of the blocks reported to roll out is about 1 meter (3.23 ft).

- According to the benchmark criteria for block size, the score for this criteria will be 27.

D.1.8 Climate and Presence of Water on Slope

The effects of precipitation, freeze/thaw cycles, and water flowing on the slope are evaluated with this category according to the benchmark criteria shown in Table 6-2.

The rainfall at Fox Glacier is around 5.6 m per annum (NZ Met Service Publications 1983) and the temperature is -2.4 to 9.5 degrees Celsius. Based on this data, it can be concluded that this area will come under the category of “High precipitation and long freezing periods”. The freezing periods are usually long in winters which may go up to 3 months. Also, most of the rockfall events are said to be associated with the event of rain storms, including the major rockfall event in January 1994.

- Hence, the score for this category is 81.

D.1.9 Rockfall History

This category rates the historical rockfall activity at a site as an indicator of future rockfall events. Typically, the frequency and magnitude of past events are used to predict the rockfall hazard in future.

Since the occurrence of the major rockfall event in January 1994, reported rockfalls have decreased at Undercite Creek. Especially, during the past sixteen months, few rockfall events has been reported. Hence this slope falls between the terms "Occasional falls" and "Many falls".

- Hence, the score for this category is 20.

Table D-2 provides the rockfall hazard field data sheet for the Undercite Creek along with the total score and remarks. The total score for the Undercite Creek is 371.

Table D-2: Rockfall hazard field data sheet.

Rockfall Hazard Field Data Sheet	
State Highway Name & No. <u>Access road to Fox Glacier</u>	
Beginning Mile Point _____	Area & Location <u>West Coast, S.I, New Zealand.</u>
(L) or R of Centerline* _____	Date of Rating <u>3 September 1997</u>
Ending Mile Point _____	Posted Speed Limit <u>50 kmph</u>
Preliminary Rating _____	Average Daily Traffic _____
Cut class A B or (C)* _____	Rater <u>Rayudu, D.N.Prasad.</u>
Proposed Correction _____	Cost Estimate \$ _____
Preliminary Rating Remarks: <u>One major event in Jan'94, only occasional rockfalls reported from past 16 months.</u>	
DETAILED RATING	
Slope Height Score <u>100</u>	Slope Height <u>450 m</u>
Ditch Effectiveness Score <u>3</u>	Catchment Letter (G) M L N*
Average Vehicle Risk Score <u>1</u>	Percent of Time _____
Sight Distance Score <u>1</u>	Percent Design Value <u>122 m</u>
Site Distance <u>182</u>	Roadway Width Score <u>5</u>
Roadway Width <u>12.5 m</u>	
GEOLOGIC CHARACTER CASE ①	
Structural Condition Score <u>81</u>	
Fracture Letter D (C)* _____	Orientation Letter F R (A)* _____
Rock Friction Score <u>52</u>	Friction Letter RI U P (CS)* _____
GEOLOGIC CHARACTER CASE 2	
Structural Condition Score _____	Erosion Feature Letter F O N M*
Diff. Erosion Rate Score _____	Diff. Erosion Rate Letter S M L E*
Block Size / Quantity / Event Score <u>27</u>	Block Size <u>1m</u>
Quantity _____	
Climate and Water Score <u>81</u>	Precipitation Letter L M (H)* _____
Freezing Period Letter N S L* _____	Water Letter N I (C)* _____
Rockfall History Score <u>20</u>	Rockfall History Letter F (O) M (C)* _____
Remarks: <u>Immediate threat to the access road by the rockfalls at this site is negligible considering the present position of access road with respect to the debris cone.</u>	
* Circle One	Total Score: 371

References

- [1] American Association for State Highway and Transportation Officials (1990). A policy on the geometric design of highways and streets, *AASHTO*, Washington, D.C. pp.1024.
- [2] Azimi C., Desvarreux P., and Giraud A. (1982). Method of calculating the dynamics of rockfalls. Application to the study of a mountainside at La Pale (Vercors). *Bull. Liaison Lab Ponts Chaussees*, N122, Nov-Dec, pp.93-102.
- [3] Azzoni A., Drigo E., Giani G.P., Rossi P.P., and Zaninetti A. (1992). In situ observation of rockfall analysis. *Proceedings of the 6th International Symposium on Landslides, Christchurch*, pp. 307-314.
- [4] Azzoni A. and de Freitas M.H. (1995). Experimentally gained parameters, decisive for rockfall analysis. *Rock Mech. and Rock Engng.* 28(2), 111-124.
- [5] Beniaowski Z.T. (1976). Rock mass classification in rock engineering. *Proceedings of Symposium on Exploration for Rock Engineering*. Balkema, Rotterdam. Vol.1., pp.97-106.
- [6] Benjamin J.R. and Cornell C.A. (1970). Probability, statistics and decision for civil engineers. *McGraw-Hill*, New York, 644p.
- [7] Bozzolo D. and Pamini R. (1982). Modello matematico per lo studio della caduta dei massi. *Laboratorio di Fisica Terrestre-ICTS, Lugano-Trevano*.
- [8] Bozzolo D. and Pamini R. (1986). Simulation of rockfalls down a valley side. *Acta Mechanica*, 63, 113-130.
- [9] Brach R.M. (1984). Friction, restitution, and energy loss in planar collisions *American Society for Mechanical Engineers (ASME) Journal of Applied Mechanics*, Vol.51, pp.164-170.
- [10] Broili L. (1977). Relations between scree slope morphometry and dynamics of accumulation processes. *Proceedings of Meeting on Rockfall Dynamics Protective Works Effectiveness 90*, 11-24.
- [11] Brown E.T. (1981). Rock Characterisation Testing and Monitoring-ISRMS Suggested Methods. *Published for the Commission of Testing Methods, International Society for Rock Mechanics (ISRM)*.
- [12] Budetta P. and Santo A. (1994). Morphostructural evolution and related kinematics of rockfalls in Campania (Southern Italy): A case study. *Engineering Geology*, 36, pp.197-210.

-
- [13] Bunce C.M. (1994). Risk analysis for rockfalls on highways. *M.Sc. thesis*, Dept. of Civil Engineering, University of Alberta.
- [14] Campanuovo G.F. (1977). ISMES experience on the model of St. Martino. *Proceedings of Meeting on Rockfall Dynamics Protective Works Effectiveness* 90, 25-39.
- [15] CAN/CSA (1991). Risk analysis requirements and guidelines, Quality management. A National Standard of Canada, Q 634-91. *Canadian Standards Association*, Rexdale, Canada.
- [16] Chan Y.C., Chan C.F. and Au W.C. (1986). Design of a boulder fence in Hong Kong. *Conference on Rock Engineering in an Urban Environment, Institute of Mineral and Metallurgy., Hong Kong*, pp. 87-96.
- [17] Chen H., Chen R.H. and Huang T.H. (1994). An application of analytical model to a slope subject to rockfalls. *Bull. Ass. Engng. Geol.* XXXI, 4, pp. 447-458.
- [18] Cundall P.A. (1971). A computer model for simulating progressive, large scale movements in blocky rock systems. *International Society for Rock Mechanics Symposium on Rock Fracture*, Nancy, Paper II-8.
- [19] Descoudres F. and Zimmermann T. (1987). Three dimensional dynamic calculation of rockfalls. *Proceedings of the 6th Int. Conf. on Rock Mechanics, Montreal*, pp. 337-342.
- [20] Dubin B. I., Watkins A.T., Chang D.C.H. (1986). Stabilisation of existing rock faces in urban areas of Hong Kong. *Conference on Rock Engineering and Excavation in an urban environment, Institution of Mining and Metallurgy*, 24-27, February Hong Kong, pp.155-171.
- [21] Elliott G. (1992). Rockfall simulation using Rockfal2. *Unpublished notes*.
- [22] Evans S.G. and Hungr O. (1993). The assessment of rockfall hazard at the base of talus slopes. *Canadian geotechnical journal*, 30, pp.620-636.
- [23] Falcetta J.L. (1985). Etude cynamatique et dynamique de chute de blocs rocheux. *These, INSA, Lyon*.
- [24] Fookes P.G. and Sweeney M. (1976). Stabilisation and control of local rockfalls and degrading rock slopes. *Quarterly Journal of Engng. Geol.* Vol. 9, pp. 37-55.
- [25] Fookes P.G. and Welman A.J. (1989). Rock slopes: stabilisation and remedial measures against degradation in weathered and fresh rock. *Proc. Instn. Civ. Engrs., Ground Engineering Group* 86, pp.359-380.
-

-
- [26] Gassen W.V. and Cruden D.M. (1989). Momentum transfer and friction in the debris of rock avalanches. *Canadian Geotechnical Journal*, vol 26, pp. 623-628.
- [27] Grigg P.V. and Wong K.M. (1987). Stabilisation of boulders at a hill slope site in Hong Kong. *Quarterly Journal of Engng. Geol.* Vol.20, pp.5-14.
- [28] Gunn B.M. (1960). Structural features of the Alpine schists of the Franz Josef-Fox Glacier region. . *New Zealand Journal of Geology and Geophysics* Vol.3, pp.287-308.
- [29] Habib P. (1977). Notes sur le rebondissement des blocs rocheux. *Proceedings of Meeting on Rockfall Dynamics Protective Works Effectiveness* 90, 123-125.
- [30] Hacar B., Bollo F. and Hacar R. (1977). Bodies falling down on different slopes. Dynamic studies. *Rock. 9th Int. Conf. Soil Mech. Found. Engng* 2, 91-95.
- [31] Hanson C.R., Norris R.J., Cooper A.F. (1990). Regional fracture patterns east of the Alpine Fault between the Fox and Franz Josef Glaciers, Westland, New Zealand. *New Zealand Journal of Geology and Geophysics*, Vol.33, pp.617-622.
- [32] Hearn G., Barrett R.K. and Henson H.H. (1995). Development of effective rockfall barriers. *Journal of Transportation Engineering, Nov/Dec*, pp.507-516.
- [33] Hoek E. (1987). A program in Basic for the analysis of rockfalls from slopes. *Unpublished notes*.
- [34] Hungr O. and Evans S.G. (1988). Engineering evaluation of fragmental rockfall hazard. *Proceedings of the Fifth Int. symposium on Landslides, Lausanne*, pp. 685-690.
- [35] Hunt R.E. (1992). Slope failure risk mapping for highways: methodology and case history. Rockfall prediction and control and landslide case histories, *Transportation Research Record, National Research Council, Washington*, No.1343, pp.42-51.
- [36] Joshi M. and Pant P.D. (1990). Causes and remedial measures for rockfalls and landslides on Naina peak, Nainital, Kumaun Himalaya, U.P., India. *Mountain research and development*, vol.10, no.4, pp. 343-351.
- [37] Kirsten H.A.D., Steffen O.K.H., Stacey T.R. (1986). Discussion on rockfall protection measures. *Conference on Rock Engineering in an Urban Environment, Institute of Mineral and Metallurgy.*, 24-27 February, Hong Kong, pp. 492-495.
- [38] Kuantsai Lee (1997). Preliminary Evaluation of rockfall programs. Report submitted to Golder Associates Inc., Hong Kong. *Unpublished notes*.
-

-
- [39] Mak N. and Blomfield D. (1986). Rock trap design for pre-splitting slopes. *Conference on Rock Engineering in an Urban Environment, Institute of Mineral and Metallurgy., Hong Kong*, pp. 263-270.
- [40] Martin D.C. (1988). Rockfall control: an update (Technical note). *Bull. Ass. Engng. Geol.* XXV No.1 pp. 137-144.
- [41] Mearns R. (1976). Solving a rockfall problem in California. *Bull. Assoc. Eng'g. Geol.*, Vol 13, No. 14, pp.329-335.
- [42] New Zealand Meteorological Service (1983). Summary of climatic observations to 1980. *New Zealand Meteorological Service Miscellaneous Publications*.
- [43] Niels Hovius (1994). A geological hazard assessment for the lower Fox Valley, anno 1994. *Department of Conservation, Conservation advisory science notes: 121*.
- [44] Paronuzzi P. (1989). Probabilistic approach for design optimisation of rockfall protective barriers. *Quarterly Journal of Eng'g Geology*, 22, 135-146.
- [45] Paterson B. (1994). Slope failure hazards on the Fox Glacier access road, South Westland. *Report submitted to the Department of Conservation*.
- [46] Paterson B. (1995). Undercite Creek & Cone rock, Fox Glacier. Slope stability assessment of rockfalls. *Report submitted to the Department of Conservation*.
- [47] Paterson B. R., McSaveney and Reyners M. E. (1992). The hazard of rockfall and rock avalanches at Zig Zag, SH73, Arthur's Pass. *Contract report No. 1992/14, for DSIR Geology & Geophysics*.
- [48] Peckover F.L. (1975). Treatment of rockfalls on railway lines. *American Railway Engineering Association, Bulletin 653*. Chicago IL.
- [49] Peckover F.L. and Kerr J.W.G. (1977). Treatment and maintenance of rock slopes on transportation routes. *Canadian Geotech. Journal*, 14, pp. 487- 507.
- [50] Pfeiffer T.J. and Bowen T.D. (1989). Computer simulation of rockfalls. *Bull. Ass. Engng. Geol.* XXVI, 135-146.
- [51] Pierson L.A., Davis S.A., and Van Vickle R. (1991). Rockfall Hazard Rating System Implementation Manual. *Federal Highway Administration (FHWA) Report. FHWA-OR-EG-90-01*. FHWA, U.S. Department of Transportation.
- [52] Piteau D.R. (1977). Computer rockfall model. *Commun. Proc. Meet. Rockfall Dynamics Protective Works Effectiveness 90*, 123-125.
- [53] Piteau D.R. and Clayton R. (1977). Discussion of paper "Computerised design of rock slopes using interactive graphics for the input and output of geometrical data"
-

- by P.A. Cundall, M.D. Voegele and C. Fairhurst. *Proceedings, 16th symposium on Rock Mechanics*, pp.62-63.
- [54] Piteau D.R. and Peckover F.L. (1978). Rock Slope Engineering. In Schuster R. L. and Krizek R.J. (editors) "Landslides: analysis and control". *Transportation Research board, Special Report 176, National Academy of Sciences*, Washington, DC, pp.489.
- [55] Reik G. and Hesselmann (1977). A study of kinematic and dynamic aspects of rock slides by means of model tests. *Proceedings of Meeting on Rockfall Dynamics Protective Works Effectiveness* 90, 97-122.
- [56] Richards L.R. (1988). Rockfall protection: a review of current analytical and design methods. *Secondo Ciclo Conferenze di Meccanica e Ingegneria delle Rocce, MIR, Politecnico di Torino*, pp. 11.1-11.13.
- [57] Ritchie A.M. (1963). Evaluation of rockfalls and its control. *Highways Research Record*. 17, 14-28.
- [58] Rochet L. (1987). Application des modeles numeriques de propagation al'etude des eboulements rocheux. *Bull. liaison Labo P. et ch.* 150/151, 84-95.
- [59] Rochet L. (1980). Protection against rockfalls. Methodology of specific studies. Application to the study of the La Praz zone of the SNCF railway between Culoz and Modane (in French). *Bull. Liasion Lab Ponts Chausses*, N106, March-April, pp.57-68.
- [60] Rochet L. (1979). Protection against rockfalls by means of metal netting (in French). *Bull. Liasion Lab Ponts Chausses*, N101, May-June, pp.21-28.
- [61] Rockfall Hazard Rating System, participant's manual (1993). *U.S. Department of Transportation, Federal Highway Administration(FHWA)*. FHWA-SA-93-057.
- [62] Romana M. (1988). Practice of SMR classification for slope appraisal. *Proceedings of the 5th International Symposium on Landslides*, Lausanne. July 10-15. Vol.2, pp. 1227-1229.
- [63] Romana M. (1991). SMR classification. *Proceedings of 7th International Congress on Rock Mechanics (ISRM)*, Aachen, Germany. Vol2., pp.955-960.
- [64] Russell S.O. (1976). Civil engineering risks and natural hazards. *The BC Professional Engineer, Journal of The Association of Professional Engineers of BC*. Vol.27, no.1, pp.9-12.
- [65] Sara W.A. (1979). Glaciers of Westland National Park. *Department of Scientific and Industrial Research information series*, 75. Wellington, New Zealand.

-
- [66] Shie-Shin Wu (1986). Rockfall evaluation by computer simulation. *Transportation Research Record, No. 1031*, pp. 1-5.
- [67] Smith C.E. (1991). Predicting rebounds using rigid body dynamics. *American Society for Mechanical Engineers (ASME) Journal of Applied Mechanics*, Vol.58, pp.754-758.
- [68] Smith C.E. and Liu P.P. (1992). Coefficients of restitution. *American Society for Mechanical Engineers (ASME) Journal of Applied Mechanics*, Vol.59, pp.963-969.
- [69] Spang R.M. (1987). Protection against rockfalls - stepchild in the design of rock slopes. *Proceedings of the 6th Int. Congress on Rock Mechanics, Montreal, Canada*, pp 551-557.
- [70] Spang R.M. and Rautenstrauch R.W. (1988). Empirical and mathematical approaches to rockfall protection and their practical application. *Proceedings of the 5th International Symposium on Landslides, Lausanne*, pp. 1237-1243.
- [71] Stacey T.R. (1989). Potential rockfalls in conventionally supported stopes - a simple probabilistic approach. *Journal of South African Inst. of Mineral and Metallurgy*, Vol 89, no.4, pp. 111-115.
- [72] Statham I. (1979). A simple dynamic model of rockfall: some theoretical principles and field experiments. *International Colloquium on Physical and Geomechanical Models*, pp. 237-258.
- [73] Stronge W.J. (1991). Unravelling paradoxical theories for rigid body collisions. *American Society for Mechanical Engineers (ASME) Journal of Applied Mechanics*, Vol.58, pp.1049-1055.
- [74] Varnes, D.J. (1978). Slope movement types and processes. *Schuster, R.L., and Krizek, R.J. Landslides - Analysis and control, transportation Research Board Special Report 176, National Academy of Sciences, Washington, D.C.*, pp. 11-33.
- [75] Tourism Resource Consultants (1995). Westland National Park. Review of visitor access to the Glaciers. *Tourism Resource Consultants Report*.
- [76] Whitehouse I.E. and McSaveney M.J. (1992). Assessment of geomorphic hazards along an alpine highway. *New Zealand Geographer*, 48, 1, pp. 27-32.
-